NOVEL EPHB RECEPTOR FORWARD SIGNALING PATHWAYS IN THE DEVELOPMENT OF MAJOR WHITE MATTER TRACTS OF THE MAMMALIAN BRAIN

by

MICHAEL ROBICHAUX

DISSERTATION

Presented to the Faculty of the Graduate School of Biomedical Sciences

The University of Texas Southwestern Medical Center at Dallas

In Partial Fulfillment of the Requirements

For the Degree of

DOCTOR OF PHILOSOPHY

The University of Texas Southwestern Medical Center at Dallas

Dallas, Texas

December, 2013

Dedication

I'd first like to thank my wife, Betsy, father Tim, mother Michele, sister Kristen, brothers Ben and Janssen, second father Curtis, and second mother Mona for their whole and true support when I moved to Dallas to begin graduate school and thereafter. Betsy, in particular, has been an exceptionally patient and loving companion throughout the long lab hours of graduate school. She always strove to prepare the most delectable and unforgettable after-work supper for me (and may one day succeed). On one early October morning this past year, another special guy showed up and turned us into a family. Besides having the enviable distinction of being born a Dallas cowboy, Jackson is already my glowing source of happiness and I marvel at him every single day. He truly inspires me to be a great person and to be a better scientist.

Speaking of being a better scientist, I couldn't have achieved my research goals without meeting Dr. Chris Cowan and subsequently joining his lab. Chris taught me how to be an efficient researcher, how to think effectively and strategically about experimental design, and how to "think big!". I'll never forget meeting Chris for the first time and instantly becoming inspired by his passion for science. I am especially grateful to him for allowing me to stay in Dallas to finish my Ph.D., while the rest of the lab moved to Boston. I hope to model my career after his, and hope to continue our collaboration/working relationship, which I value greatly.

The Cowan lab was an incredible and stimulating environment in which to work, and I am very fond of the relationships made with my labmates. I won't soon forget our lab outings to the Rangers games and to the park. Especially that time we got rained out and all crowded into Makoto's apartment for food and good times. I wish the very best for Carly, Maria, Laura,

Makoto, Nishi, Jesse, George, Adam, Yuhong, Guohong, Ben and Marissa, and hope to keep in touch with all of them in the future.

I am also in debt to Dr. Mark Henkemeyer, who was a fantastic collaborator for essentially all of my research projects. Mark was always happy to set up crosses for me in his menagerie of a mouse colony. He was also a constant presence in the development and design of many of my experiments, and he very well may have saved my paper by never giving up on ephrinB1! I'd also like to thank members of the Henkemeyer lab, including George, Sonal, Tim, Franny, and Lei, who were also very helpful, kind and sharing throughout the years.

Next, I am grateful for the advice and guidance bestowed to me by the other members of my thesis committee, Dr. Jonathan Terman and Dr. Adrian Rothenfluh. Jon and Adrian were always supportive of my work and provided many useful ideas and comments throughout our committee meeting sessions. In addition, I'd like to thank Dr. Amelia Eisch, who helped me get started here at UT Southwestern as a first year student, encouraged me to rotate in Chris' lab, and continues to provide support and guidance. Finally, I'd like to extend a broad "thank you" to all of the labs of the Psychiatry department here at UT Southwestern, who were all willing to share equipment and reagents with me this past year after the rest of the lab had moved out

I must also acknowledge my undergraduate professors from the Department of Biological Sciences at Nicholls State University in Thibodaux, Louisiana, who first inspired me and then encouraged me into pursuing graduate school in the basic sciences. They are as follows (in no particular order) (except for the first person): Dr. Michele Robichaux, Dr. Gary Lafleur, Dr. John Doucet, Dr. Raj Boopathy, Dr. Raj Nathaniel, Dr. Marilyn Kilgen, Dr. David Schultz, and Ms. Angie Corbin. I'd also like to thank Dr. Masami Yoshimura from the LSU School of Veterinary Medicine, who gave me my first real laboratory experience as an undergraduate SURF student.

Finally, I'd like to thank Licorice, who may or may not have been a constant and undying companion after long hours in the lab, and who may or may not be a fluffy black cat with lots to love.

NOVEL EPHB RECEPTOR FORWARD SIGNALING PATHWAYS IN THE DEVELOPMENT OF MAJOR WHITE MATTER TRACTS OF THE MAMMALIAN BRAIN

Publication No. _____

Michael Robichaux

The University of Texas Southwestern Medical Center at Dallas, 2013

Supervising Professor: Christopher Cowan, Ph.D.

The development of the vertebrate central nervous system (CNS), including the brain and spinal cord, progresses in a stepwise and patterned fashion that involves the function of thousands of genes. The complex processes of neurogenesis and early cell migration mark the earliest stages CNS development, and subsequent developmental steps, including axon guidance, establish the functional circuitry between young neurons. Axon guidance is characterized by the growth of axonal processes that sprout from neuronal cell bodies and navigate within the developing brain to reach target synaptic zones. This precise navigation is accomplished by the recruitment of numerous axon guidance molecules that activate essential signal transduction pathways to mediate morphological changes in developing axon. In this dissertation, I collected research data on EphB receptor forward signaling mechanisms and on the impact of these signaling pathways during the development of the major white matter tracts of the mouse brain. These major tracts include the optic nerve and optic tracts, the anterior commissure, the corpus callosum, and the reciprocal corticothalamic and thalamocortical axon pathways. I specifically present data in which I demonstrate that Vav2 and Vav3 GEF (guanine nucleotide exchange

factor) molecules form a specific forward signaling interaction with the EphB1 receptor that is essential for the proper axon guidance of retinal ganglion cell axons *in vivo*. Similarly, I demonstrated that Pak1, a signaling kinase, forms a novel interaction with the EphB2 receptor that is essential for the ephrinB2-stimulated growth cone repulsion of cortical axons.

I also present *in vivo* data using EphB mutant mouse lines to test EphB forward signaling events during the development of mouse forebrain circuitry. I show that forward signaling pathways are necessary for the proper development of the anterior commissure *in vivo*, as this tract is significantly misprojected off course in EphB deficient brains. Next, I present findings that characterize a novel role of EphB receptor forward signaling during thalamocortical axon pathfinding, where I demonstrate that, in the absence of proper EphB forward signaling, an early thalamocortical axon guidance error leads to major postnatal axon guidance defects. This data also presents strong evidence for the co-mingling of thalamocortical axons with reciprocal corticothalamic axons during their development through a selective fasciculation event. Together, these findings represent a major step forward in the understanding of axon connectivity in specific regions of the mammalian brain and also highlight the widespread function and importance of EphB receptors and EphB-mediated forward signaling during the axon guidance stage of brain development.

Table of Contents

Prior Publications

1. Soskis, M.J., Ho, H.Y., Bloodgood, B.L., **Robichaux, M.A.**, Malik, A.N., Ataman, B., Rubin, A.A., Zieg, J., Zhang, C., Shokat, K.M., Sharma, N., Cowan, C.W., Greenberg, M.E. (2012). A chemical genetic approach reveals distinct EphB signaling mechanisms during brain development. *Nat Neurosci* 15, 1645-1654. PMID: 23143520

2. Srivastava, N.*, **Robichaux, M.A.*** , Chenaux, G., Henkemeyer, M., and Cowan, C.W. (* authors contributed equally to this work) (2012). EphB2 receptor forward signaling controls cortical growth cone collapse via Nck and Pak. *Mol Cell Neurosci*, 52C , 106-116. PMID: 23147113

3. **Robichaux, M.A.***, Chenaux, G., Ho, H.Y., Soskis, M.J., Dravis, C., Kwan, K.Y., Sestan, N., Greenberg, M.E., Henkemeyer, M., and Cowan, C.W. (2013). Transient EphB Receptor Forward Signaling Coordinates Area-specific Cofasciculation of Reciprocal Thalamic and Cortical Axons during Brain Development. (IN REVIEW 07/13)

4. Cowan, C.W., **Robichaux, M.A.** "Local Signaling Strategies During Axon Guidance and Early Synaptogenesis" (book chapter). *The Neurobiology of Childhood*. CTBN. (IN EDITORIAL 07/13)

5. **Robichaux, M.A.***, Chenaux, G.*, Ho, H.Y., Soskis, M.J., Greenberg, M.E., Henkemeyer, M., and Cowan, C.W. (* authors contributed equally to this work) (2013). EphB Receptor Forward Signaling Regulates the Interhemispheric Development of Corpus Callosum and Anterior Commissure Axons. (IN PREPARATION 07/13)

List of Figures

Page

List of Tables

Page

Abbreviations

AC - anterior commissure

ACa - anterior branch of the anterior commissure

ACp - posterior branch of the anterior commissure

AD - acidic domain

AgCC - agenesis of the corpus callosum

AS - analog sensitive

ASD - autism spectrum disorder

CAM - cell adhesion molecule

CC - corpus callosum

CFA - corticofugal axon

CNS - central nervous system

CST - corticospinal tract

CTA - corticothalamic axon

DH - Dibble homology

DiI - 1,1′-Dioctadecyl-3,3,3′,3′-tetramethylindocarbocyanine perchlorate

DKO – double knockout

dLGN - dorsal lateral geniculate nucleus

DTB - diencephalic-telencephalic border

EC – external capsule

GABA - gamma-aminobutyric acid

GAP - GTPase-activating protein

GCC - growth cone collapse

GDP - guanosine diphosphate

GTP - guanosine triphosphate

GEF - gunanine nucleotide exchange factor

GFP – green fluorescent protein

GP - globus pallidus

GPI - glycosyl-phosphatidylinositol

HC - hippocampal commissure

Hy - hypothalamus

IC – internal capsule

JM - juxtamembrane

LGE - lateral ganglionic eminence

LIMK - Lim Kinase

MGE - medial ganglionic eminence

Npn - Neuropilin

OX - optic chiasm

PAK - p21 activated kinase

PDZ - postsynaptic density, discs large, zona occludens

PH - pleckstrin homology

RGC - retinal ganglion cell

ROCK - Rho-kinase

RTK - receptor tyrosine kinase

SAM - sterile alpha motif

Sema - semaphorin

SH2 - Src homology 2

SH3 - Src homology 3

TCA - thalamocortical axon

Th - thalamus

VT - ventrotemporal

VTC - ventrotemporal crescent

VTel - ventral telencephalon

WT - wild-type

ZF - zinc finger

Foreword

The development of a functioning central nervous system (CNS) involves a complex series of developmental stages that initiate the morphogenic transformation of the brain and spinal cord into highly-order and interconnected biological systems. As an elaborate circuitry, the proper formation of the CNS requires a highly regulated and effective program for axon guidance. Numerous genes, transcriptional networks and signaling transduction pathways have been characterized and linked to the process of axon guidance. Still, this critical work in the field of neurodevelopment continues, as our understanding of the development of neural circuitry is linked to our understanding of postnatal connectivity and higher order brain function. The data presented in this dissertation identify novel forward signaling mechanisms within developing axons that are downstream of the *EphB* receptor genes. This introductory chapter will present a selective literature review of the genes, structures, and mechanisms that are the subject of the following chapters.

Circuit Formation in the Developing Brain

The mammalian brain first emerges as a morphologically distinct organ segment of the neural tube at around gestational day 26 in humans and embryonic day 10 in mice. At this early stage, the future forebrain, midbrain and hindbrain are patterned as the prosencephalon, mesencephalon and rhombencephalon, respectively (for review, see (Keynes and Lumsden, 1990)). Within this rudimentary brain structure, numerous sequential and simultaneous developmental processes drive the expansion, organization and connectivity that characterize a mature functional brain. Neurodevelopmental stages, such as cell division, neurogenesis,

gliagenesis, and cell migration are required for the growth and basic cellular organization of the brain; however, brain morphology is also defined by the white matter axon fibers that interconnect neurons and hardwire brain circuitry. Indeed, one the most fascinating and complex aspects of brain development is the process by which neurons interconnect through stereotyped axon connections. Only through the developmental process of axon guidance is brain circuitry established by way of the precise navigation of growing axons to their appropriate target region(s) within the brain or periphery. Once axons arrive at their terminal destination, they will form chemical synapses with target neurons or effector cells (e.g. muscle cells). The importance and complexity of axon guidance, including the underlying molecular programs designed to carry out axon development, becomes clear when one considers that billions of neurons will form trillions of targeted synaptic connections within the developing brain.

Decades of neurobiological research have contributed to our understanding of the axon guidance "decisions" made by neurons in the developing brain during circuit formation. In most cases, the navigation of axons to appropriate target regions is determined at the local, molecular level, where complex cell signaling events are initiated when cell surface receptors encounter extracellular ligand molecules (such as axon guidance cues). During axon pathfinding, local molecular signaling events can affect axonal morphology, substrate adhesion properties and axon motility. In some cases, activated axon guidance receptors signal a long distance back to the soma and nucleus to facilitate axon outgrowth and guidance, but local signaling events within the axon's distal tip, in a structure known as the growth cone, are thought to be most critical for proper axon navigation. Research in this field aims to elucidate how these events function at the molecular and cellular level both in concert and in series to achieve the goal of trillions of properly developed synaptic connections.

Axon Guidance

Axons sprout from newly born, polar neurons and extend as morphologically distinct processes that are supported by microtubules within its axon shaft. The growth cone, a filamentous actin (F-actin)-rich structure, is formed at the distal tip of the axon shaft and is subsequently tasked with interpreting extrinsic molecular cues, referred to as guidance cues, that push (repellent cues) or pull (attractant cues) the distal growth cone. Through such encounters the growth cone effectively steers the extending axon toward its target zone. During axon growth, the growth cone extends as a flattened, lamellopodia-like structure capable of dynamic motility and structural reorientation through rapid cytoskeletal remodeling of its underlying F-actin and microtubule cytoskeleton. This underlying framework is intimately linked to numerous axon guidance receptors and cell adhesion molecules (e.g. integrins) expressed at the growth cone surface.

Axon guidance cues are broadly classified as attractive or repulsive based on the subsequent growth cone response to these cues. However, some guidance factors, including ephrins and semaphorins, promote either growth cone attraction or repulsion based on axon guidance receptor composition. In normal development, navigating axon growth cones encounter both: (1) secreted molecular cues expressed in a concentration gradient or (2) cell membrane-associated cues that require axon:cell contact. Axons navigating long distances will often encounter various guidance cues or "intermediate targets" at multiple guidance choice points en route. In addition, axons of the same origin and general destination will often bind together in large white matter bundles through an axon:axon adhesive phenomenon known as fasciculation. Fasciculated axon bundles often develop *in vivo* along the route established by pioneer axons earlier in development (reviewed in (Raper and Mason, 2010)). These fascicles

often remain as large white matter brain structures, such as the corpus callosum or the thalamocortical axon tract (Figure I). As such, pioneer axons are heavily dependent upon axon guidance cues and early guidance decisions, such that errors made by pioneer axons can result in the aberrant axon guidance of fasciculating axons that follow the misprojected pioneer axon path.

To this end, the axon growth cone must be equipped with the appropriate guidance cue detection and cytoskeletal machinery. Growth cones often express multiple axon guidance receptor proteins to bind specific cues, and these receptors are expressed in a cell type dependent pattern. In addition, navigating growth cones must possess the local signaling machinery to rapidly respond to guidance cues and direct cytoskeletal changes at a long distance from the soma. Many of these local signaling networks that are downstream of different axon guidance receptors overlap and share several common signaling cascades and effector molecules (e.g. F-actin remodeling enzymes, cell adhesion molecules, etc). Furthermore, a developing axon typically responds to many different classes of guidance cues during its navigation, and upon binding to several distinct classes of guidance receptors, intracellular signaling cascades often converge to facilitate proper F-actin cytoskeletal remodeling. Understanding how these distinct guidance receptor pathways recruit and coordinate cell signaling factors to orchestrate proper axon guidance is a critical and challenging aspect of the field.

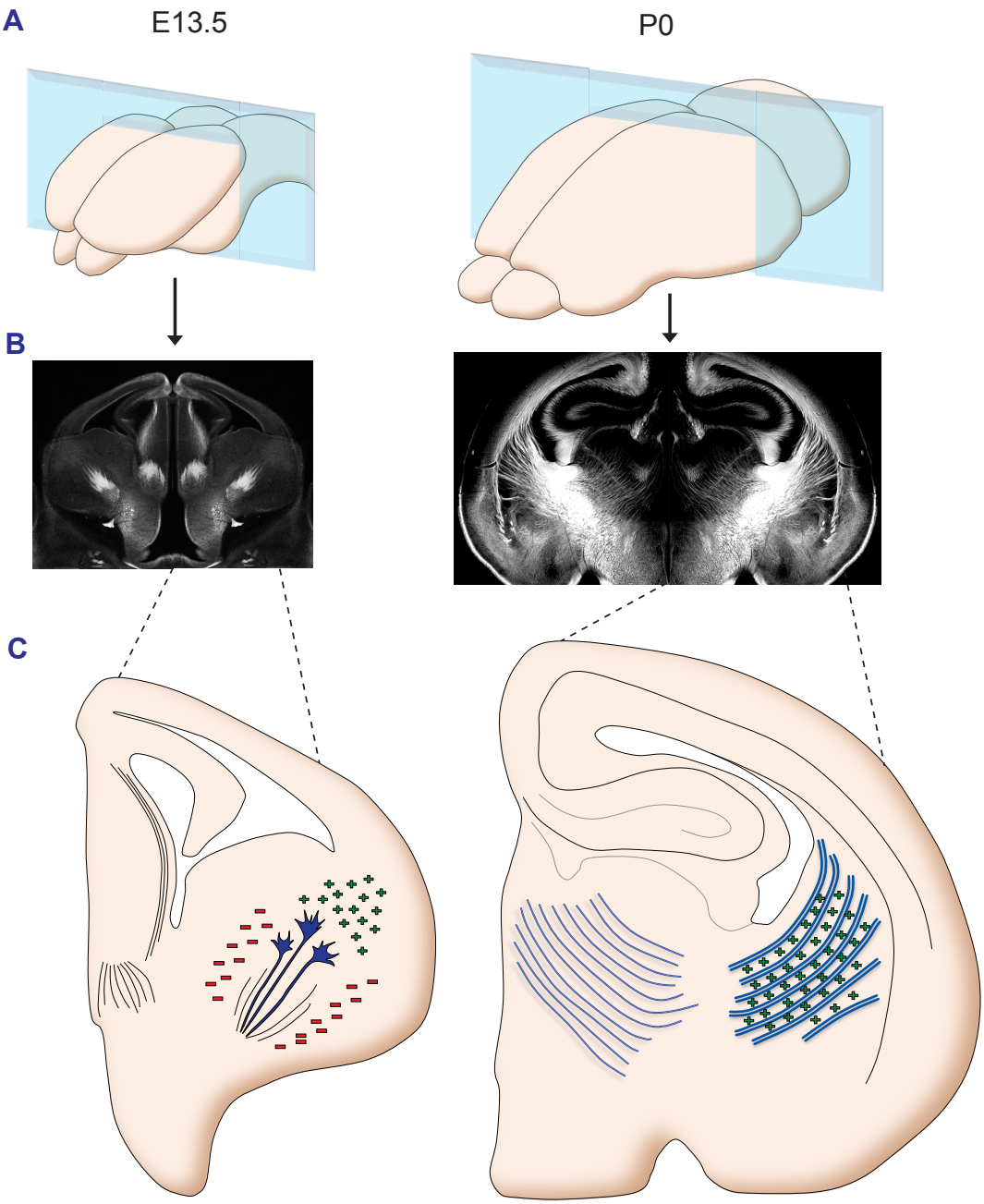

Figure I. Pioneer axons trailblaze the projection path of mature axons. *(A)* An E13.5 embryonic brain and P0 postnatal mouse brain are depicted. The brain dramatically increases in size between these periods through the processes of cell division, neurogenesis, gliagenesis, and cell migration. Brain circuitry is subsequently established through the developmental stages of

axon guidance and synaptogenesis. *(B)* Shown here are fixed sections of E13.5 and P0 mouse brains that are immunostained with a L1-CAM antibody that specifically labels developing axons (Demyanenko et al., 2011; Fukuda et al., 1997; Wiencken-Barger et al., 2004). These coronal forebrain regions contain the ventral telencephalon (VTel) (the future striatum) and internal capsule. At E13.5, L1+ pioneer thalamocortical axons (TCAs) descend from the dorsal thalamus and penetrate the VTel as a tightly organized pioneer axon population. At P0, reciprocal axons from the neocortex, including CFAs and CTAs, have formed large fasciculated bundles with ascending TCA fiber bundles that are highly organized and patterned. *(C)* An enlarged illustration of the coronal brain regions in *(B)*. At E13.5, pioneer TCA axons encounter both attractive cues, such netrin-1 (Braisted et al., 2000) (depicted as "+" symbols") and repulsive boundary cues like Slit proteins (Bagri et al., 2002) (depicted as "-" symbols) within the VTel en route to the neocortex. At P0, mature axon bundles are tightly bound together through the adhesive process of lateral fasciculation (depicted as "+" symbols).

Eph Receptors

Among the axon guidance receptor genes that direct axon pathfinding in the vertebrate brain, the *EPH* Receptors are one of the largest and most studied of these gene families. The "Eph" family of receptor tyrosine kinase proteins were first purified and cloned from Erythropoietin Producing human Hepatocellular carcinoma cells, for which they were named (Hirai et al., 1987). Several years later the ephrin proteins (previously known as "Lerks") were discovered and identified as Eph receptor ligands (Bartley et al., 1994; Beckmann et al., 1994; Cheng and Flanagan, 1994; Davis et al., 1994). Ephrins are a family of transmembrane proteins that are either bound to the membrane surface through a glycosyl-phosphatidylinositol (GPI)-anchor or a transmembrane protein domain. As the Eph and ephrin gene families grew larger and developed an inconsistent nomenclature and classification, the Eph Nomenclature Committee in 1997 consensually adopted the current nomenclature and classification of the Ephs and ephrins (Eph Nomenclature Committee 1997). Class-A Eph receptors (EphA1-8 & A10), primarily bind to ephrinAs (ephrinA1-A5), which contain a GPI surface anchor. Class-B Eph receptors (EphB1-6) primarily bind to ephrinBs (ephrinB1-3), which contain a transmembrane protein domain (Pasquale, 2005). Notable exceptions to the class A/B binding scheme are EphA4, which can bind to the ephrinBs (Kullander and Klein, 2002), and EphB2, which can bind to ephrinA5 in addition to the ephrinBs (Himanen et al., 2004; Zimmer et al., 2003).

Eph receptors reside endogenously as dimers before adopting a heterodimer-dimer conformation upon ephrin binding. These heterodimer complexes then multimerize through tight lateral clustering into large receptor complexes containing dozens of individual Eph receptor proteins (Himanen and Nikolov, 2003). The binding preference of the EphA and EphB receptors is mediated through slight differences in the N-terminal, ephrin-binding extracellular domains of

the receptor protein. Both Eph subclasses, however, share a homologous and highly-conserved intracellular domain structure, which features a critical juxtamembrane (JM) signaling region, a large Src-like tyrosine kinase domain, a sterile-alpha motif (SAM) signaling domain, and a C-terminal PDZ (postsynaptic density, discs large, zona occludens) target signaling site (Himanen and Nikolov, 2003). In the endogenous "off" state, the intracellular Eph kinase domain is conformationally clamped to the unphosphorylated JM region, and a hydrophobic pocket blocks tyrosine kinase activity (Wybenga-Groot et al., 2001). Upon ephrin binding and receptor clustering, the receptor kinase domains come into close lateral contact so that the JM regions become autophosphorlyated. Once autophosphorylated, the clustered receptors become aligned in an "on" conformation that is then capable of kinase-dependent signaling (Himanen et al., 2001).

In addition to inducing the formation of large Eph-ephrin clusters between the surface of two interacting cells membranes, the Eph-ephrin interaction establishes a bidirectional signaling complex that elicits both Eph receptor "forward" signaling and ephrin-mediated "reverse" signaling. Eph forward signaling is mediated through intracellular kinase activity, direct signaling interactions at the SAM and PDZ regions, as well as the recruitment of several signaling proteins to the JM region (Dent et al., 2011; Wybenga-Groot et al., 2001). Essential forward signaling proteins include Rho-GTPases (see next section), which are required for Eph receptor forward signaling upon ephrin stimulation in various cell types (Fournier et al., 2000; Jurney et al., 2002; Wahl et al., 2000). GTPase signaling regulators, however, such as Rho-family guanine nucleotide exchange factors (GEFs) and GTPase-activating proteins (GAPs), which would serve as the molecular link between activated Ephs and Rho-GTPases, remain largely uncharacterized. Several mechanisms have been identified that terminate Eph-ephrin

signaling, as well. Protein tyrosine phosphatases have the capability to shut off both EphA and EphB receptor kinase activity (Shintani et al., 2006; Stepanek et al., 2005); however, Eph receptor signaling *in vivo* is more likely regulated through the severing of the Eph-ephrin interaction either through receptor-ligand transendocytosis (Cowan et al., 2005; Marston et al., 2003) or extracellular protease cleavage (Georgakopoulos et al., 2006; Hattori et al., 2000; Pascall and Brown, 2004).

Ephrin reverse signaling was first described as a significant axon guidance component during the development of posterior branch of anterior commissure (ACp) in mice. ACp development is EphB2 receptor-dependent, yet EphB2-lacZ mutant mice, a transgenic line that expresses a truncated form of the EphB2 receptor lacking an intracellular signaling domain. (Henkemeyer et al., 1996). These results indicate that EphB2 must stimulate ephrin reverse signaling events. Reverse signaling pathways have since been demonstrated for both ephrinAs and ephrinBs (reviewed in (Gauthier and Robbins, 2003)).

As the largest receptor tyrosine kinase (RTK) gene family, the Eph receptors have a broad and ubiquitous function during development. Outside of the CNS, Eph receptors function during the processes of cell morphogenesis, tissue patterning and angiogenesis (Pasquale, 2005). Within the CNS, Ephs are essential for neural crest cell migration, dendritic spine formation and synaptogenesis, as well as synaptic plasticity and maintenance in postnatal neuronal circuits (Dalva et al., 2000; Henkemeyer et al., 2003; Kayser et al., 2006; Kayser et al., 2008; Pasquale, 2005; Shen and Cowan, 2010). During axon guidance, however, Eph receptors serve varied and redundant functions among various cell types throughout the brain, and, along with the ephrins, remain one the most well-studied axon guidance molecules (reviewed in (Egea and Klein, 2007; Pasquale, 2005)). Generally, the Eph-ephrin interaction induces a repulsive response in axons,

as the application of artificially clustered ephrin protein induces the dramatic repulsion of Eph-expressing neurites in culture (Birgbauer et al., 2001; Petros et al., 2010; Srivastava et al., 2013; Williams et al., 2003). Ephrin-induced axon repulsion mediates axon turning *in vivo* at key decision points during axon pathfinding and development. Indeed, the disruption of Eph receptor expression and signaling *in vivo* leads to significant axon guidance errors in the CNS (Henkemeyer et al., 1996; Kadison et al., 2006; Mendes et al., 2006; Williams et al., 2003). In addition to the *in vivo* axon pathfinding events discussed in detail in the following chapters, Eph receptors are also essential during topographic mapping of retinotectal axons and corticospinal guidance at the spinal cord midline (Harada et al., 2007; Kadison et al., 2006; Kullander et al., 2001b).

Rho GTPases

Rho GTPase signaling molecules, which are members of the Ras GTPase superfamily of nearly 200 proteins, are the most commonly employed secondary signaling molecules in the axon growth cone. Rho GTPases are discussed here because most signaling pathways that have morphological effects on the growth cone, including those downstream of Eph receptors, converge on the regulation of Rho GTPases. Like other G proteins, Rho-GTPases are active when bound to GTP (guanosine triphosphate), and are inactivated upon GTP hydrolysis to GDP (guanosine diphosphate). These "molecular switches" are highly regulated by guanine nucleotide exchange factors (GEFs), which promote the release of bound GDP and allow for binding to GTP. In contrast, GTPase-activating proteins (GAPs) regulate the inactivation of Rho GTPases by binding to GTP-bound GTPases and accelerating GTP hydrolysis (reviewed in (Colicelli, 2004; Jaffe and Hall, 2005; Schmidt and Hall, 2002)).

Rho GTPases function as key regulators of the F-actin cytoskeleton by promoting the formation, branching or disassembly of F-actin scaffolds. As such, the Rho GTPase subfamily, of which there are over 20 different genes, plays an important role in the cytoskeletal dynamics of navigating axon growth cones (reviewed in (Dickson, 2001; Hall and Lalli, 2010)). Rho-family GTPases are divided into three major subgroups: Rho, Rac, and Cdc42. In general, Rac-GTP promotes the formation of branched lamellapodia or membrane ruffles, while Cdc42-GTP promotes the formation of unbranched filopodia, and Rho-GTP regulates F-actin severing and F-actin contractility via actin-type II myosin regulation (reviewed in (Hall, 1998)). Numerous studies, however, report atypical roles for the Rho GTPases during axon guidance, such as Rho-mediated F-actin severing that generates new F-actin branch points to promote axon outgrowth (Hall and Lalli, 2010). As such, within the same growth cone, Rho GTPases are differentially regulated to control complex axon growth cone turning.

Vav-GEFs

Considering the functional importance of Rho-GTPases in the axon growth cone, much research has focused on identifying the GEFs and GAPs that link ligand-bound axon guidance receptors to the activation or inactivation of the Rho-family GTPases, respectively. Dbl homology (DH) Rho-family GEFs possess a DH protein domain that facilitates the release of bound GDP on Rho GTPases, and several of these DH-family GEFs are recruited to, and/or activated by, various axon guidance receptors. For example, the DH-family GEF, Trio, functions downstream of netrin-DCC receptor binding in mammalian spinal cord axons to promote axon attraction (Briancon-Marjollet et al., 2008). Trio selectively activates Rac, while the LARG GEFs, which selectively activate RhoA, function downstream of the PlexinB1 receptor to

facilitate growth cone repulsion in hippocampal neurons (Swiercz et al., 2002). In spinal cord axons, EphA receptors can recruit the Rho-GEF Ephexin-1 (Shamah et al., 2001), which becomes a strong RhoA activator upon EphA activation and ephexin tyrosine phosphorylation (Sahin et al., 2005). EphA and EphB receptors can also recruit Vav family GEFs in cultured retinal ganglion cells (RGCs). Vav-GEFs are DH-family members that can activate Rho, Rac and Cdc42, and are required for ephrinA-induced growth cone collapse as well as the Rac-dependent endocytosis of Eph receptors (Cowan et al., 2005).

Members of the Vav family of DH-containing Rho-GEFs in mammals (Vav1-3) have a homologous multi-domain, protein structure. Upon binding to Rho-GTPase targets, the DH domain of Vav carries out its GEF function by promoting the disassociation of GDP from bound GTPases (Bustelo, 2000). The regulatory acidic domain (AD) directly inhibits the DH region in the inactive state and is released upon the phosphorylation of a key tyrosine residue (Y-172 in Vav2) within the AD (Aghazadeh et al., 2000; Bustelo, 2000; Turner and Billadeau, 2002). A pleckstrin homology (PH) domain is also essential for Vav GEF activity onto bound Rho-GTPases. Next, a zinc finger (ZF) domain is followed an adaptor segment that features a SH2 (Src homology 2) domain that is flanked by two SH3 (Src homology 3) domains (Bustelo, 2000; Turner and Billadeau, 2002). The SH2 domain contains the positive amino acid sequence (Y(P)XEP (X = M, L, or E) (Songyang et al., 1994)) that serves as the interaction site with SH2-binding regions of signaling partners, such as at the phosphorylated (negatively-charged) JM tyrosine residues of EphA4 and EphB2 (Cowan et al., 2005).

Vav1 was first identified as an oncogene in cells of the hematopoietic system, and all of the Vav-GEFs have a well-characterized role outside of the CNS during immune cell development and function (Turner and Billadeau, 2002). Vav1 expression, however, is limited

to the hematopoietic system, while both Vav2 and Vav3 have a broader expression pattern that includes the CNS (Bustelo, 2001; Cowan et al., 2005). Vav2 was identified in a yeast-two hybrid screen with the intracellular region of EphA4 as a potential forward regulator of Eph receptor signaling. Furthermore, Vav2/3 GEFs were demonstrated to be necessary for retinogeniculate axon targeting (Cowan et al., 2005); however, the complete *in vivo* function of Vav-GEFs in the CNS, particularly during axon guidance, remains uncharacterized. However, other recent studies have demonstrated that Vav GEFs function during photoreceptor axon guidance in *Drosophila* (Malartre et al., 2010), neurite outgrowth in *Xenopus* spinal cord axons (Moon and Gomez, 2010), and during dendritic spine formation downstream of TrkB receptor activation in cultured hippocampal neurons (Hale et al., 2011).

Pak

Along with GEF proteins, which function as upstream activators of Rho family GTPases, there are several key downstream effectors of Rho GTPase signaling. *Pak* (p21-activated kinase) genes are one particular signaling effector family downstream of Rac-GTP and Cdc42-GTP. The Paks are highly-conserved serine/threonine signaling kinases that regulate F-actin dynamics indirectly via the phosphorylation of additional downstream factors (reviewed in (Bokoch, 2003)). Upon cellular stimulation, Pak1 becomes localized to actin structures, such as the leading edge lamellapodia, membrane ruffles and focal adhesions. Actin-binding Pak substrates include LIM kinase, regulatory myosin light chain, myosin light chain kinase, stathmin, and filamin (Bokoch, 2003; Dharmawardhane et al., 1997; Dharmawardhane et al., 2000; Sells et al., 2000). In addition to cell morphology and motility, Pak has a reported function in proliferative signaling downstream of MEK1 and Raf (Eblen et al., 2002; Slack-Davis et al., 2003) during

processes such as neurogenesis, angiogenesis, and cancer metastasis (reviewed in (Arias-Romero and Chernoff, 2008; Bokoch, 2003)).

The Pak family is divided into group I Paks (Pak 1-3) and group II Paks (Pak 4-6) based on homology, and although Paks are a common cellular signaling molecule for actin cytoskeleton remodeling, its precise morphological function in many areas of brain development is still unclear. A recent SAGE analysis confirmed that all Pak genes are expressed in the human brain (Arias-Romero and Chernoff, 2008). Furthermore, Pak1 is expressed in the developing and adult rodent cortex (Causeret et al., 2009), and has been localized to developing growth cones of cultured cortical neurons (Hayashi et al., 2007; Zhong et al., 2003). In these developing fibers, Pak1 activity regulates primary dendritic branching and axon sprouting (Hayashi et al., 2007; Jacobs et al., 2007b). In addition, Pak1 is believed to be essential for proper neuronal morphology *in vivo*, particularly in the mammalian neocortex, as it is expressed in major cortical axonal tracts, including the corpus callosum, the cortical intermediate zone, and axon fascicles of the internal capsule (Jacobs et al., 2007b; Zhong et al., 2003).

As a key signaling molecule during axon guidance, Pak1, and its activators Rac1 and Cdc42, are recruited to the netrin1-activated DCC receptors to stimulate axonal outgrowth of spinal cord commissural axons (Shekarabi et al., 2005). In this context, Pak1 functions "traditionally" by activating LIM kinase, which in turn phosphorylates cofilin. Cofilin, a F-actin severing protein, is inhibited upon phosphorylation, which results in stable F-actin and axon outgrowth (Edwards et al., 1999). In *Drosophila*, dPak is necessary for the proper development of photoreceptor axons (Hing et al., 1999); however, dPak is also paradoxically activated downstream of Rac1 through an interaction with Dock, an adaptor protein, to signal growth cone repulsion downstream of the Robo receptor (Fan et al., 2003). Similarly (as outlined in Chapter

2), ephrinB2 stimulation of cortical neurons stimulates an EphB2 receptor-mediated growth cone collapse, which is dependent on Pak1. Here, the Nck adaptor protein, the mammlian homolog of Dock, binds to the activated EphB2 receptor and recruits Pak1. However, unlike dPak, the kinase-dependent function of Pak in EphB2 receptor-mediated cortical growth cone repulsion does not require Rac-GTP or Cdc42 GTP (Figure II) (Srivastava et al., 2013).

Finally, as a ubiquitous signaling protein with emerging roles in the nervous system, the Pak family is not surprisingly involved in several brain pathologies. Missense mutations to the *Pak3* human gene have been linked to nonsyndromic X-linked mental retardation (Allen et al., 1998; Bienvenu et al., 2000; Gedeon et al., 2003). Pak family genes have also been associated with neurodegenerative diseases, including Alzheimer's disease (AD), as Pak3 binds to a familial AD mutant amyloid precursor protein in culture to initiate neuronal apoptosis and AD-associated DNA synthesis (McPhie et al., 2003). Furthermore, in human AD patients, a loss of Pak1 and Pak3 expression levels are observed in the hippocampus and temporal lobe (Nguyen et al., 2008; Zhao et al., 2006), and in mouse AD models, group I Pak activity is significantly reduced (Nguyen et al., 2008).

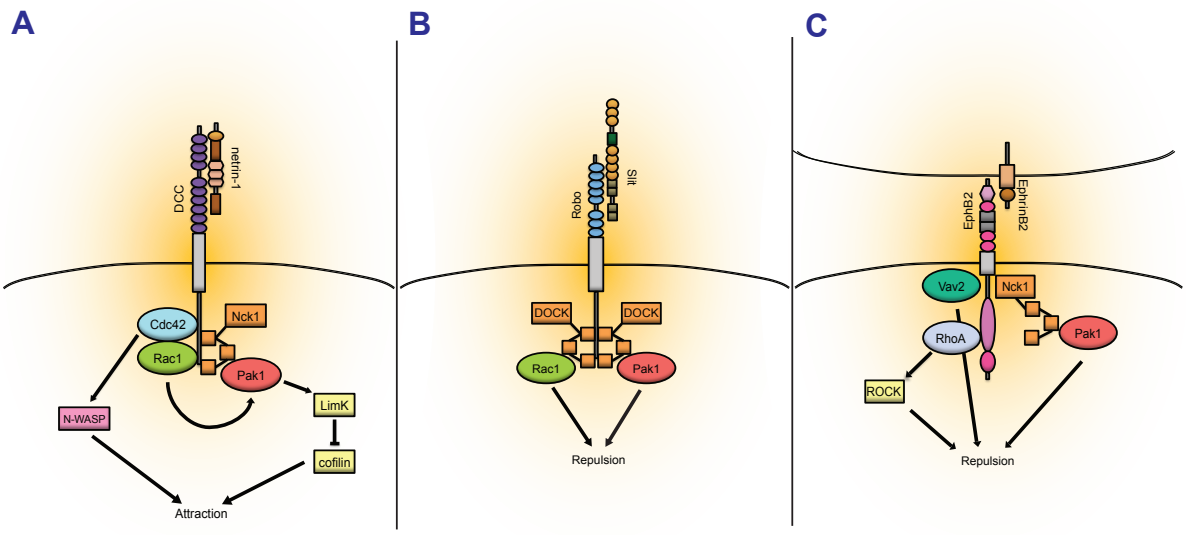

Figure II. PAK – p21-associated kinase – is a Rho GTPase downstream signaling factor essential in multiple axon guidance receptor signaling pathways. *(A)* Netrin-1 binds to and activates the DCC receptor in spinal commissural axons, which recruits Rac1 and Cdc42 GTPases. Pak1 is also recruited to DCC via the Nck1 docking protein and is activated by Rac1/Cdc42. Pak1 carries the signal further downstream by phosphorylating Lim kinase (LIMK), which inhibits cofilin F-actin severing to favor growth cone attraction (Shekarabi and Kennedy, 2002). *(B)* In *Drosophila* photoreceptor axons, Slit proteins bind to the Robo receptor, which simultaneously recruits both Rac1 and Pak1 via the DOCK *Drosophila* adaptor protein (ortholog of Nck). Together and in parallel, both Rac1 and Pak1 are necessary for Slit-induced repulsion in these neurons (Fan et al., 2003). *(C)* EphrinB2 activation of the EphB2 receptor induces strong growth cone repulsion in cortical neurons that also requires Pak1. Here, upon EphB2 activation, Pak1, via Nck1, is directly recruited to EphB2 independent of Rac GTP activation (Srivastava et al., 2013).

Retinogeniculate Axons

Retinal ganglion cells (RGCs) are located in ganglion cell layer of the retina and form stereotyped axonal connections with the dorsal lateral geniculate nucleus (dLGN) in the thalamus and the superior colliculus (or optic tectum) in the midbrain. The developmental course of RGC axons, either along the retinogeniculate (to the dLGN) or the retinotectal (to the superior colliculus) pathway, has long been used as a model system for studying axon guidance genes and mechanisms (Bao, 2008; Erskine and Herrera, 2007). RGCs are first born around age E11.5 (Drager, 1985) and sprout axons that converge into the optic disc located at the back of the retina and grow through the optic stalk to form the optic nerve bundle that projects caudally through the ventral diencephalon. A key axon guidance decision occurs when retinogeniculate axons reach the optic chiasm (OX) midline between ages E14 - E17 (Godement et al., 1990). Here, RGC axons either cross over the midline toward the contralateral hemisphere or are repelled toward the ipsilateral axon tract (reviewed in (Williams et al., 2004)). In mice, RGC axons from the ventro-temporal crescent (VTC) of the retina are specifically repelled from the midline onto the ipsilateral optic tract, while the rest of the RGC axon population crosses over to the contralateral side (Colello and Guillery, 1990; Drager, 1985; Godement et al., 1987; Shatz and Sretavan, 1986; Sretavan, 1990). To complete the retinogeniculate axon pathway, dual opposing EphA and ephrinA gradients between the retina and dLGN establish the topographic synaptic terminal mapping of RGC projections (reviewed in (Harada et al., 2007)). Recently, EphB1 was also shown to be required for RGC synaptic terminal refinement in the dLGN; however, this specific function for EphB1 has not been fully characterized (Rebsam et al., 2009).

At the OX midline, RGC axons display a “saltatory” growth pattern characterized by intermittent periods of dynamic growth and decision-making along with long periods pausing,

during which the growth cone remains fluid and dynamic (Godement et al., 1994; Mason and Wang, 1997). RGC axons at the OX form direct contact with the neurite "feet" of radial midline glia that express axon guidance cues, including ephrinB2, that are transduced by the midline RGC axons (Mason and Sretavan, 1997; Williams et al., 2003). Ultimately, ipsilateral RGC axons make the decision to turn away from the midline and continue development along the ipsilateral optic tract (Godement et al., 1994). The partial decussation at the OX segregates the RGC population based on the visual hemifield of the RGC cell bodies in the retinae of binocular animals, including mice. The number of decussating fibers at the midline is variable between species and is dependent on the binocular overlap of their respective visual fields (Fukuda et al., 1989; O'Leary et al., 1983). Thus, RGCs from the VT retina in mice are repelled from the midline to terminate in the visual centers in an overlapping fashion with the contralateral axon population from the opposing eye. This partial decussation establishes stereopsis and depth perception in these visual centers of the mouse brain (reviewed in (Petros et al., 2008; Williams et al., 2004).

Several axon guidance cues are utilized during the various stages of RGC axon pathfinding, include the long-range netrin-1, Semaphorin-5A and 3D, and Slit-1 cues (reviewed in (Williams et al., 2004)). Netrin-1 functions to promote the outgrowth of RGC axons from optic disc, through the optic stalk and onto the optic nerve tract (Deiner et al., 1997; Lauderdale et al., 1997), while Sema5A/3D and Slit-1 function as repulsive guidance cues that maintains proper RGC axon fasciculation and orientation within the optic nerve tract (Oster et al., 2003; Sakai and Halloran, 2006; Thompson et al., 2006a; Thompson et al., 2006b). The Eph receptors and ephrins serve multiple, redundant functions along the retinogeniculate pathway. EphB2 and EphB3 are necessary for early RGC axon targeting to the optic disk (Birgbauer et al., 2000;

Connor et al., 1998; Henkemeyer et al., 1996; Hindges et al., 2002a). Despite a uniform retinal expression early, EphB2 receptors form a high ventral-low dorsal expression gradient in the retina by age E16.5 (Birgbauer et al., 2000). EphB1, on the other hand, is exclusively expressed in the VT retina from ages E14.5-E15, which is consistent with its role in ipsilateral repulsion at the OX midline that occurs at this time period, when ipsilateral RGC axons encounter ephrinB2 that is simultaneously expressed on the surface of midline glia (Williams et al., 2003). Furthermore, in cultured RGC axons from the VTC, axons undergo dramatic growth cone collapse and repulsion in response to exogenous stimulation with ephrinB2 (Petros et al., 2010). Zic2, a zinc finger transcription factor, is also specifically upregulated in the VTC at around age E14 and is directly linked to the expression of EphB1 in VT RGCs (Garcia-Frigola et al., 2008; Herrera et al., 2003; Lee et al., 2008), while Islet2, a LIM homeodomain transcription factor, is simultaneously expressed in contralateral projecting RGCs of the retina (Pak et al., 2004). Together, the upregulation of these two transcriptional regulators in different regions of the retina appears to drive the transcriptional pathways that establish the fate of RGC axon projections at the OX midline.

Thalamocortical Axons

Sensory input into the mammlian brain, excluding olfactory information, is primarily directed through sensory relay nuclei in the thalamus that relay the signal to target brain areas, including the sensory regions of the neocortex. Thalamocortical axons (TCAs) interconnect these sensory relay nuclei with specific neocortical target neurons to propagate sensory processing in the brain (reviewed in (Lopez-Bendito and Molnar, 2003; Molnar et al., 2012)). The proper development of TCA axons from the thalamus to these neocortical regions is thus

critical for maintaining the fine topography that spans the length of these fibers and establishes the fine neuronal circuitry between these two regions. In addition, corticothalamic axons (CTAs) form reciprocal connections with TCA fibers, and these populations develop simultaneously (see the section below), which contributes to the complex developmental program that ultimately forms this cortical-thalamic circuit.

TCA projections first sprout from dorsal thalamic neurons at ages E11.5-E12.5 (Auladell et al., 2000). TCA fibers then project ventrally through the prethalamus and toward the hypothalamus before turning sharply in the lateral direction at the diencephalic-telencephalic border (DTB) to emerge in the ventral telencephalon (VTel) region around age E12.5. At this early age, the VTel is populated by migrating cells, which include GABAergic guidepost cells that migrate from the lateral ganglionic eminence (LGE) and into the medial ganglionic eminence (MGE) and globus pallidus (GP) (Lopez-Bendito et al., 2006). Here in the VTel, TCA fibers establish the internal capsule bundle, which becomes a major postnatal axon fascicule. Pioneer TCAs in the VTel then ascend toward the neocortex, developing as an organized and topographic web of fiber projections. TCAs reach the cortical intermediate zone at age E13.5, where they pause for ~36 hours before penetrating the cortical plate at age E15 (Auladell et al., 2000).

The axon guidance molecules, netrin-1, Slit1/2, Sema3A, and ephrinA5 (Bagri et al., 2002; Bielle et al., 2011a; Bielle et al., 2011b; Dufour et al., 2003; Powell et al., 2008; Wright et al., 2007) are all expressed in some manner within VTel during the time period of TCA development. VTel guidance cues contribute to TCA guidance through specific interactions with axon guidance receptors expressed in TCA axons themselves, including Neuropilin 1, Robo1/2, EphA3/4/7, and Sema6A (Dufour et al., 2003; Little et al., 2009; Lopez-Bendito et al., 2007;

Wright et al., 2007). In particular, ephrinA5 is expressed within the VTel along a high-rostral, low-caudal gradient that maintains the proper topographic patterning of EphA-expressing TCAs. These projections are derived from the rostro-medial thalamus and develop in a tight, highly regulated pattern through the rostral aspect of the VTel and toward the rostral cortex (Dufour et al., 2003). In addition, transcription factors, such as *Ebf-1*, *Dlx1/2*, *Lhx2,* and *Ngn2*, have also been implicated in the early growth of TCAs in the VTel (Garel et al., 2002; Lakhina et al., 2007; Seibt et al., 2003). Migrating cell populations in VTel also co-mingle with developing TCAs to regulated TC guidance. Islet1-positive GABAergic neurons migrate from the LGE to a region near the DTB where TCA axons first invade the VTel and function as guidepost cells in forming a permissive guidance "corridor" for pioneer TCAs (Bielle et al., 2011a; Lopez-Bendito et al., 2006). While collectively these various factors and mechanisms function within the VTel to properly guide TCAs, particularly along the rostrocaudal axis, more unidentified factors and cues likely function to complete the developmental trajectory of the entire TCA bundle array through the VTel. Notably, only a few axon guidance molecules function to maintain the dorsoventral aspect TCA topography, and most of these identified factors have broad effects on TCA guidance, leaving much to be elucidated on the level of individual and small populations of TCA fiber projections.

Corticothalamic Axons

Newborn neurons in the neocortex form numerous axonal connections with other cortical regions and subcortical targets (Auladell et al., 2000; McConnell, 1995). Corticothalamic axons (CTAs) target sensory relay nuclei of the thalamus to complete a reciprocal circuit with thalamocortical axons (TCAs) (discussed in the section above) that establishes the main axonal

pathway for sensory input and processing into the neocortex (Lopez-Bendito and Molnar, 2003). Numerous studies have focused exclusively on TCA development, and, in particular, ascending TCA topographic development toward neocortical target areas (Lopez-Bendito and Molnar, 2003; Price et al., 2006). As such, CTA guidance remains relatively uncharacterized even though the CTA axon pathway develops in similar, topographic manner toward stereotyped thalamic cell targets. In addition, CTA development has been hypothesized to be necessary for proper reciprocal TCA targeting within the cortex and within the VTel, where pioneer TCA fibers interact directly with CTAs near the internal capsule region (Molnar et al., 1998b; Molnar et al., 2012). As one example of this potential co-dependence, mutant mice that lack the transcription factor *Coup-tfl* also lack a cortical layer IV and proper subcortical pioneer axon projections as the result of early cortical progenitor subplate neuron differentiation errors and neuronal death, which together results in deficient TCA development in the cortex (Zhou et al., 1999). Similarly, disruption of cortex-specific transcription factor *Tbr1*, as well as the pan-expressed *Pax6* leads to aberrant CTA and TCA projections. Additionally, disruption the thalamic factors *Emx2, Dlx1/2,* and *Gbx2* result in misguided CTA projections in the VTel (Garel et al., 2002; Hevner et al., 2002; Lopez-Bendito et al., 2002). These combined results illustrate how CTA and TCA fiber projections require the establishment of the opposite, reciprocal pathway for their own proper development.

Functionally, CTAs form a feedback circuit onto sensory thalamic nuclei that is critical for complex information processing in the brain that underlies behavior (Alitto and Usrey, 2003; Temereanca and Simons, 2004). CTA projections, as the primary input onto relay nuclei, are generally denser and more abundant than reciprocal TCA fibers within the thalamus. For each cortical region innervated by TCA input, CTA projections from layer 6 of the cortical plate form

small feedback terminals onto these thalamic neurons, while layer 5 corticofugal axons (CFAs) project both into corticospinal tract (CST) and onto other thalamic nuclei to stimulate feed-forward circuits between distinct cortical regions (cortico-thalamo-cortical loops) (Bourassa and Deschenes, 1995; Bourassa et al., 1995; Rouiller and Welker, 2000). For example, in the rodent somatosensory system, thalamic input from the ventrobasal nucleus (VB) and nuclei of the posterior complex (PO) innervate the somatosensory cortex (S1). Layer 6 CTA reciprocal projections from the S1 innervate both of these nuclei in addition to sending collateral fibers to the reticular nucleus (RN) that also function within this circuit. S1 layer 5 CFA projections from this same region also send large terminal fibers to the PO as collaterals from the CST (Rouiller and Welker, 2000). CTA feedback on sensory relay nuclei has been hypothesized to regulate the sensory response to stimuli by enhancing sensory stimulation input and by modulating the activity state of thalamic sensory neurons. Proper reciprocal input onto the thalamus is thus essential for the sharpness and acuity of thalamic sensory fields (Alitto and Usrey, 2003).

In mice, descending CTA projections first pioneer into the VTel around age E13.5, one day after TCA development has begun (Auladell et al., 2000; Lopez-Bendito and Molnar, 2003). Though less studied, several axon guidance molecules, including netrin-1, Slit1/2, Sema3A/3C, and Sema5B, regulate CTA guidance within the VTel (Bagnard et al., 2001; Bagnard et al., 1998; Bagri et al., 2002; Lett et al., 2009; Metin et al., 1997). Netrin-1 acts as a chemoattractant for descending cortical projections into the early ganglionic structures of the subpallium (Metin et al., 1997), while Slit1/2 proteins are chemorepellants that regulate the guidance of both CTA and TCA fibers (Bagri et al., 2002). Analysis of the Robo receptors, which bind to Slit1/2, corroborate these findings, as CTAs in *Robo1*$^{-/-}$*Robo2*$^{-/-}$ mice aberrantly project past their internal capsule and thalamic targets and aberrantly cross over the telencephalic midline (Lopez-Bendito

et al., 2007). In the cortical plate, CTAs are preferentially attracted to Sema3C expressed in the subventricular zone and repelled by Sema3A at the ventricular zone, which is thought to initially guide CTA pioneer projections out of the cortical preplate (Bagnard et al., 2001; Bagnard et al., 1998). Finally, the transcription factors *Pax6, Nkx2,* and *Gbx2* also regulate the early development of these descending CTAs (reviewed in (Lopez-Bendito and Molnar, 2003)).

Both CFA and CTA fiber pathways, from cortical layers V and VI, respectively, grow into the IC before diverging, when CTAs turn dorsally into the thalamus and most CFAs continue into the ventral cerebral peduncle fiber bundle toward lower brain targets (O'Leary and Koester, 1993). Before reaching the IC, however, all descending cortical fiber bundles must develop in the same space as ascending TCA fibers, and these opposing pathways have been shown to cofasciculate with each other within the VTel (Molnar et al., 1998a). The "handshake hypothesis" was proposed to describe a mechanism for which the development of the opposing TCA and CTA fiber bundles, as well as the maintenance of their topographies, functionally relied on the development of the pioneer axon "tracks" established by the opposing pathway (Molnar et al., 1998a; Molnar and Blakemore, 1995; Molnar et al., 2012). The importance of the "handshake" is controversial (reviewed in (Molnar et al., 2012)); however, it is likely, at least, that descending cortical axons do require TCA axons "tracks" to properly develop into the internal capsule (Molnar et al., 1998a). Genetic models have been limited in their ability to directly test the handshake hypothesis and its implications on cortical and thalamic axon development.

Forebrain Commissures

The two hemispheres of the mammalian forebrain are highly interconnected through three major, interhemispheric white matter tracts: the corpus callosum (CC), the anterior commissure (AC), and the hippocampal commissure (HC). In mice, the CC is located in the dorsal telencephalon and is composed of axons from cortical layers II, III, and V. The CC tract serves as the major pathway for interhemispheric communication between dorsal and medial cortical subregions (Innocenti et al., 1995). The HC tract forms directly between the two hippocampi and just ventral the CC. Finally, the AC interhemispheric tract spans the ventral telencephalic midline beneath the CC and HC, and is composed of two distal axon bundles, the anterior branch (ACa) that originates from the olfactory bulbs and olfactory nuclei and the posterior branch (ACp) that is derived from cortical axons of the temporal neocortex and axons from the lateral nucleus of the amygdala. The proper interhemispheric development of the CC and AC tracts, in particular, is critical for higher functioning neural activity in postnatal brains (Raybaud and Girard, 2005; Richards et al., 2004). As my work on forebrain commissures (outlined in Chapter 4) focuses on Eph receptor forward signaling during CC and AC axon development, the formation of the HC will not be discussed here.

Corpus Callosum

The formation of the CC begins around embryonic age E15.5 (Ozaki and Wahlsten, 1992; Rash and Richards, 2001). Pioneer cortical axons from the cingulate cortex develop toward the dorsal midline, where the two dorsal hemispheres fuse together to enable pioneer callosal fibers to cross over. In addition to the CC axons that grow across the midline, cells located at the midline region also play an active and essential role during the development of the CC (Shu and Richards, 2001). First, the morphogenic fusion of the dorsal cortices is a function

of midline glia and neurons that form a "glial sling" across the two dorsal hemispheres that is evident as early as age E13.5 in mice (Katz et al., 1983; Shu et al., 2003a; Shu and Richards, 2001; Silver et al., 1982). Severing of this glial bridge leads to the failure of CC fibers to cross the midline and agenesis of the corpus callosum (AgCC) (Silver et al., 1982; Silver and Ogawa, 1983). Callosal axons also form essential axon:cell interactions with midline glia such that callosal axons are intimately associated with these cells, which is thought to enable the continuation of CC fiber development across the midline (Mendes et al., 2006).

A number of axon guidance molecules function during CC axon guidance, including netrin-1 Sema3A, Neuropilin-1, L1-CAM, Slit2, Wnt5a, and Fgfr1 (Kamiguchi et al., 1998; Keeble et al., 2006; Polleux et al., 1998; Richards et al., 2004; Shu et al., 2003a; Stein et al., 2001; Tole et al., 2006). The EphB receptors and the ephrinBs also have a well-characterized function during CC development, such that EphB1 and ephrinB3 knockout mutant mice have severe AgCC defects. *EphB2*$^{-/-}$ mutants, on the other hand, display a less severe, CC hypoplasia phenotype (Mendes et al., 2006). Furthermore, *EphB2*^{lacz} and *ephrinB3*^{lacz} truncated knockin mice, which are null for forward signaling and reverse signaling, respectively, displayed no AgCC phenotypes (Mendes et al., 2006), indicating that both forward and reverse signaling pathways are essential during CC axon pathfinding. Still, the precise roles and impact of EphB forward and ephrinBs reverse signaling on the different stages of CC development remain to be determined.

Anterior commissure

As mentioned above, the anterior branch of the AC (ACa) is formed from axon projections of the olfactory bulbs, olfactory nuclei and anterior piriform cortex, while the posterior ACp is derived from cells of the posterior piriform cortex, and other temporal cortices

of the basal telencephalon that converge together as the external capsule bundle that develops toward the anterior end of brain. The ACa and ACp converge at the ventral midline along with the stria terminalis axon bundle to form a single, large midline fascicle. Thus, axons growing along the external capsule must make a dramatic turn toward the midline at the appropriate rostral-caudal location (Bregma 3.4mm in mice) (Paxinos, 2007) to properly converge with the ACa at the midline and successfully innervate the contralateral hemisphere. This ACp axon turning event is a major axon guidance step that is highly regulated by a number of axon guidance molecules.

In mice, ACp pioneer projections first turn toward the midline around age E14 and are evident at the midline as early as E14.5 (Henkemeyer et al., 1996). Subsequent ACp axon projections develop along the pioneer ACp bundle via fasciculated growth to form the thick, postnatal white matter tract. Thus, the proper guidance of the initial pioneer ACp fibers as well as the proper fasciculation of subsequent axons is essential for proper ACp tract formation. Netrin-1, Sema3B/3F, Npn2, Nr-CAM, Tsukushi, Draxin, Fgfr1 and PlexinA4, as well as EphB2 and ephrinB2, are all necessary, in some manner, for ACp axon guidance and the completion of the ACp tract (Chen et al., 2000; Cowan et al., 2004; Falk et al., 2005; Giger et al., 2000; Henkemeyer et al., 1996; Ho et al., 2009; Hossain et al., 2013; Islam et al., 2009; Ito et al., 2010; Sahay et al., 2003; Serafini et al., 1996; Suto et al., 2005; Tole et al., 2006). For example, *Sema3B*$^{-/-}$ mutants display a significant ACp defasciculation phenotype (Falk et al., 2005), while the ACp is slightly displaced in *Fgfr1*$^{-/-}$ mutants (Tole et al., 2006). In Npn-2 and Tsukushi knockout mice, however, the ACp is completely missing (Giger et al., 2000; Ito et al., 2010). Finally, in EphB2 knockout mutants, truncated *EphB2*^{lacZ} and truncated ephrinB2lacZ mutants, the ACp is severely misprojected toward the brain floor or completely misformed and fails to

converge the ACa and cross the midline (Cowan et al., 2004; Henkemeyer et al., 1996; Ho et al., 2009), demonstrating that both EphB2 receptor forward signaling and ephrinB reverse signaling are necessary for proper ACp formation in some manner.

Goal of Thesis Research

For decades the EphB receptors have been studied throughout the mammlian CNS; however, the precise molecular mechanisms that function downstream of the EphBs represents a significant knowledge gap. Although these ubiquitous EphB receptors are expressed in many regions of mammalian brain and implicated in several axon guidance paths, most of these *in vivo* analyses have not fully considered the precise role of EphB forward signaling compared to non-autonomous effects during these critical developmental events. Thus, the goal of my thesis research is to: 1) elucidate novel EphB forward signaling pathways that are essential for EphB-mediated axon guidance processes *in vivo*, and 2) characterize, with a focus on EphB forward signaling pathways, the role of EphB receptor axon pathfinding during the development of major white matter axon tracts in the mammalian forebrain.

Chapter 1

Vav-GEFs Function as Essential Forward Signaling Molecules Downstream of the EphB1 Receptor during Ipsilateral Retinal Axon Repulsion

Summary

EphB receptors and their ligands, the ephrinBs, mediate the formation of numerous axon tracts in the mammalian brain, including the axonal projections from the retina to the thalamus (retinal nerve tract), in part through the activation of EphB-dependent forward signaling. However, the identity and regulation of critical EphB1 forward signaling molecules remains largely unknown. Here, we provide evidence that Vav2 and Vav3, which are members of the Rho-family of guanine nucleotide exchange factors (GEFs), function downstream of EphB1 receptors to facilitate the midline repulsion of ipsilateral retinal ganglion cell axons at the optic chiasm (OX) midline. Specifically, Vav2/3-deficient mutant mice show a dramatic reduction in the number of ipsilateral RGC axons that emerge from the OX, consistent with a deficit in midline repulsion. We also find that Vav2 coimmunoprecipitates with kinase-active EphB1 receptors, via SH2 domain-dependent interaction with phosphorylated EphB1 receptor juxtamembrane tyrosines. Moreover, EphB1 kinase activity can activate Vav2 GEF activity, consistent with Vav2, and likely Vav3, participating in active EphB1 forward signaling initiated upon binding to ephrinB2 at the embryonic OX midline. Finally, we use retinal explants from Vav2/3 knockout mutant embryos to confirm that Vav2 and Vav3 are essential for RGC axon repulsion in response to ephrinB2, which is the presented ligand for EphB1 at the OX midline.

Introduction

During the formation of the mammalian visual system, the growth and development of retinal ganglion cell (RGC) axons establishes the neural circuitry between the retina and visual centers of the brain that are essential for visual perception and processing. In mice, RGC are located in the ganglion cell layer of the retina and extend axons between the ages of E13 - E16 that then bundle together at the optic disc and exit the retina as the optic nerve bundle (Drager, 1985). Next, RGC axons navigate caudally through the ventral diencephalon toward the optic chiasm (OX), and then partially decussate at the OX midline to form ipsilateral and contralateral projects to the thalamus. Upon reaching the OX, the majority of mouse RGC pioneer axons cross the midline to innervate the contralateral hemisphere, while a smaller population derived from the ventrotemporal crescent (VTC) of the retina is instead repelled away from the midline to innervate the ipsilateral hemisphere (Godement et al., 1990; Godement et al., 1994). RGC axons continue along these contralateral and ipsilateral axon tracts before finally terminating onto the visual brain centers: the dorsal lateral geniculate nucleus (dLGN) of the thalamus and the superior colliculus (SC). Axonal divergence at the OX splits retinal input from each into different hemispheres, such that ipsilateral RGC axons and contralateral RGC axons from the opposite eye, which both share the same visual hemifield in mice, ultimately terminate together in the same hemispheric target zones. This partial decussation that is established at the OX is essential for stereopsis and biopic vision in binocular animals (see detailed reviews: (Petros et al., 2008; Williams et al., 2004)).

RGC axon guidance at OX midline and their precise synaptic targeting within the visual centers is also an important model system for the study of axon guidance events. This includes several retinogeniculate guidance events mediated by the Eph receptors and their transmembrane

ligands, the ephrins. Ephs comprise a large genes family of receptor tyrosine kinase that are separated into the EphA (A1-A8, A10) and EphB (B1-B4, B6) subclasses based on their binding capability to either the GPI (Glycophosphatidylinositol)-anchored ephrinAs or the ephrinBs, which contain a transmembrane protein subdomain (Pasquale, 2005). Upon Eph-ephrin interaction, clustered Eph receptors become autophosphorylated and activate signaling pathways through either their intracellular tyrosine kinase domain (kinase-dependent) or through other kinase-independent signaling interactions, such as the recruitment of signaling partners to critical phosphorylated tyrosine residues located at the juxtamembrane (JM) receptor domain (Egea and Klein, 2007). As clustered ephrins also regulate separate signaling pathways, components of the Eph-ephrin bidirectional signaling complex are separately referred to as Eph-mediated "forward" signaling or ephrin "reverse" signaling.

Eph receptors regulate numerous developmental processes within the CNS, including neural crest cell migration, axon guidance, and synapse formation (Reviewed in (Kullander and Klein, 2002; Pasquale, 2005). As axon guidance receptors, the Ephs typically function to induce growth cone repulsion and the subsequent axonal turning away from surface-expressed ephrins (Egea and Klein, 2007). During retinogeniculate axon targeting, the Ephs serve redundant functions to guide RGC axons to their visual center targets. EphAs and ephrinAs function in dual expression gradients to regulate the topographic patterning of synaptic terminals in the dLGN and SC (Feldheim et al., 2000; Feldheim et al., 1998; Frisen et al., 1998; Harada et al., 2007). In the developing mouse retina, RGC axons from the VTC exclusively express EphB1 and are specifically repelled at the OX midline onto the ipsilateral axon tract via a repulsive midline interaction between EphB1 expressed on ipsilateral RGC axons and ephrinB2 expressed on radial glia at midline (Nakagawa et al., 2000; Williams et al., 2003). This essential midline

role for EphB1 is dependent upon EphB1 forward signaling events, as ventrotemporal (VT) RGC axons fail to repel at the midline when the EphB1 intracellular regions, including all forward signaling regions, are missing (Chenaux and Henkemeyer, 2011; Petros et al., 2009). Notably, EphB2 is also expressed in the developing retina along a high ventral, low-dorsal gradient, while EphB3 is expressed throughout cells of the developing retina as well (Williams et al., 2003). EphB2, however, is not sufficient to effectively induce ipsilateral repulsion in RGC's at the OX like EphB1 (Petros et al., 2009). Additionally, ventronasal (VN) retinal explant axons, which express EphB2 but not EphB1, are less sensitive to ephrinB2 in culture (Petros et al., 2010; Williams et al., 2003). Thus, EphB1 forward signaling is the critical factor for ipsilateral OX repulsion. The potential role of EphB3 at the OX midline is undetermined.

In addition to the function of EphB1 forward signaling at the OX, EphB forward signaling is also essential for the development of major axon pathways in the developing mouse forebrain, including corticothalamic and thalamocortical axons, the anterior commissure and the corpus callosum (Henkemeyer et al., 1996; Mendes et al., 2006; Robichaux et al., 2013). Yet, fewer studies have focused on the role of downstream forward signaling genes that function during the development of these major pathways. Several studies have confirmed that Rho-GTPase molecules, including Rac1, RhoA and Cdc42, are essential for ephrin-mediated growth cone collapse in cultured primary neurons (Fournier et al., 2000; Jurney et al., 2002; Wahl et al., 2000). Furthermore, Ephexin-1, a guanine-nucleotide exchange factor (GEF), was shown to activate RhoA upon ephrinA stimulation of cultured neurons, (Sahin et al., 2005; Shamah et al., 2001). Conversely, α-chimaerin, a G-protein activating protein (GAP), turns off Rho-GTPase signaling downstream of EphA4 in hippocampal neurons (Iwasato et al., 2007). Two members of the Vav family of Dbl-GEFs, Vav2 and Vav3, which are highly expressed in the developing

CNS (Cowan et al., 2005; Movilla and Bustelo, 1999; Schuebel et al., 1998), are also necessary for RGC ipsilateral axon targeting to the dLGN *in vivo* (Cowan et al., 2005). Vav2 directly binds to the intracellular juxtamembrane (JM) region of both the EphA4 and EphB2 receptors can be transiently activated by ephrin stimulation. Finally, Vav2/3 GEFs are required for ephrinB induced growth cone collapse of cultured RGC neurons (Cowan et al., 2005). Still, the complete *in vivo* relevance and functionality of Vav-GEFs, as forward signaling genes, remain largely uncharacterized.

In this study, we define the role of Vav2 and Vav3 during retinogeniculate axon targeting by demonstrating that they are essential for RGC ipsilateral axon repulsion at the OX midline. We also characterize a strong molecular interaction between Vav2 and the EphB1 receptor, and show that Vav2/3 are required for ephrinB2-induced growth cone collapse of VT retinal explant axons. Together, our *in vivo* and culture results strongly suggest that Vav2/3 GEFs are dynamically-regulated by ephrinB2 and EphB1 and they redundantly function to mediate forward signaling functions required for *in vivo* pathfinding of ipsilateral RGC axon projections at the OX midline.

Results

EphB1 interacts with and activates Vav2

Since *Vav2$^{-/-}$3$^{-/-}$ DKO* mutants show reduced ipsilateral RGC axon terminals in the dLGN(Cowan et al., 2005), we hypothesized that Vav2/3 GEFs might be recruited to the ephrinB2 activated EphB1 receptors to mediate ipsilateral RGC axon repulsion at the OX midline. We previously demonstrated that Vav2 co-immunoprecipiates with both the EphA4 and EphB2 receptor, and binds to EphA4 in a kinase-dependent and juxtamembrane (JM) tyrosine

dependent fashion (Cowan et al., 2005). To determine whether EphB1 can bind and activate Vav2, we co-expressed these proteins in HEK293T cells and then immunoprecipitated (IPed) an epitope-tagged version of Vav2 (T7-Vav2), and found that HA-tagged EphB1 receptor co-IPed with Vav2 (n=8, Figure 1.1A). When Eph receptors are overexpressed in heterologous cells, they are typically found to be stably autophosphorylated (Holland et al., 1997; Holland et al., 1996; Shamah et al., 2001). Using a site-specific phospho-antibody to Eph receptor juxtamembrane tyrosines (Y594 and Y600 in EphB1), we observed strong autophosphorylation as expected. To test whether activated EphB1 could activate the associated Vav2, we co-expressed them and analyzed Vav2 phosphorylation at the conserved Y172 site in the Vav regulatory acidic domain (Cowan et al., 2005). While there was undetectable levels of P-Vav2 signal when Vav2 was expressed alone in the cells, we observed a robust increase in P-Y172 levels when Vav2 was co-expressed with EphB1 (Figure 1.1A). In addition, Vav2 failed to interact with an EphB1 K651R kinase-dead point mutant (n=2, Figure 1.1A), demonstrating that EphB1 kinase activity was required for its interaction with Vav2. Similarly, co-expression of EphB1 K651R did not increase Vav2 P-Y172 levels, indicating that EphB1 kinase activity is required for Vav2 phosphorylation and suggesting that Vav2 specifically interacts with the kinase activated form of EphB1.

Next, since we previously demonstrated that Vav2 interacts with the EphA4 receptor at JM tyrosine residues on the receptor (Cowan et al., 2005), we tested if the Vav2-EphB1 interaction required the autophosphorylation of the conserved JM residues of EphB1 (Y594 and Y600). To this end, we performed a co-IP of Vav2 with either WT, EphB1 Y594F/Y600F (a mutant that cannot be phosphorylated at these residues) or EphB1 Y594E/Y600E (a phosphomimetic mutant that enables EphB1 kinase activity, but does not allow for binding of

SH2 (Src homology 2-adaptor binding partners). Vav proteins contain C termianl SH2 adaptor domains, which are well known to bind to phosphotyrosine motifs, and in addition, the Vav SH2 domain is known to mediate binding to other tyrosine phosphorylated receptors (reviewed in (Bustelo, 2001)). As such, \neither EphB1 mutant coimmunoprecipitated with Vav2 (Figure 1.1B & Figure 1.2), as expected, indicating that the Vav2-EphB1 interaction requires the presence of the JM EphB1 phosphotyrosines for binding. Interestingly, we found that Vav2 was still partially phosphorylated at Y-172 when co-expressed with these JM mutants (Figure 1.1B), suggesting that Vav2 activation downstream of EphB1 is not entirely dependent upon high-affinity binding to the JM P-tyrosine, and might be indirectly activated via another EphB1 forward signaling modality.

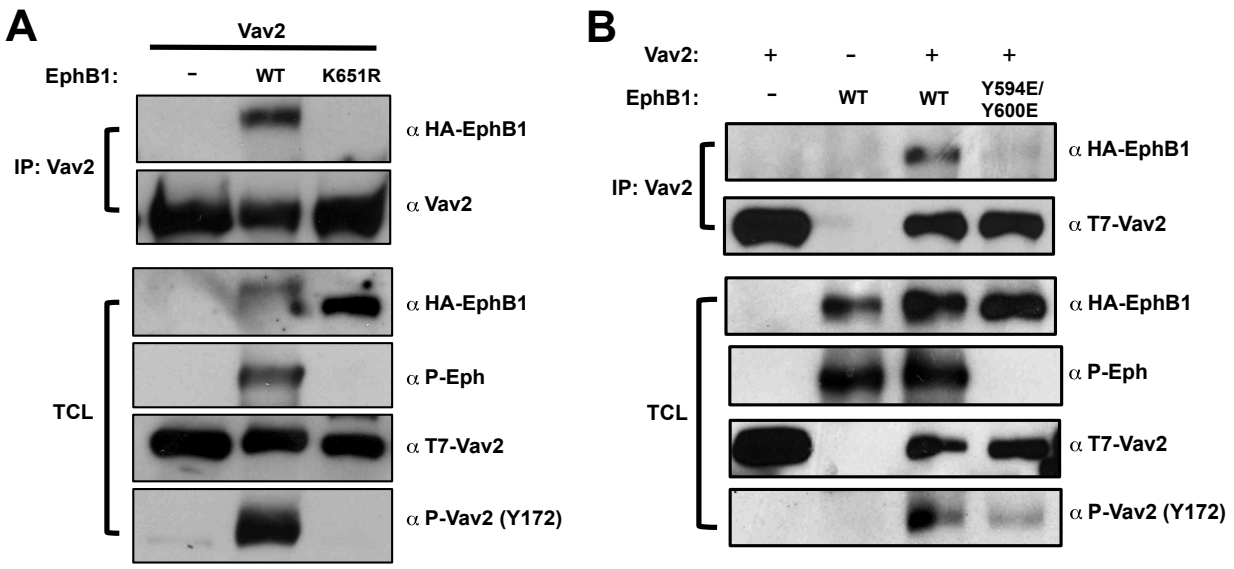

Figure 1.1. Vav2 interacts with the EphB1 receptor in mammalian cells. *(A)* Coimmunoprecipitation immunoblot results of Vav2 coexpressed with either WT EphB1 or EphB1 K651R in HEK293T cells. Cells were transfected with T7-tagged Vav2 and either HA-tagged EphB1 or EphB1 K651R. *(B)* Coimmunoprecipitation of Vav2 coexpressed with WT EphB1 and EphB1 Y594E/Y600E. Cells were transfected with T7-Vav2 alone or with HA-EphB1, HA-EphB1 Y594E/Y600E, or HA-EphB1 alone. All lysates were pulled down with T7-agarose. Total cell lysates and IP lysates (20μg) were immunoblotted with anti-HA, anti-T7, anti-Vav2, anti-P-Eph and anti-P-Vav2 (Y172) antibodies.

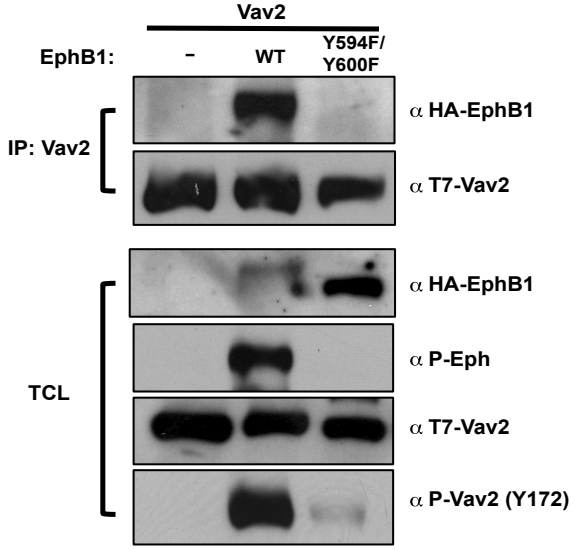

Figure 1.2. The JM region of EphB1 is required for Vav2 binding. Coimmunoprecipitation of Vav2 with WT EphB1 and EphB1 Y594F/Y600F. Cells were transfected with T7-Vav2 alone or coexpressed with HA-EphB1 or HA-EphB1 Y594F/Y600F. All lysates were pulled down with T7-agarose. Total lysates and IP lysates (20μg) were immunoblotted with anti-HA, anti-T7, anti-Vav2, anit-P-Eph and anti-P-Vav2 (Y172) antibodies.

Since Vav2 did not interact with either the EphB1 Y594E/Y600E or EphB2 Y594F/Y600G mutant, se next hypothesized that Vav2-EphB1 binding likely involves Vav2's Src-homology 2 (SH2) domain. To test this idea, we performed a co-IP of full-length WT EphB1 and a Vav2 ΔSH2 mutant. As expected, Vav2 ΔSH2 failed to interact with the full-length EphB1 receptor yet was still phosphorylated at Y172 when co-expressed with EphB1 (Figure 1.3A). Together, these results show that Vav2 forms a strong, kinase-dependent molecular interaction with the JM phosphotyrosine residues of EphB1 through its SH2 domain and is subsequently phosphorylated in an EphB1 kinase-dependent manner.

Vav2 interacts with EphB1 and EphB2

Ipsilateral RGC axons derived from the VT retina are the only retinal axons to express EphB1 in the developing retina at embryonic timepoints that correspond to RGC axon repulsion at the OX midline (~E14.5-E15.5) (Williams et al., 2003). EphB2 is also expressed in the ventral half of the retina, including the VTC, at these same timepoints (Williams et al., 2003) and previous studies have confirmed that both EphB1 and EphB2 are both expressed at the surface of RGC axons from VT explants (Chenaux and Henkemeyer, 2011; Petros et al., 2009). Despite this, the intracellular region of EphB1 is the critical determining factor for ipsilateral repulsion at the OX (Chenaux and Henkemeyer, 2011; Petros et al., 2009). Thus, we considered the possibility that EphB1 might preferentially bind and activate Vav2, whereas EphB2 might have a reduced ability to active Vav2 GEFs. To test this idea, we co-expressed full-length Vav2 with either HA-EphB1 or HA-EphB2 and analyzed Vav2-EphB binding and Vav2 P-Y172. Interestingly, we observed a similar affinity between Vav2 and EphB1 or EphB2, as well as similar levels of Vav2 P-Y172 induction (n=2, Figure 1.3B), suggesting that, at least in

heterologous cells, EphB1 does not preferentially recruit or activate Vav2 to account for EphB1-specific aspects of RGC ipsilateral axon guidance.

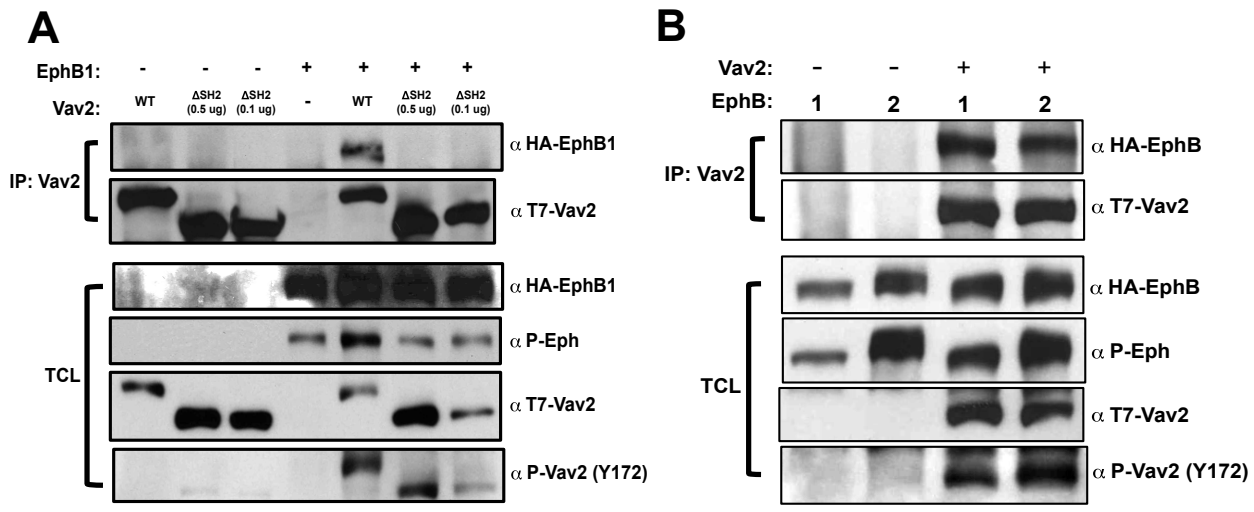

Figure 1.3. Vav2 forms a non-preferential interaction with both EphB1 and EphB2. *(A)* Coimmunoprecipitation results from Vav2 and Vav2 ΔSH2 coexpressed with EphB1 in HEK293T cells. Cells were transfected with T7-tagged WT Vav2 or either 0.5μg or 0.1μg of T7-Vav2 ΔSH2 and/or HA-tagged EphB1. *(B)* Coimmunoprecipitation of Vav2 with either EphB1 or EphB2 in HEK293T cells. Cells were transfected with HA-EphB1 and EphB2 and/or T7-Vav2. All lysates were pulled down with T7-agarose. Total lysates and IP lysates (20μg) were immunoblotted with anti-HA, anti-T7, anti-Vav2, anti-P-Eph and anti-P-Vav2 (Y172) antibodies.

Vav GEFs are required for the ipsilateral repulsion of RGC axons at the optic chiasm

Previously, we linked the VAV family GEFs, Vav2 and Vav3, to EphB receptor axon repulsion in cultured cell preparations, and demonstrated *in vivo* that Vav2 and Vav3 were required for retinogeniculate targeting to the dLGN, as *Vav2*$^{-/-}$*Vav3*$^{-/-}$ knockout mutants displayed a significant reduction in ipsilateral dLGN terminal staining (Cowan et al., 2005). Ipsilateral RGC axons are specifically repelled from the OX midline though an EphB1/ephrinB2 interaction, such that EphB1-expressing RGC axons from the vetnrotemporal crescent (VTC) of the retina are directed to innervate ipsilateral visual centers, including the ipsilateral dLGN (Godement et al., 1990; Godement et al., 1994). Thus, based on our previous findings, we hypothesize that Vav2/3 function as forward signaling molecules downstream of EphB1 within ipsilateral RGC axon projections at the optic OX.

To test this, we first performed unilateral, intraocular DiI labeling of RGC axons in wild-type (WT) and *Vav2*$^{-/-}$*Vav3*$^{-/-}$ double knockout (DKO) mouse embryos at E16.5 (n=8, n=10, respectively) (Figure 1.4A). E16.5 represents a suitable timepoint in mice when most RGC axons have already crossed the OX (Godement et al., 1990). After a two-week labeling period, serial coronal sections of these embryo heads were obtained for imaging of RGC axons past the OX (Figure 1.4B & 1.4C). Fluorescence intensity measurements were obtained for both the contralateral and ipsilateral axon tracts from both conditions. Although contralateral intensity is equal and consistent in both WT and DKO conditions, the DiI-labeled ipsilateral tract in DKO mutants is morphologically smaller in fluorescent images (Figure 1.4D) and significantly less intense compared to WT, representing a 40% reduction in total fluorescence intensity compared to WT (Figure 1.4E). The ipsilateral/contralateral intensity ratio is also significantly smaller in DKOs compared to WT embryos, confirming that the contralateral tract intensity is relatively

consistent and unchanged between conditions (Figure 1.4F). Thus, Vav2/3 are essential for complete ipsilateral RGC axon repulsion at the OX midline.

Although both Vav2 and Vav3 are expressed in the embryonic and adult mouse retina (Cowan et al., 2005; Fujikawa et al., 2010) and have a homologous protein structure (Movilla and Bustelo, 1999; Schuebel et al., 1998), we sought to test whether these genes perform separate or redundant functions during retinogeniculate axon guidance. We thus performed dual anterograde optic tracing of RGC axon projections to the dLGN terminals in WT, *Vav2*$^{-/-}$ and *Vav3*$^{-/-}$ single knockout mice. Dual tracing labels the larger region of contralateral RGC terminals in dLGN with one dye (Alexa 488, Green) that surrounds a smaller, central patch of ipsilateral RGC axon projections (Alexa 555, Red) in WT brains (Figure 1.5A). Interestingly, we observed no difference in the fluorescent intensity of ipsilateral axon projections at the dLGN in either Vav single mutant condition compared to WT (WT n=8, *Vav2*$^{-/-}$ n=9, *Vav3*$^{-/-}$ n=5) (Figure 1.5B-1.5D). Therefore, Vav2 and Vav3 appear to function redundantly at the optic chiasm midline to thus compensate for the missing gene in single knockout mutants. We did, however, observe an atypical and expanded zone of ipsilateral RGC staining in both *Vav2*$^{-/-}$ and *Vav3*$^{-/-}$ mice, which was more prominent in *Vav3*$^{-/-}$ mutants (see arrows in Figure 1.5C). Although the ipsilateral pattern was not as divergent as we previously reported for *Vav2*$^{-/-}$*Vav3*$^{-/-}$ double mutants (Cowan et al., 2005), this finding supports a potential role for Vav2/3 in the topographical patterning of ipsilateral axon projection terminals at the dLGN.

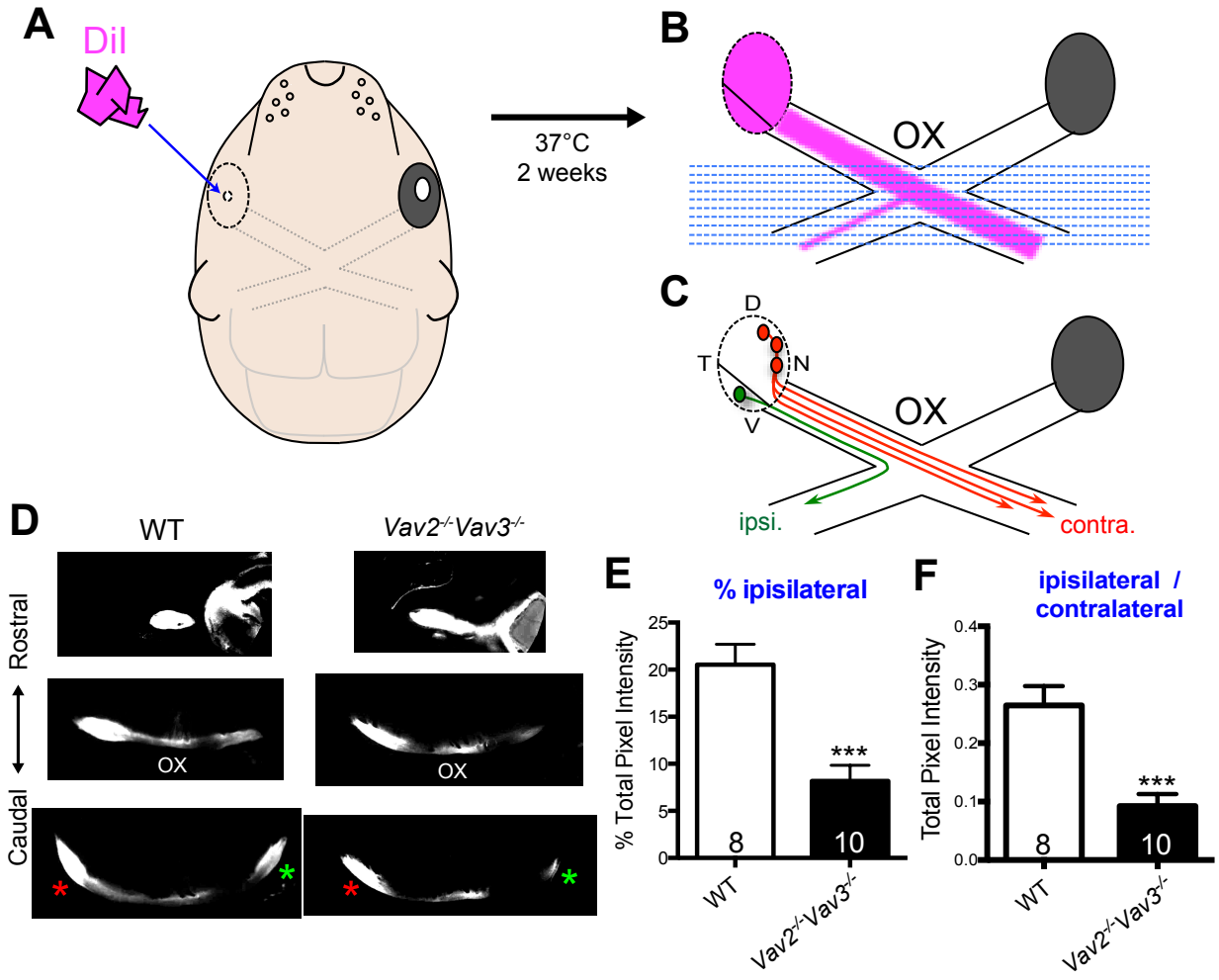

Figure 1.4. Vav2/3 are required for ipsilateral RGC axon turning at the OX midline. *(A)* Diagram of unilateral DiI tracing in fixed E16.5 mouse embryo heads. A large DiI crystal is placed directly onto the optic disc at the back of the retina. *(B)* Diagram of the retinae, optic nerve and optic chiasm midline of DiI-labeled embryos indicating the OX region in the ventral diencephalon that is serially sectioned along the coronal plane. *(C)* Similar diagram of the OX midline with example contralateral RGC axons (red) from the dorsal and nasal regions of the retina and an example ipsilateral RGC axon from the VTC. *(D)* Fluorescent images of labeled WT and *Vav2*$^{-/-}$*Vav3*$^{-/-}$ mutant embryos after 2 weeks of unilateral DiI tracing. Shown are representative coronal sections through the optic nerve, OX midline, and a region past the OX

containing clear and distinct contralateral (red asterisk) and ipsilateral (green) axon tracts. *(E)* Data graph comparing the % ipsilateral tract DiI intensity between WT and *Vav2*$^{-/-}$*Vav3*$^{-/-}$ embryos. *(F)* Data graph comparing the ipsilateral / contralateral DiI intensity ratio between WT and *Vav2*$^{-/-}$*Vav3*$^{-/-}$ embryos. (*** $p<0.001$, Students t-test).

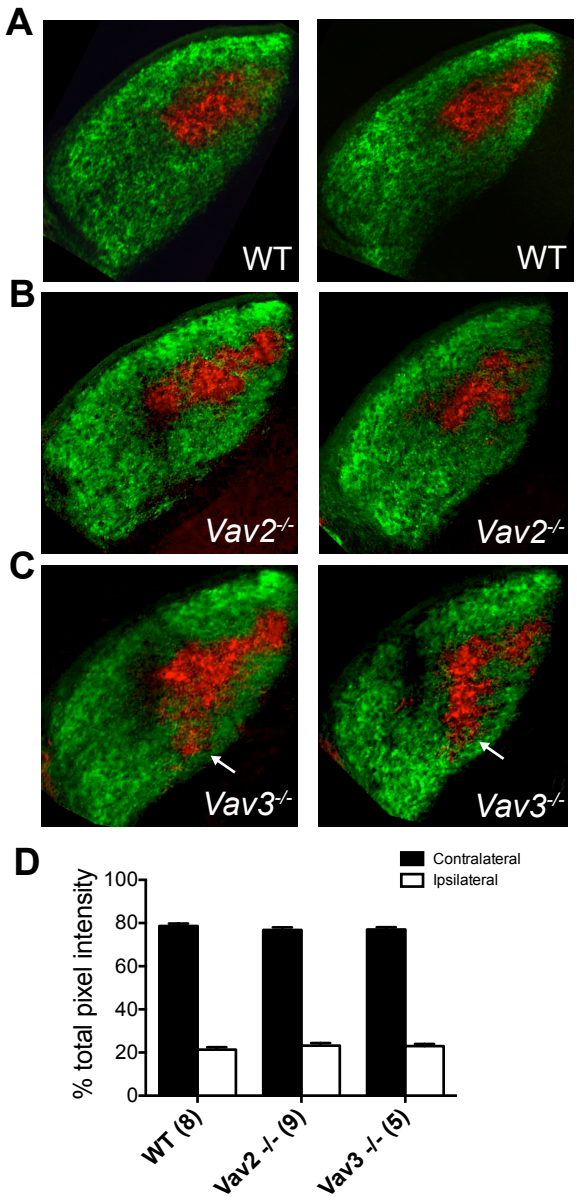

Figure 1.5. Ipsilateral retinogeniculate dLGN axon terminals are not diminished in *Vav2*$^{-/-}$ and *Vav3*$^{-/-}$ mutants. Two examples of anterograde contralateral (green) and ipsilateral (red) axon projections in the dLGN of *(A)* WT, *(B) Vav2*$^{-/-}$ and *(C) Vav3*$^{-/-}$ mutants. Arrows indicate the expanded ipsilateral zones in *Vav3*$^{-/-}$ dLGN examples. *(D)* Data graph of terminal staining intensity measurements (% of total axon projections) of contralateral (black bars) and ipsilateral projections (white bars) in the dLGN for each genotype. (n-values in parenthesis).

EphrinB2 repulsion of RGC axons requires Vav2 and Vav3

Previously, we demonstrated that Vav2/3 are required for ephrinA1-induced growth cone collapse (GCC) in cultured RGC neurons, and that Vav2 is dynamically activated upon ephrinA1 and ephrinB1 stimulation of primary cortical neurons (Cowan et al., 2005). These results established Vav2/3 as forward signaling factors downstream of activated Eph receptors; however, the function of Vav2/3 has not been shown in the context of ipsilateral axons at OX midline that encounter ephrinB2. In cultured retinal explants, long-term ephrinB2 application inhibits neurite outgrowth from VT retinal explants (Williams et al., 2003), and exogenous stimulation of artificially clustered ephrinB2/Fc induces a higher rate of growth cone collapse in VT retinal explants compared to DT control explants (Petros et al., 2010). As such, we hypothesized that Vav2/3, which, based on our results, are forward signaling factors downstream of EphB1, are necessary for ephrinB2-induced growth cone collapse of VT explant axons.

To test this hypothesis, we cultured retinal explants from WT, $Vav2^{+/-}Vav3^{+/-}$ double heterozygous, and $Vav2^{-/-}Vav3^{-/-}$ double homozygous E14.5 embryos as described previously (Erskine et al., 2000) with slight modification. We initially stimulated explants with a low level of ephrinB2 (0.3 μg/ml) to identify a concentration of the repulsive ligand that would stimulate growth cone collapse (GCC) of VT explants, but would not stimulate collapse of DT explants. However, at this concentration, neither DT nor VT explant axons significantly collapsed following the addition of clustered ephrinB2/Fc (Figure 1.6). Therefore, we next stimulated WT explant axons with a higher concentration - 1.0 ug/ml - of clustered ephrinB2/Fc, which elicited strong GCC from both DT and VT explant axons (~80%) (Figure 1.7E, 1.8A & 1.8B). We then simulated Vav2/3 knockout mutant explants with the same 1.0 μg/ml concentration of clustered ephrinB2/Fc to test if Vav2 and Vav3 are required for ephrinB2 stimulated collapse. Using these

conditions, we observed decreased GCC in VT explants from both *Vav2*$^{+/-}$*Vav3*$^{+/-}$ and *Vav2*$^{-/-}$ *Vav3*$^{-/-}$ mutants in response to clustered ephrinB2/Fc compared to Fc control stimulation (Figure 1.7). In addition, we also observe a general reduction in GCC rates from expalnts of various other Vav2/3 mutant genotypes tested (Figure 1.8A & 1.8B). Together, these results demonstrate that Vav2/3 are necessary, to some degree, for ephrinB2 induced growth cone collapse in EphB1-expressing VT RGC axons. Next, to assess the rates of RGC axonal outgrowth from these culture explants, we measured in the number of explant axons per explant in addition to axon length (measured in μm) in both control and ephrinB2/Fc stimulation conditions. In VT explants we found no changes in axon number or outgrowth in either condition (Figure 1.8D & 1.8F); however, in DT explants we did observe an overall reduction in both axon number and outgrowth from most Vav2/3 mutant genotypes compared to WT controls in either stimulation condition (Figure 1.8C & 1.8E). Thus, based on these analyses, Vav2/3, in addition to functioning during GCC in response to ephrinB2 stimulation, are required for the basal outgrowth of DT RGC axons but not VT RGC axons.

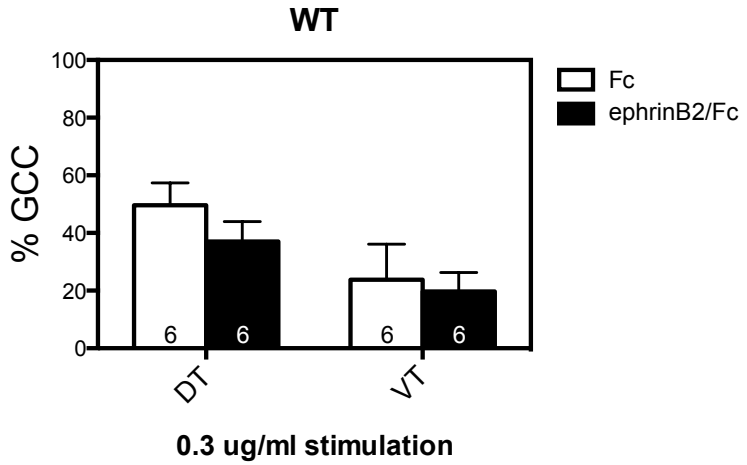

Figure 1.6. Retinal explant axons are not sensitive to low levels of ephrinB2. GCC analysis of WT retinal explants from either the DTC or VTC that are stimulated with either clustered Fc alone (white bars) or clustered ephrinB2/Fc (black bars) at 0.3 μg/ml. Data represented as %GCC.

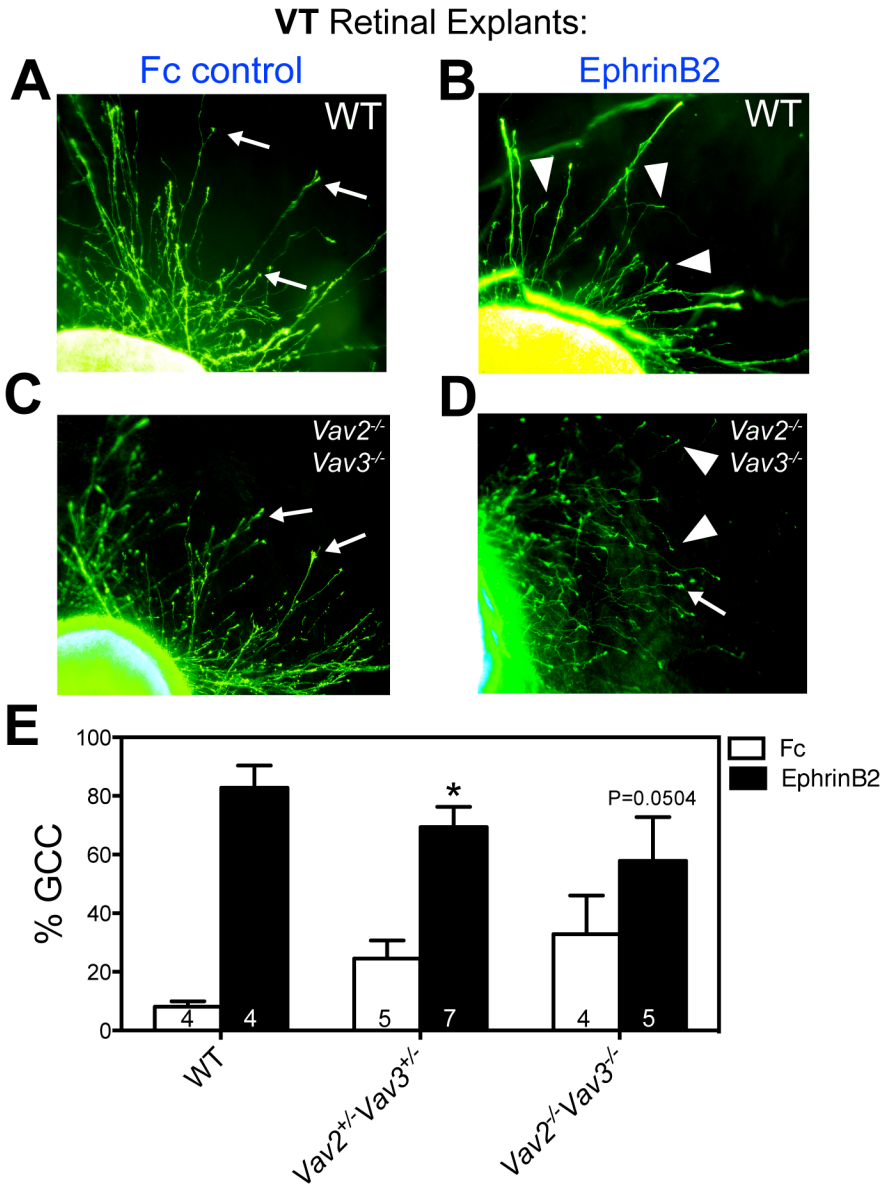

Figure 1.7. RGC axons from VT retinal explants require Vav2/3 for ephrinB2 induced growth cone collapse. Phalloidin-green stained ventrotemporal (VT) retinal explants from WT E14.5 embryos stimulated with either *(A)* clustered Fc alone or *(B)* clustered ephrinB2/Fc (at 1.0 µg/ml). VT retinal explant examples from *Vav2*$^{-/-}$*Vav3*$^{-/-}$ stimulated with either 1.0 µg/ml of *(C)* clustered Fc alone or *(D)* clustered ephrinB2/FC. Uncollapsed growth cones (arrows), and instances of growth cone collapse (GCC) (arrowheads) are indicated. *(E)* Data graph of GCC analysis from WT, *Vav2*$^{+/-}$*Vav3*$^{+/-}$ double heterozygous or *Vav2*$^{-/-}$*Vav3*$^{-/-}$ double knockout VT

explants. Explants were stimulated with either clustered Fc alone (white bars) or clustered ephrinB2/Fc (black bars) (1.0 μg/ml). Data are represented as %GCC and mutant conditions were analyzed for statistical significance against WT controls using Two-way ANOVA (*P<0.05).

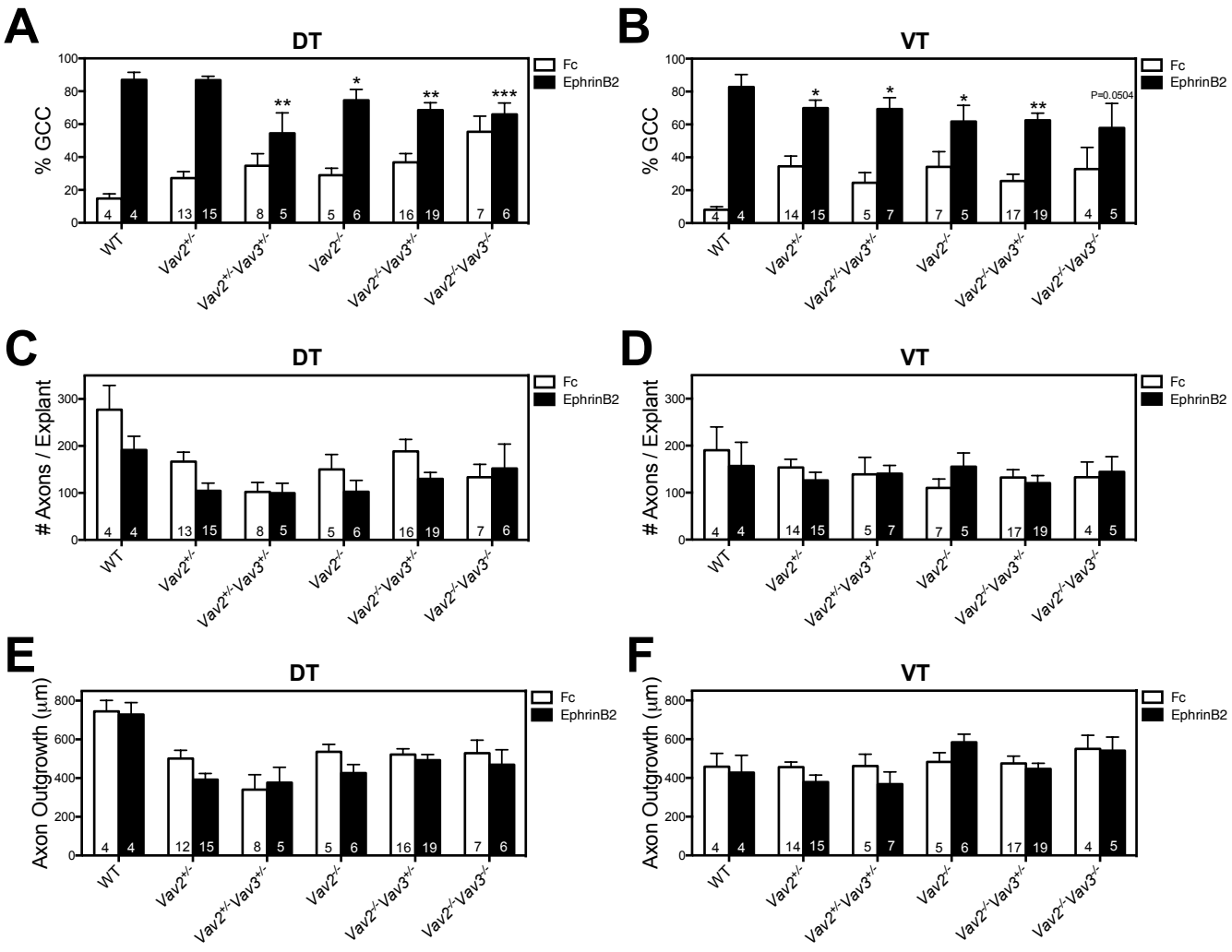

Figure 1.8. Summary of morphological axon analyses from Vav2/3 mutant retinal explants. Summary of data compiled from retinal explants experiments (DT and VT) for WT, *Vav2*$^{+/-}$, *Vav2*$^{+/-}$*Vav3*$^{+/-}$, *Vav2*$^{-/-}$, *Vav2*$^{-/-}$*Vav3*$^{-/-}$ and *Vav2*$^{-/-}$*Vav3*$^{-/-}$ mutant genotypes stimulated with either clustered Fc alone (white bars) or clustered ephrinB2/Fc (black bars) at 1.0 μg/ml. The following morphological data are presented: *(A)* GCC, *(B)* axon number/explant, and *(C)* axon outgrowth that are represented as %GCC, #Axons/Explant or Axon ougrowth (μm), respectively. Data were analyzed for statistical significance against WT controls using Two-way ANOVA (*P<0.05, **P<0.01, ***P<0.001).

Discussion

In this study we demonstrate that Vav2 and Vav3 GEFs are essential for the axon repulsion of ipsilateral RGC axons at the OX midline during embryonic development. We used a series of molecular binding assays in culture to demonstrate that 1) Vav2/3 forms a strong molecular interaction with EphB1 at critical juxtamembrane phosphotyrosine residues, and 2) Vav2 GEF function is activated by EphB1 kinase activity. Finally, we use cultured retinal explants from Vav2/3 knockout mice to confirm that Vav2/3 are necessary for ephrinB2 induced growth cone collapse of axons from the VT retina. Together, these findings are consistent with our hypothesis that Vav2/3 GEFs are critical forward signaling molecules downstream of the EphB1 receptor in ipsilateral RGC axons *in vivo*.

Although we previously reported a novel role for Vav2/3 at the OX midline during retinogeniculate axon targeting, our DiI tracing analysis of *Vav2/3 DKOs* confirms its function at the OX midline as Vav2/3 mutant pups have a significantly reduced ipsilateral tract as the RGC axons decussate at the OX at E15.5. The magnitude of the reduced ipsilateral axons in Vav2/3 DKO mice is similar to the reduced Ipsilateral RGC axons in the dLGN target field previously observed (Cowan et al., 2005), and to the reduction observed in *EphB1*$^{-/-}$ and EphB1 truncated mutant mice that lack forward signaling (Chenaux and Henkemeyer, 2011; Williams et al., 2003). Using the DiI labeling method, we observed a ~40% reduction in ipsilateral axons in the *Vav2/3 DKOs* compared to WT, whereas we previously observed a slightly more robust, 55% decrease in ipsilateral dLGN axon terminal staining in these same mutants (Cowan et al., 2005). Furthermore, ipsilateral DiI intensity in *EphB1*$^{-/-}$ and *EphB1*$^{-/-}$*EphB2*$^{-/-}$*EphB3*$^{-/-}$ mutant mice were measured at a 43% and 56% reduction, respectively, compared to WT mice (Williams et al., 2003). Chenaux et al (2011), on the other hand, reported a near complete loss of ipsilateral

terminal staining in the dLGN of *EphB1*$^{T\text{-}lacZ}$ truncated mutants (a 90% reduction compared to WT).

These differences in ipsilateral measurements between genotypes may be explained in a number of ways besides the various technical differences between preparations. First, although previous studies have demonstrated a clear and dominant role for EphB1 at the OX midline, EphB2 has been proposed to account for a minor number of ipsilateral deflections from the OX (Chenaux and Henkemeyer, 2011; Petros et al., 2009). Thus, EphB2, and possibly EphB3, mediated ipsilateral repulsion could account for the difference in ipsilateral axons measured between *EphB1*$^{-/-}$ and *EphB1/2/3* triple knockouts. Considering that our results from *Vav2/3 DKOs* better match the ipsilateral reduction in EphB1 single KOs, Vav2/3 likely functions specifically downstream of EphB1 *in vivo* despite our interaction studies reported here, which show no preference for the interaction of Vav2 with either EphB1 and EphB2. Second, Vav2/3 DKOs and *EphB1*$^{T\text{-}lacZ}$ truncated mutants may also have dLGN terminal defects that lead to axonal pruning and retraction that might explain the more robust ipsilateral reduction recorded at the dLGN in these studies. Indeed, Vav2/3 DKOs display an abnormal targeting defect in dLGN, which further suggests that these mutant RGC fibers undergo terminal pruning (Cowan et al., 2005). Also, EphB1 was recently shown be required for RGC terminal refinement in the dLGN, although this specific function for EphB1 has not been fully characterized (Rebsam et al., 2009). Finally, it remains possible, if not likely, that there are additional signaling molecules that can compensate for Vav2/3 in the process of EphB1-mediated axonal repulsion. For example, Nck-family adaptor proteins can bind to ephrin-activated EphB receptors and recruit additional signaling proteins that might facilitate F-actin remodeling in axon growth cones.

In addition to ephrinB2, RGC axons encounter several other axon guidance forces at the OX midline, including Slit1-3, Semaphorin6D, and Nr-CAM (Erskine et al., 2000; Kuwajima et al., 2012; Williams et al., 2006; Williams et al., 2004). As such, it remains possible that the loss of Vav2/3 in our knockout mutants also disrupts the signal transduction pathways downstream of these other midline guidance factors, which could directly affect RGC axon guidance at the OX. Our complete knockout of Vav2/3 DKO mutant mice may also disrupt radial glia morphology at the OX, which could subsequently have a dramatic effect on ephrinB2 expression and the midline repulsion RGC axons. In addition to axon guidance, proper fasciculation is also critical for RGC axon guidance at the OX, as Neuropilin 1 mutants have a clear mutant defasciculation defect at the OX (Erskine et al., 2011). Therefore, Vav2/3 may also be necessary for either the effective defasciculation of VT RGC at the midline from the contralateral optic nerve bundle or in the proper fasciculation of these same axons onto the ipsilateral optic nerve tract past the midline. In either scenario Vav2/3 DKO mutant axons may become stalled at the OX midline and fail to either cross over or be repelled, which would also account for the decreased ipsilateral optic tract in these mutants. Based on our results, however, it is most likely that Vav2/3 GEFs function directly downstream of EphB1 in ipsilateral RGC axons such that in their absence, a significant portion of VT RGCs fail to repel from the OX midline due to ineffective EphB1 forward signaling and instead aberrantly project along the contralateral optic tract. In the future, more targeted approaches will be necessary in the future to 1) identify the fate of ipsilateral RGC axons at the OX midline in Vav2/3 DKO mutants, and 2) specifically label individual VT RGC axons with high acuity to observe their behavior at the midline on the single fiber level in the absence of either EphB1 or Vav2/3.

Using culture-based binding assays, we also demonstrate that Vav2 strongly interacts with EphB1 at the JM tyrosine residues 594 and 600, and that EphB1 phosphorylates Vav2 at the Y-172 residue in a kinase-dependent manner. Additionally, we find Vav2 does not preferentially interact with either EphB1 or EphB2, indicating that Vav2 is not intrinsically recruited to EphB1 instead of EphB2. Petros et al (2009), however identified that the intracellular domain of EphB1 as the critical signaling region responsible for ipsilateral RGC axon repulsion *in vivo*. Therefore, it is likely that other forward signaling events function to specifically recruit Vav2/3 to the EphB1 JM domain to carry out forward signaling in ipsilateral axons. One potential signaling partner for Vav2/3 are the Src kinases, which are known to form complexes with Vav-GEFs, and are recruited downstream of EphB2 (Zisch et al., 1998). In the future, a comparative assay of EphB1 and EphB2 forward signaling partners will be extremely useful in determining the essential signaling molecules that are preferentially recruited by EphB1.

Although Vav-GEFs target other downstream signaling molecules, including CD co-receptors and Grb2 (reviewed in (Bustelo, 2001)), small Rho-GTPases are the likely effectors of Vav2/3 in VT RGC axons upon their recruitment and activation by EphB1. Small Rho-GTPases, which are divided into the three subgroups, Rac1, RhoA, and Cdc42, have an abundant and varied effect on growth cone dynamics during axon guidance (reviewed in (Bashaw and Klein, 2010)). RhoA, specifically, is activated downstream of EphA/B and PlexinB receptors in response to repulsive ephrin and semaphorin cues. RhoA-GTP then activates its downstream effector ROCK (Rho-kinase) to modulate the local F-actin cytoskeleton in the growth cone (Dickson, 2001; Schmandke and Strittmatter, 2007; Wahl et al., 2000). Ephexin-1, another DH-family GEF, functions downstream of the EphAs to activate Rac, Cdc and Rho GTPases, but switches to a strong RhoA activator in response to ephrinA stimulation (Sahin et al., 2005).

Vav2 is also capable of activating all three small Rho-GTPases (Abe et al., 2000; Kawakatsu et al., 2005; Liu and Burridge, 2000; Schuebel et al., 1998), and thus, if Vav2/3 are critical forward signaling factors downstream of EphB1 at the OX midline, it is logical to predict that Vav2/3 may act like ephexin1 and also become a strong RhoA activator when recruited to EphB1 to carry out growth cone repulsion in RGC ipsilateral axons. On the other hand, we previously showed that Vav2/3 were essential for Eph-ephrin transendocytosis in cultured RGC neurons, which is a Rac1-dependent mechanism (Cowan et al., 2005; Marston et al., 2003). Receptor-ligand transendocytsis is potentially a critical step for Eph receptor mediated growth cone repulsion, as the internalization of the Eph-ephrin complex breaks the adhesive cell-cell contact point of receptor-ligand binding. If Rac-dependent transendocytosis were disrupted in Vav2/3 DKO mutants, we hypothesize that VT RGC axons would stall at the OX midline, as the Eph-ephrin interaction would not be severed.

We also demonstrate in this study that *Vav2/3 DKO* VT retinal explant axons are less sensitive to 1.0 μg/ml of clustered ephrinB2 compared to WT control explants (Figure 1.7E), which establishes a role for Vav2/3 for axon repulsion downstream of EphB1 in this VT axonal population. Petros et al (2010) previously reported a significant growth cone collapse (GCC) response in both VT and DT retinal explants upon 0.5 μg/ml clustered ephrinB2 stimulation. Therefore, it is not surprising that we also observe significant GCC in DT explants stimulated with a higher concentration (1.0 μg/ml) of ephrinB2 (Figure 1.8A). Interestingly, we also find that DT explant axons from Vav2/3 mutants have a higher basal level of GCC in addition to an overall reduction in basal axonal outgrowth (Figure 1.8A & 1.8E). Together, these retinal explant results demonstrate that in VT explants, Vav2/3 appear to function specifically downstream of EphB1 for axonal repulsion, whereas in DT explants, Vav2/3 function in general

axon outgrowth and maintenance, potentially downstream of EphB2. This role for Vav2/3 in DT explant axon outgrowth is consistent with previous findings, which established that Vav was required for midline axon crossing during Drosophila embryogenesis (Malartre et al., 2010) and that Vav2 was necessary for neurite extension from *Xenopus* spinal neurons (Moon and Gomez, 2010).

Although the specific function of Vav2/3 GEFs at the OX midline remains to be elucidated, our findings define an essential forward signaling role for these proteins downstream of EphB1 in ipsilateral RGC axon projections in response to ephrinB2. More targeted approaches, such as the generation of conditional EphB1 receptor and Vav2/3 knockout mice will be needed to fully elucidate the signaling mechanisms of these molecules at the OX midline. However, based on our results, we promote Vav2/3 as one of the few axon guidance signaling effector molecules that link guidance receptor activation to a clear effect on growth cone behavior *in vivo*.

Materials and Methods

Animals: The *Vav2*$^{-/-}$*Vav3*$^{-/-}$ knockout mice used in this study were described previously (Cowan et al., 2005; Marston et al., 2003). *Vav2*$^{-/-}$ and *Vav3*$^{-/-}$ single knockout mice were derived by cross-breeding *Vav2*$^{-/-}$*Vav3*$^{-/-}$ mutants with WT mice to yield double heterozygous mutants. Double het mutants were then cross bred to yield single mutants as well as the different het and knockout genotypes used for the retinal explant analysis. All mice were maintained in either a C57BL/6 or mixed (C57BL/6 + 129) background strain.

DNA Constructs: Plasmids for full-length EphB1 and EphB2 were generated in standard pcDNA3 vectors with an N-terminal interleukin-3 signal peptide sequence followed by an N-terminal HA-tag. EphB1 K651R, EphB1 Y594E/Y600E and EphB1 Y594F/Y600F point mutants were generated using standard quick-change mutagenesis. The human Vav2 WT and ΔSH2 mutant constructs were packaged in a modified pA1 vector with a T7 epitope and six histidine tag on the C-terminus as previously described (Cowan et al., 2005; Marston et al., 2003).

Antibodies: The following antibodies are commercially available: anti-T7 epitope (Novagen) (1:1000 dilution) and anti-HA epitope (Sigma) (1:20,000 dilution). Anti-Vav2 and antibodies against P-Eph receptors were described previously (Cowan et al., 2005; Shamah et al., 2001). The anti-P-Y172 Vav2 phospho-antibody (1:1000; 1 μg/ml) was also described previously (Hale et al., 2011). Briefly, antibodies were generated in rabbits from synthesized phosphorylated peptide (C-AEGDEI*Y*EDLMRL) and affinity purified by standard procedures using a Pierce Sulfo-link resin and 100 mM glycine, pH 2.3, elution.

Axon tracing: Unilateral optic nerve DiI tracing was performed similar to previous studies (Plump et al., 2002; Williams et al., 2003). A large DiI (1,1′-Dioctadecyl-3,3,3′,3′-tetramethylindocarbocyanine perchlorate) crystal (Sigma) was placed directly onto the optic disc of E16.5 fixed embryo heads. Heads were incubated at 37°C for 2 weeks in 30% sucrose solution for adequate anterograde labeling past the optic chiasm midline. Heads were then flash frozen and cryosectioned at 25μm. Sections were imaged and ipsilateral and contralateral axon tracts were analyzed with ImageJ software. Axon tracts past the midline were individually

isolated and measured for total pixel intensity. Background subtraction was performed by 50 pixel rolling ball method as previously described (Torborg and Feller, 2004). Analysis and fluorescent intensity measurements were performed experimenter-blinded. % Ipsilateral was calculated as the intensity of the ipsilateral tract over the total contra. plus ipisi. intensity value. Ipsilateral/contralateral was calculated as a direct ratio of intensity values.

Binocular anterograde tracing of retinogeniculate axon projections was described previously (Cowan et al., 2005). Postnatal day 15 mouse pups were injected binocularly with either Alexa-488 or Alexa-555 labeled Cholera Toxin B subunit (Molecular Probes). After 36 hours, pups were killed and brains were dissected and fixed in 4% PFA for 48 hr at 4°C. 100μm coronal vibratome sections were imaged on a Zeiss LSM 510 Meta confocal microscope at 10x magnification.

Retinal Explants: Ventrotemporal (VT) and dorsotemporal (DT) retinal explants were dissected from E14.5 mouse embryos and plated in a collagen matrix: a 50:50 mix of bovine dermis collagen (BD) and rat tail collagen (BD). Explants were grown in serum-free media for 40-48 hr. before stimulation. Clustered ephrinB2/Fc or Fc control (R&D systems) was prepared by incubation of 100 μg/ml ephrinB2/Fc or Fc alone with 450 μg/ml goat anti-human Fc (Jackson ImmunoResearch Labs) for 60 min at room temp and then diluted to the appropriate final concentrations in conditioned culture medium. Explants were stimulated for 30 minutes at 37°C. Treated explants were fixed for 1 hr. with 3.7% formaldehyde and stained with Phalloidin-green (Life Technologies) for 30 min.

Cell Transfections and Immunoprecipitations: HEK-293T cells were transfected using the calcium phosphate method. After ~16 hr., T7-Vav2 and HA-EphB transfected cells were lysed in a modified RIPA buffer (20 mM Tris–HCl, pH 7.4, 150 mM NaCl, 1 mM EDTA, 1% Triton X-100, 5 mM NaF, 1 mM activated Na_3VO_4, 1 mM PMSF). Lysates were incubated with 15µl anti-T7 epitope agarose (Novagen) (50% slurry) for Vav2 immunoprecipitation. Beads were washed 3 times with modified RIPA lysis buffer prior to immunoblotting for anti-HA or anti-T7.

Immunoblotting: Samples were run on SDS-PAGE gels and transferred to PVDF membrane (GE Healthcare). The membranes were blocked in 10% milk/TBS-T (tween-20 at 0.05% v/v) for 1 hr and probed with 1° antibody for 2 hr at room temperature or overnight at 4°C. The membranes were then incubated with a 2° antibody (1:10,000 G∝R IgG or G∝M IgG, Jackson ImmunoResearch Labs) for 1 hr at room temperature and developed with a homemade enhanced chemiluminescence (ECL) solution.

Morphological Analysis: Measurements of growth cone collapse in phalloidin stained retinal explant axons were performed under blinded conditions using the standard criteria (Shamah et al., 2001). Only growth cones located in the periphery of the retinal explant axon outgrowth were scored. %GCC collapse was calculated as ratio of collapsed growth cone over total number of growth cones counted (collapsed and uncollapsed). Axon number is a quantification of the total number of axons scored for growth cone collapse. Axon outgrowth was measured using ImageJ software and represents the mean length of the 3 longest axon processes per explant.

Data Analysis: Two-way ANOVA or Student's t-test was used to determine statistical significance in growth cone collapse assay and DiI tracing experiments. Statistical analysis and graphs were performed using GraphPad Prism software.

Chapter 2

EphB2 Receptor Forward Signaling Controls Cortical Growth Cone Repulsion via Nck and Pak

(*Originally published as*: Srivastava, N.*, Robichaux, M.A.*, Chenaux, G., Henkemeyer, M., and Cowan, C.W. (*authors contributed equally to this work) (2013). EphB2 receptor forward signaling controls cortical growth cone collapse via Nck and Pak. *Mol Cell Neurosci* 52, 106-116.)

Summary

EphB receptors and their ephrinB ligands transduce bidirectional signals that mediate contact-dependent axon guidance primarily by promoting growth cone repulsion. However, how EphB receptor-mediated forward signaling induces axonal repulsion remains poorly understood. Here, we identify Nck and Pak proteins as essential forward signaling components of EphB2-dependent growth cone repulsion in cortical neurons. We show that kinase-active EphB2 binds to Pak and promotes growth cone repulsion via Pak kinase activity, Pak-Nck binding, RhoA signaling and endocytosis. However, Pak's function in this context appears to be independent of Rac/Cdc42-GTP, consistent with the absence of Rac-GTP production after ephrinB treatment of cortical neurons. Taken together, our findings suggest that ephrinB-activated EphB2 receptors recruit a novel Nck/Pak signaling complex to mediate repulsive cortical growth cone guidance, which may be relevant for EphB forward signaling-dependent axon guidance *in vivo*.

Introduction

The Eph family of receptor tyrosine kinases (Ephs) function with their membrane-bound ligands, the ephrins, to regulate the proper organization and connectivity of the developing nervous system (Egea and Klein, 2007; Pasquale, 2005; Shen and Cowan, 2010). Eph-ephrin binding requires cell-cell contact and can stimulate both forward and reverse signaling events that facilitate complex attractive and adhesive or repulsive cell responses. The Ephs comprise two subgroups in mammals, the EphA subclass (A1-A8, A10) and EphB subclass (B1-B4, B6), based in part on their binding affinities for ephrinA or ephrinB proteins, respectively (Pasquale, 2005). Eph forward signaling plays a major role in several repulsive axon guidance events during normal brain and spinal cord development, including roles in retinal ganglion cell (RGC) midline repulsion at the optic chiasm (Williams et al., 2003), topographic mapping of RGC axons within the thalamus and superior colliculus (Feldheim et al., 1998; Hindges et al., 2002b), midline repulsion of corticospinal tract axons (Kullander et al., 2001a; Kullander et al., 2001b; Yokoyama et al., 2001), and thalamocortical axon topographic mapping (Dufour et al., 2003; Torii and Levitt, 2005).

In the developing brain, EphB receptors are highly expressed in the developing cortical plate, and are known to contribute to aspects of cortical axon guidance *in vivo*, including the formation of the corpus callosum (CC), an interhemispheric tract that connects layer 2/3 and layer 5 cortical neurons from one hemisphere to the other (Innocenti et al., 1995; Mendes et al., 2006), and the posterior branch of the anterior commissure (ACp), another interhemispheric tract that connects cortical axons from temporal regions of the cerebral cortex (Henkemeyer et al., 1996; Orioli et al., 1996). While several studies have characterized EphB receptor-associated

proteins, the critical signaling and cellular events that mediate Eph receptor signaling-dependent axonal repulsion remain poorly understood.

Here, we studied embryonic cortical neurons in culture to characterize EphB2 forward signaling pathways that are required for ephrinB2-induced cortical growth cone collapse. Interestingly, we find that several intracellular signaling proteins, including Nck, Pak, RhoA and Rho kinase, are all required for EphB2-dependent cortical growth cone repulsion. Interestingly, Pak's novel kinase-dependent function in this process is dependent on Nck binding, but independent of Rac/Cdc42 binding or activity, suggesting a novel role and regulation for Pak in EphB2-mediated growth cone collapse.

Results

Cortical neuron EphB2 receptors are required for ephrinB2-induced growth cone collapse

To study the potential role of EphB receptors in cortical growth cone collapse, we cultured embryonic rodent cortical neurons and treated them with clustered ephrinB2/Fc, a major repulsive ligand for EphB receptors, or clustered Fc control (1 mg/ml) for various times (3-60 minutes) before assessing either endogenous EphB receptor autophosphorylation at juxtamembrane (JM) tyrosines or the extent of growth cone collapse (GCC) (Figure 2.1A-C). Compared to clustered Fc control, treatment with clustered ephrinB2 led to a time-dependent increase in autophosphorylated Eph receptors and robust GCC as early as 10 minutes after treatment (Figure 2.1A and C). In the absence of clustering anti-Fc antibody, ephrinB2/Fc failed to increase P-Eph levels (data not shown), consistent with many previous studies. Interestingly, treatment with clustered ephrinB1/Fc, which is also an EphB receptor ligand, led to a much

weaker stimulation of Eph receptor phosphorylation than ephrinB2 and failed to induce GCC (Figure 2.1A and 2.1D), suggesting that ephrinB2 is a more potent repulsive cue, at least *in vitro*, than ephrinB1 when presented at similar concentrations or that ephrinB1 binding to EphB2 does not promote repulsive signaling. Even at 3- or 10-fold higher concentrations of clustered ephrinB1/Fc (10 mg/ml), we observed little or no cortical GCC (Figure 2.1E).

To determine which EphB receptors mediate the ephrinB2-induced growth cone collapse in cortical neuron cultures, we cultured E16.5 cortical neurons from wild-type, *EphB1*$^{-/-}$, *EphB2*$^{-/-}$ or *EphB3*$^{-/-}$ mutant mice (Henkemeyer et al., 1996; Orioli et al., 1996; Williams et al., 2003), or combinations of these mutant alleles (data not shown). We then treated the neurons with clustered ephrinB2/Fc (1 mg/ml) and measured GCC. EphrinB2 induced robust GCC in all genotype combinations, except for neurons cultured from *EphB2*$^{-/-}$ mice (Figure 2.2A), which indicates the EphB2 receptor is required to mediate ephrinB2-induced GCC in this context. As expected, neurons cultured from *EphB2*$^{Tr/Tr}$ forward signaling mutant mice also failed to undergo GCC in response to ephrinB2 treatment (Figure 2.2A, right), indicating that EphB2 forward signaling is essential for mediating ephrinB2-induced GCC in the cultured cortical neurons. Interestingly, even *EphB2*$^{+/-}$ cortical neurons had profound defects in ephrinB2-induced GCC (Figure 2.2B), and this could be rescued by transiently expressing Flag-EphB2 in the neurons (Figure 2.2B). Together these data suggest that ephrinB2-induced GCC is highly dependent on normal levels of EphB2 expression and forward signaling in the cortical neuron cultures.

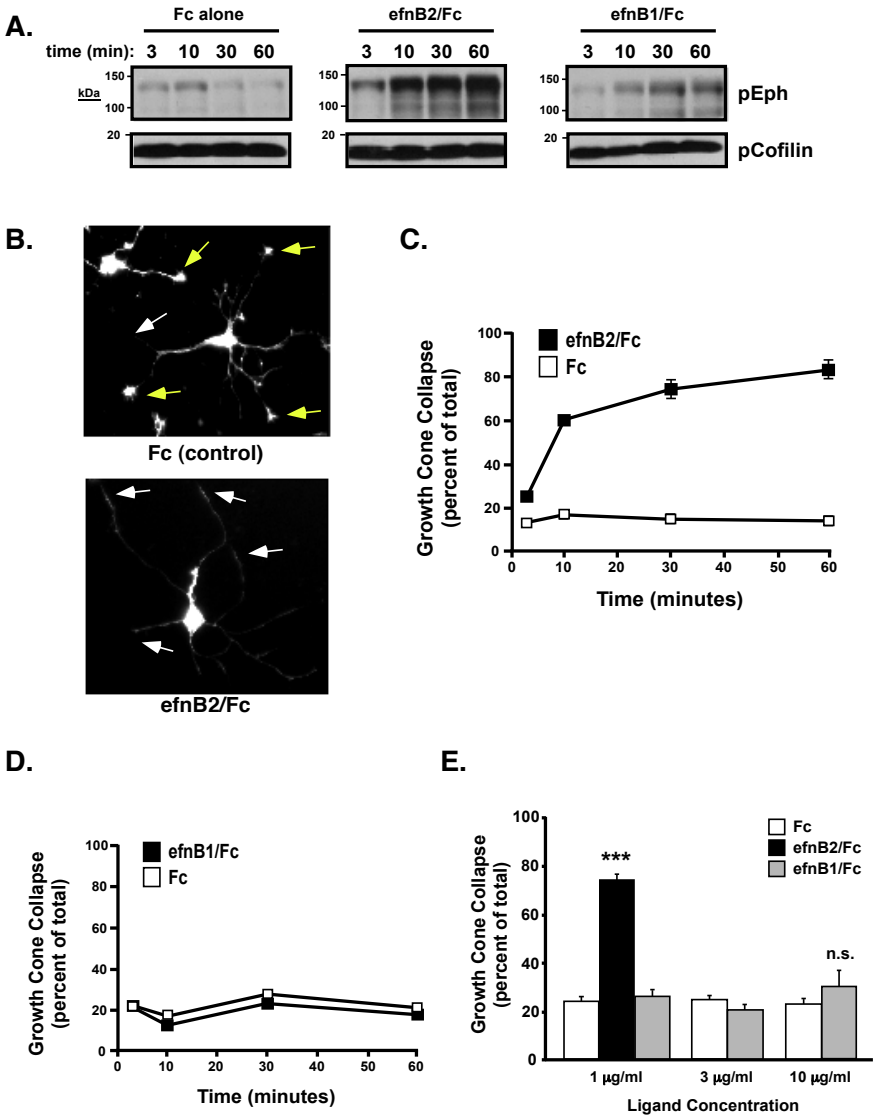

Figure 2.1. EphrinB2 stimulates EphB activation and growth cone collapse of cultured cortical neurons. *(A)* E18 rat cortical neurons were stimulated with clustered ephrinB2 (efnB2), ephrinB1 (efnB1) or Fc control for 3, 10, 30 or 60 mins, and then lysates were immmunoblotted with anti-phospho-Eph or anti-phospho-cofilin antibodies. *(B)* Growth cone morphology of Fc-control (top) and EphrinB2 (bottom) stimulation conditions. Uncollapsed (yellow arrows) and

collapsed (white arrows) growth cones were visualized with phalloidin (Oregon-green). *(C)* Time-course analysis of cortical (E18 + 2 DIV) neuron growth cone collapse upon preclustered Fc-control or ephrinB2/Fc addition (mean +/- SEM, n=9 from 3 independent experiments). *(D)* Time-course analysis of cortical (E18 + 2 DIV) neuron growth cone collapse upon preclustered Fc-control or ephrinB1/Fc addition (mean +/- SEM, n=9 from 3 independent experiments). *(E)* Cortical GCC (E18 + 2DIV) after 1 hr treatment with indicated preclustered ephrins or Fc control (mean +/- SEM, n=3, ***$p<0.001$ ephrin/B2 vs. Fc control, Student's t-test).

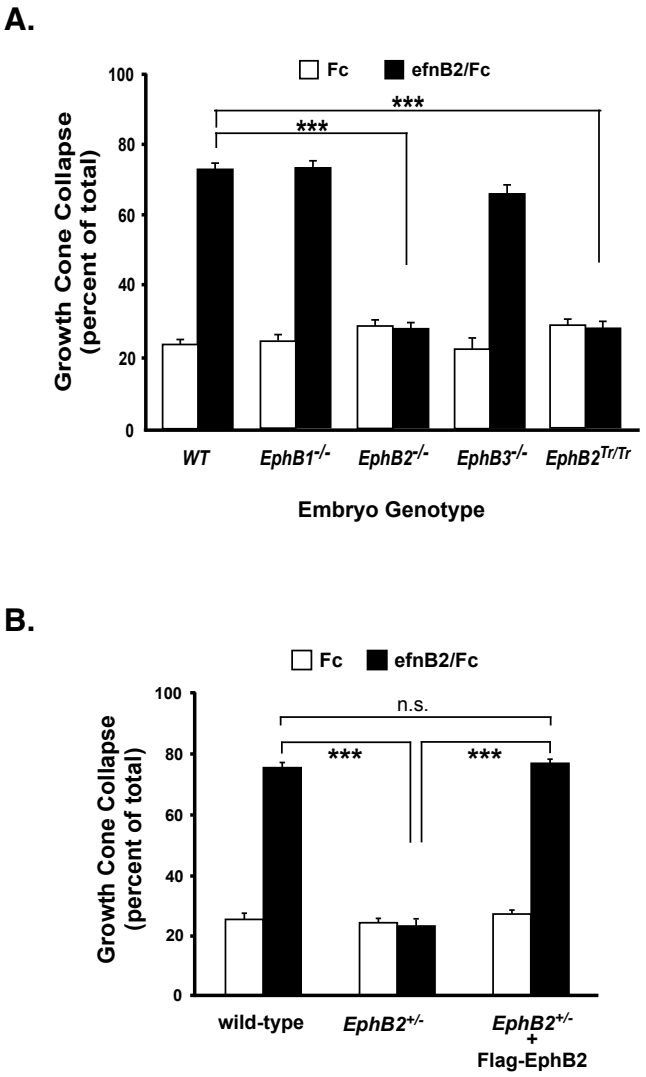

Figure 2.2. EphB2 is required for ephrinB2-induced cortical neuron growth cone collapse. *(A)* Growth cone collapse assay from *EphB1*$^{-/-}$, *EphB2*$^{-/-}$, *EphB3*$^{-/-}$, *EphB2*$^{T\text{-}lacZ/T\text{-}lacZ}$, and wild-type cultured mouse cortical neurons. Cultured neurons (E16.5 + 3 DIV) were treated with 1 m/ml clustered Fc or ephrinB2/Fc for 1 hour prior to fixation, staining and blinded scoring (***$p<0.001$, Two-way ANOVA). *(B)* Expression of EphB2 rescues the EphB2 deficit in ephrinB2/Fc induced GCC. *EphB2*$^{-/-}$ cortical neurons were transfected with pcDNA3-Flag-

EphB2 or vector alone following dissociation. After ~72 hours in culture, the neurons were treated with clustered ephrinB2/Fc for 1 hr prior to fixation and analysis of GCC as in 3A (***$p<0.001$, Two-way ANOVA).

EphB2 receptor-mediated growth cone collapse requires the adaptor protein, Nck

Since the cultured cortical neurons provided a tractable, reductionist system in which to study EphB2-dependent GCC in primary neurons, we next tested candidate forward signaling molecules in ephrinB2-induced GCC. The Nck adaptor proteins have been implicated in EphB2 receptor forward signaling (Holland et al., 1997). Nck1 contains one Src homology type II (SH2) domain, which mediates binding to phosphorylated tyrosines, and three SH3 domains, which mediate physical interactions with proteins containing proline-rich regions. The second SH3 domain has been shown to mediate binding to a number of signaling proteins, including the p21-activated kinases (Paks) (Buday et al., 2002; Li et al., 2001). To test whether Nckα is required for EphB2-mediated GCC, we transiently transfected plasmids expressing wild-type or function-blocking, dominant negative Nck proteins (*i.e.* a SH2 domain (DSH2) deletion mutant or a middle SH3 domain deletion mutant (DSH3-#2)) into freshly-dissociated embryonic cortical neurons just prior to plating. This approach allows for rapid plasmid-directed protein expression for 2-3 days prior to ephrinB2 treatment. Transfected primary cortical neurons were treated with clustered ephrinB2/Fc (1 mg/ml) or Fc alone for 1 hour, and then the transfected neurons (detected by co-transfected mCherry expression) were analyzed for F-actin content (phalloidin) and general growth cone morphology. Whereas expression of vector alone or wild-type Nckα had no effect on basal or ephrinB2-induced GCC, the expression of either the DSH2 Nck or the DSH3-#2 Nck significantly blocked ephrinB2-induced GCC without altering basal GCC (Figure 2.3A). In addition, we also analyzed the basal outgrowth of neurite extensions of these transfected neurons in the Fc-alone control condition. Here, we observe a modest but significant decrease in neurite length between vector control and Nck mutant conditions (Figure 2.4). Together, these findings indicate that Nck is an essential downstream signaling molecule that

mediates growth cone collapse and basal neurite outgrowth through functions requiring both its SH2 and middle SH3 domain. Together, these findings indicate that Nck is an essential downstream signaling molecule that mediates growth cone repulsion through functions requiring both its SH2 and middle SH3 domain.

Since the second Nck SH3 domain binds Pak-family proteins, which are known to regulate the F-actin cytoskeleton, we tested whether EphB2 receptors might physically interact with Pak. When co-expressed in HEK-293T cells, Pak1 (myc-tagged) was co-immunoprecipitated by wild-type EphB2 receptor (HA-tagged). However, a kinase-inactive mutant EphB2 receptor (K643M) failed to co-immunoprecipitate Pak1 (Figure 2.3B). Together, these data suggest that activated EphB2 receptors bind to Nck and Pak to form a functional signaling complex necessary for GCC.

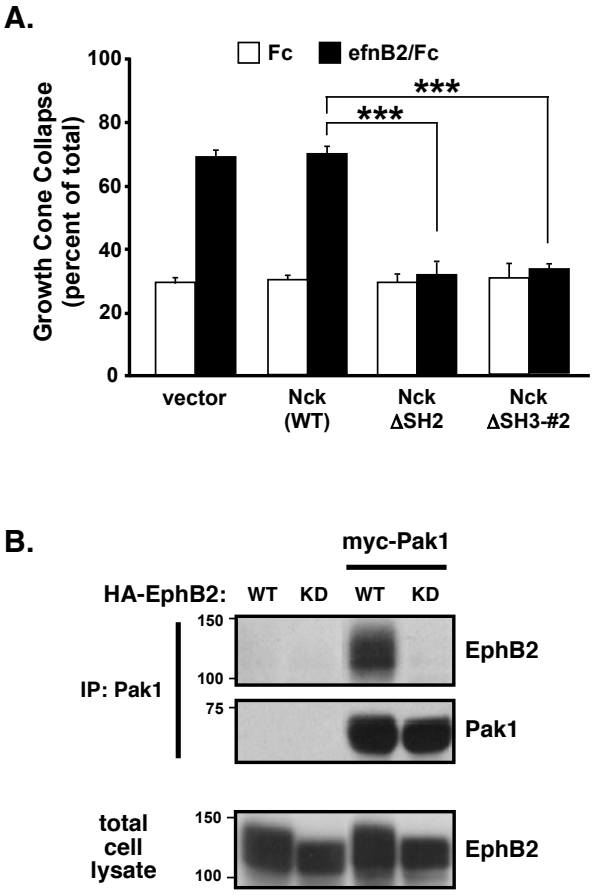

Figure 2.3. Role for Nck1 and Pak1 in ephrinB2-induced growth cone collapse. *(A)* Cultured rat cortical neurons (E18 + 2 DIV) were transfected with wild-type Nck1, the ΔSH2 deletion Nck1 mutant (Nck ΔSH2), a Nck1 mutant lacking a functional second SH3 domain (Nck ΔSH3-#2), or vector control and then treated with clustered Fc control (white bars) or ephrinB2/Fc (black bars) for 1 hr prior to analysis of GCC. (***$p<0.001$, Two-way ANOVA, n=9, data are mean of 3 independent experiments). *(B)* Coimmunoprecipitation of Pak1 and EphB2 co-expressed in HEK293T cells. Cells were transfected with HA-tagged wild-type or kinase-dead (K643M) EphB2 with or without myc-tagged Pak1 prior to anti-myc IPs. IP and total cell lysates (30 mg) were Western blotted with anti-HA (EphB2) or anti-Pak1 antibodies.

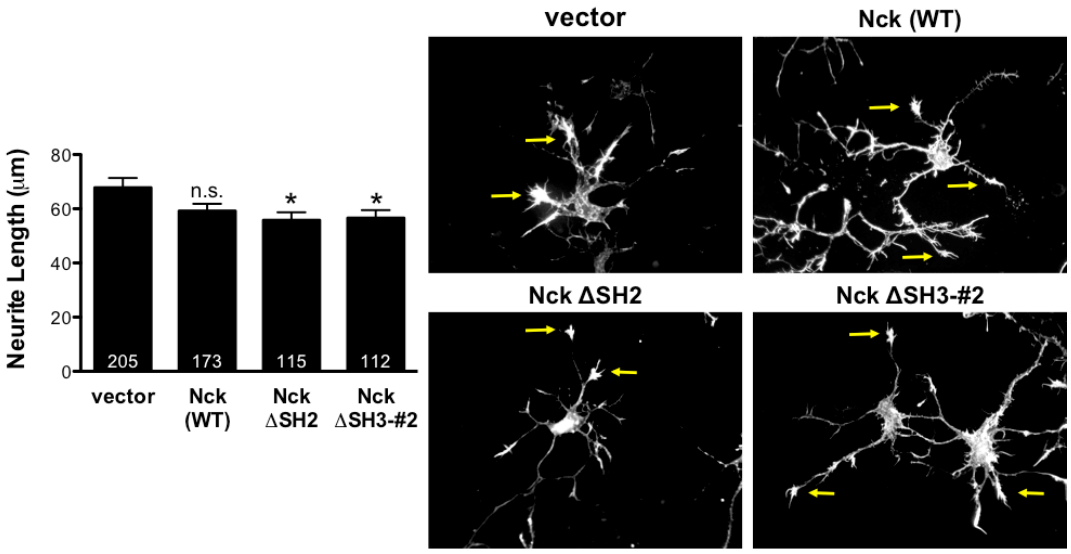

Figure 2.4. Cortical neurite outgrowth requires Nck1. *(A)* Cultured rat cortical neurons (E18 + 2 DIV) transfected with wild-type Nck1, Nck ΔSH2, Nck ΔSH3-#2, or vector control were stimulated for GCC analysis (described above). Neurite outgrowth was measured in transfection-positive, phallodin-labeled neurons from the Fc-alone control condition using the ImageJ line tool. (*$p<0.05$, One-way ANOVA, data are mean of measured neurites from transfected neurons in 3 independent experiments). *(B)* Representative images of transfected neurons that are stained for F-actin with a phalloidin antibody are depicted. Arrows indicate large growth cones with complex morphologies in each ectopic condition.

Pak kinase activity is required for ephrinB2/EphB2-mediated growth cone collapse.

We next tested whether Pak kinase activity was important for ephrinB2-induced GCC in the cortical neurons. Similar to the Nck findings, we found that transfection of an empty vector or wild-type Pak1 plasmid into primary cortical neurons had no effect on ephrinB2-induced GCC, but transfection of a kinase-inactive Pak1 (K299R) plasmid significantly blocked GCC (Figure 2.5A). Interestingly, overexpression of constitutively-active Pak1 (King et al., 2000) had no effect on basal or ephrinB2-induced GCC (Figure 2.5A, right). These results indicate that Pak1 kinase activity is necessary for EphB2-mediated GCC, but expression of a hyperactive Pak1 kinase alone was not sufficient to promote GCC in the absence of ephrinB2 treatment. To test whether all Pak proteins are involved in this process, we expressed kinase-inactive or constitutively-active Pak5, a member of the group II Pak genes (Pak4-6), and measured ephrinB2-induced GCC. Unlike the Pak1 kinase-inactive mutant, expression of the kinase-inactive Pak5 mutant did not alter normal ephrinB2-induced GCC (Figure 2.5B), suggesting that ephrinB2-induced GCC may preferentially involve the group I Pak genes (Pak1-3).

To determine if other group I Pak genes are expressed in cortical neurons, we performed quantitative real-time PCR (qRT-PCR) on total RNA isolated from E16.5 cortex and retina, and compared relative expression of all three group I Pak genes in the cortex and retina (Figure 2.5C). Our findings indicated that all group one Paks are expressed at similar levels. To test the importance of Pak1, we transfected plasmids expressing a pre-validated Pak1 shRNA to reduce endogenous Pak1 mRNA and protein levels (Yi et al., 2008). We found that reducing Pak1 dramatically blocked ephrinB2-induced GCC in a Pak1 shRNA plasmid concentration-dependent manner (Figure 2.5D and data not shown). Furthermore, the induced GCC phenotype could be rescued by co-transfection with an RNAi-resistant human Pak1 expression plasmid (Figure 2.5D,

right), suggesting that the Pak1 shRNA effects are not due to off-target RNAi effects. These data suggest an important functional role for Pak1 in EphB2 receptor-mediated GCC in cultured cortical neurons.

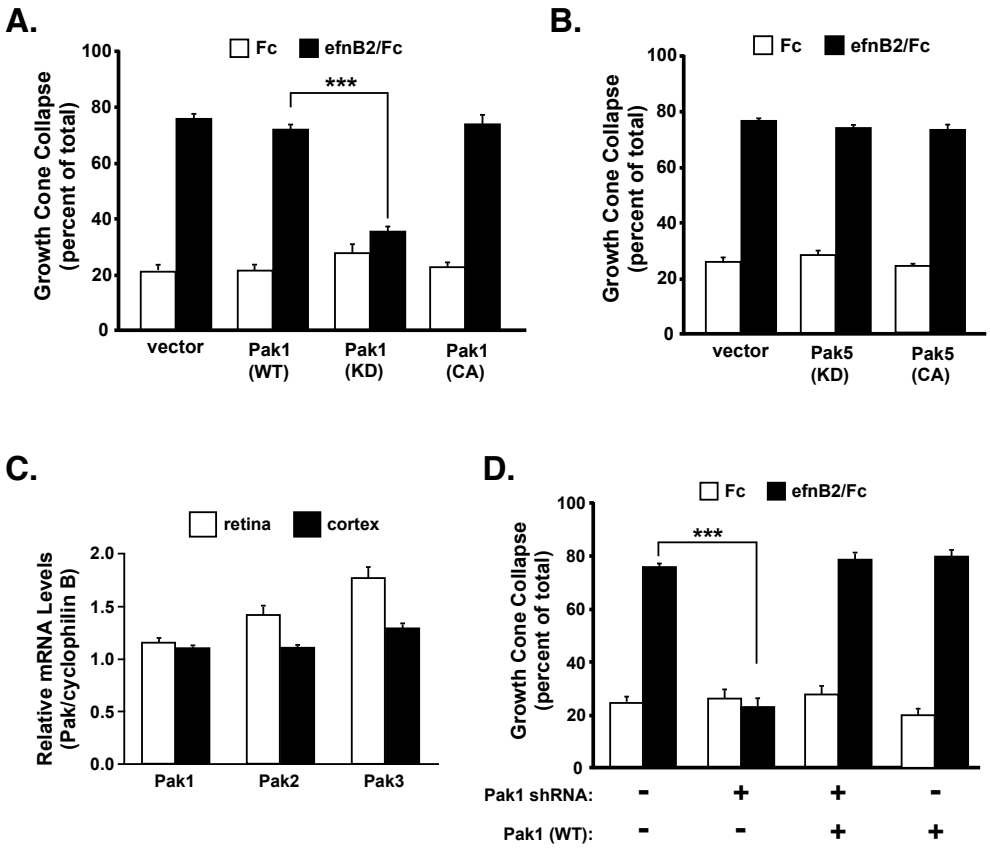

Figure 2.5. EphrinB2-induced growth cone collapse requires Pak1 kinase activity. *(A)* Growth cone collapse assay of E18 cultured rat cortical neurons transfected with wild-type Pak1, a kinase-dead Pak1 mutant (K299R), a constitutively active Pak1 mutant (L107F), or vector control (***$p<0.001$, Two-way ANOVA, n=9 from 3 independent experiments). *(B)* Growth cone collapse assay of cultured cortical neurons transfected with WT or kinase activity mutants of Pak5. *(C)* Relative mRNA expression of Pak1, Pak2 and Pak3 in whole retina (white bars) or cerebral cortex (black bars) from indicated developing mouse tissues (E16.5) and normalized to mRNA levels of the housekeeping gene, cyclophilin B (PpiB). *(D)* Growth cone collapse assay of cultured cortical neurons transfected with a Pak1 shRNA plasmid with or without a wild-type, RNAi-resistant human Pak1 plasmid (***$p<0.001$, Two-way ANOVA, n=9 from 3 independent experiments).

EphrinB2 stimulation does not regulate basal Pak1 kinase activity

Having established a role for Pak1 kinase activity in ephrinB2-induced GCC, we next tested whether ephrinB2/EphB2 activation regulates Pak1 kinase activity. Previous studies have shown that Rac-GTP-activated Pak1 induces autophosphorylation of two Pak1 serines (S198/S203) (Bokoch, 2003). Using a phosphorylation site-specific antibody to these autophosphorylation sites (Tolias et al., 2007)), we treated cultured neurons with clustered ephrinB2/Fc (1 mg/ml) for 3-60 minutes prior to analysis of autophosphorylated Pak1 (P-Pak1, Figure 2.5A). Unlike treatment with brain-derived neurotrophic factor (BDNF), which induced a rapid and robust induction of P-Pak1 (Figure 2.6A and (Hale et al., 2011)), treatment with clustered ephrinB2/Fc failed to induce a detectable increase in P-Pak1 levels at any time point analyzed (Figure 2.6A). Using these same experimental conditions, we also performed a kinase assay in cultured neurons to analyze Pak1 kianse activity in response to clustered ephrinB2 treatment. Kinase activity, as measured by MBP phosphorlyation, was relatively high in control conditions and only modestly increased upon ephrinB2 stimulation (Figure 2.7). In addition, ephrinB2 treatment did not increase Rac-GTP levels at any time point (3-60 minutes) in the cultured cortical neurons using a standard GST-PBD pulldown assay (Figure 2.6B). Therefore, despite the importance of basal Pak1 kinase activity for ephrinB2-induced GCC (Figure 2.5A and 2.6C), ephrinB2 treatment does not appear to modulate Rac-GTP or Pak1 kinase activity levels under these conditions.

Since basal Rac-GTP levels are not altered by ephrinB2 treatment, we sought to test whether the function of Pak1 in GCC was independent of Rac/Cdc42 GTPase regulation. Unlike the kinase-inactive Pak1 mutant, overexpression of a Pak1 mutant (H83L/H86L) that cannot bind Rac/Cdc42-GTP (Sells et al., 1997) did not alter either basal or ephrinB2-induced GCC (Figure

2.6C). Consistent with this finding, expression of Rac1 (T17N) or Cdc42 (T17N) dominant negative mutants (Nofer et al., 2003; Palmieri et al., 2000) did not reduce ephrinB2-induced GCC (Figure 2.8A). This suggests that Rac/Cdc42 GTPase activities are not regulated by ephrinB2 and may not be required for ephrinB2-induced GCC in cortical neurons. In contrast, expression of the Nck binding-deficient Pak1 mutant (P13A) or the kinase-inactive Pak1 mutant (K299R) significantly reduced ephrinB2-induced GCC (Figure 2.6C). Moreover, a double Pak1 mutant that contained both the kinase-inactivating mutation and the Nck-binding mutation (K299R/P13A) did not result in a more severe dominant negative effect than either mutant alone (Figure 2.6C), indicating that Pak-Nck binding and Pak1 kinase activity likely function in the same molecular pathway to mediate ephrinB2-induced GCC. Interestingly, overexpression of a Pak1 mutant (P191G/P192A, (Manser et al., 1998)) that disrupts binding to the constitutive binding partner, PIX/COOL (a Rho-family GEF), dramatically reduces ephrinB2-induced GCC (Figure 2.6C). Taken together, these findings suggest that ephrinB2-induces the recruitment of Nck and kinase-active Pak1, and possibly PIX/COOL, to activated EphB2 receptors to promote cortical GCC. However, Rac/Cdc42 binding to Pak1 and activation of Rac/Cdc42-GTP appear to be non-essential for ephrinB2-induced GCC in this context.

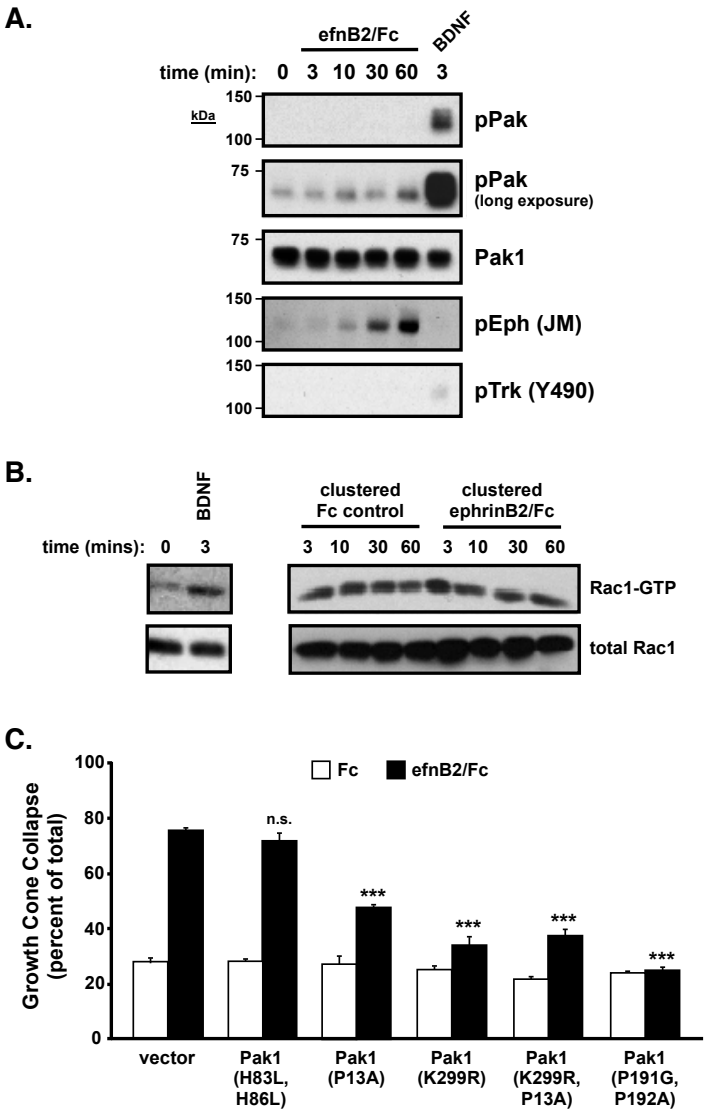

Figure 2.6. EphrinB2-stimulated cortical GCC requires Rac/Cdc42-independent Pak1 kinase activity and Nck and PIX/COOL binding to Pak1. *(A)* Cultured cortical neurons (E18) were stimulated with clustered ephrinB2/FC for 0, 3, 10, 30 and 60 mins or human BDNF for 3 mins. Total cell lysates were immunoblotted with anti-phospho-Pak1 (S198/S203), anti-total Pak1, anti-phospho-Eph (JM) and anti-phospho-Trk (Y490) antibodies. *(B)* Cultured rat cortical neurons were stimulated with clustered ephrinB2/Fc or Fc control for the indicated times prior to performing GST-PBD assays. GST-PBD bound Rac1-GTP or total cellular Rac1 levels

were assessed by Western blotting with anti-Rac1 antibodies. Data are representative of 6 independent experiments. *(C)* Standard GCC assay of cultured cortical neurons (rat E18 + 2 DIV) transfected with a Rac/Cdc42-GTP binding-deficient Pak1 mutant (H83L/H86L), a Nck-binding deficient Pak1 mutant (P13A), a kinase-dead Pak1 mutant (K299R), a double Pak1 mutant (P13A/K299R), a PIX/COOL-binding deficient mutant (P191G/P192G), or a vector only control (***$p<0.001$, Two-way ANOVA, n=9 from 3 independent experiments).

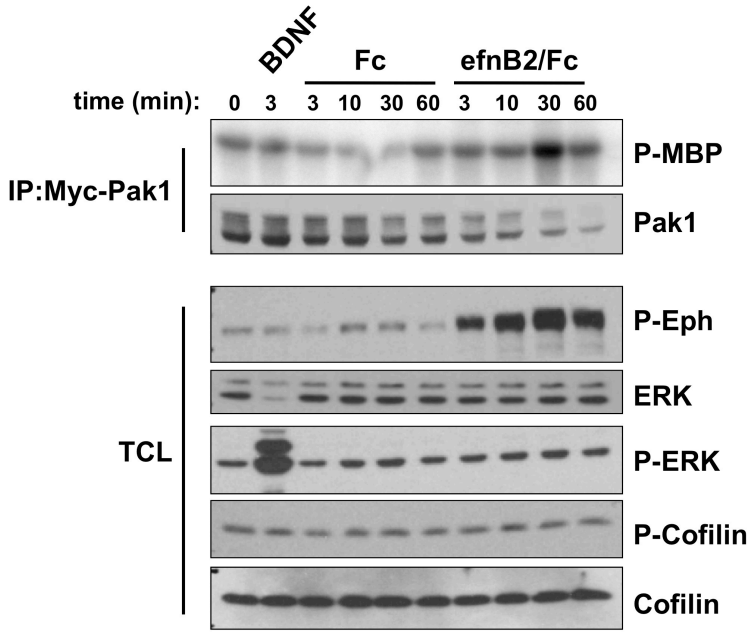

Figure 2.7. Pak1 kinase activity is not strongly regulated by EphrinB2. Cultured cortical neurons (E18) were stimulated with clustered ephrinB2/FC for 0, 3, 10, 30 and 60 mins or human BDNF for 3 mins. ^{32}P-MBP levels were obtained from Myc-Pak1 lysates and total cell lysates were immunoblotted with anti-phospho-Pak1 (S198/S203), anti-total Pak1, anti-phospho-Eph (JM), anti-cofilin, anti-phospho-cofilin, anti-phospho-ERK, and a loading control anti-ERK antibody.

The RhoA/Rho Kinase signaling cascade is required for EphrinB2-induced GCC

Numerous studies have reported an essential role for RhoA-GTP, and one of its effectors, Rho kinase, in the process of GCC in culture (Dickson, 2001; Schmandke and Strittmatter, 2007; Wahl et al., 2000). To test the importance of RhoA GTPases, we expressed dominant-interfering forms of RhoA (T19N) and measured the extent of ephrinB2-induced GCC. Consistent with previous studies, the dominant-negative RhoA robustly blocked ephrinB2-induced GCC (Figure 2.8A). Interestingly, expression of a constitutively-active form of RhoA (Q63L) did not collapse growth cones in the absence of ephrinB2 treatment, suggesting that RhoA-GTP is necessary, but not sufficient, for GCC (Figure 2.8A, right). Since RhoA-GTP is required for GCC, we next sought to test the importance of one of its known downstream effectors, Rho kinase (ROCK), which has been reported previously to be important for ephrin-induced GCC and axon retraction ((Harbott and Nobes, 2005). Incubation of the cortical neurons with the Rho kinase inhibitor, Y-27632 (10 mM), resulted in a partial reduction in ephrinB2-induced GCC (Figure 2.8B), indicating that RhoA/Rho kinase signaling is required for EphB2 receptor-mediated GCC.

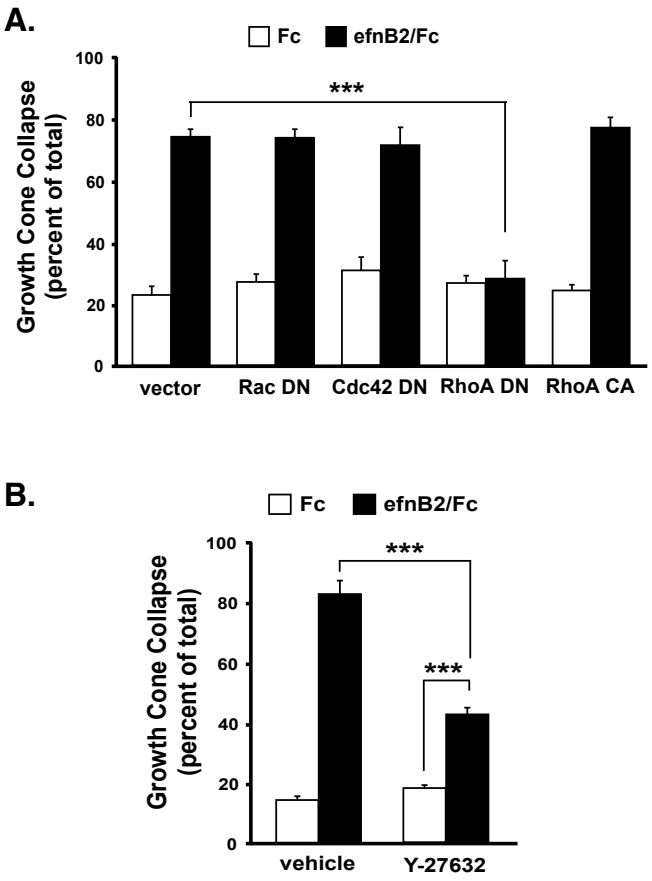

Figure 2.8. RhoA and Rho-kinase activity are required for EphrinB2-induced growth cone repulsion. *(A)* Growth cone collapse assay of cultured rat cortical neurons (E18 + 2 DIV) transfected with dominant-negative Rac1 (T17N), Cdc42 (T17N), RhoA (T19N) mutants, a constitutively-active RhoA (Q63L) mutant or a vector only control (***$p<0.001$, Two-way ANOVA, n=3). *(B)* Growth cone collapse assay of E18 cultured cortical neurons pre-treated with the Rho kinase inhibitor (Y-27632, 10 mM) or vehicle. Data represent the mean +/- SEM of 3 independent experiments. (***$p<0.001$, Two-way ANOVA) (Y-27632 inhibitor: ***$p<0.001$ ephrin/B2 vs. Fc control, Student's t-test).

Endocytosis is required for ephrinB2-induced cortical GCC

Several previous studies have indicated an important role for Eph receptor endocytosis in the process of cell and growth cone retraction (Cowan et al., 2005; Marston et al., 2003; Zimmer et al., 2003). To test the importance of endocytosis, we transiently-transfected a dominant-interfering mutant of Dynamin (K44A), a small GTPase required for receptor endocytosis, and measured ephrinB2-induced GCC. We observed that neurons expressing dynamin (K44A), a GTP binding deficient mutant that blocks endocytosis (Huang et al., 2010), had a significant reduction of ephrinB2-induced GCC (Figure 2.9A), suggesting that endocytosis is an important cellular process for ephrinB2-induced growth cone collapse. We observed similar effects by treating the neurons with phenylarsine oxide (PAO) (Figure 2.9B), a chemical inhibitor of clathryn-mediated receptor endocytosis (Gray et al., 2001; Hertel et al., 1985; Xia et al., 2009). These combined findings suggest an important role for endocytosis in ephrinB2-induced GCC.

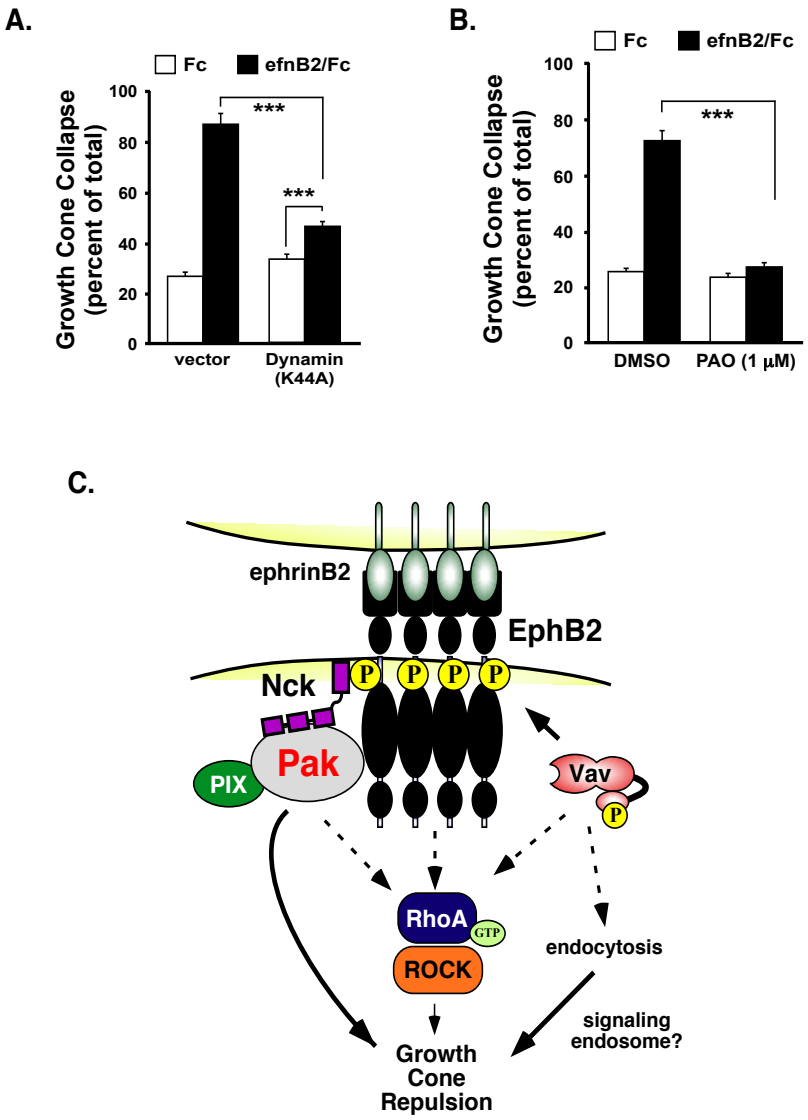

Figure 2.9. Endocytosis is required for ephrinB2-induced cortical growth cone collapse. *(A)* Growth cone collapse assay of cultured rat cortical neurons (E18 + 2 DIV) transfected with dominant-negative Dynamin (K44A) or a vector control. Neurons were stimulated with clustered Fc control (white bars) or ephrinB2/Fc (black bars) for 60 mins prior to analysis of GCC. Data represent the mean of 3 independent experiments. (***$p<0.001$, Two-way ANOVA, n=9) (Dynamin K44A: ***$p<0.001$ ephrin/B2 vs. Fc control, Student's t-test). *(B)* Growth cone collapse assay of E18 cultured rat cortical neurons pre-treated with PAO (1 mM) or vehicle

alone. (***p<0.001, Two-way ANOVA, n=6, from 2 independent experiments). *(C)* Working model for the EphB2 forward signaling complexes required for growth cone repulsion.

Discussion

In this study, we identified several key signaling molecules and cellular processes required for endogenous EphB2-mediated cortical neuron GCC (Figure 2.9C), including a novel role for Pak in this process. We report a novel interaction between kinase-active EphB2 and Pak1, which likely occurs via interaction with the EphB2-interacting adaptor protein, Nck, and we show that Pak kinase activity and Nck are required for ephrinB2-induced GCC. However, our data suggest that ephrinB2 binding to EphB2 does not elevate Rac1-GTP to levels detectibly above baseline, which is consistent with a lack of effect by Rac/Cdc42 dominant negative expression on EphB2-mediated GCC. We also provide evidence that Pak1 function in EphB2-dependent GCC requires binding to Nck, Pak kinase activity, and residues that are known to mediate binding to the PIX/COOL GEFs. However, a direct interaction between Pak1 and Rac/Cdc42-GTP does not appear to be required. These data suggest that recruitment of Pak to the ephrinB2/EphB2 receptor complex is necessary and sufficient to mediate its role in GCC. Consistent with previous studies, RhoA-GTP, Rho Kinase and endocytosis are all required for GCC, suggesting that the ephrinB2/EphB2 complexes recruit multiple key signaling components to orchestrate growth cone F-actin remodeling during repulsive guidance.

While our findings reveal a novel role for Pak signaling in EphB2-mediated GCC, these findings also raise many new questions for future study. Classically, Pak is thought to be an effector of Rac/Cdc42-GTP, and subsequent enhancement of Pak kinase activity results in F-actin remodeling through sequential activation of Lim kinase and phosphorylation of the F-actin binding protein, cofilin (Edwards et al., 1999). However, this pathway often results in generation of lamellapodia, membrane ruffles and focal adhesions (reviewed in (Bamburg, 1999)), which is in apparent conflict with presumed dynamics in growth cone repulsion. In our

study, we did not observe any evidence that ephrinB2 treatment stimulates this Rac/Pak/LimK signaling cascade, as we do not observe an increase P-cofilin levels in response to ephrinB2 (Figure 2.1A & Figure 2.7). Rather, we now report an important role for Pak1 and Nck in ephrinB2-induced GCC largely independent of Rac/Cdc42-GTP, which suggests that recruitment of Pak1/Nck to the activated EphB2 receptor complex has a distinct cellular function than Pak activated in response to upregulated Rac/Cdc42-GTP.

Previous work has reported a critical role for drosophila Pak and the Nck homolog, Dock, in the process of photoreceptor axon guidance *in vivo* (Garrity et al., 1996; Hing et al., 1999). In loss-of-function Dock or Pak mutant flies, R photoreceptor cell axons are mistargeted and disorganized within the lamina and medulla of the brain. Rescue studies *in vivo* revealed a critical role for Pak kinase activity, binding to PIX and Dock, and Rac/Cdc42-GTP binding (Hing et al., 1999). However, in the fruit fly, Rac/Cdc42 binding to Pak is required for R photoreceptor cell axon guidance (Hing et al., 1999), and as such, represents a significant departure from the mechanisms of EphB2-mediated cortical GCC in rodents. Interestingly, in both flies and mammals, the recruitment of Pak to the cell membrane appears to be sufficient to activate Pak kinase activity (Hing et al., 1999; Lu et al., 1997), so it is possible that Nck-mediated recruitment of Pak1 to the activated EphB2 receptor at the cell surface increases its intrinsic kinase activity, but Pak1 autophosphorylation of the S/T sites only occurs upon Rac/Cdc42-GTP binding. As such, we speculate that either: (1) the basal Pak kinase activity, recruited to the EphB2 receptors, is sufficient for its role in GCC or (2) the recruitment of Pak to the activated EphB2 receptors at the plasma membrane increases Pak1 kinase activity in a Rac-independent manner.

Nck genes are critical for proper cortical axon guidance *in vivo* such that the conditional deletion of both Nck1 and Nck2 genes leads to deficits in corticospinal tract axon guidance and a reduced posterior anterior commissure (Fawcett et al., 2007). Interestingly, individual Nck1 or Nck2 KO mice appeared normal, suggesting that these two genes serve largely redundant functions during development or can compensate for the loss of the other gene. Similar to this study, we found that expression of the Nck2 (DSH3-2) mutant also blocked ephrinB2-induced GCC (N. Srivastava, unpublished observations), suggesting functional redundancy in EphB2-mediated GCC *in vitro*. Interestingly, Nck2 recruits Pak1 to mediate ephrinB3 reverse signaling-dependent axonal pruning of hippocampal dentate gyrus neurons during development (Xu and Henkemeyer, 2009), suggesting that Nck/Pak may be a common signaling complex for both forward (Eph receptor) and reverse (ephrinB) repulsive axon guidance signaling.

In addition to ephrin-induced recruitment of signaling proteins to the clustered Eph receptors, ephrin-induced endocytosis has emerged as an important step for forward signaling and GCC (Cowan et al., 2005; Fournier et al., 2000; Jurney et al., 2002; Marston et al., 2003; Zimmer et al., 2003). Our present findings that both dynamin (K44A) mutant and PAO block ephrinB2-induced GCC (Figure 2.9A & 2.9B) are consistent with a key role for EphB2 and/or plasma membrane internalization in GCC. Surprisingly, we do not observe a key role for Rac-GTP in ephrinB2-induced GCC, which is distinct from findings of ephrinB2/EphB4-mediated cell-cell repulsion in a Swiss 3T3 cultures (Marston et al., 2003). However, it is interesting to note that Pak1 kinase activity, independent of Rac/Cdc42 binding, has been linked to a form of endocytosis, macropinocytosis, in non-neuronal cells (Dharmawardhane et al., 2000). It is admittedly difficult to interpret a negative result from the Rac dominant negative experiments in our study, but taken together with the absence of ephrinB2-induced Rac-GTP and P-Pak

production (Figure 5A,B) and the failure of the Rac/Cdc42-binding mutant of Pak (H83L,H86L) to reduce ephrinB2-induced GCC (Figure 2.6C), these combined findings suggest that Rac-GTP function is likely dispensable for Pak's role in ephrinB2-induced GCC in this context.

Taken together, our findings reveal important EphB2 receptor forward signaling mechanisms that are required for ephrinB2-induced cortical growth cone repulsion. Considering the importance of axon guidance for proper cortical neuronal connectivity *in vivo*, the discovery of new repulsive signaling factors, such as Nck and Pak, may reveal new therapeutic targets for the treatment of neurodevelopmental disorders or axonal regeneration following brain injury.

Materials and Methods

Animals: The EphB receptor knockout and knock-in mice used in this study, including *EphB1*$^{-/-}$, *EphB2*$^{-/-}$, *EphB2*$^{Tr/Tr}$ and *EphB3*$^{-/-}$ mice, were previously described (Genander et al., 2009; Henkemeyer et al., 1996; Orioli et al., 1996; Williams et al., 2003) and maintained in a CD1 background. *EphB2*$^{Tr/Tr}$ mice express C-terminal truncated fusion proteins containing the extracellular and trans-membrane domain of EphB2 conjugated to β-galactosidase (Henkemeyer et al., 1996). The resulting EphB2-bgal fusion proteins lack their respective intracellular tyrosine kinase catalytic domain and PDZ binding motif. For PCR genotyping, DNA was extracted from tails samples of dissected mice embryos with 100% isopropanol after an intervening lysis step. PCR was performed using the extracted DNA in a total volume of 15ul using the primer sets described previously (Henkemeyer et al., 1996; Orioli et al., 1996; Williams et al., 2003).

DNA Constructs: Expression plasmids for wild-type and mutant Pak1, Pak5, Rac1, Cdc42, and RhoA were described previously (Cotteret et al., 2003; Galisteo et al., 1996; Manser et al., 1994; Manser et al., 1998; Sells et al., 1997; Zhang et al., 1995) and obtained from Addgene. The

compound mutant Pak1 (K299R/P13A) was generated by standard subcloning. The Pak1 shRNA plasmid and vector control for rodent Pak1 was previously described and validated (Yi et al., 2008). Expression plasmids for Nck1 and Dynamin K44A were also described previously (Hu et al., 2009; van der Bliek et al., 1993).

Antibodies: In most cases, the antibodies were commercially available and all were used at a 1:1000 dilution for immunoblotting, except where noted): Pak1 (CST), Nck (BD), anti-T7 epitope (Novagen), anti-M2 Flag epitope (Sigma), anti-Myc (MBL), anti-HA (Roche) (1:285 dilution), anti-Rac1 (Millipore), anti-pY490 TrkA (CST), anti-pY, 4G10 clone (Millipore). Antibodies against P-Eph receptors and anti-P-S198/S203 Pak1 were described previously (Shamah et al., 2001).

Dissociated Cortical Neuron Cultures: Embryonic cortical neurons were cultured from embryonic day 18 Long Evans Rats (CRL) or CD-1 mice at E16.5. The cortices were dissected and treated with 100 U papain (Worthington) for 3 min. The digestion was terminated by the addition of trypsin inhibitor (Sigma). The tissue was washed for a total of 3X with trypsin inhibitor, followed by 3 washes with plating medium consisting of DMEM (Invitrogen) supplemented with 10% fetal bovine serum (Invitrogen), 1% L-glutamine (Sigma), and 1% penicillin-streptomycin (Sigma). Neurons were mechanically dissociated with a pipet and plated on Poly-D-Lysine (Sigma)- and Laminin (Invitrogen)-coated coverslips in a 24-well plate at a density of 100,000 viable cells per dish. The culture medium was replaced with Neurobasal medium (Invitrogen) supplemented with B-27 (Invitrogen), L-glutamine (Sigma), and 1% penicillin-streptomycin (Sigma) at 24 hr after plating. For experiments analyzing EphB mutant

mice, heterozygous crosses were used, and individual embryos were processed for cortical cultures, and PCR genotyping was performed the next day using tail snip DNA.

Cortical neuron transfections at 0 DIV: Following dissociation of rat or mouse cortical neurons with papain, and before plating, the neurons were co-transfected in solution with indicated expression vectors together with a plasmid expressing mCherry ($1/10^{th}$ of total DNA in transfection) using Lipofectamine 2000 (protocol available upon request). The total amount of plasmid DNA in the transfection was held constant, such that empty vector was included to increase levels where appropriate.

Immunoblotting: Samples were run on SDS-PAGE gels and transferred to PVDF membrane (GE Healthcare). The membranes were blocked in 10% milk/TBS-T (tween-20 at 0.05% v/v) for 1 hr and probed with 1° antibody for 2 hr at room temperature or overnight at 4°C. The membranes were then incubated with a 2° antibody (1:10,000 G∝R IgG or G∝M IgG, Jackson ImmunoResearch Labs) for 1 hr at room temperature and developed with a homemade enhanced chemiluminescence (ECL) solution or Amersham™ ECL Plus Western Blotting Detection System (GE Healthcare).

GST-PBD Assay: At 6 days in culture, dissociated cortical neurons (plated at a density of 8 million cells per dish in a 10 cm dish) were treated with clustered EphrinB2/Fc or Fc alone or BDNF (0.1 μg/mL; Peprotech). GST-PBD assays were performed as described previously (Hale et al., 2011). In brief, the treated neurons were lysed in a buffer consisting of 50 mM Tris (pH 7.2), 1% (v/v) Triton X-100, 250 mM NaCl, and 10 mM $MgCl_2$ and containing 10 μg GST-PBD

per condition. Following incubation with 20 μL glutathione beads (50% slurry; GE Healthcare) for 1 hr at 4°C, beads were washed 3 times with a wash buffer consisting of 50 mM Tris (pH 7.2), 1% Triton X-100, 150 mM NaCl, and 5 mM $MgCl_2$). Samples were eluted with 2X sample buffer, boiled and then loaded onto SDS-PAGE gels for Western blotting with anti-Rac antibodies (Santa Cruz).

Cell Transfections and Immunoprecipitations: HEK-293T cells were transfected using a calcium phosphate method. After ~24 hours, Pak1 and EphB2 transfected cells were lysed in a modified RIPA buffer (20 mM Tris-HCl, pH 7.4, 150 mM NaCl, 1 mM EDTA, 1% Triton X-100, 5 mM NaF, 1mM activated Na_3VO_4, 1 mM PMSF). Pak1 was immunoprecipitated with 5 ml of anti-Myc epitope antibody (MBL) followed by incubation with 4 ml of protein-A agarose beads (Roche). Beads were washed 3 times with modified RIPA lysis buffer, prior to immunoblotting for anti-Pak1 or anti-HA.

Growth Cone Collapse Assays: Rat (E18) or mouse (E16.5) cortical neurons were prepared as previously described (Cowan et al., 2005) and cultured on PDL/Laminin-coated glass coverslips (100,000 neurons/well in a 24-well plate). After 48 hrs (rat) or 72 hrs (mouse) in culture, the neurons were treated with pre-clustered ephrinB2-Fc or Fc control (1-10 μg/ml final concentration) for 60 minutes at 37°C. Clustered ephrinB2/Fc, ephrinB1/Fc or Fc control (all from R&D systems) was prepared by incubation of 100 μg/ml ephrinB/Fc or Fc alone with 450 μg/ml goat anti-human Fc (Jackson ImmunoResearch Labs) for 60 min at room temp, then diluted to the final concentrations indicated in conditioned culture medium. Treated cortical neurons were fixed with paraformaldehyde (PFA) (4% PFA/2% sucrose/D-PBS) for 8-10

minutes and stained with Phalloidin-green (Molecular Probes) for 30 min. Collapsed or un-collapsed growth cones were scored under experimenter-blinded conditions using standard criteria (Shamah et al., 2001). In experiments with plasmid transfection, only neurons with detectable expression of mCherry fluorescence were analyzed.

RNA Isolation and Reverse Transcription: Whole cortices and retinae were dissected from E16.5 mice of either sex at various ages and processed immediately or snap frozen on ethanol/dry-ice. The samples were homogenized in TRIzol (Invitrogen) using a tissue homogenizer, and the RNA was precipitated with chloroform (Sigma). The remaining steps were carried out using the RNeasy® Micro kit (Qiagen). The RNA concentration of each sample was determined using a NanoDrop spectrophotometer and was reverse transcribed using the Superscript™ III First-Strand Synthesis System for RT-PCR (Invitrogen).

Quantitative Real-time PCR: All primers were designed to amplify a 150-200 base-pair product. The qRT-PCR primers for mouse Pak1-3 were as follows: (1) Pak1 forward, 5'-CTTGCTTCTCCCATTTCCTG-3', and Pak1 reverse, 5'-GGGTAAACCCTTGCTCATCA-3', (2) Pak2 forward, 5'-ACCGCGCTTGACGTTCGCATA-3', and Pak2 reverse, 5'-AGAGGAAGGGAAGGTCACGAAGGA-3', (3) Pak3 forward, 5'-GCCAGTAGTGAATCCCCTCA-3', and Pak3 reverse, 5'-CGTTGGGTAAGGGATTTTGA-3'. The primers used to amplify mouse cyclophilin B were 5'-CATCTATGGTGAGCGCTTCCC-3' (forward) and 5'-GCCTGTGGAATGTGAGGGGTG-3' (reverse). The reactions were carried out using the SYBR Green PCR Master Mix (Ambion) and the ABI 7500 real-time PCR thermal cycler (ABI). Pak1-3 expression in the developing cortex and retina were determined by running

reactions of 32 ng of RT-generated single-stranded cDNA. Fold changes relative to cyclophilin B were determined using the ΔΔCt method, in which mean fold change ($2^{-\Delta\Delta CtAVE}$) and s.e.m. ($abs(((2^{-\Delta\Delta CtAVE} \times 2^{-\Delta\Delta CtSEM}) - (2^{-\Delta\Delta CtAVE} / 2^{-\Delta\Delta CtSEM})) / 2)$) were determined.

Pak1 Kinase Assay: Primary cortical neurons (rat, E18) were cultured for 6 days prior to stimulation with pre-clustered ephrinB2-Fc or control Fc. Neurons were lysed in a modified RIPA buffer (20 mM Tris–HCl, pH 7.4, 150 mM NaCl, 1 mM EDTA, 1% Triton X-100, 5 mM NaF, 1 mM activated Na_3VO_4, 1 mM PMSF), and the soluble lysate fraction was incubated with 5 µl anti-Pak1 antibody (CST) to immunoprecipitate Pak1 with protein-A agarose beads (Roche). Immunoprecipitated Pak1 was then incubated with 5 µg MBP (myelin basic protein (Sigma)) plus gamma ^{32}P-ATP (10 µCi/reaction) (75 µM ATP final) for 30 min at 30 °C in kinase reaction buffer (25 mM HEPES, pH 7.5, 5 mM $MgCl_2$, 1 mM $MnCl_2$). Samples were run on a 12% SDS-PAGE gel to visualize MBP phosphorylation *via* Storm phosphorimager (Molecular Dynamics).

Data Analysis: Two-way ANOVA or Student's t-test was used to determine statistical significance in growth cone collapse assay experiments.

Chapter 3

Transient EphB Receptor Forward Signaling Coordinates the Area-Specific Cofasciculation of Reciprocal Thalamic and Cortical Axons during Brain Development.

Summary

In early brain development, ascending thalamocortical axons (TCAs) navigate through the ventral telencephalon (VTel) to reach their target regions in the young cerebral cortex. Descending, deep-layer cortical axons subsequently target appropriate thalamic and subcortical target regions. However, precisely how and when corticothalamic axons (CTA) identify their appropriate, reciprocal thalamic targets remains unclear. We show here that EphB1 and EphB2 receptors control proper reciprocal navigation of a subset of TCA and CTA projections through the VTel. We show *in vivo* that EphB receptor forward signaling and the ephrinB1 ligand are required during the early navigation of TCA fibers in the VTel, and that the misguided TCA fibers in EphB1/2 KO mice interact with cortical subregion-specific axon populations during reciprocal cortical axon guidance. As such, our findings suggest that descending cortical axons identify specific TCA subpopulations in the dorsal VTel to coordinate reciprocal cortical-thalamic connectivity in the early developing brain.

Introduction

In the mammalian forebrain, proper neural circuitry is established through the development of intricate axonal fiber pathways between brain regions (Reviewed in (Chedotal and Richards, 2010; O'Leary and Koester, 1993; O'Leary et al., 1994)). Thalamocortical axons (TCAs) make up one such pathway, which interconnects individual thalamic relay nuclei with corresponding regions of the neocortex (Lopez-Bendito and Molnar, 2003; Molnar et al., 2012). These fibers develop in a highly topographical manner and form fasciculated axon bundles as they ascend toward the neocortex. Reciprocal, descending corticothalamic axons (CTAs) from cortical layer VI project feedback fibers onto appropriate thalamic nuclei. They also navigate in a highly organized and topographic manner alongside corticofugal axons (CFA) from layer V, which innervate both forebrain and lower brain targets (O'Leary and Koester, 1993). Together, these cortical and thalamic fiber pathways establish critical circuits in the forebrain that mediate sensory processing and motor output (Alitto and Usrey, 2003).

During early embryonic brain development (~E11.5-E12.5), pioneer TCA fibers grow through the prethalamus before making a sharp turn past the diencephalic-telencephalic border (DTB) and into the ventral-most aspect of the ventral telencephalon (VTel), or subpallium, where they establish the internal capsule (IC). TCAs continue to ascend through the VTel toward the developing cortical plate and cross the pallial-subpallial border to reach the cortical intermediate zone by age E13.5 (Auladell et al., 2000). At these early ages, the developing VTel comprises the medial and lateral ganglionic eminences (MGE, LGE) and globus pallidus (GP), which together function as critical intermediate targets for TCA pathfinding involving several known axon guidance ligands (Bagri et al., 2002; Bielle et al., 2011b; Dufour et al., 2003; Little et al., 2009; Powell et al., 2008; Wright et al., 2007) and their receptors (Dufour et al., 2003;

Lopez-Bendito et al., 2007; Torii and Levitt, 2005; Wright et al., 2007). In addition, Islet1-positive GABAergic neurons migrate from the LGE to a region near the DTB where TCA axons first invade the VTel and are thought to provide a permissive "corridor" for pioneer TCAs to properly penetrate the DTB (Bielle et al., 2011a; Bielle et al., 2011b; Lopez-Bendito et al., 2006).

Reciprocal, descending cortical axons first pioneer into the VTel around age E13.5, one day after TCA development into the VTel (Auladell et al., 2000; Kwan et al., 2012; Lopez-Bendito and Molnar, 2003). Several axon guidance molecules, including netrin-1 (Metin et al., 1997), Sema3A/3C (Bagnard et al., 2001; Bagnard et al., 1998) and Sema5B (Lett et al., 2009), regulate the initial outgrowth of these descending cortical fibers. Initially, the CFA and CTA fiber pathways, from cortical layers V and VI, respectively, grow together into the IC, but then diverge. CTAs turn dorsally into the thalamus, whereas most of the CFAs continue into the ventral cerebral peduncle fiber bundle *en route* to lower brain targets (O'Leary and Koester, 1993; Price et al., 2006). Prior to the development of these mature axon tracts; however, descending pioneer cortical fibers from the developing cortical subplate extend in the same physical space as ascending TCA fibers, and these opposing pathways have been demonstrated to cofasciculate with each other within the VTel (Auladell et al., 2000; Molnar et al., 1998a; Molnar et al., 1998b). Over two decades ago, the "handshake hypothesis" proposed that TCAs navigate to their appropriate cortical regions by cofasciculating with reciprocal descending cortical axons encountered near the pallial/subpallial boundary (Blakemore and Molnar, 1990; Molnar et al., 1998a; Molnar and Blakemore, 1995); however, the functional importance of the "handshake" between ascending TCAs and descending CTAs for controlling topography remains controversial (Molnar et al., 2012).

Eph receptors and ephrins have broad functions in the development of the mammalian nervous system (Egea and Klein, 2007; Pasquale, 2005; Shen and Cowan, 2010), and are expressed in unique, but often overlapping, spatial and temporal patterns in the brain and body. The Eph family of receptor tyrosine kinases is divided into two subgroups: the A-class (A1-A8, A10) and B-class (B1-B4, B6), based largely on their similarity and binding preferences for ephrinA and ephrinB transmembrane ligands (Pasquale, 2005). The Eph-ephrin interaction primarily occurs upon cell-cell contact, such as when a developing axonal growth cone contacts a guidepost cell. This induces both Eph receptor forward signaling via clustering of Eph receptors and autophosphorylation of conserved tyrosine residues, as well as ephrin reverse signaling, via ephrin intracellular tyrosine phosphorylation and binding to reverse signaling adaptor molecules. In many cases, EphB receptor activation stimulates a cell-cell or axonal repulsion event coordinated by various signaling events and the reorganization of the F-actin cytoskeleton (Cowan et al., 2005; Egea and Klein, 2007; Srivastava et al., 2013). In particular, EphB1 receptors are expressed in a restricted region of the developing retina that gives rise to ipsilateral retinal ganglion cell (RGC) projection axons. EphB1 receptor forward signaling in these RGCs mediates midline turning away from the ephrinB2 ligand expressed on optic chiasm midline radial glia (Chenaux and Henkemeyer, 2011; Petros et al., 2009; Williams et al., 2003). In addition, EphB1 receptor forward signaling mediates proper interhemispheric development of the corpus callosum (Mendes et al., 2006; Soskis et al., 2012) and anterior commissure (Henkemeyer et al., 1996).

Several studies have reported developmental abnormalities in white matter tracts in autism spectrum disorder (ASD) individuals (Minshew and Williams, 2007; Mizuno et al., 2006; Wolff et al., 2012) suggesting that deficits in normal axon guidance and neuronal connectivity in

the developing brain may contribute to the pathophysiology of ASDs. The recent identification of a *de novo* nonsense mutation in the *EPHB2* kinase domain in an autistic individual (Sanders et al., 2012) potentially implicates EphB receptor forward signaling in this role. As such, understanding the role of EphB receptor forward signaling *in vivo* may provide important insights into both normal brain development and neurodevelopmental disorders such as autism. Using a variety of mouse genetic approaches, we show here that EphB1 and EphB2 receptor forward signaling, in cooperation with the ephrinB1 ligand expressed in regions surrounding the TCA fiber pathway, control reciprocal navigation of a subset of TCA and CTA fibers in the developing mouse brain. Our findings reveal that descending cortical axons selectively cofasciculate with specific TCA subpopulations in the dorsal VTel to coordinate reciprocal cortical-thalamic connectivity in the early developing brain, and they provide supportive evidence for the functional relevance of the cortical-thalamic "handshake".

Results

EphB1 and EphB2 receptors are required for proper cortical-thalamic axon guidance in the ventral telencephalon.

EphB1 and EphB2 receptors are both expressed in the developing cortex (Mendes et al., 2006; North et al., 2009), suggesting a possible role in the regulation of cortical axon guidance to subcortical target zones. To test the potential role for these receptors during cortical-thalamic axon guidance, we assessed L1-CAM-positive axons traversing the ventral telencephalon (VTel) in wild-type (WT), *EphB1*$^{-/-}$, *EphB2*$^{-/-}$, and *EphB1/2 DKO* (*EphB1*$^{-/-}$*EphB2*$^{-/-}$) total knockout mice at postnatal day 0 (P0). In *EphB1*$^{-/-}$ mice, we observed significant axon patterning defects within the VTel and adjacent to the internal capsule (IC) where descending cortical axons and TCAs

normally form a web of topographically organized axon bundles (Figure 3.1A & 3.1B). Compared to WT or *EphB2*$^{-/-}$ mouse brains, EphB1-deficient mice showed a clear disorganization of the radial array of cortical and thalamic axons spanning between the cortical intermediate zone (IZ) and the IC. In addition, we observed large axon bundles that veered away from their normal trajectory toward the IC and aberrantly projected toward the ventral brain floor at a location just medial to the external capsule (EC) (Figure 3.1D & 3.1E). Interestingly, *EphB2*$^{-/-}$ mice showed a normal axon patterning in this same region (Figure 3.1C), but *EphB1/2 DKO* mutant mice revealed a more severe axon mistargeting phenotype within the VTel compared to *EphB1*$^{-/-}$ mice (Figure 3.2A, 3.2G). In addition, we analyzed L1+ *EphB1/2 DKO* mice brains at age P0 along the sagittal plane and identified the presence of ventral axon misguidance errors almost exclusively in the lateral aspect of the ventral VTel (Figure 3.3).

EphB receptor forward signaling mediates proper axon patterning in the VTel.

To test whether the EphB1/2 receptor-dependent axon guidance in the VTel requires EphB1/2 receptor forward signaling, we analyzed truncated EphB knock-in mutant mice (*EphB1*$^{Tr/Tr}$ or *EphB2*$^{Tr/Tr}$) in which the EphB1 or EphB2 receptor intracellular domains are replaced with bacterial β-galactosidase (*lacZ*) (Chenaux and Henkemeyer, 2011; Henkemeyer et al., 1996). In *EphB1*$^{Tr/Tr}$ or *EphB2*$^{Tr/Tr}$ mutant mice, chimeric EphB receptors are expressed normally at the cell surface and mediate ephrinB-mediated reverse signaling *in vivo* while blocking intracellular forward signaling events. *EphB1*$^{Tr/Tr}$ mice showed similar axon guidance defects in the VTel as *EphB1*$^{-/-}$ mice (Figure 3.2B), suggesting that EphB1 forward signaling is critical for proper VTel cortical and/or thalamic axon guidance. Consistent with our previous findings in the total *EphB2*$^{-/-}$ knockout mice, mice lacking EphB2 forward signaling (*EphB2*$^{Tr/Tr}$)

had normal L1+ axon patterning in the VTel (Figure 3.2C), whereas *EphB1*$^{Tr/Tr}$*EphB2*$^{Tr/Tr}$ double mutant mice displayed a severe, hyperfasciculated VTel misprojection phenotype (Figure 2D). As such, our findings reveal that EphB1 and EphB2 receptor forward signaling is required for normal cortical-thalamic axon guidance *in vivo* (Figure 3.2G, Figure 3.4).

Since these truncated mutants lack the entire receptor intracellular domain, we next asked whether EphB1/2-dependent guidance defects depended upon EphB kinase domain activity, specifically, or upon another function of the intracellular domain (PDZ binding, etc). To address this question, we used an analog-sensitive EphB receptor knock-in mouse (*AS-EphB*) that possesses a point mutation in the conserved EphB kinase domain that renders mutant EphB receptors that are sensitive to the reversible kinase inhibitor, 1-NA-PP1, *in vivo* (Soskis et al., 2012). We injected timed-pregnant *AS-EphB* mutant or WT control mice twice daily with either vehicle or 1-NA-PP1 (80 mg/kg) from E12.5 to E19.0, and then assessed L1+ axons in the VTel (Figure 2E). Compared to control mice, 1-NA-PP1-injected *AS-EphB* embryos at E19.5 had significant VTel axon guidance errors, including severe ventral misprojections (Figure 3.2F), essentially phenocopying the axon guidance errors in the *EphB1/2 DKO* and *EphB1/2* truncated mutant mice (Figure 3.2G). WT vehicle- and drug-injected mice had normal axon circuitry at E19.5 (Figure 3.5). Taken together our findings indicate that EphB receptor tyrosine kinase activity is required for normal cortical-thalamic axon guidance in the VTel during brain development.

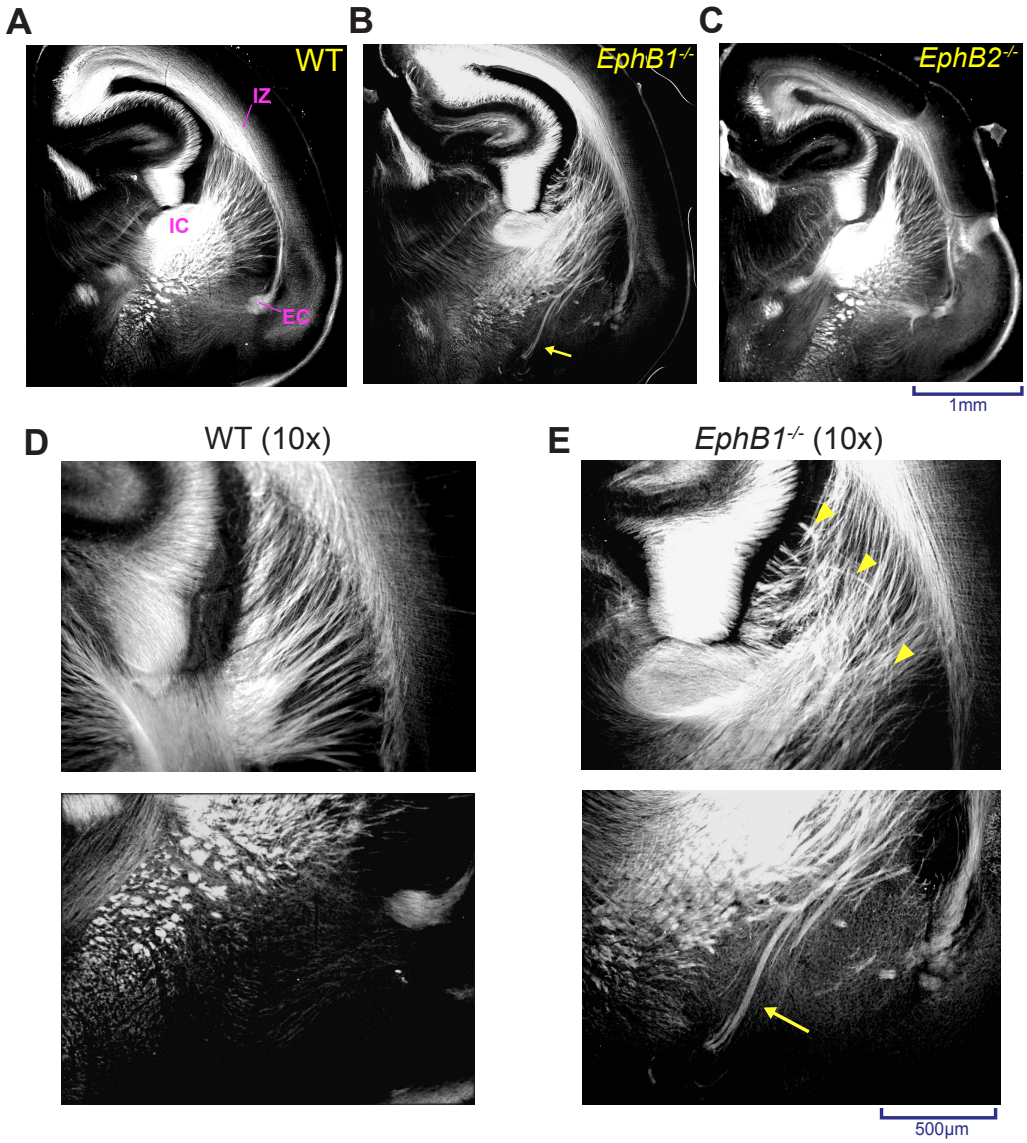

Figure 3.1. *EphB1* knockout mutants have significant axon pathfinding errors in the ventral telencephalon. *(A)* Coronal vibratome section (~ Bregma 3.7mm) through the forebrain of a wild-type (WT) mouse at postnatal day P0 immunostained with anti-L1-CAM. L1+ thalamocortical axon (TCA) and deep-layer cortical axon fiber bundles are located within the region of the ventral telencephalon (VTel) between the internal capsule (IC) and subcortical intermediate zone (IZ). The external capsule (EC) is also indicated. *(B)* Age-matched coronal section of an *EphB1*$^{-/-}$ mutant mouse forebrain, where L1+ axons in VTel is misprojected toward

the ventral floor of the VTel (arrow). *(C)* Age-matched coronal section of an *EphB2*$^{-/-}$ mutant with normal L1+ axons. *(D)* 10x magnified image of the WT brain section from *(A)* highlighting the fine topographic organization of axon bundles in the dorsal half of the VTel. (E) 10x magnified image of the *EphB1*$^{-/-}$ mutant brain from *(B)* demonstrating disorganized axon fibers in the dorsal VTel (arrowheads) and the significant axon bundle misprojection in the ventral half of the VTel (arrow), a region which is devoid of L1+ fibers in WT brains.

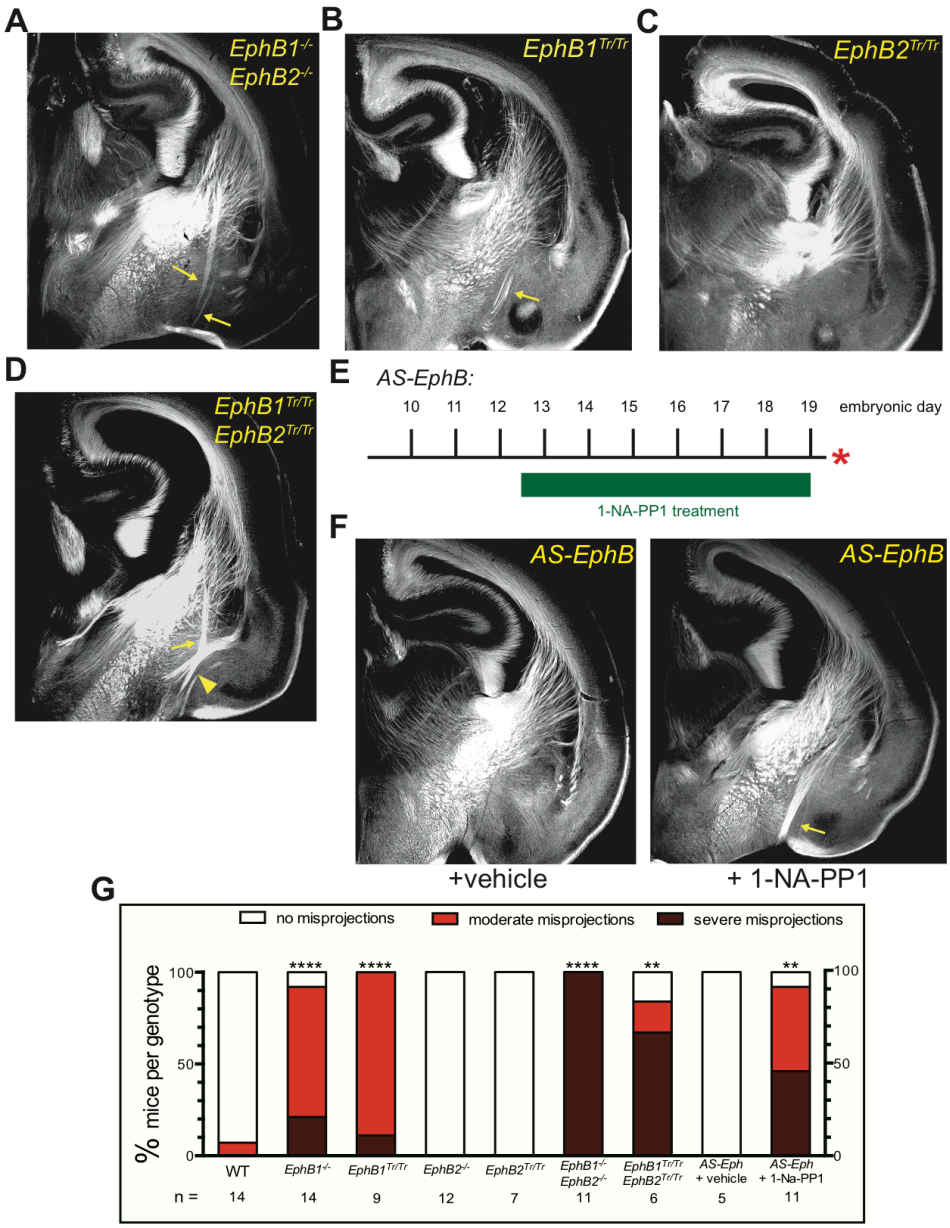

Figure 3.2. EphB receptor forward signaling mutants have forebrain axon misprojections similar to knockout mutants. *(A)* Coronal vibratome section of an *EphB1*$^{-/-}$*EphB2*$^{-/-}$ double knockout mutant mouse at postnatal day P0 immunostained with anti-L1-CAM. These compound mutants have more severe L1+ axon misprojections in the ventral half of the VTel (arrows). *(B)* L1-CAM immunostained coronal brain section of the truncated *EphB1*$^{Tr/Tr}$ mutant mouse at age P0 that is deficient for EphB1 forward signaling. A moderate L1+ axon

misprojection (that phenocopies the *EphB1*$^{-/-}$ condition - see Figure 1B) is evident in the ventral half of the VTel (arrow). *(C)* Age-matched coronal section of an *EphB2*$^{Tr/Tr}$ truncated mutant mouse with normal L1+ axons. *(D)* Age-matched coronal section of a double truncated *EphB1*$^{Tr/Tr}$*EphB2*$^{Tr/Tr}$ mutant with a severe axon misprojection in the ventral VTel (arrow). The misprojected posterior branch of the anterior commissure (ACp), a separate bundle population of interhemispheric cortical axons (Henkemeyer et al., 1996; Orioli et al., 1996), is also located in this same ventral region (arrowhead). *(E)* Drug injection schedule for 1-NA-PP1 drug treatment of timed-pregnant *AS-EphB* mutants. These mutants were administered twice-daily subcutaneous injections of 80 mg/kg body weight 1-NA-PP1 or vehicle from E12.5 - E19.0. Embryos were collected for analysis at E19.5 (asterisk). *(F)* Representative L1-CAM stained E19.5 coronal sections of *AS-EphB* embryos that were either administered 1-NA-PP1 or vehicle and immunostained with anti-L1-CAM. 1-NA-PP1-administered embryos, and not vehicle controls, demonstrate significant axon misprojections in the ventral VTel (arrow). *(G)* Combined graphical representation of VTel misprojection scores from EphB mutant conditions outlined in Figures 1 and 2. All brains were scored for either moderate VTel misprojections (as in *(B)*) or severe VTel misprojections (as in *(A)* and *(D)*). **$p<0.001$, ****$p<0.0001$, Fisher's exact test (see Figure 3.4).

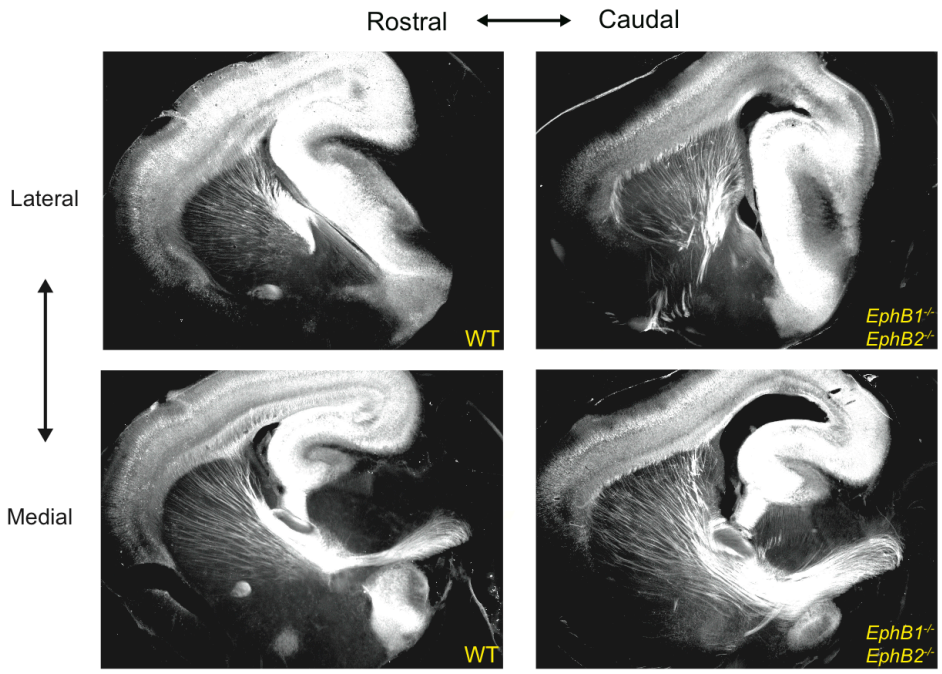

Figure 3.3. Axon misprojections in EphB-deficient mice are localized in the lateral ventral telencephalon. Sagittal vibratome sections of either P0 wild-type or *EphB1*$^{-/-}$*EphB2*$^{-/-}$ *DKO* mutant brains at a matching medial and lateral sagittal plane. Misprojected axons are largely present in the lateral *DKO* aspect. In addition, the rostral-caudal topography of axons in the VTel is maintained in *DKO* mutants.

A

	# brains with **no** misprojections	# brains with **any** misprojections	n-value
WT	13	1	14
EphB1$^{-/-}$	1	13	14
EphB1$^{Tr/Tr}$	0	9	9
EphB2$^{-/-}$	12	0	12
EphB2$^{Tr/Tr}$	7	0	7
EphB1$^{-/-}$EphB2$^{-/-}$	0	11	11
EphB1$^{Tr/Tr}$EphB2$^{Tr/Tr}$	1	5	6
AS-EphB Vehicle	5	0	5
AS-EphB Drug	1	10	11

**** p<0.0001 (Chi Square test)

B

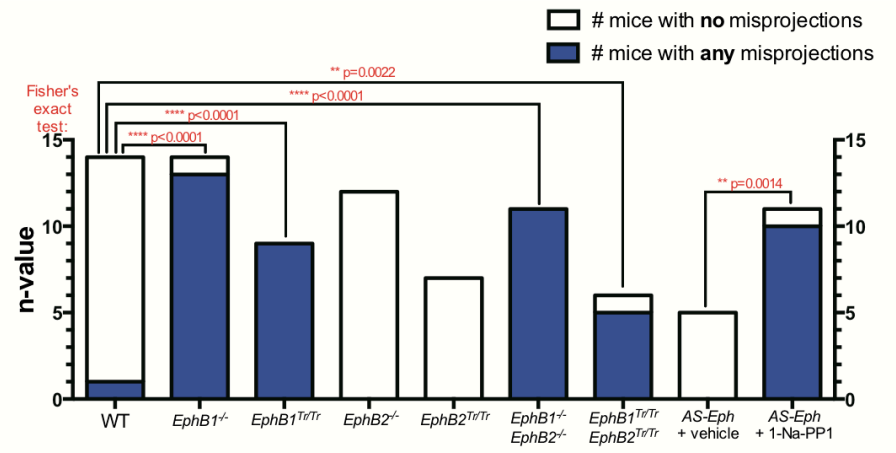

Figure 3.4. EphB mutants have a statistically significant axon misprojection phenotype. *(A)* Contingency table of scored axon misprojection phenotypes outlined in Figure 2G for Chi Square statistical analysis. All mutant misprojection scores from Figure 2G are combined in the second column. *(B)* Graphical representation of *(A)* with P-values from Fisher's exact tests performed to directly compare various mutant genotypes.

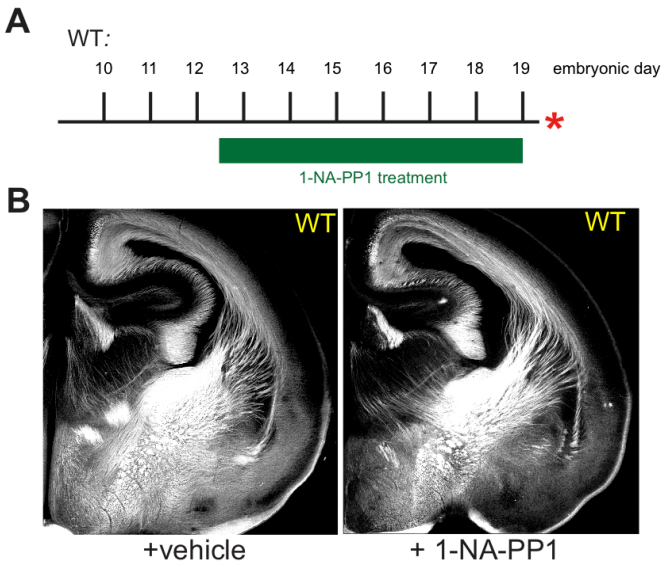

Figure 3.5. Wild-type embryos have normal VTel axon morphology upon 1-NA-PP1 drug adminstration. *(A)* Drug injection schedule for 1-NA-PP1 drug treatment of timed-pregnant *WT* mutants. These mice were administered twice-daily subcutaneous injections of 80 mg/kg body weight 1-NA-PP1 or vehicle from E12.5 - E19.0. Embryos were collected for analysis at E19.5 (asterisk). *(F)* Representative L1-CAM stained E19.5 coronal sections of *WT* embryos that were either administered 1-NA-PP1 or vehicle and immunostained with anti-L1-CAM. For both conditions, WT embryonic brains have normal L1+ VTel axon morphology (drug: n=6 & vehicle: n=4).

EphB1/2 receptors are required for thalamocortical axon guidance in the ventral telencephalon.

Since descending cortical fibers are thought to cofasciculate along TCA fascicle bundles that arrive near the cortical plate prior to the extension of subplate pioneer cortical axons, we sought to determine if either cortical and/or thalamic axons were initially misguided at embryonic timepoints. To this end, we analyzed control or *EphB1/2 DKO* mice at E14.5, a developmental stage when ascending TCAs, which are L1-CAM-positive (Fukuda et al., 1997), exclusively populate the ventral portion of the VTel and have already reached the intermediate zone (IZ) beneath the cortical plate. In contrast, descending pioneer cortical axons have only penetrated the dorsal half of the VTel at this age (Auladell et al., 2000; Jacobs et al., 2007a). We confirmed that the cortical pioneers had not yet fully extended into the VTel at this embryonic age by analyzing two different transgenic mice that express GFP in the developing cortical subplate and mature deep-layers: (1) FezF2-GFP mice that express GFP in both deep layer and subplate cortical neurons during development and in layer 5 cortical neurons specifically at postnatal ages (corticofugal axons; CFAs) (Figure 3.6A) (Kwan et al., 2008) and (2) Golli-tau-GFP mice that express tau-GFP in the subplate and selectively in layer 6 cortical neurons (CTAs) (Figure 3.6B) (Jacobs et al., 2007a). In *Fezf2-GFP; EphB1/B2 DKO* E14.5 reporter mutants, we observed clear L1+ TCA guidance defects in the ventral VTel at a time prior to the arrival of descending GFP+ cortical axons (Figure 3.6C). Finally, we confirmed that L1-CAM staining was efficiently labeling early TCA fibers at E14.5 via dual L1-CAM immunolableing and thalamic axon labeling with a lipophilic fluorescent tracer (Figure 3.6D). Thus, our findings indicate that a subset of TCAs are mistargeted in the VTel prior to the arrival of reciprocal, descending cortical fibers.

To determine when the initial TCA guidance errors occur in the VTel, we next analyzed TCA growth patterns of control or *EphB1/2 DKO* mice at E13.0, an earlier developmental stage when L1-positive TCAs have reached the floor of the brain and are turning dorsally across the diencephalic:telencephalic border (DTB) and are reported to project between the medial ganglionic eminence (MGE) and the developing globus pallidus (GP) *en route* to the cortical plate (Reviewed in (Lopez-Bendito and Molnar, 2003; Molnar et al., 2012)). Similar to E14.5 *EphB1/2 DKO* brains, we observed a mutant subpopulation of L1+ fibers that misproject laterally in the ventral VTel at E13.0 (Figure 3.6F). Some of these astray fibers show a delayed dorsal turn into the dorsal VTel (Figure 3.6G) that are reminiscent of the laterally misprojected fibers that we observed in E14.5 and P0 mutant brains.

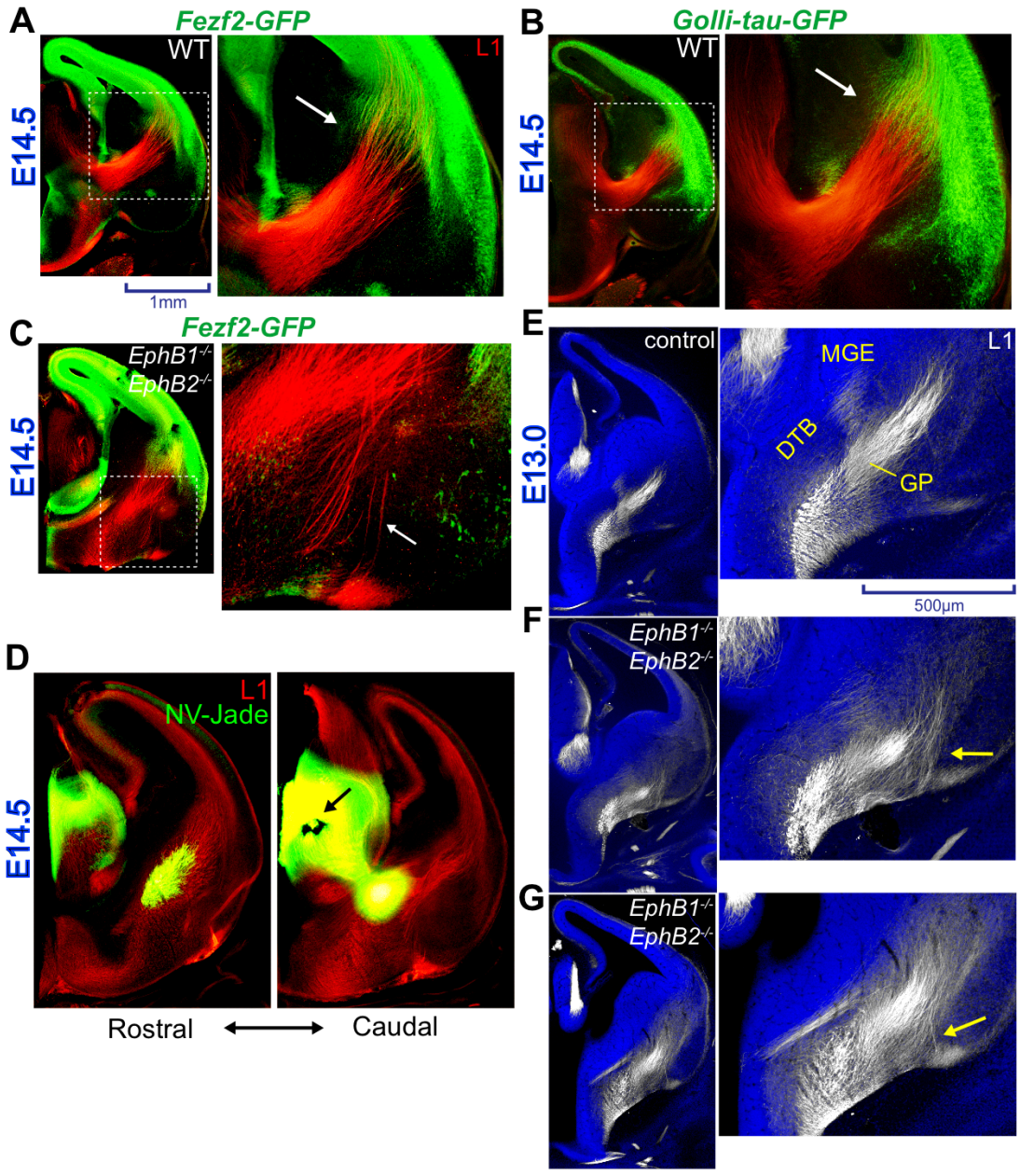

Figure 3.6. Thalamocortical axons are initially misguided in EphB-deficient mutants during early forebrain development. *(A)* A coronal section of an E14.5 *Fezf2-GFP* embryonic brain that has wild-type (WT) EphB receptor expression and is dual immunostained with anti-L1-CAM (red) and anti-GFP (green). GFP+ cortical pioneer axons have only penetrated the dorsal half of the developing VTel at this early embryonic age (arrow), while L1+ thalamocortical axons (TCAs) have developed extensively through the VTel toward the cortical

intermediate zone. *(B)* E14.5 coronal brain section of a *Golli-tau-GFP* reporter embryonic mouse that is also WT for EphB expression, and which also demonstrates the partial development of GFP+ cortical pioneers in the early VTel (arrow). *(C)* Age-matched coronal brain section of a *Fezf2-GFP* reporter mouse that is *EphB1*$^{-/-}$*EphB2*$^{-/-}$. In these mutants, L1+ TCA axons are misprojected in the ventral VTel (arrow). *(D)* Coronal brain section of a E14.5 *EphB1/B2 DKO* brain in which the thalamus is labeled with a NeuroVue-Jade fluorescent tracer (green) for 1 week at 37°C. The thalamic implantation point of the tracer is shown (arrow). NV-Jade positive axons from the thalamus grow throughout the VTel and properly overlap with L1+ TCA fibers. *(E)* Coronal brain sections of an E13.0 littermate control embryo (*EphB1*$^{+/-}$*EphB2*$^{-/-}$) that is immunostained with anti-L1-CAM (white), which labels the earliest L1+ TCA fibers in the VTel. TCA fibers in these control brains are tightly associated in a large bundle that traverses the medial VTel just lateral to the diencephalic-telencephalic border (DTB) and between the developing regions of the medial ganglionic eminence (MGE) and globus pallidus (GP). Brain sections were counterstained with Hoechst nuclear stain (blue). *(F) EphB1*$^{-/-}$*EphB2*$^{-/-}$ double mutant embryo brain sections at E13.0 that are immunostained with anti-L1-CAM (white). L1+ TCA fibers in the ventral half of the VTel of these mutants are significantly shifted toward the ventral brain floor compared to control littermates. Also, TCA fibers extend more laterally in these EphB1/2 knockout mutants compared to controls (arrow). *(G)* Another example of an *EphB1*$^{-/-}$*EphB2*$^{-/-}$ brain section at E13.0. A significant, L1+ TCA misprojection bundle is evident in the lateral VTel (arrow).

Since these findings suggest that the earliest TCA pioneer projections are misguided, we next assessed the expression patterns of the EphB1 and EphB2 receptors in the developing thalamus (Th) and VTel during the time frame when the initial TCA guidance errors occur (~E12.5). We analyzed the protein expression of EphB1 and EphB2 in *EphB1*$^{Tr/+}$ or *EphB2*$^{Tr/+}$ knock-in mice (Chenaux and Henkemeyer, 2011; Henkemeyer et al., 1996), which express β-galactosidase (*lacZ*) as a fusion protein with the extracellular domain and transmembrane region of the respective EphB protein. Using X-gal staining in these mice to detect the EphB fusion protein, we observed strong expression of EphB1-lacZ in the caudal thalamus at E13.0, particularly in a restricted dorsal-lateral region (Figure 3.7A). EphB1-lacZ receptor expression was also detected in the ventral VTel region where the ascending TCAs are located. Similar expression patterns of EphB1 in caudal thalamus and ventral VTel were observed using *in situ* hybridization at age E12.5 (data not shown), confirming that EphB1 is expressed in both regions. EphB2-*lacZ* expression was also observed in a low rostral to high caudal thalamic gradient at E13.0 (Figure 3.7B). Together, these data reveal that EphB1 and EphB2 receptors are expressed in the developing caudal thalamus and are positioned to influence TCA guidance in the VTel at ages E12.5-E13.5, when TCA guidance errors are first observed.

We next considered the possibility that the TCA guidance errors could be a result of a defective cell "corridor" between the MGE and GP regions (Lopez-Bendito et al., 2006) in *EphB1/2 DKO* mice, resulting in lateral TCA misprojections. Analysis of *Nkx2.1* expression, a marker of the MGE and GP cell populations, revealed no obvious differences in the corridor region between control and *EphB1/2 DKO* mice (Figure 3.7C). Unexpectedly, in E13.5 wild-type mice we observed that the vast majority of L1+ TCAs grow through the region of Nkx2.1-expressing neurons (GP) rather than avoiding it. At this early stage, the Nkx2.1-positive GP

neuronal population appears to roughly define the brain region through which most or all of the ascending TCAs project in the VTel, suggesting that the GP does not exclude ascending thalamic fibers at this early developmental age. However in the *EphB1/2 DKO* mice, we observed misprojected TCAs that extended laterally beyond the Nkx2.1-positive boundary (Figure 3.7C), suggesting that EphB receptors might promote avoidance of the region lateral to the Nkx2-positive GP region.

Since EphB1 and EphB2 are most highly expressed in the caudal thalamus, we labeled the rostral thalamus (Th) and caudal Th with two different anterograde lipophilic dyes to study their trajectory through the ventral VTel at the time when mutant guidance errors first occur. Interestingly, we found that caudal Th fibers in control mice, where EphB1/2 are highly expressed, populate the ventral-lateral axons within the ascending TCA fiber bundle, whereas the rostral Th fibers, where EphB1/2 expression is lower, populate the dorsal-medial TCA fiber bundle that is closest the future "corridor" region (Figure 3.7D). As such, the caudal Th axons appear to navigate through the VTel in a more ventral-lateral position within the ascending TCA fiber population, and as such, are located in a physical space closest the boundary where misprojected axon bundles are observed in the *EphB1/2 DKO* mice at E13.5. Furthermore, we found that in a similar dual anterograde dye labeling experiment in E14.5 *EphB1/B2 DKOs*, lateral VTel misprojections were exclusively labeled with the dye from the caudal Th, which demonstrates that the caudal, high-EphB1/B2 expressing Th region is indeed the origin of TCA misprojections in *DKO* mice (Figure 3.7E).

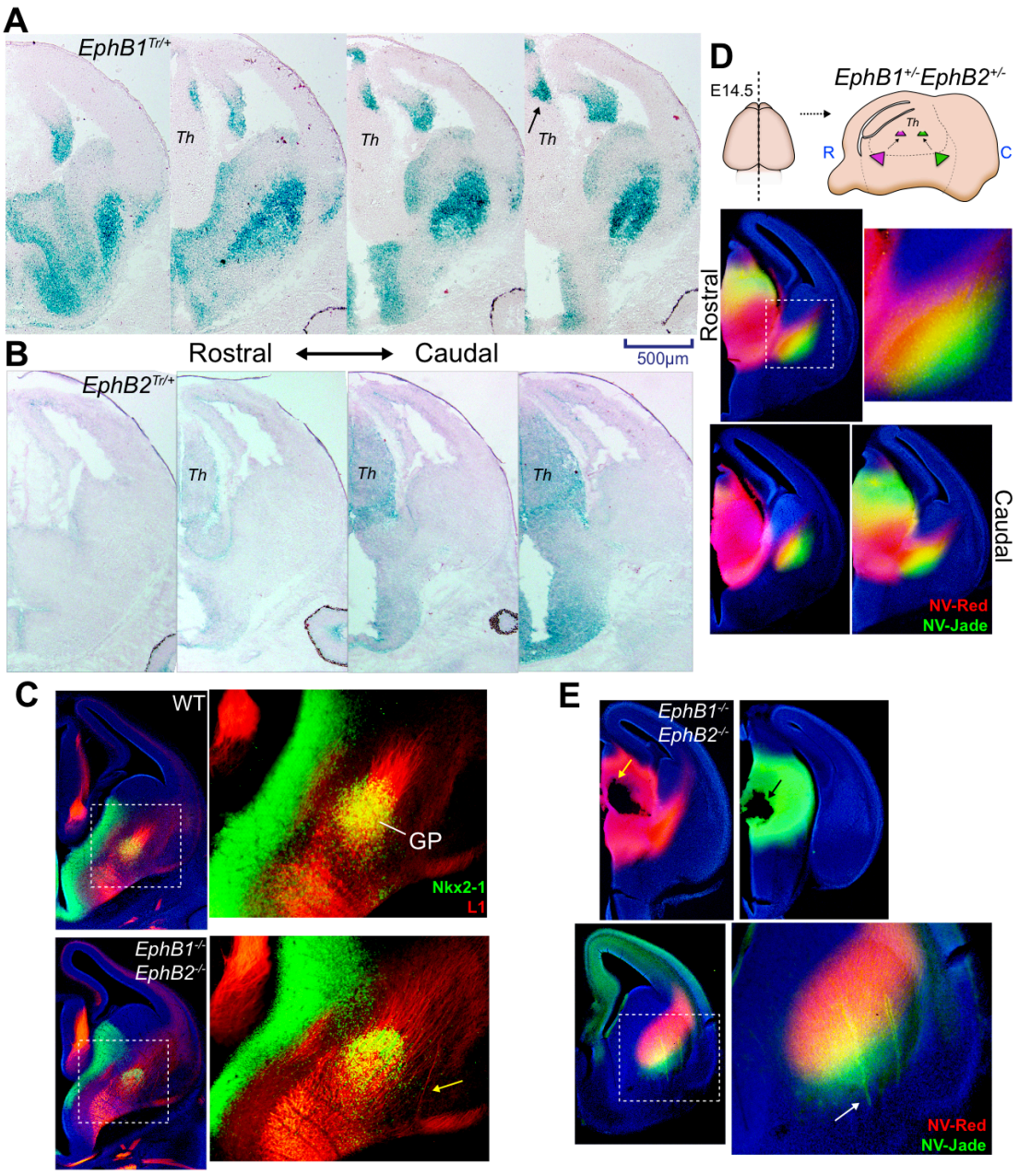

Figure 3.7. *EphB1* is expressed in the caudal thalamus, where TCA fibers are exclusively projected into the ventrolateral region of the ventral telencephalon.

(A) Coronal brain sections of *EphB1*$^{Tr/+}$ truncated mutants at embryonic age E13.0 that are stained with X-gal to label beta-galactosidase containing EphB1 truncated receptor protein. Images are arranged in sequence along the rostral-caudal plane. A strong subregion of EphB1 protein expression is concentrated in the dorsal-caudal thalamus (Th) (arrow) (n=2). *(B)* An age-

matched *EphB2*$^{Tr/+}$ mutant brain stained with X-gal. EphB2 expression is more ubiquitously expressed throughout the caudal thalamus (n=3). *(C)* E14.5 coronal brain section of a WT and *EphB1*$^{-/-}$*EphB2*$^{-/-}$ knockout mice that are dual immunostained with anti-Nkx2-1 (green) and anti-L1-CAM (red). Nkx2-1 labeled cells (green) are localized in the GP regions of the VTel, and L1-positive TCA fibers pass directly through this cell population (WT: n=2, *EphB1/B2 DKO*: n=4). The L1+ misprojection in the *EphB1/B2 DKO* mutant brain (arrow) is located lateral to the Nkx2-1-positive GP region. *(D)* Diagram of the dual thalamic axon-labeling paradigm in E14.5 *EphB1*$^{+/-}$*EphB2*$^{+/-}$ control brains. Brains were hemisected along the midline prior to dye insertion. NeuroVue-Red (NV-Red) tracer was placed in the rostral thalamus (Th) and NeuroVue-Jade (NV-Jade) was placed in the caudal thalamus. Brains were incubated for 1 week at 37°C before coronal vibratome sectioning. Coronal sections of labeled brains with TCA fibers from the rostral Th (red) project through the dorsal half of the VTel alongside TCAs from the caudal Th (green) that project through the ventrolateral region of the VTel. The two axon populations overlap in the medial VTel (yellow). *(E)* Labled coronal brains sections from the same dual thalamic axon tracing paradigm as (D) but in E14.5 *EphB1/B2 DKO* mutants. Implantation points for NV-Red in the rostral Th (yellow arrow) and NV-Jade in the caudal thalamus (black arrow) are shown. Caudal-traced axons (green) are exclusively miswired in the ventrolateral region of the VTel (white arrow) (n=3).

Corticofugal and corticothalamic axons are misprojected in EphB mutant mice.

We next sought to address whether the misprojected L1+ axons observed at P0 in the VTel of *EphB1/2 DKO* mice were exclusively astray thalamic fibers or whether they were cofasciculated with descending cortical axons. During normal development, CFA (layer 5) and CTA (layer 6) fiber projections navigate together through the VTel and into the IC (O'Leary and Koester, 1993; Price et al., 2006), and are thought to cofasciculate with ascending thalamic fibers. To address this question, we crossed *EphB1/2 DKO* mice with the aforementioned transgenic reporter mice - *FezF2-GFP* mice to identify postnatal layer 5 CFAs (Kwan et al., 2008) and *Golli-tau-GFP* mice to detect layer 6 CTAs (Jacobs et al., 2007a) - and analyzed both L1+ and GFP+ axons at P0. In *EphB1/2 DKO* mice, misguided L1+ axons co-localized nearly completely with GFP in either transgenic mouse line (Figure 3.8). We also observed colocalization of GFP with most of the disorganized fibers within the ventral aspect of the caudate putamen (Figure 3.9), indicating that these disorganized fiber bundles also contain CTA and CFA axons. We did not observe GFP+ axons that were not co-localized with L1+ fascicles, suggesting that CTA/CFA fibers do not display TCA-independent axon guidance errors in *EphB1/2 DKO* mice. Together, these findings strongly suggest that a subpopulation of CTAs/CFAs navigate along the aberrant TCA fiber tracks that are established earlier during mutant brain development.

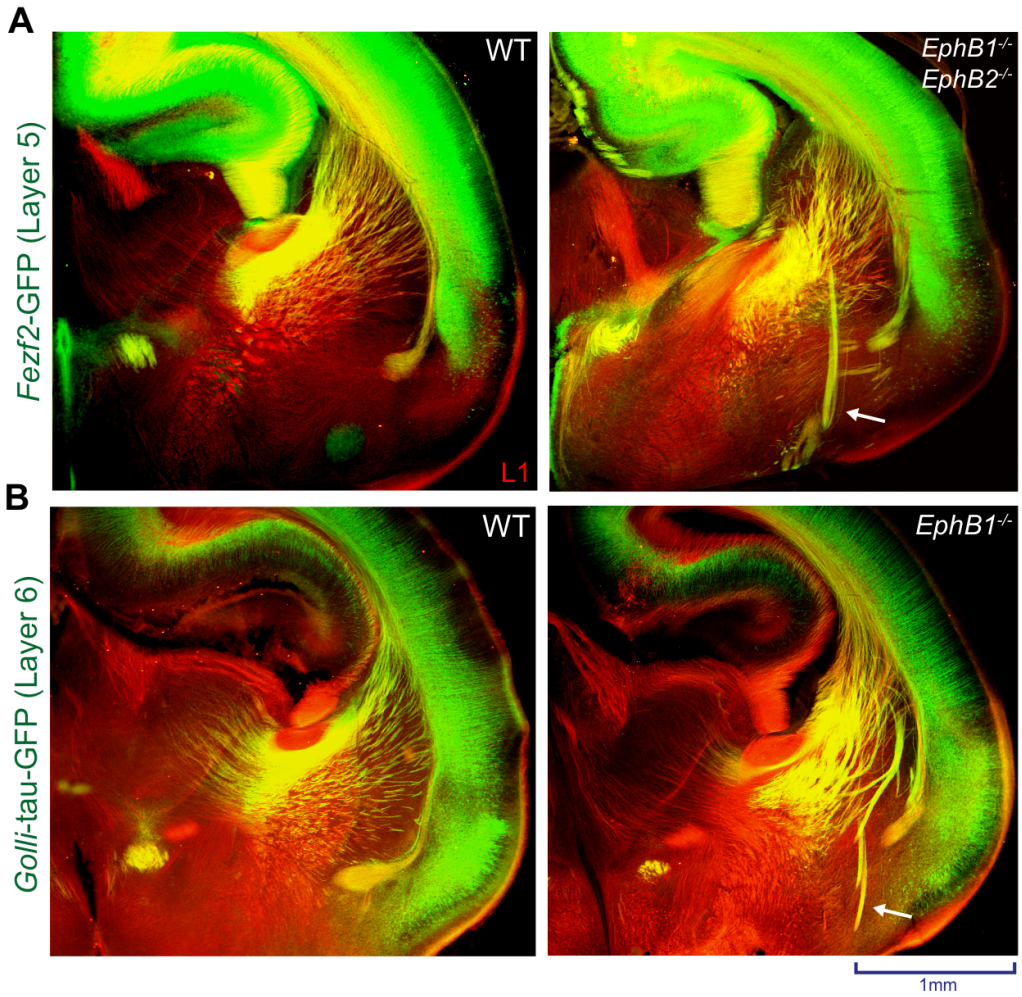

Figure 3.8. Deep layer corticothalamic and corticofugal axons are misprojected in the ventral telencephalon of EphB-deficient mice. *(A)* Coronal sections (~ Bregma 3.7mm) of postnatal P0 brains from cortical layer 5 specific *Fezf2-GFP* reporter mice that are either WT for EphB receptor expression or EphB-deficient: *EphB1*$^{-/-}$*EphB2*$^{-/-}$. GFP+ axons from cortical layer 5 (green) are misprojected in *EphB1/B2 DKO* reporter brains and directly co-localize with L1+ misprojected axons (arrow) (n=3). *(B)* Similar coronal brain sections of P0 cortical layer 6 specific *Golli-tau-GFP* reporter mice that are either WT or *EphB1*$^{-/-}$ single knockout mutants. GFP+ axons from cortical layer 6 are also misprojected in *EphB1*$^{-/-}$ brains, and these axon bundles also directly co-localize with L1+ misprojected axon fascicles (arrow) (n=2).

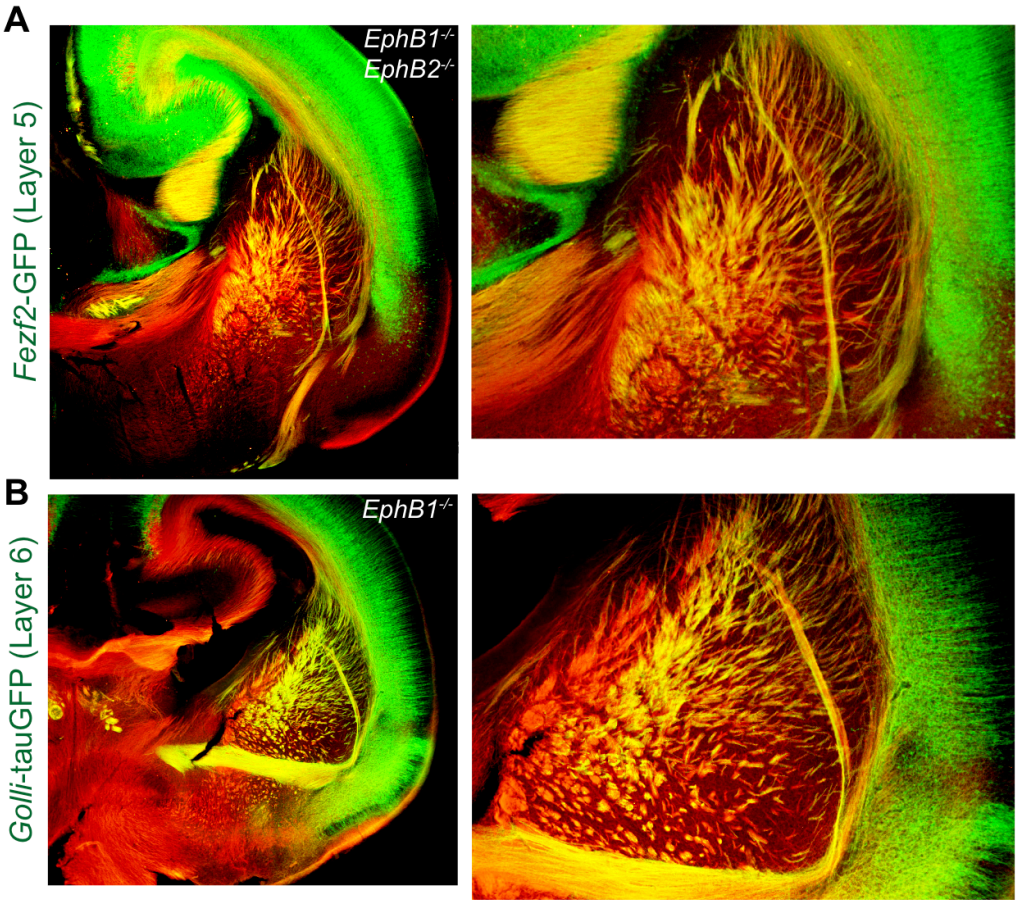

Figure 3.9. Deep layer corticothalamic and corticofugal axons are miswired in a disorganized fashion in the ventral telencephalon of EphB-deficient mice. *(A)* Coronal sections (~ Bregma 3.4mm) of postnatal P0 brains from cortical layer 5 specific *Fezf2-GFP* reporter mice that are either WT for EphB receptor expression or EphB-deficient: *EphB1*$^{-/-}$ *EphB2*$^{-/-}$. A large GFP+ axon bundle from cortical layer 5 (green) is severely misplaced within the VTel (caudate putamen area) of EphB1/B2 DKO reporter brains and is directly co-localized with a L1+ miswired axon bundle. *(B)* Similar coronal brain sections of P0 cortical layer 6 specific, *Golli-tau-GFP* reporter mice that are either WT for EphB1 or are *EphB1*$^{-/-}$ mutants. Here again, a large GFP+ axon bundle from cortical layer 6 is also miswired in the VTel of *EphB1*$^{-/-}$ brains. This axon bundle also directly co-localizes with an L1+ misprojected bundle.

Aberrant CTA/CFA misprojections navigate along misguided TCA fascicles in EphB-deficient mutants.

Our findings strongly suggest that in the absence of EphB1/2 receptor kinase activity, the cortical axon guidance mutant phenotype is an indirect result of the cofasciculation of descending cortical axons along misguided TCA fiber fascicles. To explore this idea further, we analyzed *Fezf2-GFP; EphB1/2 DKO* mice at E16.0, a developmental stage when GFP+ cortical axons are rapidly descending through the VTel and approaching the IC. We observed that individual aberrant descending cortical axons (GFP) exclusively co-localize with misprojected L1-positive TCA fascicles in the VTel (Figure 3.10A). We failed to observe GFP-positive fibers that misprojected independent of TCA fascicles, suggesting that mistargeted, mature CTA/CFA fibers are an indirect result of pioneer cofasciculation with aberrant TCA fibers tracts established earlier in development. At an earlier time point (E14.5) when cortical fibers are midway through the VTel, we also observe descending cortical fibers that are extending along, and highly intermingled with, thalamic fibers tracks (Figure 3.6A), strongly suggesting that cortical axons become misprojected due to cofasciculation with pre-existing aberrant thalamic axon bundles.

To further test whether CTA/CFA guidance errors were an indirect result of earlier TCA guidance errors, we transiently inhibited EphB kinase activity in the *AS-EphB* knock-in mice during an early developmental period when TCA axons are navigating through the ventral half of the VTel, but prior to the period of cortical axon extension into the VTel. Injection of timed-pregnant *AS-EphB* dams with 1-NA-PP1 from E12.0-E14.5, a time frame that spans early TCA guidance through the VTel, resulted in robust axon guidance defects when analyzed at E19.0 (Figure 3.10B). Indeed, only two 1-NA-PP1 injections at E12.0 and E12.5 was sufficient to produce misguided VTel axons reminiscent of the total knockout mice (Figure 3.10B), albeit to a

weaker degree, indicating that the EphB receptor kinase activity is essential during this early critical period of TCA guidance through the ventral half of the VTel. Moreover, our findings strongly support the conclusion that mutant cortical misprojections are an indirect consequence of earlier TCA guidance errors.

Misprojected cortical axons in EphB receptor knockout mice originate from localized subregions of the neocortex.

Axon guidance molecules are often expressed as gradients, and these molecular gradients often assist with maintaining general topographic organization of brain structures. Since EphB1/2 receptors are expressed in the caudal thalamus, and reciprocal connectivity of the developing TCA and CTA projections maintains topographic organization (Dufour et al., 2003; Lopez-Bendito and Molnar, 2003; Seibt et al., 2003; Torii and Levitt, 2005), we speculated that the aberrant descending cortical axons would originate preferentially from caudal-regions of the neocortex. Alternatively, the descending cortical fibers might randomly associate with TCA fibers during the "handshake" period. To explore this idea in an unbiased manner, we placed NeuroVue® carbocyanine dye-soaked filters (MTTI) into random positions across the entire cerebral cortex in WT or *EphB1/2 DKO* fixed mouse brains (P0), and analyzed anterograde-labeled, descending axons under experimenter-blinded conditions (Figure 3.10C). Using this assay, we efficiently labeled only a limited number of descending cortical axon fibers for each implanted brain (Figure 6D), and traced the dye through the entire cortical axon trajectory past the IC and into the thalamus or cerebral peduncle (Figure 3.11). Using a heat map of original dye placements along the neocortex (Figure 3.10E), we observed that the misguided VTel fibers in the *EphB1/2 DKO* brains did not concentrate in caudal cortical regions, nor were they evenly

distributed across the entire cortex as predicted in a random handshake model, but instead the aberrant cortical fibers originated from two discrete cortical subregions (Figure 3.10E, red boxes). The largest cortical subregion mapped to an area within the putative somatosensory cortex, whereas the smaller cortical subregion localized to the border regions of the somatosensory and auditory cortex. Taken together our findings suggest that descending axons from discrete cortical subregions selectively cofasciculate with the aberrant TCA fiber bundles in *EphB1/2 DKO* mice. These findings also suggest that EphB1/2-mediated TCA guidance does not simply function to maintain rostral-caudal topographic organization, but might selectively regulate reciprocal connectivity of cortical-thalamic subregions during the initial interaction between thalamic and cortical fibers in the dorsal VTel region below the developing cortical subplate.

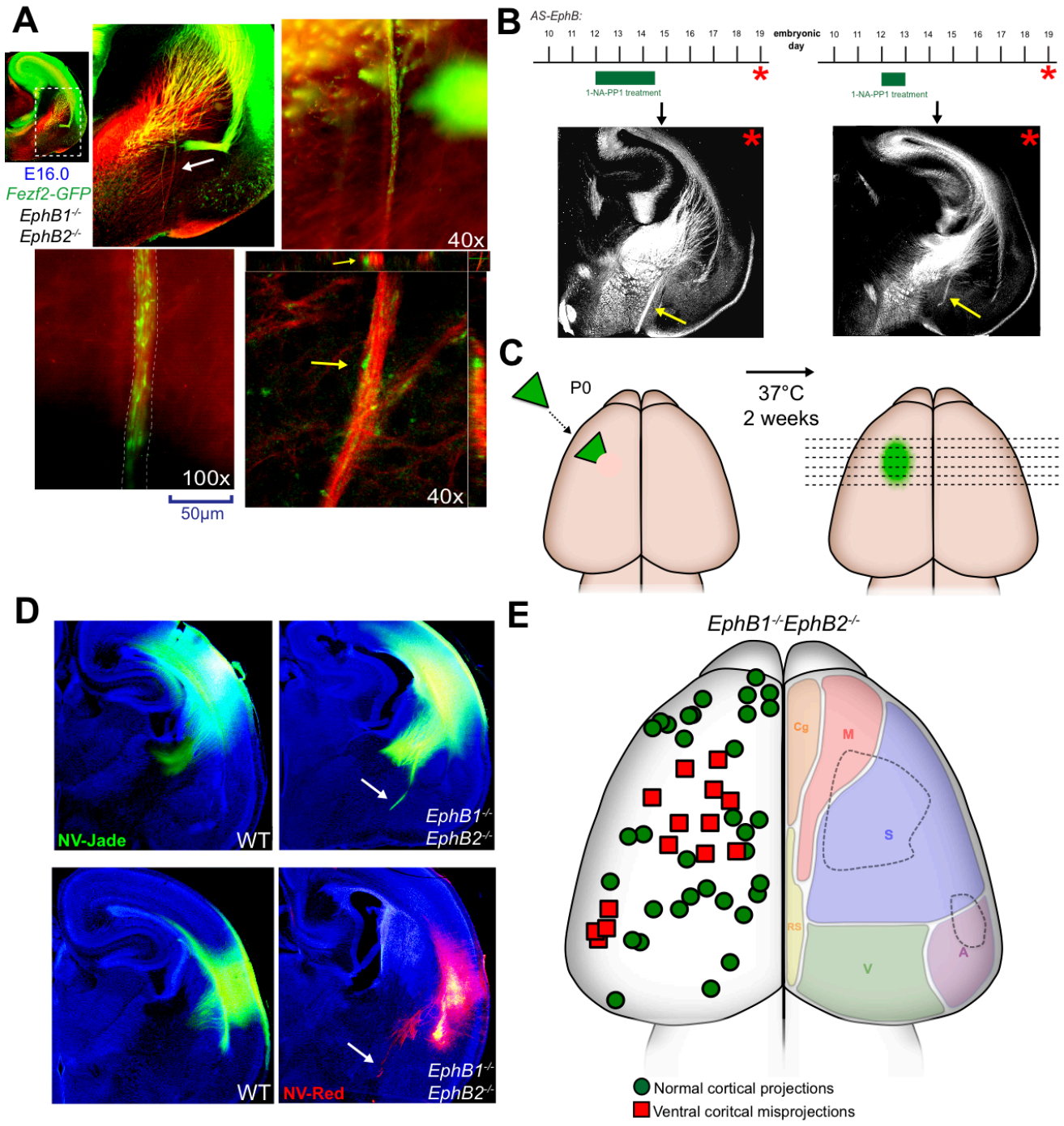

Figure 3.10. Descending cortical axon misprojections originate from two specific neocortical subregions and co-fasciculate with misprojected thalamocortical axons fascicles. *(A)* Coronal section of a *Fezf2-GFP*; *EphB1*$^{-/-}$*EphB2*$^{-/-}$ reporter mutant mouse brain at

mid-embryonic age E16.0 that is dual immunostained with anti-GFP (green) and anti-L1-CAM (red). L1+ misprojected TCA axon bundles in the ventral regions of VTel are colocalized with GFP+ cortical axons that have cofasciculated onto the misprojected TCA bundle (white arrow). At high magnification (40x & 100x), individual axon fibers and growth cones (green) are discernable along the L1+ misprojected bundle (the L1+ bundle is outlined with dashed white line at 100x). A confocal X-Y-Z reconstruction at 40x magnification of the dual stained misprojection bundle demonstrates the direct association and cofasciculation of a GFP+ cortical axon with the L1+ bundle (yellow arrows). *(B)* Drug injection schedule for short-term 1-NA-PP1 drug treatment in timed-pregnant *AS-EphB* mutants. Twice daily injections of 80 mg/kg body weight drug were administered for the embryonic time points indicated (green box). Embryos were collected for analysis at E19.0 (asterisk) and fixed for immunoanalysis with anti-L1-CAM. Most short-term drug injected *AS-EphB* E19.0 brains, for both injection schedules, had significant L1+ VTel misprojections (arrows) (E12.0-E14.5 schedule: 4/6 = 66.6% & E12.0-E13.0 schedule: 4/6 = 66.6%). *(C)* Diagram of the subregion-targeted, neocortical anterograde axon tracing assay in P0 brains with NeuroVue-Jade (or NV-Red) fluorescent tracer filters. *(D)* P0 coronal brain sections of either WT or *EphB1/B2 DKOs*, in which the NV tracer was inserted into neocortical regions that labeled VTel axon misprojections in *EphB1/B2 DKO* brains (arrows). Brain sections were counterstained with Hoechst nuclear stain (blue). *(E)* Neocortical heat map of 48 separate neocortical labeling experiments. The left hemisphere of the heat map diagram indicates the NV tracer insertion points that represent the cell body origins of labeled CTAs within the VTel. Labeled regions with normal CTA projections are marked with a green circle on the heat map and ventral CTA misprojections are marked with a red square. The right hemisphere diagrams the functional regions of the mouse cortex (A - auditory, Cg - cingulate, M

- motor, RS - retrospenial, S - somatosensory, V- visual). The two localized cortical subregions of VTel misprojections are outlined with a dashed line the right side of the diagram.

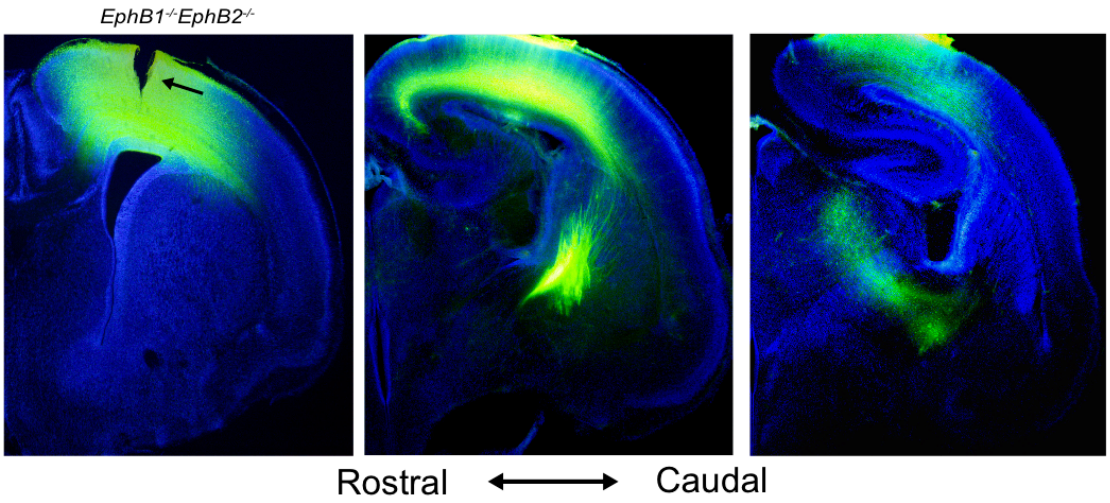

Figure 3.11. Anterograde dye tracing from the neocortex labels the entire length of descending cortical axons. P0 coronal sections of an *EphB1/B2 DKO* brain at postnatal day P0 that are labeled with NV-Jade tracer that is implanted into the dorsal neocortex (arrow). Descending CFAs from this neocortical origin point are labeled along their entire shaft length through the VTel, IC and Th. Labeled axons from this example *DKO* brain do not become misprojected in VTel. Brain sections were counterstained with Hoechst nuclear stain (blue).

EphrinB1 is required for the proper TCA guidance in the ventral telencephalon.

In most cases, EphB receptors are activated by binding to their high-affinity, transmembrane ephrinB ligands. To determine the potential *in vivo* ligand for EphB1/2-dependent TCA guidance, we first assessed a likely candidate, *ephrinB2*. In retinal development, midline glial expression of ephrinB2 stimulates repulsive axon turning of EphB1-expressing RGC axons originating from the ventrotemporal retina. This gives rise to the ipsilateral component of the developing optic tract (Williams et al., 2003). In addition, we observed that ephrinB2 is expressed in the ventral-lateral VTel at E13.0 (Figure 3.12). Since *ephrinB2*$^{-/-}$ mutant mice die prenatally at ages E9 - E10 due to cardiac valve formation defects (Cowan et al., 2004), we used floxed *ephrinB2* conditional knockout (cKO) mice (*ephrinB2*^{loxp}) to create conditional deletions of *ephrinB2* (Gerety and Anderson, 2002). Mutant *ephrinB2*$^{loxP/loxP}$ mice were crossed with Cre recombinase-expressing transgenic mice to generate cKO mice. We generated *ephrinB2* cKOs using either *Nestin*^{Cre}, which generated cortical plate-specific recombination by E13.5, or *FoxG1*^{Cre}, which generated brain-wide recombination by E13.5 (Figure 3.12). Neither of these ephrinB2 cKO mice had any apparent cortical-thalamic guidance defects (Supp. Figure 3.12), revealing that *ephrinB2* is dispensable for TCA guidance.

We next analyzed ephrinB1 protein expression levels at E12.5 – E14.5 using a Tet-inducible *ephrinB1*^{rtTA}*;TetO-tdTomato* reporter mouse line. In these reporters at E12.5 and E13.5, we observed high levels of ephrinB1 expression in ventral-lateral VTel regions, dorsal VTel regions, and throughout the cortical plate but no detectable expression in the thalamus (Figure 3.13, Figure 3.8: *ephrin*$^{+/+}$ control). Interestingly, at E13.5 we also observed a strong subregion of ephrinB1 expression along the ventral brain border where TCA fibers are misguided in EphB-deficient conditions (see Figure 3.6E & 3.6F), as well as the near complete

absence of ephrinB1 in the TCA axon-spanning region of the ventral VTel (Figure 3.13A). At E14.5, the expression of ephrinB1 has retreated from the VTel and is observed within the cortical plate in a radial-like pattern reminiscent of radial glial cells. To test whether *ephrinB1* was the relevant ligand for TCA guidance, we created early, brain-wide *ephrinB1* cKO mice (*FoxG1*$^{Cre/+}$*; ephrinB1*$^{loxP/Y}$). In this case, we observed significant TCA guidance errors at E13.5 that were similar to those seen in the *EphB1/2 DKO* mice, strongly suggesting that ephrinB1 is the relevant ligand for EphB1 in normal TCA guidance (Figure 3.13B). Taken together, the strong expression of ephrinB1 in the regions surrounding the ascending TCA fiber bundles, and the appearance of TCA guidance errors in the ventral region of the VTel in brain-specific ephrinB1 cKO mice, strongly suggest that ephrinB1 protein in the lateral VTel functions to promote proper EphB1/B2-dependent dorsal-medial turning of caudal TCAs in the VTel.

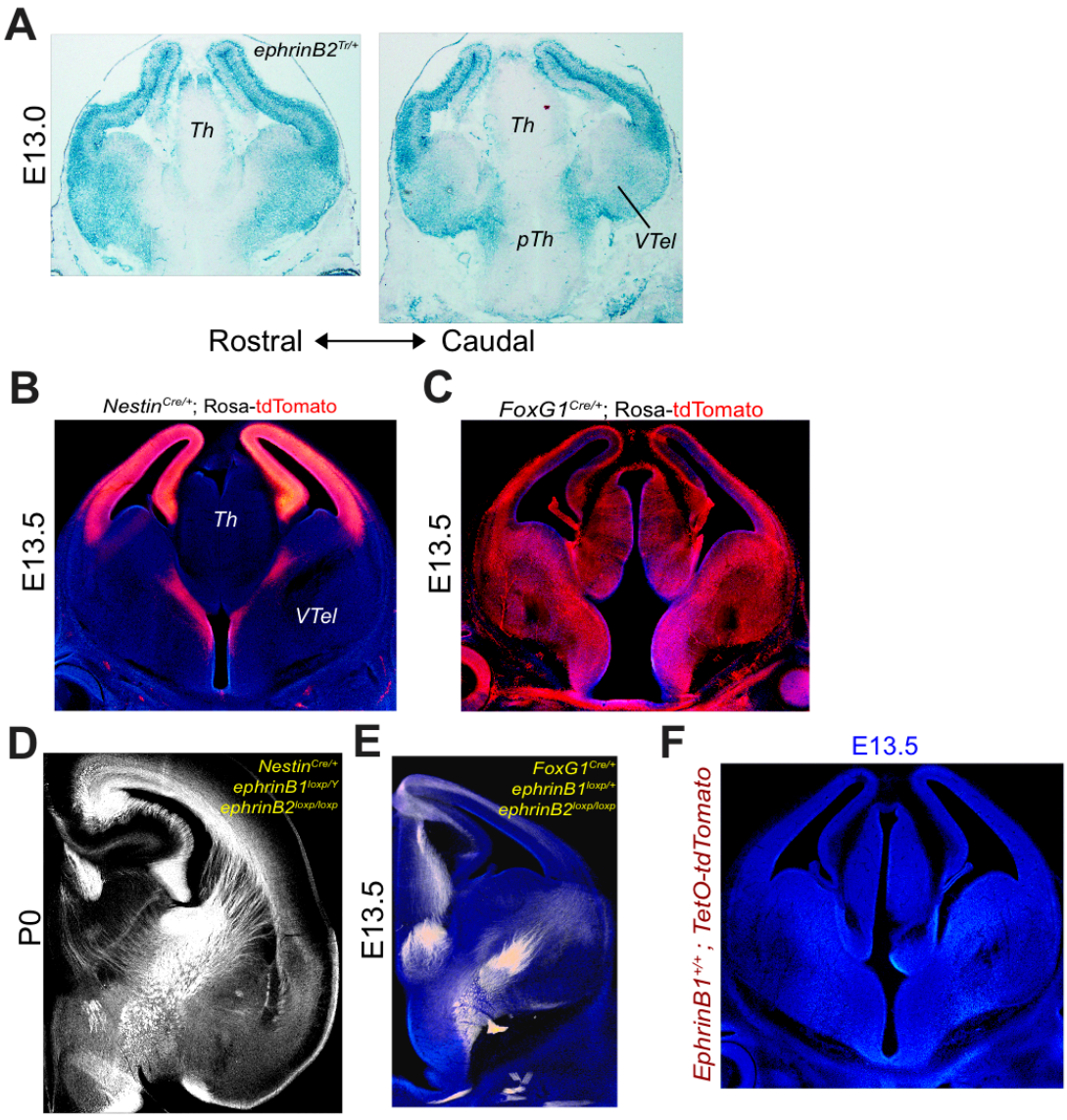

Figure 3.12. EphrinB2 is not required for proper TCA guidance in the ventral telencephalon. *(A)* Coronal brain sections of an *ephrinB2*$^{Tr/+}$ truncated mutant brain at embryonic age E13.0 stained with X-gal to label beta-galactosidase containing ephrinB2 truncated receptor protein. At this age, ephrinB2 is highly expressed throughout the entire telencephalon including in the VTel where TCA axons are located; however, ephrinB2 is only lightly expressed in the thalamus (Th) and prethalamus (pTh) (n=3). *(B)* Representative coronal section of an E13.5 embryonic brain containing the Nestin-Cre driver allele and *Rosa-tdTomato*

reporter gene. Tomato signal (red) represents Nestin-Cre expression, which is specifically localized to the dorsal telencephalon including the developing cortical plate and hippocampal anlage, as well as migrating cells at the ventral midline. *(C)* Coronal section of a P0 *ephrinB1*$^{loxp/Y}$;*ephrinB2*$^{loxp/loxp}$ conditional mutant containing the Nestin-Cre driver allele. These conditional knockout brains have normal axon wiring (n=6), which indicates that the Nestin-Cre driven conditional deletion of ephrinB1/2 is not sufficient to phenocopy EphB receptor knockout axon miswiring phenotypes. *(D)* Representative coronal section of an E13.5 embryonic brain containing the FoxG1-Cre driver allele and *Rosa-tdTomato* reporter gene. Unlike Nestin-Cre, FoxG1-Cre expression (red) at this age is ubiquitously expressed throughout the entire brain and other regions of the embryonic head (n=3).

(E) Coronal brain section of an E13.0 *ephrinB1*$^{lox/+}$; *ephrinB2*$^{loxp/loxp}$ conditional knockout embryo containing the FoxG1-Cre driver allele. These conditional knockout embryos also have normal TCA axon wiring at this early age (n=3) demonstrating that a single copy of ephrinB1 is sufficient for proper TCA axon development, and that ephrinB2 in VTel is not necessary for the proper guidance of these axons. *(F)* Control brain section of an *ephrinB1*$^{+/+}$*; TetO-tdTomato* reporter embryo at age E13.5 that is clear of non-specific tdTomato fluorescence.

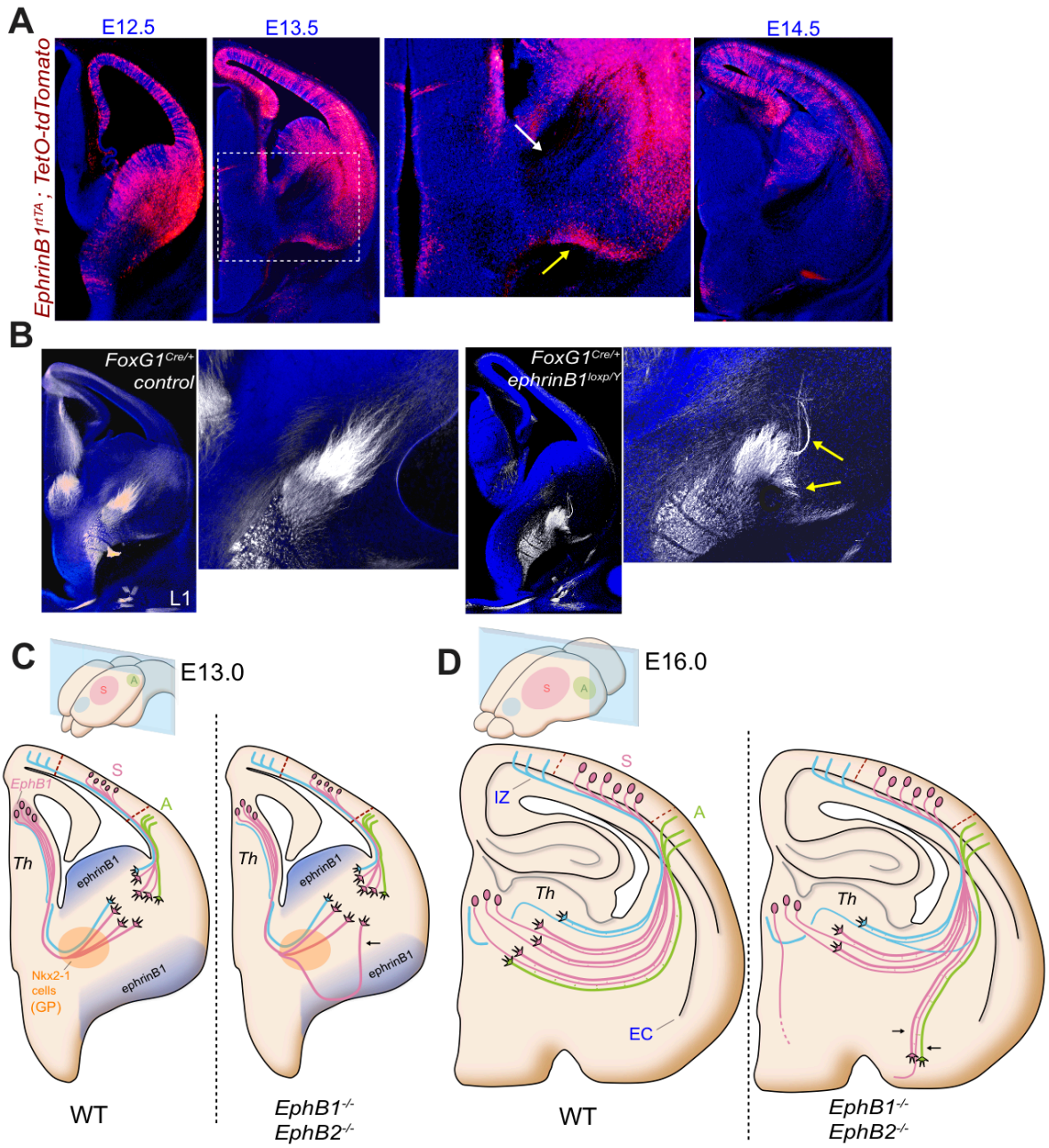

Figure 3.13. EphrinB1 conditional knockout mutants have significant axon pathfinding errors in the ventral telencephalon. *(A)* Coronal brain sections of *ephrinB1-rtTA; TetO-tdTomato* reporter embryos from ages E12.5, E13.5 and E14.5 (each n=2). Tomato fluorescence (red) represents ephrinB1 protein expression in these sections, which is high in the VTel at ages E12.5 and E13.5, but absent in this region at E14.5. In E13.5 reporter embryos, ephrinB1 is

expressed as a boundary around the medial VTel where developing TCA axons are located (white arrow: region devoid of counterstain). A strong region of ephrinB1 expression forms the boundary along the ventral floor of the brain (yellow arrow) where TCA fibers are misprojected in EphB-deficient conditions. *(B)* Coronal sections of FoxG1-Cre positive ephrinB1 control (*ephrinB1*$^{loxp/+}$) and *ephrinB1*$^{loxp/Y}$ hemizygous conditional knockout (cKO) embryonic brains immunostained with anti-L1-CAM (white). L1+ TCA fibers develop normally and in a tight bundle through the medial VTel in FoxG1-Cre positive controls (n=2), whereas ventrolateral TCAs are significantly miswired in FoxG1-Cre positive *ephrinB1*$^{loxp/Y}$ hemizygote cKO embryos (n=5 for FoxG1-Cre+ male *ephrinB1*$^{loxp/Y}$, n=2 for FoxG1-Cre+ female *ephrinB1*$^{loxP/loxp}$ (not shown)). Brain sections were counterstained with the Hoechst nuclear stain. *(C)* Model diagrams depicting the mechanism of EphB receptor mediated TCA guidance through the VTel at age E13.0 in wild-type and *EphB1/B2 DKO* conditions. A subset of TCA fibers is misprojected in the ventral region of the VTel in the knockout diagram (arrows). *(D)* Model diagrams of cortical-thalamic wiring at embryonic age E16.0 in wild-type and *EphB1/B2 DKO* conditions. A subpopulation of descending cortical fibers from the somatosensory cortex (“S”, pink) and auditory cortex (“A”, green) selectively cofasciculates along TCA misprojections that originate, in part, from the caudal thalamus where EphB1 is highly expressed. EC - external capsule, IZ - cortical intermediate zone, Th – thalamus

Discussion

In this study, we find that EphB1, and to a lesser extent EphB2, receptor kinase-dependent signaling play an essential role in the proper guidance of thalamocortical axons in the ventral telencephalic region of the developing mammalian forebrain *in vivo*. We find that EphB1 and EphB2 receptors are highly expressed in the developing caudal thalamus, at a time when these TCAs are turning from the ventral-portion of the VTel toward the developing cortical plate, and we show that EphB kinase inhibition during this critical time frame results in TCA guidance errors. In addition, we show that the *ephrinB1* ligand is expressed in regions surrounding the developing TCA fibers in the VTel, and ephrinB1 conditional brain knockout mice have TCA guidance errors similar to *EphB1/2 DKO* mice. Finally, we find that CTA fibers from discrete cortical subregions selectively navigate along the misprojected, EphB1/2-dependent TCA fibers. This suggests that specific thalamic relay nuclei might interact selectively with descending cortical axons from specific functional cortical subregions and specify reciprocal connectivity at the point of the initial TCA/CTA interactions in the VTel.

While revealing a novel role for EphB receptor forward signaling in TCA guidance, our findings also raised a number of interesting observations and important questions for future investigation. The major contributor to the TCA/cortical-thalamic guidance phenotypes, the EphB1 receptor, is highly expressed in the caudal thalamus during TCA navigation in the VTel (Figure 3.7A). Interestingly, this caudal Th region preferentially populates the most ventral-lateral portion of the ascending TCA axons (Figure 3.7B), which are just adjacent to the lateral VTel region (i.e. lateral to the Nkx2.1-expressing GP region) that highly expresses ephrinB1 at this developmental time window (Figure 3.13A & 3.13C). Based on the expression patterns of EphB1 and ephrinB1, and the timing and location of axon guidance errors in the VTel, our

findings suggest that EphB1 receptors in the caudal Th neurons mediate the avoidance of regions lateral to Nkx2.1+ GP that express ephrinB1. We also detect EphB1-lacZ protein in the VTel regions where ascending TCA axons are located. Some of this EphB1-lacZ signal likely represents axonal EphB1, but clearly the cells within the GP region also express EphB1, which could also be contributing to the TCA guidance process. In the future, the generation of conditional knockout mice with thalamic or VTel-selective EphB1 gene deletion will better address the question of whether EphB1 in dorsal thalamic neurons functions cell-autonomously to mediate normal TCA guidance or whether EphB1 in cells of the VTel mediates its function.

Despite the expression of both EphB1 and EphB2 in caudal thalamus, only the EphB1 receptors are essential for TCA guidance, with EphB2 appearing to play only a partial compensatory role. A similar observation was made in developing retinogeniculate projections that express both EphB1 and EphB2 in the ventro-temporal crescent of the retina; however, only the EphB1 receptor is required for ephrinB2-dependent midline repulsion at the optic chiasm (Chenaux and Henkemeyer, 2011; Petros et al., 2009; Williams et al., 2003). There are a number of possible non-mutually exclusive reasons for the differences between EphB1 and EphB2, including: (1) EphB1 is more highly expressed in dorsal thalamic neurons or their axon growth cones than EphB2 receptors, (2) EphB1 has a higher affinity for the cell surface-encountered ephrinB1 ligand, or (3) EphB1 receptors are more efficient at stimulating repulsive axon guidance signaling, possibly via EphB1-specific signaling pathways. Recently we found that addition of soluble, clustered ephrinB2/Fc to cultured embryonic cortical neurons stimulated EphB2 receptor-dependent growth cone collapse (Srivastava et al., 2013). However, addition of soluble, clustered ephrinB1/Fc, even at very high concentrations, failed to induced collapse, suggesting that ephrinB1 inefficiently stimulates EphB2 receptor-mediated repulsive axon

guidance in some contexts. Interestingly, overexpression of wild-type, but not kinase inactive, EphB1 receptors in the developing retina resulted in the conversion of some axons destined for the contralateral optic tract to the ipsilateral path (Petros et al., 2009). In contrast, overexpression of EphB2 in the retina did not efficiently generate ipsilateral projecting axons. Chimeric receptors of EphB1 and EphB2 revealed that the extracellular domain and transmembrane region of EphB1 were critical for its ability to promote midline repulsion at the optic chiasm, suggesting that EphB1 has unique functional properties that enable it to preferentially mediate repulsive axon guidance in some contexts.

Our findings revealed that descending cortical axons from two discrete cortical subregions (somatosensory and auditory cortex) closely intermingle with misprojected TCAs in the *EphB1/2 DKO* mice (Figure 3.13C), suggesting that cortical and thalamic axons do not randomly cofasciculate during development, but instead are more specifically targeted. Based on our findings, we propose that descending axons from specific cortical subregions selectively interact with specific thalamic axons, and that this selective interaction is critical for pre-establishing reciprocal connectivity between specific thalamic relay nuclei and specific functional subregions within the developing cortex. Since select somatosensory/auditory region CTAs appear to tightly co-mingle with the misguided TCAs in the EphB mutant mice (Figure 6E), we speculate that unique and specific cell surface proteins (*e.g.* cell adhesion molecules) are expressed on the surface of select cortical and thalamic axons, and this molecular "code" might determine specific cortical and thalamic axons interactions and subsequent reciprocal cofasciculation. Our current findings suggest that EphB1 receptors and ephrinB1 are assisting in the proper navigation of caudal thalamic axons within the VTel. However, EphB1 and ephrinB1 do not likely specify the selective cofasciculation of somatosensory and auditory CTAs with

these caudal TCAs. Rather, the spatial location of the caudal TCAs during the dorsal turn in the VTel places them near the outermost boundary of TCA fibers, where repulsive axon guidance may be critical for navigation toward the cortical subplate region. In the future, it will be important to identify the exact cortical neurons that fasciculate with mistargeted TCAs in the EphB1 KO mice in order to better understand the mechanisms by which cortical axons selectively interact with the TCAs, and to test the role of these interactions in reciprocal connectivity later in development.

The handshake hypothesis, first proposed more than 20 years ago, was based on the observation that deep layer cortical axons and TCAs closely interact or "co-mingle". As such, it was proposed that the handshake between these reciprocal fibers might be critical for guiding these axons to their target synaptic zones (Blakemore and Molnar, 1990; Molnar and Blakemore, 1995; Molnar et al., 2012). Here, we propose that cofasciculation between ascending TCAs and descending CTAs might depend upon precise developmental timing and thalamic/cortical subregion specificity. However, several past studies have provided evidence against the general handshake hypothesis, including the demonstration that axons from cortical and thalamic explant (or dissociated neuron) co-cultures do not directly cofasciculate or co-mingle (Bagnard et al., 1998; Deck et al., 2013). Perhaps the absence of cofasciculation in these studies might be explained by the experimental conditions used. For instance, precisely timed cofasciculation signals might be expressed primarily during the time when TCAs and cortical pioneer axons first interact. Thus thalamic explants taken from later developmental stages (*e.g.* E16.0) might grow indiscriminately into any cortical region *in vitro* (such as in (Molnar and Blakemore, 1991; Molnar and Cordery, 1999)) once the critical time window has passed. Similarly, if there were subregion-specific cofasciculation molecules, as we propose here, then analysis of specific

thalamic and cortical axon subpopulations would be critical for analyzing cofasciculation in *in vitro* studies. In the future, it will be important to determine whether other cortical subregions selectively co-mingle with unique thalamic subregion axons, or whether our observations are unique to the caudal Th and the somatosensory/auditory cortex subregions identified. While our current study doesn't directly test the selective interaction hypothesis, our findings do strongly support the general idea of the handshake hypothesis, and further extend its implications for coding reciprocal connectivity.

Many studies have described the guidance mechanisms that properly guide TCA fibers along their lateral and longitudinal pathways to the developing neocortex (reviewed in (Lopez-Bendito and Molnar, 2003)). Other systems, such as cell migration within the developing VTel have been proposed to organize a permissive corridor that is essential for the proper topographic development of TCAs (Bielle et al., 2011a; Bielle et al., 2011b; Deck et al., 2013; Lopez-Bendito et al., 2006). These studies have established that *Nkx2.1*-expressing cells in the GP migrate from the MGE during early development to mark the ventral corridor boundary. In our studies, we observed that most TCA fibers migrate through the Nkx2.1+ GP region at E12.5-E13.5, the timepoint when the TCAs are first extending through the VTel region. Using a dual anterograde dye labeling method, we observed that the rostral Th neurons extend axons proximal to the future "corridor" region, consistent with earlier studies; however, caudal Th regions extend axons through the ventral-lateral Nkx2.1 region (Figure 3.7C). As such, it appears that the rostral-caudal Th axis corresponds roughly to a medial-lateral axis of ascending TCAs at E13.0. In prior studies, the TCA "corridor" was defined in large part based on anterograde dye labeling from rostral dTh regions and analysis of TCA tracts at E17.5. By analyzing earlier time-points and multiple positions with the Th, our data suggest that the Nkx2.1+ GP region is largely permissive

at E13.0 and is populated predominantly with caudal thalamic axons. Our "corridor" analysis did not extend beyond E13.5; therefore, it is possible that at later developmental stages (e.g. E17.5), the GP helps to organize TCA fibers into a more structured bundle within the IC.

A recent study by Deck et al. (2013) proposes that layer VI CTA descending projections follow a distinct pathway through the IC corridor from layer V CFAs which develop directly through the ventral globus pallidus (GP) region. In our study using transgenic mice that label cortical layer V postnatally (Fezf2-GFP, (Kwan et al., 2008)) or cortical later VI (Golli-tau-GFP, (Jacobs et al., 2007a)) axons throughout the entire cortex, we observe a close overlap of the total population of CTA and CFA projection paths, suggesting that as a global population, cortical axons from layers V and VI descend toward the internal capsule by growing along the entire TCA fiber population. In the former study (Deck et al., 2013), the authors specifically labeled cortical axon projections from one cortical location (i.e. a region of the somatosensory neocortex). Their findings suggest that descending layer V and VI axons from the same cortical subregion adopt distinct trajectories within the VTel toward the IC. In the future, it will important to explore why the global projection patterns of deep layer cortical projections are distinct from specific subregions.

Previous studies have demonstrated a key role for ephrinA5, as well as EphA4/A7 receptors, in the rostral-caudal development of TCA fibers in the VTel (Dufour et al., 2006; Dufour et al., 2003; Torii and Levitt, 2005). In null mutant mice lacking these genes, a large population of TCAs is shifted caudally within the striatum due to the disruption of a low rostral - high caudal ephrinA5 striatal gradient that normally directs EphA-expressing TCA fibers toward the rostral cortex. In contrast to these studies, our findings reveal a distinct function for EphB1/2 receptors in TCA development. In our experiments, EphB1 appears to be expressed in discrete

subregions of the thalamus and VTel at E13.5 (Figure 3.7A), and ephrinB1 is largely expressed in the intermediate target vicinity, and appears to function as a repellant lateral boundary for developing TCAs. Other guidance factors, such as Slit11/2 and Sema5B, have also been reported to be necessary for TCA guidance and display a boundary expression in the VTel (Bagri et al., 2002; Lett et al., 2009) suggesting that during TCA axon development, rostral-caudal topography in the VTel is maintained by repulsive gradients, whereas medial-lateral topography is dependent upon local, repulsive boundaries.

Autism spectrum disorders (ASDs) are characterized by early developmental deficits in social interactions, language development, and repetitive or restrictive behaviors. In addition, sensory hyper- or hyposensitivity is common in ASD (Ben-Sasson et al., 2008; Crane et al., 2009; Leekam et al., 2007). Recent studies suggest that autism may be a result of abnormal white matter tract development and abnormal cortical and thalamic connectivity (Cheng et al., 2010; Just et al., 2004; Minshew and Williams, 2007; Mizuno et al., 2006; Shukla et al., 2011; Wolff et al., 2012). Interestingly, whole-exome sequencing of ASD families from the Simons Simplex Collection (SSC) identified a significant overabundance of *de novo* nonsynonymous single nucleotide variants (SNVs) in probands compared to unaffected siblings (Sanders et al., 2012). The most significant finding involves the excess of extremely rare, highly disruptive *de novo* nonsense mutations in probands, which collectively carry large effects (odds ratio >5). One of these identified nonsense mutations was found in the kinase domain of the *EPHB2* gene, revealing it as a new candidate autism risk gene. In light of our present findings implicating EphB1 and EphB2 receptors in thalamocortical development, it will be interesting to explore the possible role of these genes, and this developmental process to the pathophysiology of autism. However, it is also important to note that EphB2 receptors also play roles in formation of the

anterior commissure and corpus callosum, as well as the formation and plasticity of excitatory synapses in the brain (Henkemeyer et al., 2003; Henkemeyer et al., 1996; Kayser et al., 2006; Mendes et al., 2006; Orioli et al., 1996; Soskis et al., 2012).

Taken together, our findings here describe a novel role for EphB1 and EphB2 receptors in the process of thalamocortical axon guidance, and indirectly reveal that select cortical axons cofasciculate with specific, ascending thalamic axons adjacent to the cortical intermediate zone, strongly supporting the handshake hypothesis. This suggests that selective interactions between specific ascending TCAs and descending cortical axons establish proper reciprocal connectivity in early development via selective cofasciculation.

Materials and Methods

Animals: EphB receptor knockout and knock-in transgenic mice used in this study, including *EphB1*$^{-/-}$ and *EphB2*$^{-/-}$ mice, were previously described (Henkemeyer et al., 1996; Williams et al., 2003). *EphB1*$^{-/-}$*EphB2*$^{-/-}$ receptor double knockout mice were generated through the cross breeding of single knockouts. *EphB1*$^{Tr/Tr}$ and *EphB2*$^{Tr/Tr}$ truncated knocking mice (previously notated as *EphB1*$^{T\text{-}lacz}$ and *EphB2*^{lacz}) express a C-terminal truncated fusion protein that contains the extracellular and transmembrane domains of the receptor fused to beta-galactosidase (Chenaux and Henkemeyer, 2011; Henkemeyer et al., 1996). The resulting EphB-beta-galactosidase fusion proteins lack their respective intracellular tyrosine kinase catalytic domain and PDZ binding motifs, and in the case of *EphB1*$^{Tr/Tr}$, also lack critical juxtamembrane tyrosine residues. *EphB1*$^{Tr/Tr}$*EphB2*$^{Tr/Tr}$ compound mutants were generated through the cross breeding of single truncated knock-ins. The generation of *EphB1*^{T697G}*EphB2*^{T699A}*EphB3*^{T706A} analog sensitive EphB triple knockin mice (*AS-EphB*) has been recently reported (Soskis et al., 2012).

EphrinB1^{loxp} and *EphrinB2*^{loxp} conditional knockout mice were previously characterized (Davy et al., 2004; Gerety and Anderson, 2002). X-linked, floxed ephrinB1 is deleted in both male hemizygotes (*ephrinB1*$^{loxp/Y}$) and female homozygotes (ephrinB1$^{loxp/loxp}$) upon Cre recombination (Davy et al., 2004). Floxed ephrin mutants were crossed with both *Nestin*^{Cre} recombinase mice (a generous gift from Dr. Amelia Eisch) and *Foxg1*^{Cre} mice were acquired from Jackson Laboratories (Strain: B6.129P2(Cg)-*Foxg1*$^{tm1(cre)Skm1}$*/J*, Stock #006084) (Hebert and McConnell, 2000). *EphrinB2*^{Tr} transgenic mice (previously notated as *EphrinB2*^{lacZ}*)* express a truncated ephrinB2 protein fused to beta-galactosidase that does reach the cell surface (Dravis et al., 2004). *Rosa-tdTomato* and *TetO-tdTomato* mice were acquired from Jackson laborartories (Strain: B6;129S6-Gt(ROSA)26Sor$^{tm9(CAG-tdTomato)Hze}$/J, Stock #007905 & Strain: STOCK Tg(tetO-tdTomato,-Syp/EGFP*)1.1Luo/J, Stock #012345) (Li et al., 2010; Madisen et al., 2010). The *Fezf2-GFP* reporter line was previously described and expresses GFP overwhelmingly in mature layer V cortical neurons and cortical pioneer axons (Kwan et al., 2008). The *Golli-tau-GFP* reporter mouse line was previously characterized to express GFP exclusively in mature layer VI cortical neurons and pioneer cortical axons during early developmental stages (Jacobs et al., 2007a). Reporter mice containing deleted *EphB* alleles were generated through cross breeding. For PCR genotyping, DNA was extracted from tissue samples of dissected mouse embryos or pups with 100% isopropanol after an intervening lysis step. PCR was performed using the extracted DNA in a total volume of 25µl using the primer sets described previously (Chenaux and Henkemeyer, 2011; Davy et al., 2004; Gerety and Anderson, 2002; Henkemeyer et al., 1996; Williams et al., 2003). All animal procedures were in accordance with the Institutional Animal Care and Use (IACUC) guidelines.

Generation of BAC-Tg-ephrinB1-rtTA mice: *BAC-Tg-ephrinB1-rtTA* (abb: *ephrinB1-rtTA*) mice contain the second generation reverse tetracycline transactivator, *rtTA-2sM2*, knocked into the ORF of BAC *ephrinB1* sequences. Transgenic mice were generated as follows: BAC clone RP23-110A15, a BAC from a C57BL/6J background containing 27 kb upstream of the ephrin-B1 start codon, was purchased from the BACPAC resources center at the Children's Hospital Oakland. The cDNA for *rtTA-2sM2* was targeted into the *ephrin-B1* ORF in RP23-110A15 using bacterial homologous recombination:

(http://web.ncifcrf.gov/research/brb/recombineeringInformation.aspx).

Briefly, RP23-110A15 was first transformed into EL250 strain cells, and then targeted with a modified pL451 vector containing an Frt-sandwiched Neo/Kan cassette and the cDNA for *rtTA-2sM2*, flanked by 500 bp homology arms (the targeting vector is thus *500bpLHA-rtTA-2sM2-Frt/Neo/Kan/Frt-500bpRHA*) guiding the cassette to the ORF of *ephrinB1*. Arabinose induction of *flpe* activity in the targeted BAC was then utilized to excise the Frt-Neo/Kan-Frt cassette, leaving *rtTA-2s-M2* followed by a single copy of *Frt* in the ephrinB1 ORF. Proper targeting of the *ephrinB1* ORF was confirmed by PCR and restriction endonuclease digests. Pronuclear injection of fertilized oocytes with this *BAC-Tg-ephrin-B1-rtTA* construct was performed by Transgenic Core facilities at the Department of Developmental Biology at the University of Texas Southwestern Medical Center. *EphrinB1*^{rtTA} mutants were cross bred with *TetO-tdTomato* mice to yield the *ephrinB1*^{rtTA}*;TetO-tdTomato* reporter line. Doxycylcine (Dox) induction of *ephrinB1-rtTA*;*TetO-tdTomato* animals was performed systemically for ~48 hrs. by feeding animals Dox-treated chow (0.625 g/kg doxycycline hyclate, Harlan #TD.08541) and including Dox in the drinking water (3 mg/ml).

Tissue Processing: Embryonic brains used in this study were obtained at appropriate time points from timed-pregnant dams, where embryonic day 0 (E0) is defined as midnight prior to the morning a vaginal plug is observed. Pregnant dams were killed by CO_2 asphyxiation, after which embryos were immediately harvested for processing. Postnatal P0 pups were killed via quick decapitation. For E12.5 - E14.5 embryos, heads were removed and immediately post-fixed in 3.7% formaldehyde. For E15.5 and older embryos, as well as for P0 postnatal pups, brains were dissected away before post fixation in 3.7% formaldehyde or a 4% paraformaldehyde /2% sucrose solution. All post-fixed tissue was fixed at 4°C for 48 hours before rinsing with phosphate-buffer saline (PBS) and storage at 4°C in PBS + 0.02% Na-Azide.

Beta-Galactosidase Staining: Procedure previously described (Chenaux and Henkemeyer, 2011; Henkemeyer et al., 1996). Briefly, unfixed brain tissue was quickly frozen with optimal cutting temperature medium. Frozen brains were then sectioned on a cryostat at 25µm thickness and allowed to air-dry overnight. Sections were washed with PBS and incubated in Beta-Gal Staining Solution (Mirus Bio #2600B) overnight at 37°C. Stained sections were washed again with PBS, counterstained with 0.025% nuclear fast red, and mounted with Aquamount (Thermo Scientific).

Immunohistochemistry: Immunohistochemical staining of free floating brain sections was performed on 70 µm coronal brain sections obtained from fixed brains embedded in a 1.5% (w/v) mix of 0.75% Low-Melting Point Agarose (Promega) and 0.75% standard Agarose (Fisher) and cut on a Leica VT 1000P vibratome. Sections were immersed in blocking solution (5% normal donkey serum, 1% BSA, 0.2% glycine, 0.2% lysine with 0.3% TritonX-100 in PBS)

and incubated on a rotating shaker for 1 hour at room temperature. Sections that were previously labeled with carbocyanine dye (see section below) were blocked with the same blocking solution except with 0.01% TritonX-100. Sections were next incubated overnight at 4°C with either rat anti-L1-CAM, 1:200 (Millipore, MAB5272MI), rabbit anti-GFP, 1:2000 (Life Tech., A11122), and/or rabbit anti-TTF1 (anti-Nkx2-1), 1:200 (Abcam, 20441) diluted in blocking solution. Sections were washed three times with PBS before fluorescent secondary antibody incubation with either Cy3-conjugated donkey anti-rat IgG (Jackson) and/or Alexa488-conjugated goat anti-rabbit IgG (Life Tech). Sections were counterstained with 50µg/ml Hoechst 33342 nuclear stain (Life Tech. #H21492) diluted in 1xPBS for 5 minutes at room temperature and serially mounted onto glass slides with Aquamount.

Axon Tracing: Anterograde dye tracing of deep layer cortical axons and thalamic axons was performed using focal application of NeuroVue® Jade or NeuroVue® Red carbocyanine dye filters (MTTI) placed directly into either the neocortex of fixed P0 brains or the thalamus of fixed hemisected E14.5 brains. Dye-implanted P0 brains were incubated 2 weeks at 37°C and implanted E14.5 brains were incubated for 1 week at 37°C for adequate anterograde axon tracing before sectioning. All dye-labeled brains were embedded in 1.5% agarose before 70µm coronal vibratome sectioning. Sections were either serially mounted onto glass slides with Aquamount (Thermo Scientific) and counterstained with Hoechst 33342 (Life Tech. - 50ug/ml) or were subsequently immunolabeled for anti-L1-CAM (see above section). Focal application points of the NeuroVue dye filter within the neocortex were mapped and diagramed using a P0 developing mouse brain atlas (Paxinos, 2007).

In Vivo 1-Na-PP1 Delivery: 1-NA-PP1 was synthesized as described previously (Blethrow et al., 2004; Soskis et al., 2012). Pregnant female WT or *AS-EphB* triple knockin mice were injected subcutaneously twice daily with 80mg/kg 1-NA-PP1 dissolved in 10%DMSO, 20% Cremaphor-EL, 70% saline for the embryonic timepoints required. E19.0 or E19.5 dams were killed by CO_2 asphyxiation and embryonic brains were harvested and processed as described above.

Analysis of Axon Misguidance Phenotypes: L1-CAM or GFP immunolabeled brain sections, dye-labeled sections, and counterstained sections were imaged on an epifluorescent microscope using standard Cy2, Cy3, and UV filters. Photomicrograph images were produced using an Olympus DP70 CCD digital camera, and images were prepared using MS PowerPoint and Adobe Photoshop. Confocal z-stack images were obtained on a Zeiss LSM 510 Meta confocal microscope and X-Y-Z plane image analysis was performed with Volocity software (Perkin Elmer). Pseudocoloring and adjustments to image brightness, contrast, and color balance were made for image clarity. Model diagrams were made on MS PowerPoint and Adobe Illustrator software. Cortical and thalamic "misprojections" were scored as L1-CAM positive axon fibers that turned in a ventral fashion away from the internal capsule. The moderate misprojection phenotype was classified by the observation of a few thin axon bundles that became misprojected, whereas severe misprojection brains were classified by the presence of several misprojected fibers or thick misprojected fiber bundles. All scoring analyses were experimenter-blinded.

Data Analysis: The Chi Square analysis and Fisher's exact test were used to determine statistical

significance in the axon misguidance phenotype scoring experiments. Statistics were compiled and graphs were designed using GraphPad Prism software.

Chapter 4

EphB Receptor Forward Signaling Regulates the Interhemispheric Development of Corpus Callosum and Anterior Commissure Axons

Summary

The two hemispheres of the mammalian forebrain are linked together by major white matter tracts that bridge the telencephalic midline to complete essential intracortical circuit pathways. Two of these are the corpus callosum (CC) and anterior commissure (AC) that develop across the dorsal and ventral midlines, respectively. The development of these two pathways requires numerous subtle molecular interactions and events, many of which remain uncharacterized. Here, we analyze the role of EphB1 and EphB2 receptor forward signaling during the axon guidance of CC and AC axons. We observe a partial and complete agenesis of the corpus callosum (AgCC) as well the comple misprojection of the posterior branch of the AC (ACp) in EphB1/2 forward signaling deficient mutants. We also show that EphB1/2 are required for the earliest stages of ACp axon guidance during embryonic development, and uncover a novel function for these EphB receptors in early axon fate determination within the developing neocortex.

Introduction

The Eph receptors are a large family of axon guidance receptor molecules that interact with their surface bound ligands, the ephrins, to mediate many developmental processes in the central nervous system (CNS), including growth cone turning during axon pathfinding (Egea and Klein, 2007; Pasquale, 2005; Shen and Cowan, 2010). The molecular interaction between the Ephs and ephrins generally triggers growth cone repulsion through the activation of bidirectional intracellular signaling pathways. Eph receptor-mediated signaling is termed "forward" signaling, while ephrin-mediated signaling is termed "reverse" signaling. Both forward and reverse signaling mechanisms are essential for Eph-ephrin axon repulsion (Cowan and Henkemeyer, 2002; Egea and Klein, 2007; Holland et al., 1996). The Eph receptors are classified as either EphAs or EphBs based on their binding preference to either the GPI (Glycophosphatidylinositol) anchored ephrinAs or the transmembrane ephrinB ligand proteins, respectively. In particular, EphBs and ephrinBs have been found to be key regulators of axon guidance during the development of white matter tracts in the mammalian CNS. These include *in vivo* studies of the optic nerve tract, thalamocortical pathway, and commissural spinal cord midline development (Chenaux and Henkemeyer, 2011; Kadison et al., 2006; Kullander et al., 2001b; Robichaux et al., 2013; Williams et al., 2003), in addition to developmental studies on two major commissural axon tracts of the mammalian forebrain: the corpus callosum (CC) and anterior commissure (AC) (Henkemeyer et al., 1996; Mendes et al., 2006; Orioli et al., 1996).

The CC is an interhemispheric tract that connects layer II/III and layer V cortical neurons, and is essential for the integration of motor, sensory and cognitive circuits between the cortical hemispheres (Innocenti et al., 1995). The formation of the CC occurs between embryonic stages E15.5 - E18 and is a complex process involving multiple axon guidance factors

and stages, including CC axon-glial interaction around the midline (Mendes et al., 2006; Ozaki and Wahlsten, 1992; Rash and Richards, 2001; Shu and Richards, 2001). In the developing brain, EphB1 and EphB2 are both highly expressed in the cortical plate near the dorsal zone where CC axons eventually cross the midline (Mendes et al., 2006; North et al., 2009). EphB2 expression at the dorsal midline, in particular, was clearly shown to be expressed in CC axons as well in critical midline glial structures (Mendes et al., 2006). In addition, both EphB receptor forward signaling and ephrinB reverse signaling appear necessary for proper CC axon pathfinding, as both *EphB1*$^{-/-}$ and *EphB2*$^{-/-}$ single null mutant mice display partially penetrant agenesis of the CC (AgCC) (Mendes et al., 2006; Orioli et al., 1996). Moreover, inducible kinase-dead EphB receptor knock-in mutants also display a partial CC agenesis phenotype (Soskis et al., 2012). However, it remains unclear how EphB1/B2 forward signaling, ephrinB reverse signaling, or both processes together function during the complex series of CC axon pathfinding steps across the dorsal midline.

The AC is another large, interhemispheric white matter tract of the rodent forebrain that interconnects the temporal cortical regions of the basal telencephalon. The AC tract is a bipartite axon bundle with an anterior AC and posterior AC branch (abb. ACa & ACp) that converge with the stria terminalis axon bundle into a single, large fascicle at the ventral telencephalic midline. In rodents, the ACa is composed of axons from the olfactory nuclei and anterior piriform cortex, and the ACp is composed of both cortical axons from the posterior piriform cortex and other temporal cortices in addition to axons from the lateral nucleus of the amygdala. Posterior ACp fibers initially migrate together along the rostral-caudal oriented external capsule before converging with other ACp axons and turning toward the midline (Cummings et al., 1997; Jouandet and Hartenstein, 1983; Pires-Neto and Lent, 1993). Thus, ACa and ACp axons must

travel a considerable distance across the ventral midline to innervate the contralateral hemisphere; however, the precise guidance mechanisms that establishes AC fiber circuitry is still unclear. The EphB2 receptor has previously been implicated in ACp axon tract development, as *EphB2*$^{-/-}$ and *EphB2*$^{-/-}$*EphB3*$^{-/-}$ mutants have a mutant ACp misprojection phenotype, in which the entire ACp tract fails to cross the ventral midline and is misplaced to the ventral floor of the brain (Henkemeyer et al., 1996; Ho et al., 2009; Orioli et al., 1996). However, the potential role and cooperation with other EphB receptors, including EphB1, during AC axon pathfinding was not established.

In this study, we analyze the role of EphB1 and EphB2 forward signaling during the development of the CC and ACp forebrain midline tracts. We demonstrate that, along with the previously characterized role of ephrinB reverse siginaling, EphB1/B2 forward signaling is also essential for the complete midline crossing of CC axons and for the maintenance of the ACp axon trajectory toward the ventral midline. Our results indicate that forward and reverse EphB1/2 signaling processes cooperatively regulate the axon guidance of these interhemispheric axon tracts *in vivo*. We also show that EphB1/B2 are critical for ACp development at an early E14.5 timepoint where we characterize an early ACp developmental defect in EphB mutant embryos. Finally, we uncover a novel function for EphB1/B2 in directing deep-layer cortical axons along their proper subcortical trajectories into either the ACp tract or the striatum.

Results

EphB Receptor forward signaling is required for the formation of the corpus callosum.

To explore the importance of EphB1 and EphB2 signaling in callosal axon pathfinding, we analyzed serial coronal sections through the entire CC region from a variety EphB1, EphB2,

and EphB1/2 combination mutant mice. Adult mouse brains were serially sectioned imaged, and the extent of partial or complete agenesis of the CC (AgCC) was determined under genotype-blinded conditions. The phenotypes were defined as follows: *No agenesis* describes intact CC with a clearly visible CC connecting the two hemispheres of the brain (Figure 4.1A). The hippocampal commissure was chosen as the structural landmark that divided the rostral and caudal domains of the CC since we observed several distinct phenotypes of partial AgCC surrounding this structure. *Partial AgCC* was divided into three distinct categories: (1) agenesis of the rostral CC region only, (2) agenesis of the caudal CC region only, or (3) agenesis of both the rostral and caudal regions, but with some intact CC evident over the hippocampal commissure (Figure 4.1B). *Complete AgCC* was defined as a lack of any crossing fibers, whereas partial AgCC phenotypes were grouped as any of the three distinct subcategories described above (Figure 4.1D). Distinctions between partial AgCC phenotypes are delineated in Table 1.

Very little spontaneous AgCC is present in our wild-type mice (1 in 27, Figure 4.1D), and this was only partial AgCC. Alternatively, 58% of *EphB1*$^{-/-}$ single mutant mice displayed evidence of AgCC with the majority of mice displaying partial AgCC (Figure 4.1D). This result is in agreement with previous results showing *EphB1*$^{-/-}$ and *EphB2*$^{-/-}$ single mutant mice display AgCC (Mendes et al., 2006). Since the complete loss of EphB receptors does not distinguish between its role as a receptor or ligand, we also analyzed the CC of *EphB1*$^{Tr/Tr}$ and *EphB2*$^{Tr/Tr}$ truncated mutant mice, which contain knock-in mutations that replace their respective EphB intracellular domains with a β-galactosidase coding region. As such, these mutant mice produce a surface-expressed EphB1 or EphB2 receptor that is still capable of supporting reverse signaling (Chenaux and Henkemeyer, 2011; Henkemeyer et al., 1996), but lack the intracellular kinase

domain that is essential for both kinase-dependent forward signaling and a kinase-independent forward signaling such as through the PDZ binding motif at the extreme C-terminus. In comparison, 27% of the *EphB1*$^{Tr/Tr}$ forward signaling mutant mice had evidence of AgCC (Figure 4.1D), suggesting that EphB1 receptors contribute to CC formation via both forward and reverse signaling mechanisms. *EphB2*$^{Tr/Tr}$ forward signaling mutant mice displayed an even higher proportion of mice with AgCC, although, these animals displayed mostly partial AgCC confined to the caudal region (Table 1). A previous study reported no evidence of AgCC in these mice (Mendes et al., 2006), but since agenesis is only observed in the caudal CC, this phenotype might have been overlooked previously.

Interestingly, reducing one allele of EphB1 forward signaling (*EphB1*$^{Tr/+}$*:EphB2*$^{Tr/Tr}$) increased the EphB2 forward signaling mutant AgCC phenotype to a greater extent (75% vs 43% AgCC, respectively), suggesting that these receptors are functioning in the same genetic pathway. Similarly, removing one allele of EphB2 forward signaling (*EphB1*$^{Tr/Tr}$*:EphB2*$^{Tr/+}$) increased the EphB1 forward signaling mutant phenotype (57%. vs. 27%, respectively, Figure 1D). When both EphB1 and EphB2 receptor forward signaling was removed (*EphB1*$^{Tr/Tr}$*:EphB2*$^{Tr/Tr}$), 91% of the mice had partial or complete AgCC (Figure 4.1D), suggesting that there is partial functional redundancy *in vivo*. Consistent with these findings, combining the *EphB1*$^{-/-}$ with either *EphB2*$^{Tr/Tr}$ or a kinase-inactive EphB2 point mutant mouse (*EphB2*$^{K661R/K661R}$) resulted in a more severe AgCC phenotype than the EphB1 mutant alone (100% vs. 58%, respectively, Figure 4.1D). Taken together, these analyses indicate that: (1) EphB1 and EphB2 receptor forward signaling contribute essential functions during proper formation of the corpus callosum *in vivo*, (2) there is partial functional redundancy between EphB1 and EphB2 forward signaling in this process, and (3) there is a partial role for the

extracellular domain of EphB1 and EphB2 in CC formation, likely as a ligand for ephrinB reverse signaling.

A previous study by Mendes et al (2006) documented the expression of EphB1 in the cortical axon tracts of the corpus callosum using antibody labeling, but a precise and localized analysis of EphB1 expression in dorsal midline regions during CC formation has not been performed. Since the *EphB1*$^{Tr/+}$ mutant mice express a fusion protein of EphB1 and β-galactosidase (β-gal) that traffics to the plasma membrane and to axons, we monitored the expression of the EphB1-β-gal fusion protein during callosal axonal pathfinding at embryonic day 16.5. EphB1-β-gal expression was observed in the cingulate cortex and extended to an area matching the path of axons stemming from this region during callosal axon pathfinding (Figure 4.1E). EphB1 receptor was also expressed in the indusium griseum (Ig) and the dorsal portion of the glial wedge (GW), key glial structures, and within the ventral midline zipper glia (Figure 4.1E). As such, EphB1 receptors are expressed in locations that enable them to function as potential repellant ligands (glial structures) or to mediate EphB1 receptor forward repulsive signaling in navigating callosal fibers.

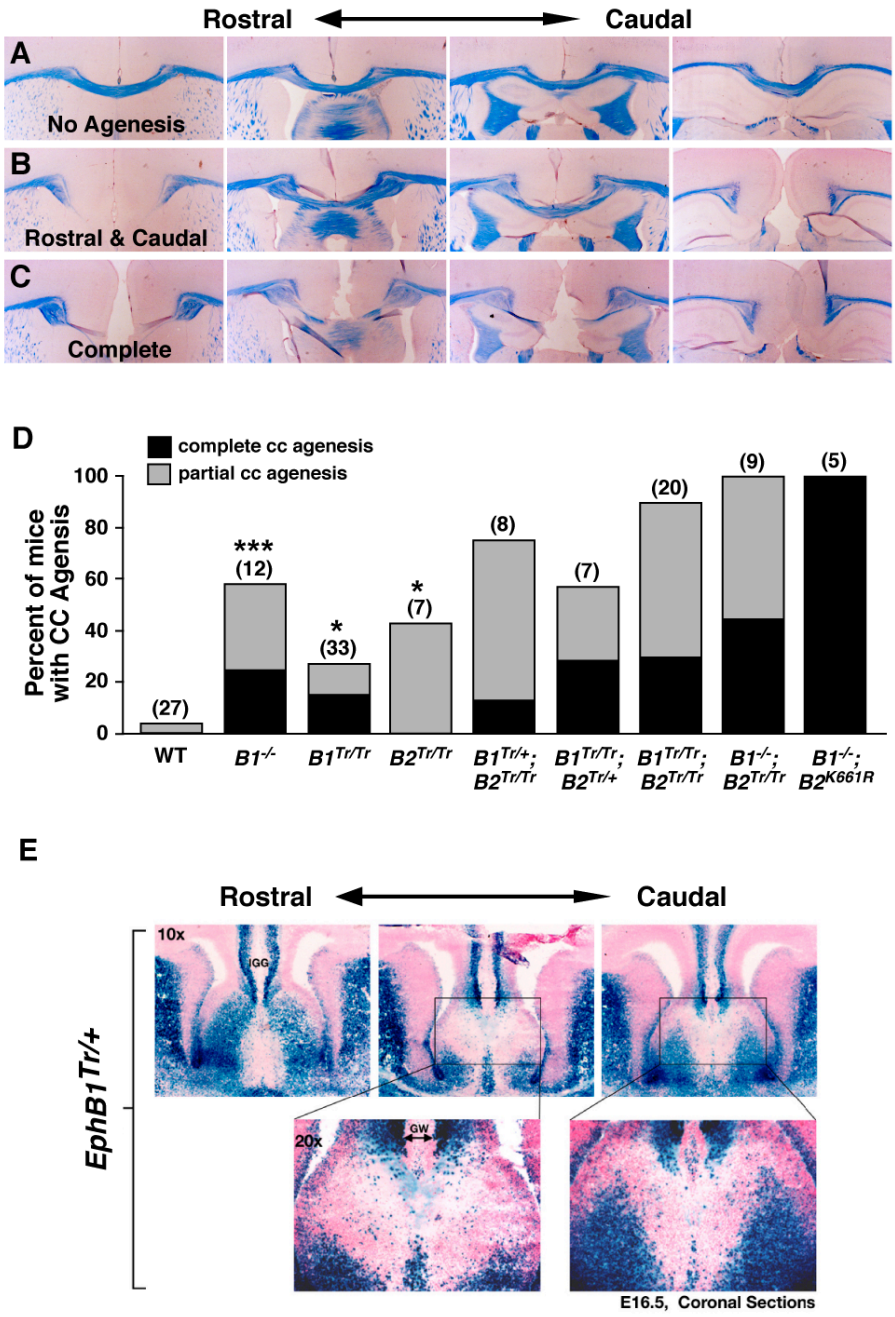

Figure 4.1. EphB1 and EphB2 forward signaling mediate the formation of the corpus callosum. *(A)* Luxol blue stains of serial coronal sections through a WT adult mouse with a normal corpus callosum. *(B)* An *EphB1*$^{Tr/Tr}$ homozygous mutant mouse brain with partial rostral and caudal AgCC. *(C)* Another *EphB1*$^{Tr/Tr}$ mutant example with complete AgCC. *(D)* Data graph displaying the percentage of each mouse genotype that displayed partial (grey) or

complete (black) agenesis of the corpus callosum (*p<0.05, ***p<0.001, Fisher's exact test). *(E)* X-gal stained E16.5 *EphB1*$^{Tr/+}$ mutant mouse brains sectioned coronally through the region of the developing corpus callosum. Representative images from rostral to more caudal portions of the developing corpus callosum are presented. β-Gal expression is evident in the indusium griseum (IGG), glial wedge (GW), ventral midline zipper glia (vMZG), as well as within the cingulate cortex (CGC). Higher magnification of X-Gal staining ventral to the cingulate cortex and dorsal to the ventral portion of the glial wedge is shown below. *(Figure arranged by George Chenaux)*

Genotype	Total mice	Agenesis							
		None	Rostral Only	Caudal Only	Both Rostral and Caudal	Complete	ratio partial	ratio complete	combined
WT	27	26	0	1	0	0	4%	0%	4%
***EphB1*$^{-/-}$**	12	5	1	1	2	3	33%	25%	58%
***EphB1*$^{Tr/Tr}$**	33	24	1	0	3	5	12%	15%	27%
***EphB2*$^{Tr/Tr}$**	7	4	0	3	0	0	43%	0%	43%
***EphB1*$^{Tr/+}$:*EphB2*$^{Tr/Tr}$**	8	2	0	4	1	1	63%	13%	75%
***EphB1*$^{Tr/Tr}$:*EphB2*$^{Tr/+}$**	7	3	0	2	0	2	29%	29%	57%
***EphB1*$^{Tr/Tr}$:*EphB2*$^{Tr/Tr}$**	22	2	0	12	2	6	64%	27%	91%
***EphB1*$^{-/-}$:*EphB2*$^{Tr/Tr}$**	9	0	0	5	0	4	56%	44%	100%
***EphB1*$^{-/-}$:*EphB2*$^{K661R/K661R}$**	5	0	0	0	0	5	0%	100%	100%

Table 1. Quantification of AgCC phenotypes in EphB mutants. *(Table arranged by George Chenaux)*

Both EphB1 and EphB2 are required for the formation of the anterior commissure

EphB2 is required for the proper development of the ACp axon tract (Henkemeyer et al., 1996; Ho et al., 2009), yet EphB1 is also expressed in the developing cortical plate during mid-development (Mendes et al., 2006; North et al., 2009). A recent study also highlighted the cooperative function for EphB1 and EphB2 during the development of corticothalamic axons within the striatum (Robichaux et al., 2013). Thus, we tested if EphB1 was necessary for ACp axon pathfinding using an axon labeling analysis of the ACp in wild-type, *EphB1*$^{-/-}$, *EphB2*$^{-/-}$, and EphB1/2 DKO (*EphB1*$^{-/-}$*EphB2*$^{-/-}$) double knockout mice at postnatal day 0 (P0). Using L1-CAM immunostaining as a marker for cortical axons, we observed the ACp white matter tract traversing the ventral midline in coronal sections of WT brains at Bregma 3.4-3.5 mm (Paxinos, 2007) (Figure 2A). At Bregma 3.6mm, the external capsule bundle, which contains ACp fibers traversing the rostral-caudal axis, is also evident in WT brains (Figure 4.2A). Compared to WT, however, *EphB1*$^{-/-}$ and *EphB2*$^{-/-}$ single knockout mice had ACp misprojection errors within these regions, in which a subset of ACp axons failed to grew toward the midline and instead grow toward the ventral brain floor (*moderate* ACp misprojections, Figure 4.2B, 4.2C & 4.5C, orange arrows). In EphB1/B2 DKO mutants, the ACp axon misprojection phenotype was more severe, with a complete misprojection and misplacement of the entire ACp bundle such that no ACp axons link the two temporal cortices of *DKO* brains (*severe* ACp misprojections, Figure 4.2D & 4.5C, yellow arrows). These ACp misprojections are a distinct mutant phenotype from CTA misprojections that are juxtaposed to ACp misprojections that are also evident near the ventral floor of the brain in EphB1/2 DKO mutants (Figure 4.2D). Misprojection phenotype examples are shown in (Figure 4.3).

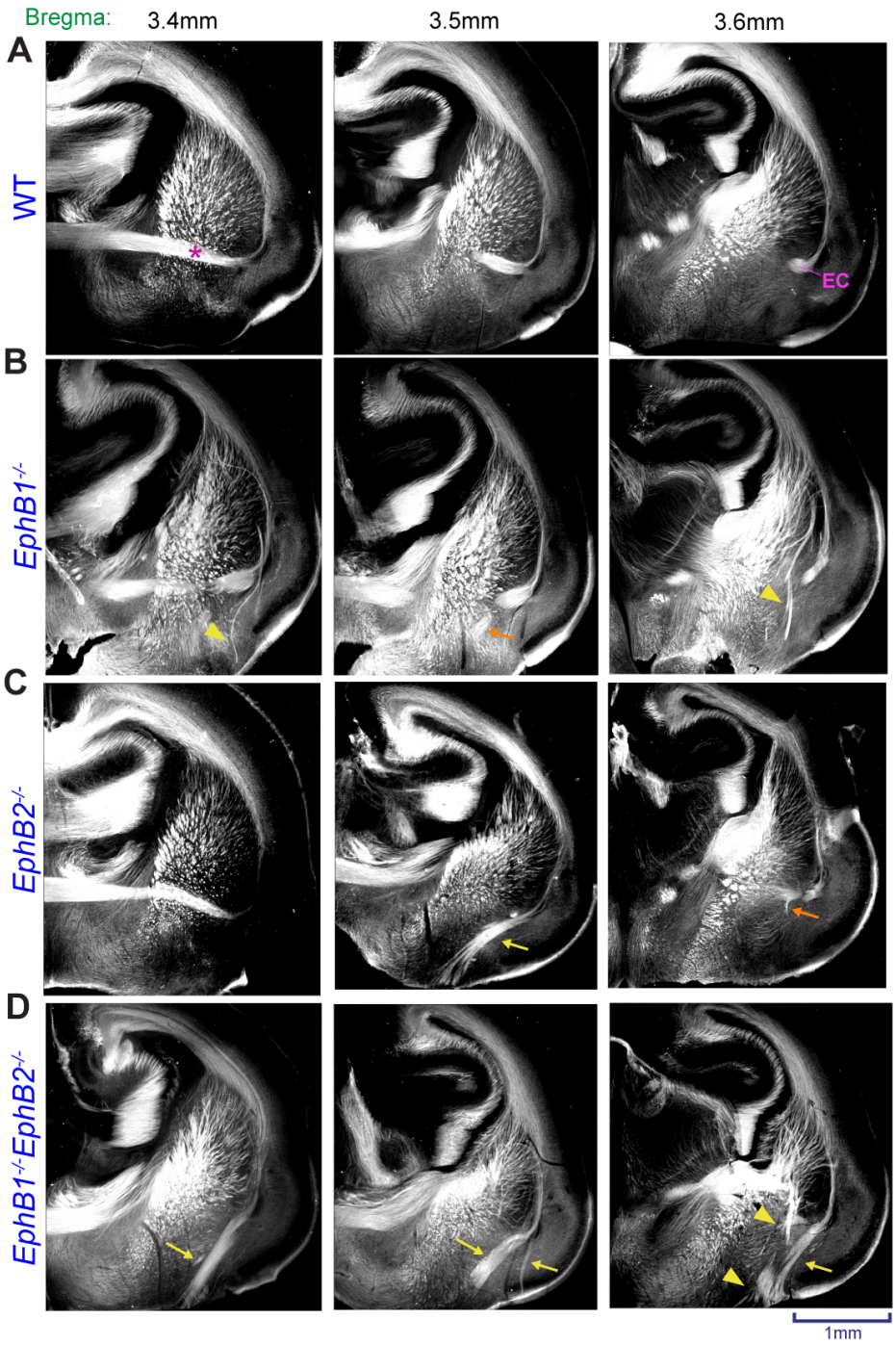

Figure 4.2. EphB1 and EphB2 are necessary for complete ACp tract development. *(A)* Coronal sections of WT mice at age P0 from Bregma 3.4mm - 3.6mm (Paxinos, 2007) stained with anti-L1-CAM. The normal ACp bundle (asterisk) and external capsule (EC) are indicated. Matched L1-CAM sections from *(B) EphB1*$^{-/-}$, *(C) EphB2*$^{-/-}$ and (D) *EphB1*$^{-/-}$*EphB2*$^{-/-}$ knockout

mutants. Moderate ACp misprojections (orange arrows) and severe ACp misprojections (yellow arrows) are indicated. Other misprojected CTA fibers from the VTel are also indicated at Bregma 3.6mm in *EphB1*$^{-/-}$ and *EphB1*$^{-/-}$*EphB2*$^{-/-}$ examples (arrowheads).

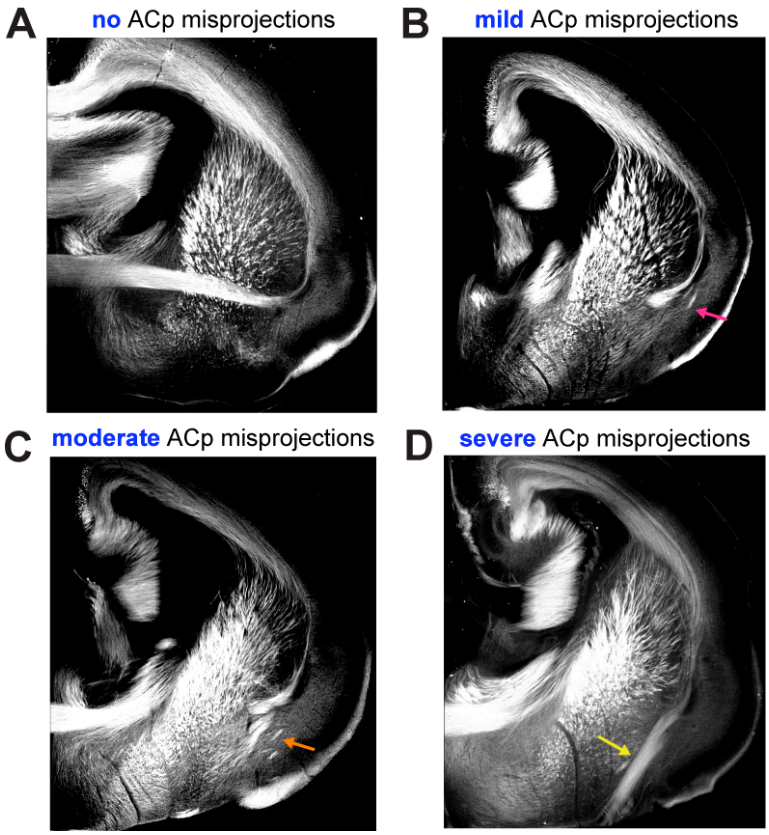

Figure 4.3. ACp misprojection phenotypes observed in EphB mutants. Example images of ACp misprojection phenotypes scored in P0 mouse brains used in this study. *(A)* No misprojection phenotype example from a WT brain. *(B)* Mild ACp misprojection example brain taken from a WT mouse example that was administered 1-NA-PP1 as outlined in Figure 4.6A (pink arrow – mild misprojection). *(C)* Moderate ACp misprojection phenotype example brain from an *AS-EphB* mouse example that was administered 1-NA-PP1 as outlined in Figure 4.6A (orange arrow – moderate misprojection). *(D)* Severe ACp misprojection phenotype example from an *EphB1*$^{-/-}$*EphB2*$^{-/-}$ mutant brain (yellow arrow – severe misprojection).

Next, to identify the axonal composition of the misprojected ACp tract in EphB1/2 DKO mutants, we used two different transgenic reporter mouse lines that selectively express GFP in the deep cortical layers. (1) Fezf2-GFP mice express GFP predominantly in the layer V of the cortex, while (2) Golli-tau-GFP express tau-GFP exclusively in layer VI (Jacobs et al., 2007a; Kwan et al., 2008; Robichaux et al., 2013). The rodent ACp is composed of axons from cortical layers II, III, V & VI (Jouandet and Hartenstein, 1983); however, a specific cortical layer labeling analysis has not previously been performed. In postnatal day 0 (P0) WT and EphB1/2 knockout mice that carry either the *Fezf2-GFP* or *Golli-tau-GFP* reporter allele, we observed that the ACp bundles, including in the severely misprojected ACp of EphB mutants, were composed of GFP-positive deep-layer axons nearly complete colocalizatopm with L1-positive ACp axons (Figure 4.4). These results demonstrate that layer V and VI cortical axons make up a significant population of the ACp axon bundle.

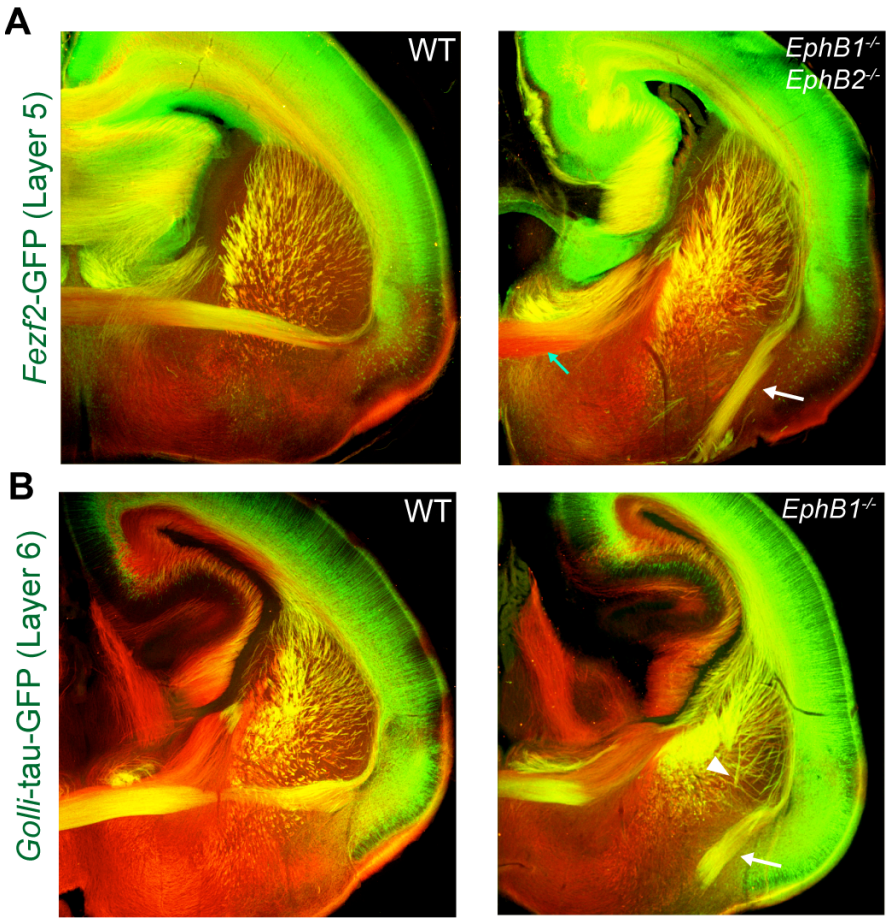

Figure 4.4. The ACp tract is composed of deep layer cortical axons. *(A)* Coronal sections of postnatal P0 brains from cortical layer 5 specific Fezf2-GFP reporter mice that are either WT for EphB receptor expression or EphB-deficient: *EphB1*$^{-/-}$*EphB2*$^{-/-}$. GFP+ axons from cortical layer 5 (green) are localized to the ACp in both WT and EphB1/B2 DKO reporter brains (arrow) and directly colocalize with L1+ misprojected axons (n=3). (B) Similar coronal brain sections of P0 cortical layer 6 specific Golli-tau-GFP reporter mice that are either WT or *EphB1*$^{-/-}$ single knockout mutants. GFP+ axons from cortical layer 6 also localize to the ACp in these reporters (n=2). The misprojected ACp (arrow) and CTA misprojections (arrowhead) are indicated.

EphB receptor forward signaling is required for normal anterior commissure formation

Next, we examined whether ACp axon guidance toward the midline requires EphB1/2 receptor forward signaling, so we again utilized truncated *EphB1*$^{Tr/Tr}$ and *EphB2*$^{Tr/Tr}$ mutant knock-in mice. *EphB1*$^{Tr/Tr}$ mice have a normal and completely formed ACp, unlike *EphB1*$^{-/-}$ knockout mutants (Figure 4.5A, 4.5C), and *EphB2*$^{Tr/Tr}$ mutants have only a slightly penetrant ACp misprojection phenotype (data not shown, Figure 4.5C). However, double truncated EphB mutants (*EphB1*$^{Tr/Tr}$*EphB2*$^{Tr/Tr}$) have severe ACp misprojections that are similar to the EphB1/B2 DKO phenotype (Figure 4.5B, 4.5C, yellow arrows). Thus, taken together, our analyses of total knockout and truncated EphB mutant mice demonstrate that (1) EphB1/2 forward signaling is essential for ACp axon development, (2) EphB1 and EphB2 forward signaling pathways likely function redundantly during ACp axon guidance, and (3) ephrinB reverse signaling, as previously demonstrated (Gale et al., 1996; Henkemeyer et al., 1996), is also required by ACp axons to some degree, as *EphB1*$^{-/-}$ and *EphB2*$^{-/-}$ mutants, in which reverse signaling is impaired, both have an ACp misprojection phenotype compared to *EphB1*$^{Tr/Tr}$ and *EphB2*$^{Tr/Tr}$ mutants, which have normal reverse signaling (Figure 4.5C).

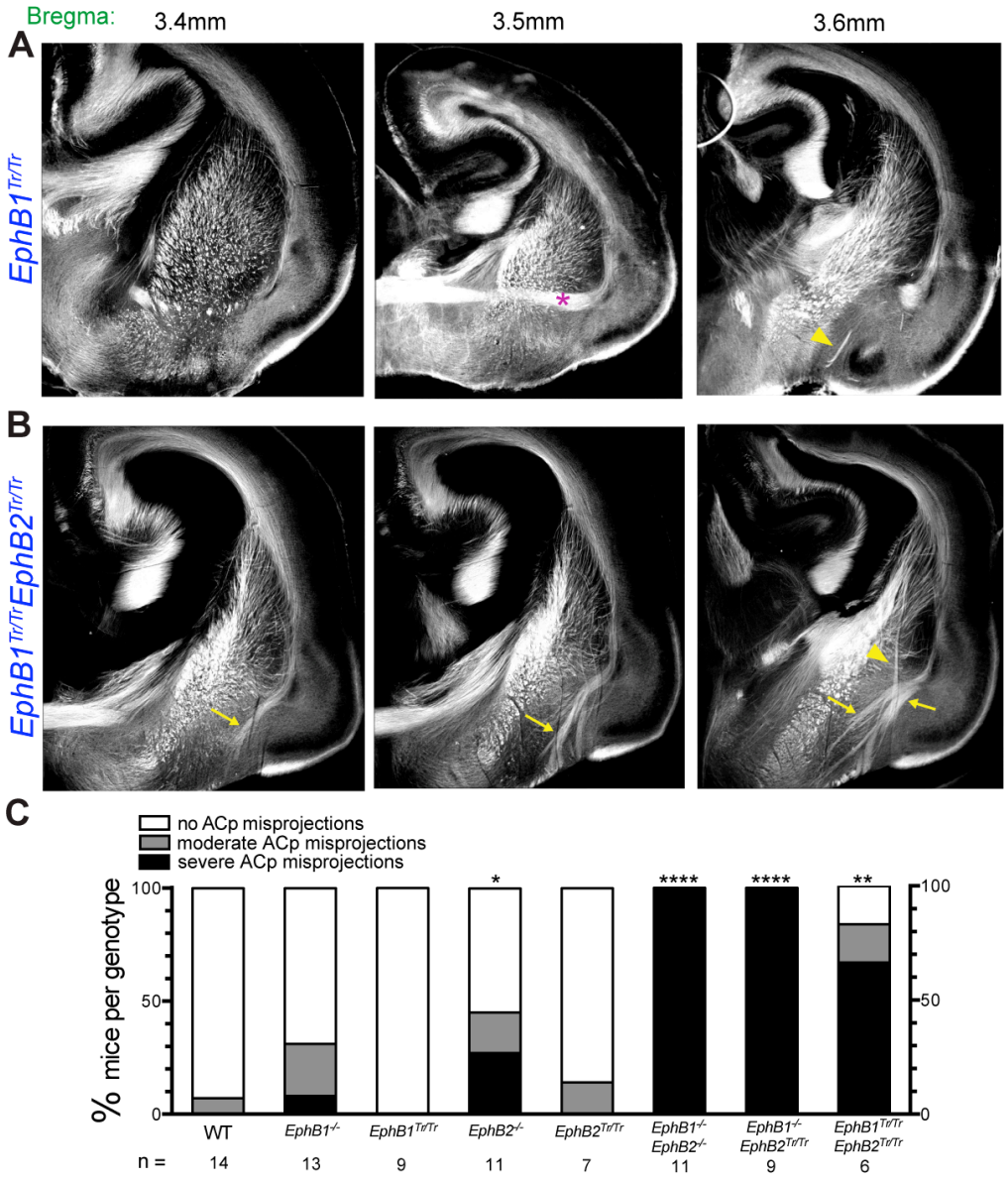

Figure 4.5. EphB1 and EphB2 forward signaling mediate proper ACp formation. *(A)* Coronal sections of *EphB1*$^{Tr/Tr}$ mutant mice at age P0 from Bregma 3.4mm - 3.6mm stained with anti-L1-CAM. The ACp bundle is indicated (asterisk). (B) Matched L1-CAM sections from *EphB1*$^{Tr/Tr}$*EphB2*$^{Tr/Tr}$ doubled truncated mutants. Severe ACp misprojections are indicated (yellow arrows). Misprojected CTA fibers from the VTel are also indicated for both genotypes (arrowhead). *(C)* Data graph of mutant ACp phenotype scores from L1-CAM stained EphB

knockout and truncated mutants analyzed in this study. (*$p<0.05$, **$p<0.01$, ****$p<0.0001$, Fisher's exact test).

Truncated EphB mutants eliminate EphB forward signaling, which requires the intracellular EphB signaling domains, including the tyrosine kinase domain, and kinase-independent SAM domain and PDZ C-terminal motif. Each of these intracellular regions is the potential site of distinct forward signaling events; therefore, we next targeted the EphB intracellular tyrosine kinase domain specifically to determine if it is necessary for ACp formation *in vivo*. For this, we used analog-sensitive EphB receptor triple knock-in mice (*AS-EphB*), which express intracellular point mutant versions of the EphB1, EphB2, and EphB3 receptors whose tyrosine kinase activity is reversibly inhibited by the ATP analog inhibitor 1-NA-PP1 (Soskis et al., 2012). We administered either vehicle or 1-NA-PP1 drug (80 mg/kg) to WT and *AS-EphB* mice from E12.5 to E19.0, and then assessed L1-positive ACp axons in treated E19.5 embryonic brains (Figure 4.6A). Using this paradigm, drug-injected *AS-EphB* mutant embryos displayed a completely penetrant, ACp misprojection phenotype (Figure 4.6E, 4.6F, orange arrows) compared to control mice. WT embryos that were administered 1-NA-PP1 displayed a non-significant, mild ACp defect (*mild* ACp misprojections, Figure 4.6D, 4.6F, pink arrows). As such, these results demonstrate that EphB kinase-dependent forward signaling mechanisms regulate ACp axon development.

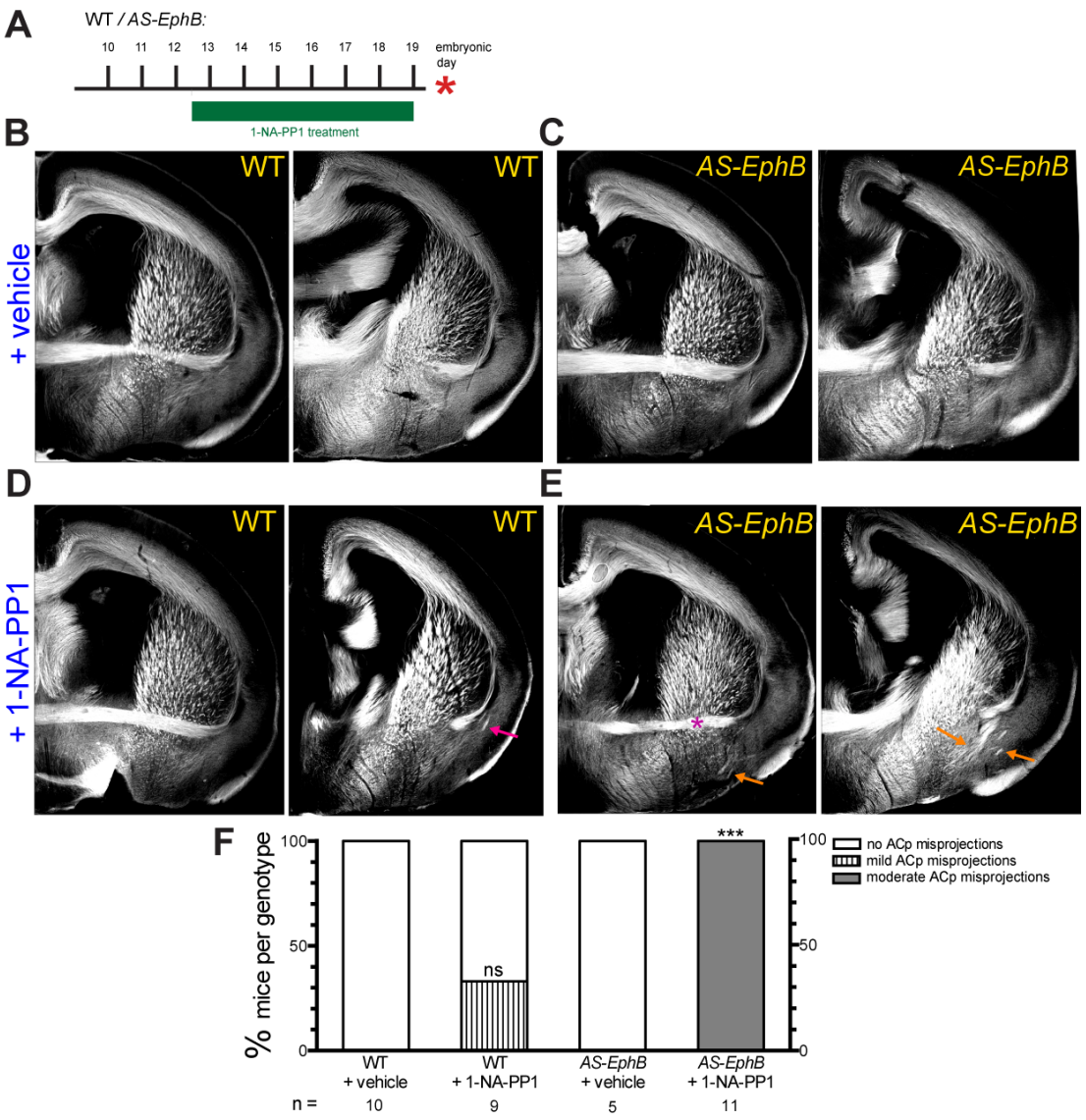

Figure 4.6. EphB receptor tyrosine kinase activity is necessary for complete ACp formation. *(A)* Drug injection schedule for subcutaneous 1-NA-PP1 delivery to timed-pregnant WT and *AS-EphB* mutant mice. Pregnant dams were administered either vehicle or 1-NA-PP1 (80 mg/kg body weight) twice daily between the embryonic stages of E12.5 and E19.0. Mice were sacrificed and embryos were harvested at stage E19.5 (asterisk). Coronal sections of L1-CAM stained *(B)* WT and *(C) AS-EphB* embryos brains treated with vehicle, and *(D)* WT and *(E) AS-EphB* embryo brains treated with 1-NA-PP1 (as outlined in *(A)*). The ACp tract in *(E)* is morphologically smaller than controls (asterisk). Mild ACp misprojections (pink arrow) and

moderate ACp misprojections (yellow arrows) are indicated. *(F)* Data graph of ACp misprojection scores for WT and *AS-EphB* brains that underwent vehicle or 1-NA-PP1 treatment. (***p<0.001, Fisher's exact test).

EphB1/2 direct the early development of anterior commissure axons at embryonic stages

Although the anterior commissure is a well-documented axon tract in neonatal and adult mouse brains (Jouandet and Hartenstein, 1983; Katz et al., 1983; Silver et al., 1982), the precise time-course of AC axon guidance events has not been fully characterized. The AC tract has been observed in the mouse brain as early as embryonic age E14.5, where EphB2 protein expression was not detected in ACp axons but localized to ventral forebrain regions underneath and surrounding ACp axons as they approach the midline (Henkemeyer et al., 1996). Thus, it is unclear if EphB1/2 is required during the earliest stages of ACp axon guidance at embryonic developmental timepoints. Here, we first analyzed EphB1 protein expression E14.5 using an *EphB1^{lacZ}* reporter mouse (Williams et al., 2003), which expresses β-gal fused to the extracellular domain of EphB1 as an intracellular protein marker for EphB1. We find that the EphB1-β-gal signal at E14.5, like EphB2, is not detectable in the ACp tract, but is highly expressed in the developing striatum dorsal to the ACp. We also observe EphB1 expression throughout the cortical plate that, including in the temporal cortices where ACp axons originate (Figure 4.7A).

To test if EphB1 and EphB2 are required for ACp guidance during embryonic timepoints, we first analyzed embryonic brains at stages E12.5 - E14.5 to determine the earliest stage in which L1-positive AC axons were evident. In WT brains analyzed at E12.5 and E13.5 we observed no ACp axons near regions of the ventrolateral cortical intermediate zone, the ventral telencephalon (VTel) or around the ventral midline (data not shown). However, at E14.5, the ACp tract is clearly present (Figure 4.7B), indicating that ACp axons penetrate the VTel as midline-projecting fibers between the ages of E13.5 and E14.5. We next addressed if EphB1 and EphB2 were required for the early development of the ACp at E14.5 by analyzing L1-positive axons in *EphB1$^{-/-}$EphB2$^{Tr/Tr}$* compound mutants at this stage. In these mutants, we observed that

the developing ACp tract is already completely misprojected toward the ventral brain floor (Figure 4.7C), indicating the EphB1/2 are required for the earliest stages of ACp development.

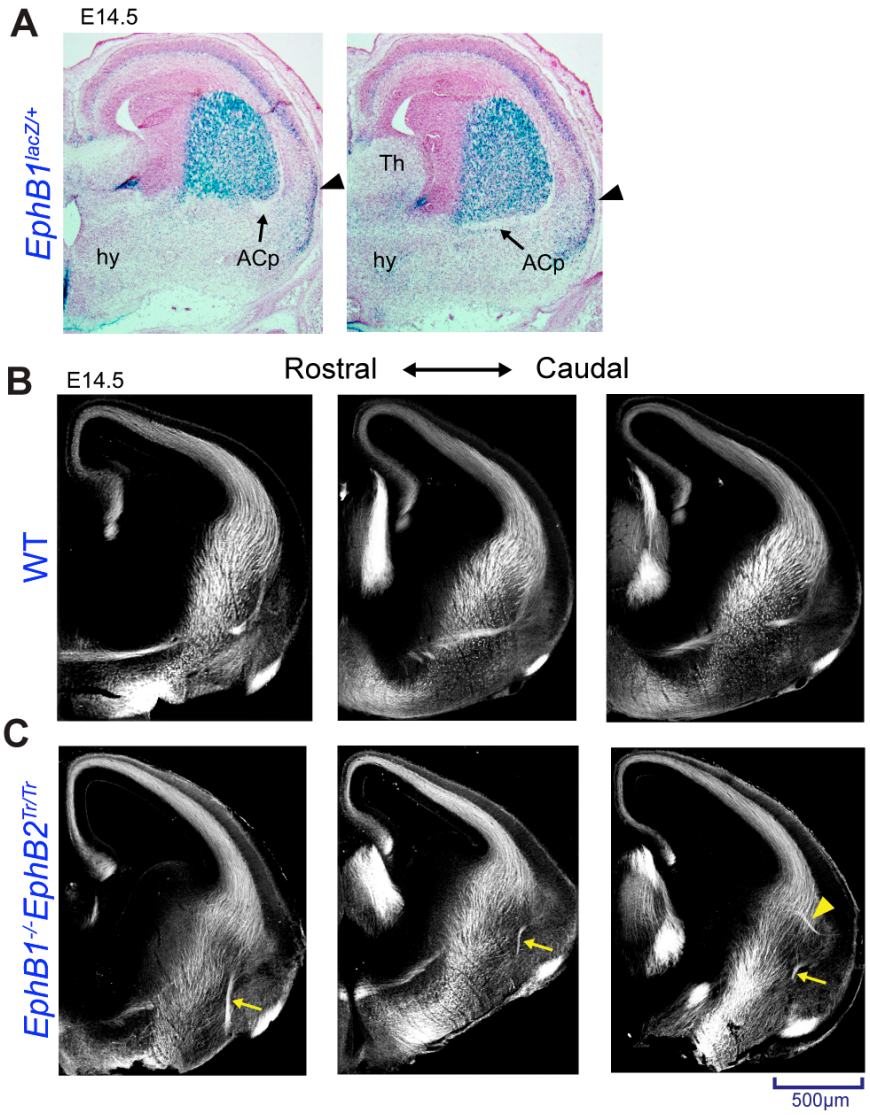

Figure 4.7. EphB1 and EphB2 are required for early embryonic formation of the ACp. *(A)* X-gal stained E14.5 *EphB1*$^{lacZ/+}$ mutant mouse brain sectioned coronally through the region of the developing ACp. The temporal region of the developing cortical plate is indicated (arrowhead). *(B)* Coronal sections of E14.5 WT brains stained with anti-L1-CAM and ordered from the rostral-caudal position. The developing ACp bundle is apparent in all example sections. *(C)* Matched sections of L1-CAM stained *EphB1*$^{-/-}$*EphB2*$^{Tr/Tr}$ compound mutants at E14.5. Misprojection of the early ACp is indicated (yellow arrows). Aberrant L1+ CTA fibers are also indicated (arrowhead). Th - thalamus, hy - hypothalamus.

EphB1/2 Receptors Regulate the Trajectory of Descending Subcortical Axons

ACp axons of cortical origin are completely derived from the temporal cortices that make up the lateral most zones of the rodent neocortex (Cummings et al., 1997; Jouandet and Hartenstein, 1983; Pires-Neto and Lent, 1993). Axons from these temporal cortical regions converge along with axons from the amygdala into a tight bundle to form the ACp near the rostral end of the forebrain (Bregma 3.4mm at P0). In *EphB1/2 DKO* mutants, the misprojected ACp bundle is not only misprojected away from the midline but appears larger in size, as we observe the misprojected tract along a broader rostral-caudal range in these mutants (Bregma 3.4mm - 3.6mm) compared to WT (Figure 4.2A & 4.2D). Furthermore, in a previous study, CTA axons that were misprojected in the ventral telencephalon of EphB1/2 DKO mutants were derived from two separate subregions of the neocortex (Robichaux et al., 2013). Therefore, we hypothesized that the larger, misprojected ACp axon tract in EphB1/2 DKO mutants may also be composed of axons from other, non-temporal cortical subregions. To identify the cortical origin of ACp axons in an unbiased manner, we placed NeuroVue® carbocyanine dye-soaked filters (MTTI) into different positions of the neocortex of WT and *EphB1/2 DKO* mutant brains at age P0 to analyze anterograde labeled cortical axons from these labeled subregions under experimenter-blinded conditions (Figure 4.8A). When placed into temporal regions of the cortex, the dye efficiently labeled a subset of cortical axons that projected either into the normal WT ACp or the misprojected DKO ACp tract (Figure 4.8B). From this collection of experiments in WT and DKO brains, we mapped the original dye placements onto a diagram of the neocortex (Figure 4.8C & 4.8D). Based on these diagrams, we demonstrate that ACp projecting axons originate from the temporal cortices in both WT and DKO brains, as expected. However, in *DKO* brains, ACP fibers also originate from a large, non-temporal cortical subregion that

roughly maps to the anterior half of the somatosensory cortex (Figure 4.8D). Thus, in the absence of EphB1 and EphB2, cortical axons from these regions incorrectly migrate toward the ACp tract, indicating that EphB1/2 are not only essential for the midline guidance of ACp axons, but also for regulating the proper subcortical trajectory of other cortical axons.

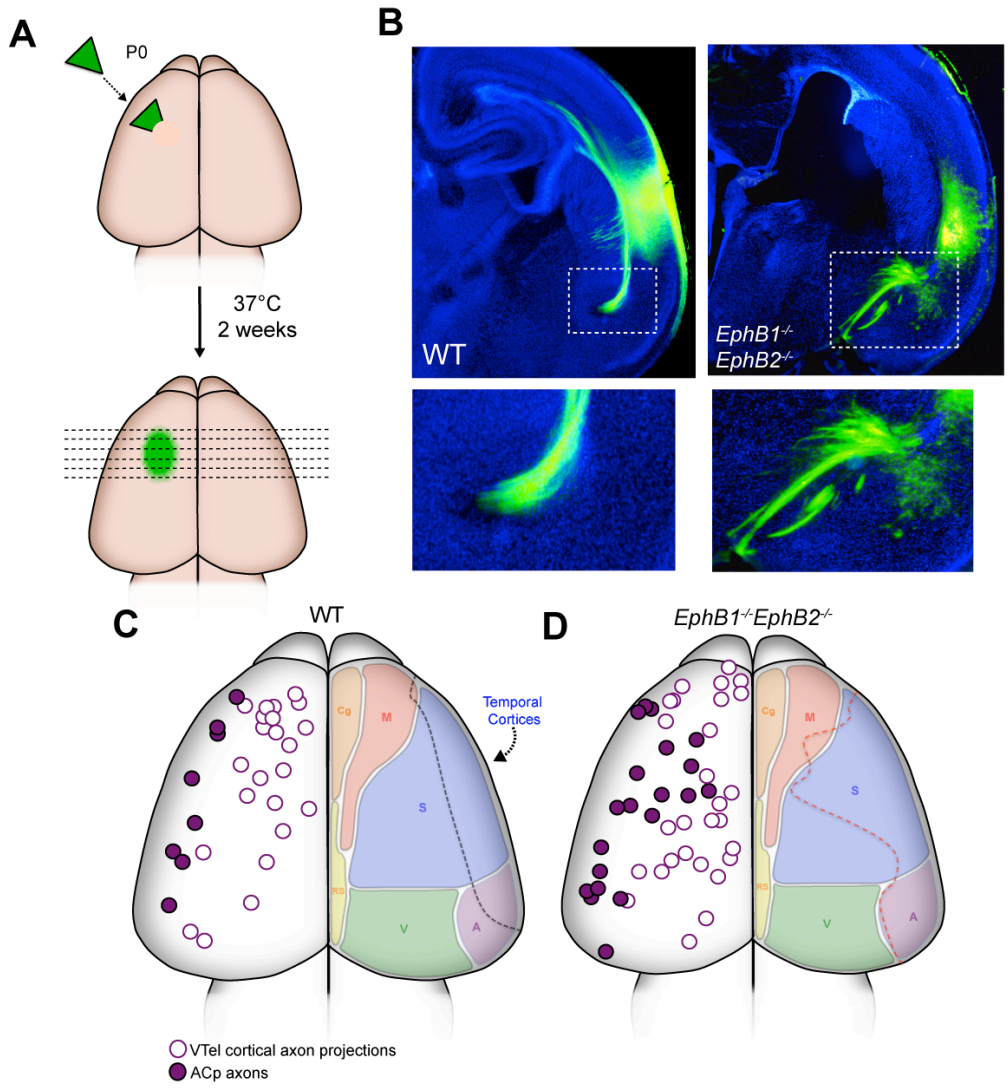

Figure 4.8. Non-temporal cortical axons are misprojected into the ACp of EphB mutants. *(A)* Diagram outlining the neocortical anterograde tracing experiments in P0 brains with the NeuroVue-Jade lipophilic tracer. *(B)* Example coronal sections of dye-labeled WT and *EphB1*$^{-/-}$ *EphB2*$^{-/-}$ mutant brains with dye placement in a similar temporal cortical location. Dye-labeled ACp axons in WT brains and misprojected ACp axons EphB1/2 DKO mutants are enlarged below. Sections were counterstained with Hoechst. *(C)* Neocortical dye placement diagram with indicator points for dye placement origins in WT (n=31) and EphB1/2 DKO (n=48) labeling experiments. In the left hemispheres of the diagrams, open circles indicate cortical regions that

project axons that traverse the striatum and do not develop along the ACp bundle. Purple shaded circles indicate regions that project along the ACp. In the right hemispheres, functional cortical subregions are outlined and the neocortical regions that encompass the origin points for ACp-projecting axons are outlined with a dashed line in both WT and DKO diagrams.

A - auditory, Cg - cingulate, M - motor, RS - retrospenial, S - somatosensory, V - visual.

Discussion

In this study we use several mutant mouse lines to dissect the function of EphB1 and EphB2 receptor forward signaling during the development of the CC and ACp, two major telencephalic commissures in the mammalian brain. Our detailed analysis of partial CC agenesis (AgCC) phenotypes in truncated, forward signaling null EphB mutants reveals that EphB1 and EphB2 forward signaling are critical for the complete formation of the CC fiber tract. In addition, we demonstrate that the ACp tract is misprojected in EphB1/2 deficient brains, as well as EphB1/2 truncated mutants and drug-inhibited, kinase dead mutants. Commissural agenesis is a common and prevalent form of CNS malformation in the developing human brain (Raybaud and Girard, 2005) with 50 known congenital human syndromes leading to instances of AgCC (Richards et al., 2004). Notably, commissural agenesis observed in human patients is characterized as either complete or partial, and cases of complete CC agenesis are often accompanied by the loss of the AC (Raybaud and Girard, 2005). Also in this study, we find that the ACp is already misprojected at E14.5 in EphB1/2 mutants, indicating that the earliest guidance steps of ACp axon formation require EphB1/2. Finally, we use anterograde tracing techniques to demonstrate that ACp axons fibers are derived from an expanded neocortical zone in EphB1/2 DKO mutants, implicating EphB1/2 in the regulation of subcortical axons fate determination into either the ACp tract or to other subcortical targets.

Along with previous findings (Bush and Soriano, 2009; Henkemeyer et al., 1996; Hu et al., 2003; Mendes et al., 2006; Orioli et al., 1996; Soskis et al., 2012), our results indicate that EphB1/2 forward signaling and ephrinB reverse signaling, to various degrees, all function during the development of the CC and ACp with potentially overlapping and redundant roles. Our analysis of AgCC in EphB1/2 mutants focuses on partial phenotypes and in a region-specific

manner, in addition to the complete agenesis phenotype. This is unlike previous EphB studies that did not consider partial phenotypes (Mendes et al., 2006; Orioli et al., 1996). Here, we show that truncated EphB1 and EphB2 mutants display partially penetrant AgCC phenotypes that becomes nearly completely penetrant in the compound truncated *EphB1*$^{Tr/Tr}$*EphB2*$^{Tr/Tr}$ mutant, which demonstrates that EphB forward signaling is necessary for CC formation. Similarly, we observe no ACp misprojection phenotype in *EphB1*$^{Tr/Tr}$ and *EphB2*$^{Tr/Tr}$ mutants and a partial ACp phenotype in *EphB2*$^{Tr/Tr}$, which becomes more severe and nearly completely penetrant in double truncated *EphB1*$^{Tr/Tr}$*EphB2*$^{Tr/Tr}$ mutants. Thus, EphB1 and EphB2 forward signaling appear to be functioning redundantly during both CC and ACp formation. Furthermore, we also confirm a cooperative function with ephrinB reverse signaling, as the *EphB1*$^{Tr/Tr}$*EphB2*$^{Tr/Tr}$ mutant phenotypes are not as complete and severe as the *EphB1*$^{-/-}$*EphB2*^{K661R} AgCC phenotype or the *EphB1*$^{-/-}$*EphB2*$^{-/-}$ ACp misprojection phenotype,

Our analysis of the role of the *ephrinB* genes (*ephrinB1-3)* during CC and ACp development was incomplete due to the unavailability of appropriate mutant mouse lines (most notably *ephrinB2*$^{-/-}$, which is embryonic lethal at E8 (Cowan et al., 2004)). We did, however, analyze postnatal brains from *ephrinB1*$^{-/-}$ and *ephrinB3*$^{-/-}$ knockout mutants and observed normal CC and ACp development with no signs of agenesis or ACp misprojection (Figure 4.9)(n=5, n=6, respectively). Notably, ephrinB2 protein is highly expressed in the ACp of postnatal brains (Henkemeyer et al., 1996), and additionally, the ACp tract of *ephrinB2*^{lacz} truncated mutants (which are reverse signaling null) is severely attenuated, suggesting that ephrinB2 reverse signaling pathways are highly involved in ACp axon guidance. Future analysis of conditional ephrinB2 null mutants and compound ephrinB mutants will be required to fully determine which of these genes are essential during forebrain commissural development.

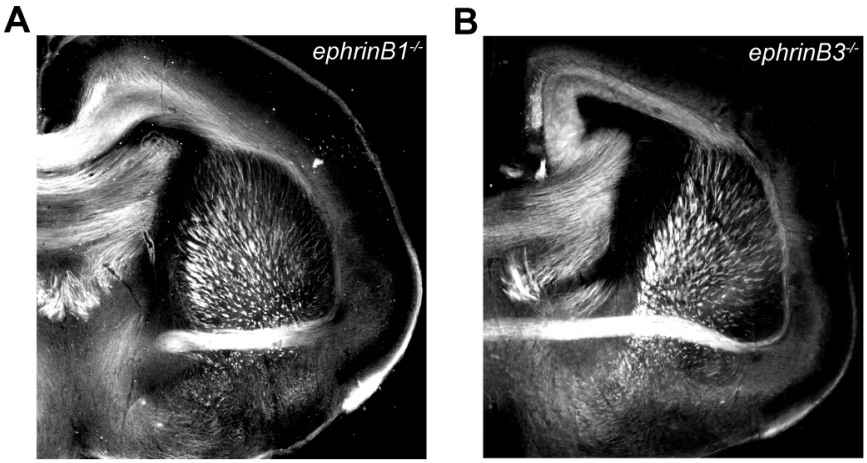

Figure 4.9. EphrinB1 and ephrinB3 are not necessary for ACp formation. *(A)* Coronal sections of *ephrinB1*$^{-/-}$ and *ephrinB3*$^{-/-}$ knockout mutant mice at age P0 stained with anti-L1-CAM. The large ACp tract is present and fully formed in these mutants.

In addition to the significant role of EphBs and ephrins, several previous studies have characterized a role for other axon guidance molecules during the development of the CC, including L1-CAM, Slit2, netrin-1, and Fgfr1 (Richards et al., 2004; Shu et al., 2003b; Stein et al., 2001; Tole et al., 2006). However, the bidirectional signaling capability of the EphB/ephrinB interaction may be particularly useful for the number of cell-cell interactions that occur during CC midline development. Before cortical axons from layers II, III & V cross the dorsal telencephalic midline to form the CC, the two dorsal telencephalic hemispheres must first undergo a morphogenic fusion that physically links the two structures (Silver et al., 1982). Blocking and rescuing this interhemispheric fusion directly effects the formation of the CC axons across the midline (Silver et al., 1982; Silver and Ogawa, 1983). Upon telencephalic fusion, midline glia initially bridge the midline by forming a "glial sling" across the dorsal hemispheres as a pathway for the development of future CC axons (Katz et al., 1983; Shu and Richards, 2001; Silver et al., 1982). Thus, in mutant studies where CC axons fail to cross the midline and instead misdirect into Probst bundles, AgCC may be due to other defects besides axon misguidance, such as the failure of hemispheric fusion or the misdevelopment of the glial sling. Such glial defects at the dorsal midline have previously been considered during the formation of commissural tracts (reviewed in (Lindwall et al., 2007)), and, indeed, several of our mutants demonstrate display an unfused dorsal telencephalon that could possibly inhibit CC axon growth over the dorsal midline (Figure 4.1B & 4.1C).

In EphB1/2 mutant brains we also observe the failure of ACp axons to reach the ventral midline, but unlike CC axons that apparently stall at the midline, ACp fibers become misprojected in a region lateral to midline and extend in an aberrant direction towards the floor of the ventral forebrain. This significant difference suggests that EphB1/2 function to direct

pioneer ACp axon guidance early during tract development. Several previous studies have reported roles for other guidance axon molecules in the development and establishment of the ACp tract, including netrin-1, Sema3B/3F, Npn2, Nr-CAM, Tsukushi, Draxin, Fgfr1 and PlexinA4 (Chen et al., 2000; Falk et al., 2005; Giger et al., 2000; Hossain et al., 2013; Islam et al., 2009; Ito et al., 2010; Sahay et al., 2003; Serafini et al., 1996; Suto et al., 2005; Tole et al., 2006). These studies report various ACp defects in addition to misprojections, such as axon defasciculation and midline guidance errors. Expression of these genes is also variable as some, such as *Npn2* and *ephrinB2*, are expressed in ACp axons themselves (Giger et al., 2000), while other genes, such as *netrin-1* & *Sema3B* (Falk et al., 2005; Serafini et al., 1996), are expressed in the cells surrounding the developing ACp.

Although the results from our expression analyses are ambiguous, it is still likely, based on the mutant phenotypes of EphB truncated and inducible kinase dead mutants, that EphB1 and EphB2 forward kinase activity are, in part, required within the CC and ACp axons themselves to mediate proper midline guidance. It is also probable that EphB forward signaling and ephrinB reverse signaling have non-autonomous effects on commissural guidance. Thus, future studies will require the targeted disruption of these genes to fully characterize the mechanism of EphB and ephrinB signaling during these axon guidance events.

Our results also confirm that EphB1/2 receptors establish the ACp tract early in development (prior to E14.5), such that in postnatal EphB mutant brains, the ACp tract is misprojected to the brain floor in the ventral telencephalon. Interestingly, these mutant misprojections are located near the same region that CTA axons are misprojected in these same EphB mutant brains (Figure 4.2D, (Robichaux et al., 2013)). In WT brains, CTA projections grow along an organized and topographic array of fiber bundles within the dorsal half of the

ventral telencephalon (VTel) where they cofasciculate with reciprocal TCA bundles; however, in EphB1/2 mutants, CTAs cofasciculate and misproject along mutant TCA axon fascicles that were misprojected earlier in developmental (E13.0). Thus, early TCA guidance is dependent on EphB1/2, and in EphB1/2 mutant embryos, these misprojected TCA fascicles localize near the bottom of the VTel at E13.5 & E14.5 in a region that is near to the embryonic ACp mutant misprojections that we observe at E14.5. Thus, it is possible that these two mutant phenotypes are related, such that, like CTA fibers, pioneer ACp axons in EphB1/2 mutant brains may aberrantly cofasciculate with misprojected TCA axons near in the floor of the VTel and become permanent misprojections. It is also possible that ACp axons are miswired in another non-cell autonomous fashion independently of misprojected TCA fibers or any other axon misguidance phenotype.

Finally, to investigate if axons from the correct temporal neocortical origin project along the misprojected ACp in EphB1/2 mutants, we performed a series of anterograde tracings of the mutant neocortex, and revealed that ACp axons are, in fact, derived from a broader region of the neocortex that includes a large portion of the somatosensory cortex (Figure 4.8D). Thus, EphB1/2 also appear to regulate early cortical axon development and direct non-temporal fibers away from the basolateral ACp tract. Control tracing experiments in WT animals also confirmed previous tracing studies in rodent, which characterized the origin of the ACp to the posterior pirifiorm cortex, temporal cortices and dorsal amygdalar nucleus (Jouandet and Hartenstein, 1983; Silver et al., 1982). Similarly, in rhesus monkey brains, ACp axons exclusively originate from the temporal lobe of the neocortex (Jouandet and Gazzaniga, 1979). However, the forebrain circuitry of the cat brain is more divergent, as ACp axons are not restricted to temporal neocortical regions but are derived from a more expansive zone that stretches into the

somatosensory areas (Jouandet, 1982). This is an intriguing similarity to the neocortical ACp origin in EphB1/2 knockout mouse brains as depicted by our anterograde tracing studies (Figure 4.8D), which suggests EphB1/B2 may have evolved a molecular function to restrict somatosensory and other cortical axons from developing in the basolateral direction along the external capsule and into ACp. Although this potential function in early axon steering requires further investigation, it demonstrates the redundancy in which the developing brain utilizes the ubiquitous EphB receptors to properly build complex brain circuits through axon pathfinding mechanisms.

Materials and Methods

Animals: The EphB receptor knockout and knock-in mice used in this study, including *EphB1*$^{-/-}$, *EphB1*$^{Tr/Tr}$ (previously annotated as *EphB1*$^{T\text{-}lacZ}$), *EphB1*^{lacZ} *EphB2*$^{-/-}$, *EphB2*$^{Tr/Tr}$ (previously annotated as *EphB2*^{lacZ}), *EphB2*$^{K661R/K661R}$, and *EphB3*$^{-/-}$ mice, were previously described (Chenaux and Henkemeyer, 2011; Genander et al., 2009; Henkemeyer et al., 1996; Orioli et al., 1996; Williams et al., 2003) and maintained in a CD1 background. *EphB1*$^{Tr/Tr}$ and *EphB2*$^{Tr/Tr}$ mice express C-terminal truncated fusion proteins containing the extracellular and trans-membrane domains of EphB1 or EphB2 conjugated to β-galactosidase (Chenaux and Henkemeyer, 2011; Henkemeyer et al., 1996). The resulting EphB1/2-β-gal fusion proteins lack their respective intracellular tyrosine kinase catalytic domain, SAM domain and PDZ binding motif. The generation of *EphB1*^{T697}*EphB2*^{T699A}*EphB3*^{T706A} analog sensitive EphB triple knockin mice (AS-EphB) has been recently reported (Soskis et al., 2012). The *Fezf2-GFP* reporter line was previously described, and expresses GFP overwhelmingly in mature layer V cortical neurons and cortical pioneer axons (Kwan et al., 2008). The *Golli-tau-GFP* reporter mouse line was also

previously characterized to express GFP exclusively in mature layer VI cortical neurons and pioneer cortical axons during early developmental stages (Jacobs et al., 2007a). GFP reporter mice containing deleted EphB alleles were generated through cross breeding. For PCR genotyping, DNA was extracted from tails samples of dissected mice embryos with 100% isopropanol after an intervening lysis step. PCR was performed using the extracted DNA in a total volume of 25ul using the primer sets described previously (Chenaux and Henkemeyer, 2011; Genander et al., 2009; Henkemeyer et al., 1996; Orioli et al., 1996; Williams et al., 2003). All animal procedures were in accordance with the Institutional Animal Care and Use (IACUC) guidelines.

Tissue Processing: Embryonic brains used in this study were obtained at appropriate time points from timed-pregnant dams, where embryonic day 0 (E0) is defined as midnight prior to the morning a vaginal plug is observed. Pregnant dams were killed by CO2 asphyxiation, after which embryos were immediately harvested for processing. Postnatal P0 pups were killed via quick decapitation. For E14.5 embryos, heads were removed and immediately post-fixed in 3.7% formaldehyde. For P0 postnatal pups, brains were dissected away before post fixation in 3.7% formaldehyde. All post-fixed tissue was fixed at 4°C for 48 hours before rinsing with phosphate-buffer saline (PBS) and storage at 4°C in PBS + 0.02% Na-Azide.

L1-CAM Immunohistochemistry: Immunohistochemical staining of free floating brain sections was performed on 70 μm coronal brain sections obtained from fixed brains embedded in a 1.5% (w/v) mix of 0.75% Low-Melting Point Agarose (Promega) and 0.75% standard Agarose (Fisher) and cut on a Leica VT 1000P vibratome. Sections were immersed in blocking solution

(5% normal donkey serum, 1% BSA, 0.2% glycine, 0.2% lysine with 0.3% TritonX-100 in PBS) and incubated on a rotating shaker for 1 hour at room temperature. Sections were next incubated overnight at 4°C with rat anti-L1-CAM, 1:200 (Millipore, MAB5272MI) diluted in blocking solution. Sections were washed three times with PBS before fluorescent secondary antibody incubation with Cy3-conjugated donkey anti-rat IgG (Jackson). Sections were counterstained with 50µg/ml Hoechst 33342 nuclear stain (Life Tech. #H21492) diluted in 1xPBS for 5 minutes at room temperature and serially mounted onto glass slides with Aquamount .

Axon Tracing: Anterograde dye tracing of deep layer cortical axons was performed using focal application of NeuroVue® Jade or NeuroVue® Red carbocyanine dye filters (MTTI) placed directly into the neocortex of fixed P0 brains. Dye-implanted P0 brains were incubated 2 weeks at 37°C for adequate anterograde axon tracing before sectioning. All dye-labeled brains were embedded in 1.5% agarose before 70µm coronal vibratome sectioning. Sections were serially mounted onto glass slides with Aquamount (Thermo Scientific) and counterstained with Hoechst 33342 (Life Tech. - 50ug/ml). Focal application points of the NeuroVue dye filter within the neocortex were mapped and diagramed using a P0 developing mouse brain atlas (Paxinos, 2007).

In Vivo 1-Na-PP1 Delivery: 1-NA-PP1 was synthesized as described previously (Blethrow et al., 2004; Soskis et al., 2012). Pregnant female WT or AS-EphB triple knockin mice were injected subcutaneously twice daily with 80mg/kg 1-NA-PP1 dissolved in 10%DMSO, 20% Cremaphor-EL, 70% saline for the embryonic timepoints required. E19.0 or E19.5 dams were killed by CO2 asphyxiation and embryonic brains were harvested and processed as described above.

X-Gal Staining: To stain cryosections, unfixed brain tissue was quickly harvested and frozen under OCT medium or else cryopreserved in 30% sucrose in 0.1M PO_4 buffer pH 7.3 prior to freezing. Tissue was then sectioned on a cryostat (25 mm), immediately mounted on charged slides, and allowed to air dry. Sections were then washed in wash buffer (2mM $MgCl_2$ and 0.02% Nonidet p-40 in 0.1 M PO_4 buffer pH 7.3) and placed in X-gal solution (2% gluteraldehyde, 0.02% Nonidet p-40, 2mM $MgCl_2$, 5mM EGTA,, 1mg/mL X-gal (Roche), 2.12 mg/mL K4[Fe(CN)6]•3H2O, 1.64 mg/mL K3[Fe(CN)6] (Sigma)in 0.1M PO_4 buffer pH 7.3) O/N at 37 °C. Slides were washed, post-fixed in 4% PFA, and counterstained with nuclear fast red.

Luxol Blue Staining: Adult wild-type and mutant mice were perfused with 1x PBS followed by 4% PFA. Brains were removed and post-fixed in 4% PFA overnight at 4°C, and were then serial sectioned to 40 μm thickness on vibratome and postfixed in 1% PFA overnight at 4°C. Sections were dehydrated for one hour in 70% EtOH followed by overnight incubation with agitation in 100% EtOH at room temperature. Sections were transferred to luxol blue staining solution (0.1% Luxol fast blue and 0.5 Acetic acid in 95% EtOH), which was preheated to 60 °C, and were stained overnight. Sections were washed 3x in 95% EtOH at 60°C, rehydrated in deionized water, and differentiated in 0.05% lithium carbonate for one to five minutes. Slides were washed in deionized water, mounted on charged slides, dehydrated in ethanol and then xylene, sealed with coverslips, and imaged with an Olympus BX50 microscope.

Analysis of ACp Misguidance Phenotypes: L1-CAM immunolabeled brain sections, dye-labeled sections, and counterstained sections were imaged on an epifluorescent microscope using

standard Cy2, Cy3, and UV filters. Photomicrograph images were produced using an Olympus DP70 CCD digital camera, and images were prepared using MS PowerPoint and Adobe Photoshop. Pseudocoloring and adjustments to image brightness, contrast, and color balance were made for image clarity. ACp "misprojections" were scored as L1-CAM positive axon fibers from the AC bundle that turned in a ventral fashion toward the brain floor. The moderate ACp misprojection phenotype was classified by the observation of significant axon bundles that became mistargeted toward the ventral floor, whereas the severe ACp misprojection phenotype was classified by the complete misplacement of the entire ACp fiber bundle. For analysis of mutant phenotypes in 1-NA-PP1 administered AS-EphB mutants, the mild ACp misprojection phenotype was distinguished by the presence of only a few mistargeted ACp axons. All scoring analyses were experimenter blinded.

Data Analysis: AgCC and ACp misprojection phenotype scores in EphB Receptor mutants were assessed for statistical significance using Fisher's exact test (FET) to directly compare mutant scores to wild-type brains. Statistics were compiled and graphs were designed using GraphPad Prism software.

Conclusion and Future Directions

Conclusion

Over the last few decades, developmental research in the specialized fields of axon guidance and synaptogenesis has greatly illuminated the complex and multifaceted nature of neural circuit formation on a molecular and cellular level. Although dozens of genes have been identified with signaling roles during axon guidance, most of the signaling processes within the growth cone occur rapidly and at a long range from cell bodies and thus necessitate local pathways that converge on the local F-actin cytoskeleton. Additionally, while we can pinpoint some signaling factors that become activated in response to a specific guidance cue, such as those downstream of the EphB receptors in response to ephrinB, these signaling molecules must still carry out the daunting task of assembling and disassembling the vast cytoskeletal structure, which invariably must require the orchestrated support of several other unidentified signaling partners. Meanwhile, fascinating research continues to emerge from the developmental fields as more axon guidance "decision points" are identified, more *in vivo* studies support previous cell culture findings, and high-definition, ultrastructural analyses of developing axon and growth cones provide an even closer look at EphB receptor and other essential guidance pathways.

Future directions: Molecular Analysis of EphB Forward Signaling

Vav

Undoubtedly, elucidating the function of Vav2 and Vav3 downstream of EphB1 receptor activation upon ephrinB2 stimulation in ipsilateral RGC axons remains the most important task left towad fully understanding the role of these GEFs during RGC repulsion at the OX. Our

analysis of DiI-labeled ipsilateral RGC axons in *Vav2*$^{-/-}$*Vav3*$^{-/-}$ mutants is strong evidence that Vav2/3 do indeed function downstream of EphB1 during repulsion, and these *in vivo* results are nicely corroborated with my culture binding assays and retinal explant analyses. However, a more targeted analysis of Vav2/3 *in vivo* through the specific knockdown, perhaps, of these Vav2/3 in the VT retina would finally allow for direct and unmistakable evidence of this pathway. Such an experiment could be envisioned using retinal *in utero* electroporation methods or the development of a conditional Vav2/3 knockout mouse line. Testing any potential function of Vav2/3 in RGCs upon ephrinB2 stimulation would be rather straightforward using retinal explants; however, a direct test of this function *in vivo* would be more challenging. An initial step towards this goal would be to use the phospho-Vav2 (Y172) antibody to label P-Vav2 in OX midline brain slice preparations. If successful, dual immunolabeling of Vav2 with potential targets could be performed.

Pak

Based on our identification and analysis of the forward signaling role of Pak1 downstream of EphB2 in cultured cortical neurons, group I *Pak* genes likely function *in vivo* during the development of cortical axon pathways. Early in the study, I analyzed *Pak1*$^{-/-}$ knockout mice (a gracious gift from Dr. J. Chernoff (Fox Chase Cancer Center)) using L1-CAM pan-axonal immunolabeling to look for any guidance defects. Specifically, I was looking for defects in the major commissural axons of the forebrain or CTA misguidance in the VTel, but failed to see any disruption of axon morphology. Thus, I hypothesize that Pak2 and Pak3, which are both also expressed in the cortex at E16.5, are compensating for the loss of Pak1 in *Pak1*$^{-/-}$ mice. Thus, in my opinion, a triple *Pak1*$^{-/-}$*Pak2*$^{-/-}$*Pak3*$^{-/-}$ knockout mutant will be needed to fully test the function of Pak1 and the group I Pak's during cortical axon pathfinding *in vivo*. As such,

I hypothesize that Pak2 and Pak3 also function as forward signaling molecules downstream of EphB2, and it would be interesting to test those interactions via side-by-side coimmunoprecipitations. Finally, it is still unclear how Pak1 and RhoA/ROCK function together downstream of EphB2 receptor activation. More elaborate experiments using our primary neuron transfection assay will be needed to test these and other, perhaps more downstream, forward signaling mechanisms.

Future directions: *In Vivo* Analysis of EphB Forward Signaling

TCAs and CTAs

My characterization of the novel function of EphB receptor forward signaling during the early development of the TCA pathway establishes a clear guidance mechanism for EphB1 and EphB2 in these fibers but leaves a number of important questions unanswered. First, despite my efforts, I was unable to properly show that EphB1 drove either TCA or CTA guidance in a cell autonomous fashion. I attempted cortical *in utero* electroporation at age E12.5, a timepoint necessary to target newborn deep layer cortical neurons, but was unsuccessful with the assay. In more experienced hands, a targeted knockdown of EphB1 in deep layer neurons using such an *in utero* approach would simultaneously test if cortical EphB1 was necessary for CTA guidance and if CTA misprojections are the result of cofasciculation with aberrant TCA misprojection fascicles, which is my standing hypothesis. Thalamic *in utero* electroporation, if even possible, would also address cell autonomy and test this same hypothesis. A conditional EphB1 knockout is currently being developed by the Cowan lab through the UC Davis Mouse Biology Core and will be used for the continued study of EphB1-mediated cortical-thalamic axon development. Crossed with a cortical-specific or thalamic-specific Cre driver, the EphB1 cKO mouse

(designed by George Chenaux), which features loxp sites flanking exon 3 of the EphB1 ORF, will also address the cell autonomy question.

I would like to note, however, that a thorough expression analysis of EphB1 in the TCA and CTA axon populations could help address if EphB1 truly functions in a cell autonomous fashion during early TCA guidance. This is potentially confounded because: (1) EphB1 is highly enriched in the cell bodies located within the developing striatum at all embryonic ages that I analyzed through X-gal staining of EphB1$^{Tr/Tr}$ mice, and (2) no trusted EphB1 antibody has been developed for immunostaining (or otherwise). However, an experiment could theoretically be performed in EphB1$^{Tr/Tr}$ through dual immunolabeling with the L1-CAM antibody to label TCA axons and a β-galactosidase antibody to label EphB1. Although the immunostaining may be muddled with background EphB1 staining in the striatum, colocalization of the L1-CAM and EphB1 signals may be possible. Co-culture assays with thalamic, cortical and possibly VTel explants could also be utilized in addressing a number of these same questions.

Another interesting line of potential experiments based on my results would test if misprojected CTA axons in the VTel are permanently miswired in EphB deficient animals. Although they appear to be stuck at the brain floor in DKO mutants at postnatal ages, we cannot rule out the possibility that they may somehow still reach the thalamus, considering that they cofasciculate (at least at E16.5) with thalamic axons that originate in the dorsal thalamus. Targeted dye labeling of CTA terminals from the somatosensory origin of CTA misprojections in *EphB1/2 DKOs* would be the most straightforward, however challenging way of testing if these axons properly reach the thalamus. It would also be interesting to test if surrounding cortical regions have a disrupted terminal staining pattern in the thalamus of EphB mutants due to the CTA misprojections and the theoretical loss of CTA input into the thalamus. Similarly, it

would be very useful to identify the thalamic origin of misprojected TCAs in EphB1/2 DKO mutants. This would not only clarify the mechanism of TCA misguidance in EphB mutants, but it would also allow one to address if these misprojected TCA axons are actually able to "reintegrate" with the normal TCA population (as it appears in our stained embryonic brain sections). This finding would be fascinating as it would help explain the selective cofasciculation of CTAs with TCAs, and may help open to door into the elucidating the apparent "molecular code" that topographically lines up CTAs and TCAs for a precise and consistent handshake in the VTel during mid-development.

Finally, as one last acknowledgement to the consensus favorite question posed to me by the neuroscience community over the years, yes, behavior analysis will be performed in both EphB1/2 knockout and truncated animals by the Cowan lab in the future.

Anterior Commissure

My analysis of ACp tract formation in truncated *EphB*$^{Tr/Tr}$ mutants and drug-mediated kinase dead EphB mutants (*AS-EphB*) demonstrates that EphB forward signaling is essential for the proper development of ACp axons. Based on these results, however, ephrinB reverse signaling is also somehow necessary for ACp development. Thus, in the future, it will critical to analyze ACp tract development when stable, whole-brain *ephrinB2*$^{-/-}$ knockout or ephrinB compound knockout mice are developed. My study also included an embryonic analysis of the ACp at E14.5, but this line of axon labeling in embryonic tissue could be expanded for the analysis pioneer ACp axons at ~E14.0. A more precise labeling method would aid in visualizing the behavior of pioneer ACp axons, perhaps through stereotaxic dye injection into the temporal neocortex or even more targeted DiI labeling of these regions. The most surprising and

intriguing finding from this work was the expansion of the neocortical origin zone of ACp axons in *EphB1*$^{-/-}$*EphB2*$^{-/-}$ DKOs into more medial regions of the somatosensory cortex, which suggests that EphB1 and EphB2 also function during early subcortical axon fate determination. An early analysis of cortical axon outgrowth from the developing plate around age E13.5 in *EphB1*$^{-/-}$ *EphB2*$^{-/-}$ may demonstrate new EphB-mediated cortical guidance phenotypes. Finally, ACp misprojections in *EphB1/2* DKOs occur near the ventral region where CTA projections are misprojected in these same mutants. Thus, it would be interesting to test if these two phenotypes are related. Since CTA fibers are misprojected to the brain floor through cofasciculation onto misprojected TCA fascicles, a dual thalamic/temporal cortex dye labeling assay would be a starting experiment for determining if misprojected ACp axons also aberrantly cofasciculate with misprojected TCA fibers in *EphB1/2* DKOs.

Afterword

The experimental fields of neurodevelopment continue to grow and become more complex and interesting as more questions become answered and more targeted questions arise. What I have found most fascinating about brain development through working on axon guidance problems is the incredible consistency and precision in which the developmental program builds circuitry. Related to my work, it's particularly interesting how different cell types at different timepoints use EphB receptors and EphB signaling transduction pathways to make different axon guidance decisions. Only slight variations in the expression a different signaling effector, for example, enable this redundancy among various pathways. I sincerely hope that, in the field of axon guidance, molecular research of EphB receptor signaling and other guidance signaling mechanisms continue, as these pathways and their convergence and cooperativity will help build the “bigger picture” and enlighten our understanding of CNS development.

Though I am thoroughly satisfied with the progress made in all of my graduate research projects, I am most proud and excited about the novel EphB receptor thalamocortical phenotype that I discovered and characterized. This project took a number of exciting twists and turns over the years, as I was able explain a complex phenotype with interesting and exciting data. In addition, Chris and I were able to use our results to address the handshake hypothesis, which for over 20 years has been debated and tested by investigators. The impact of our findings in this regard has already been evident. Still, my hope is that these findings are well received by colleagues in the field and that I have, in some manner, stimulated future science in our lab and beyond.

References

Abe, K., Rossman, K.L., Liu, B., Ritola, K.D., Chiang, D., Campbell, S.L., Burridge, K., and Der, C.J. (2000). Vav2 is an activator of Cdc42, Rac1, and RhoA. J Biol Chem *275*, 10141-10149.

Aghazadeh, B., Lowry, W.E., Huang, X.Y., and Rosen, M.K. (2000). Structural basis for relief of autoinhibition of the Dbl homology domain of proto-oncogene Vav by tyrosine phosphorylation. Cell *102*, 625-633.

Alitto, H.J., and Usrey, W.M. (2003). Corticothalamic feedback and sensory processing. Curr Opin Neurobiol *13*, 440-445.

Allen, K.M., Gleeson, J.G., Bagrodia, S., Partington, M.W., MacMillan, J.C., Cerione, R.A., Mulley, J.C., and Walsh, C.A. (1998). PAK3 mutation in nonsyndromic X-linked mental retardation. Nat Genet *20*, 25-30.

Arias-Romero, L.E., and Chernoff, J. (2008). A tale of two Paks. Biol Cell *100*, 97-108.

Auladell, C., Perez-Sust, P., Super, H., and Soriano, E. (2000). The early development of thalamocortical and corticothalamic projections in the mouse. Anat Embryol (Berl) *201*, 169-179.

Bagnard, D., Chounlamountri, N., Puschel, A.W., and Bolz, J. (2001). Axonal surface molecules act in combination with semaphorin 3a during the establishment of corticothalamic projections. Cereb Cortex *11*, 278-285.

Bagnard, D., Lohrum, M., Uziel, D., Puschel, A.W., and Bolz, J. (1998). Semaphorins act as attractive and repulsive guidance signals during the development of cortical projections. Development *125*, 5043-5053.

Bagri, A., Marin, O., Plump, A.S., Mak, J., Pleasure, S.J., Rubenstein, J.L., and Tessier-Lavigne, M. (2002). Slit proteins prevent midline crossing and determine the dorsoventral position of major axonal pathways in the mammalian forebrain. Neuron *33*, 233-248.

Bamburg, J.R. (1999). Proteins of the ADF/cofilin family: essential regulators of actin dynamics. Annu Rev Cell Dev Biol *15*, 185-230.

Bao, Z.Z. (2008). Intraretinal projection of retinal ganglion cell axons as a model system for studying axon navigation. Brain Res *1192*, 165-177.

Bartley, T.D., Hunt, R.W., Welcher, A.A., Boyle, W.J., Parker, V.P., Lindberg, R.A., Lu, H.S., Colombero, A.M., Elliott, R.L., Guthrie, B.A.*, et al.* (1994). B61 is a ligand for the ECK receptor protein-tyrosine kinase. Nature *368*, 558-560.

Bashaw, G.J., and Klein, R. (2010). Signaling from axon guidance receptors. Cold Spring Harb Perspect Biol *2*, a001941.

Beckmann, M.P., Cerretti, D.P., Baum, P., Vanden Bos, T., James, L., Farrah, T., Kozlosky, C., Hollingsworth, T., Shilling, H., Maraskovsky, E.*, et al.* (1994). Molecular characterization of a family of ligands for eph-related tyrosine kinase receptors. EMBO J *13*, 3757-3762.

Ben-Sasson, A., Cermak, S.A., Orsmond, G.I., Tager-Flusberg, H., Kadlec, M.B., and Carter, A.S. (2008). Sensory clusters of toddlers with autism spectrum disorders: differences in affective symptoms. J Child Psychol Psychiatry *49*, 817-825.

Bielle, F., Marcos-Mondejar, P., Keita, M., Mailhes, C., Verney, C., Nguyen Ba-Charvet, K., Tessier-Lavigne, M., Lopez-Bendito, G., and Garel, S. (2011a). Slit2 activity in the migration of guidepost neurons shapes thalamic projections during development and evolution. Neuron *69*, 1085-1098.

Bielle, F., Marcos-Mondejar, P., Leyva-Diaz, E., Lokmane, L., Mire, E., Mailhes, C., Keita, M., Garcia, N., Tessier-Lavigne, M., Garel, S.*, et al.* (2011b). Emergent growth cone responses to combinations of Slit1 and Netrin 1 in thalamocortical axon topography. Curr Biol *21*, 1748-1755.

Bienvenu, T., des Portes, V., McDonell, N., Carrie, A., Zemni, R., Couvert, P., Ropers, H.H., Moraine, C., van Bokhoven, H., Fryns, J.P.*, et al.* (2000). Missense mutation in PAK3, R67C, causes X-linked nonspecific mental retardation. Am J Med Genet *93*, 294-298.

Birgbauer, E., Cowan, C.A., Sretavan, D.W., and Henkemeyer, M. (2000). Kinase independent function of EphB receptors in retinal axon pathfinding to the optic disc from dorsal but not ventral retina. Development *127*, 1231-1241.

Birgbauer, E., Oster, S.F., Severin, C.G., and Sretavan, D.W. (2001). Retinal axon growth cones respond to EphB extracellular domains as inhibitory axon guidance cues. Development *128*, 3041-3048.

Blakemore, C., and Molnar, Z. (1990). Factors involved in the establishment of specific interconnections between thalamus and cerebral cortex. Cold Spring Harb Symp Quant Biol *55*, 491-504.

Blethrow, J., Zhang, C., Shokat, K.M., and Weiss, E.L. (2004). Design and use of analog-sensitive protein kinases. Curr Protoc Mol Biol *Chapter 18*, Unit 18 11.

Bokoch, G.M. (2003). Biology of the p21-activated kinases. Annu Rev Biochem *72*, 743-781.

Bourassa, J., and Deschenes, M. (1995). Corticothalamic projections from the primary visual cortex in rats: a single fiber study using biocytin as an anterograde tracer. Neuroscience *66*, 253-263.

Bourassa, J., Pinault, D., and Deschenes, M. (1995). Corticothalamic projections from the cortical barrel field to the somatosensory thalamus in rats: a single-fibre study using biocytin as an anterograde tracer. Eur J Neurosci *7*, 19-30.

Braisted, J.E., Catalano, S.M., Stimac, R., Kennedy, T.E., Tessier-Lavigne, M., Shatz, C.J., and O'Leary, D.D. (2000). Netrin-1 promotes thalamic axon growth and is required for proper development of the thalamocortical projection. J Neurosci *20*, 5792-5801.

Briancon-Marjollet, A., Ghogha, A., Nawabi, H., Triki, I., Auziol, C., Fromont, S., Piche, C., Enslen, H., Chebli, K., Cloutier, J.F.*, et al.* (2008). Trio mediates netrin-1-induced Rac1 activation in axon outgrowth and guidance. Mol Cell Biol *28*, 2314-2323.

Buday, L., Wunderlich, L., and Tamas, P. (2002). The Nck family of adapter proteins: regulators of actin cytoskeleton. Cell Signal *14*, 723-731.

Bush, J.O., and Soriano, P. (2009). Ephrin-B1 regulates axon guidance by reverse signaling through a PDZ-dependent mechanism. Genes Dev *23*, 1586-1599.

Bustelo, X.R. (2000). Regulatory and signaling properties of the Vav family. Mol Cell Biol *20*, 1461-1477.

Bustelo, X.R. (2001). Vav proteins, adaptors and cell signaling. Oncogene *20*, 6372-6381.

Causeret, F., Terao, M., Jacobs, T., Nishimura, Y.V., Yanagawa, Y., Obata, K., Hoshino, M., and Nikolic, M. (2009). The p21-activated kinase is required for neuronal migration in the cerebral cortex. Cereb Cortex *19*, 861-875.

Chedotal, A., and Richards, L.J. (2010). Wiring the brain: the biology of neuronal guidance. Cold Spring Harb Perspect Biol *2*, a001917.

Chen, H., Bagri, A., Zupicich, J.A., Zou, Y., Stoeckli, E., Pleasure, S.J., Lowenstein, D.H., Skarnes, W.C., Chedotal, A., and Tessier-Lavigne, M. (2000). Neuropilin-2 regulates the development of selective cranial and sensory nerves and hippocampal mossy fiber projections. Neuron *25*, 43-56.

Chenaux, G., and Henkemeyer, M. (2011). Forward signaling by EphB1/EphB2 interacting with ephrin-B ligands at the optic chiasm is required to form the ipsilateral projection. Eur J Neurosci *34*, 1620-1633.

Cheng, H.J., and Flanagan, J.G. (1994). Identification and cloning of ELF-1, a developmentally expressed ligand for the Mek4 and Sek receptor tyrosine kinases. Cell *79*, 157-168.

Cheng, Y., Chou, K.H., Chen, I.Y., Fan, Y.T., Decety, J., and Lin, C.P. (2010). Atypical development of white matter microstructure in adolescents with autism spectrum disorders. Neuroimage *50*, 873-882.

Colello, R.J., and Guillery, R.W. (1990). The early development of retinal ganglion cells with uncrossed axons in the mouse: retinal position and axonal course. Development *108*, 515-523.

Colicelli, J. (2004). Human RAS superfamily proteins and related GTPases. Sci STKE *2004*, RE13.

Connor, R.J., Menzel, P., and Pasquale, E.B. (1998). Expression and tyrosine phosphorylation of Eph receptors suggest multiple mechanisms in patterning of the visual system. Dev Biol *193*, 21-35.

Cotteret, S., Jaffer, Z.M., Beeser, A., and Chernoff, J. (2003). p21-Activated kinase 5 (Pak5) localizes to mitochondria and inhibits apoptosis by phosphorylating BAD. Mol Cell Biol *23*, 5526-5539.

Cowan, C.A., and Henkemeyer, M. (2002). Ephrins in reverse, park and drive. Trends Cell Biol *12*, 339-346.

Cowan, C.A., Yokoyama, N., Saxena, A., Chumley, M.J., Silvany, R.E., Baker, L.A., Srivastava, D., and Henkemeyer, M. (2004). Ephrin-B2 reverse signaling is required for axon pathfinding and cardiac valve formation but not early vascular development. Dev Biol *271*, 263-271.

Cowan, C.W., Shao, Y.R., Sahin, M., Shamah, S.M., Lin, M.Z., Greer, P.L., Gao, S., Griffith, E.C., Brugge, J.S., and Greenberg, M.E. (2005). Vav family GEFs link activated Ephs to endocytosis and axon guidance. Neuron *46*, 205-217.

Crane, L., Goddard, L., and Pring, L. (2009). Sensory processing in adults with autism spectrum disorders. Autism *13*, 215-228.

Cummings, D.M., Malun, D., and Brunjes, P.C. (1997). Development of the anterior commissure in the opossum: midline extracellular space and glia coincide with early axon decussation. J Neurobiol *32*, 403-414.

Dalva, M.B., Takasu, M.A., Lin, M.Z., Shamah, S.M., Hu, L., Gale, N.W., and Greenberg, M.E. (2000). EphB receptors interact with NMDA receptors and regulate excitatory synapse formation. Cell *103*, 945-956.

Davis, S., Gale, N.W., Aldrich, T.H., Maisonpierre, P.C., Lhotak, V., Pawson, T., Goldfarb, M., and Yancopoulos, G.D. (1994). Ligands for EPH-related receptor tyrosine kinases that require membrane attachment or clustering for activity. Science *266*, 816-819.

Davy, A., Aubin, J., and Soriano, P. (2004). Ephrin-B1 forward and reverse signaling are required during mouse development. Genes Dev *18*, 572-583.

Deck, M., Lokmane, L., Chauvet, S., Mailhes, C., Keita, M., Niquille, M., Yoshida, M., Yoshida, Y., Lebrand, C., Mann, F.*, et al.* (2013). Pathfinding of corticothalamic axons relies on a rendezvous with thalamic projections. Neuron *77*, 472-484.

Deiner, M.S., Kennedy, T.E., Fazeli, A., Serafini, T., Tessier-Lavigne, M., and Sretavan, D.W. (1997). Netrin-1 and DCC mediate axon guidance locally at the optic disc: loss of function leads to optic nerve hypoplasia. Neuron *19*, 575-589.

Demyanenko, G.P., Siesser, P.F., Wright, A.G., Brennaman, L.H., Bartsch, U., Schachner, M., and Maness, P.F. (2011). L1 and CHL1 Cooperate in Thalamocortical Axon Targeting. Cereb Cortex *21*, 401-412.

Dent, E.W., Gupton, S.L., and Gertler, F.B. (2011). The growth cone cytoskeleton in axon outgrowth and guidance. Cold Spring Harb Perspect Biol *3*.

Dharmawardhane, S., Sanders, L.C., Martin, S.S., Daniels, R.H., and Bokoch, G.M. (1997). Localization of p21-activated kinase 1 (PAK1) to pinocytic vesicles and cortical actin structures in stimulated cells. J Cell Biol *138*, 1265-1278.

Dharmawardhane, S., Schurmann, A., Sells, M.A., Chernoff, J., Schmid, S.L., and Bokoch, G.M. (2000). Regulation of macropinocytosis by p21-activated kinase-1. Mol Biol Cell *11*, 3341-3352.

Dickson, B.J. (2001). Rho GTPases in growth cone guidance. Curr Opin Neurobiol *11*, 103-110.

Drager, U.C. (1985). Birth dates of retinal ganglion cells giving rise to the crossed and uncrossed optic projections in the mouse. Proc R Soc Lond B Biol Sci *224*, 57-77.

Dravis, C., Yokoyama, N., Chumley, M.J., Cowan, C.A., Silvany, R.E., Shay, J., Baker, L.A., and Henkemeyer, M. (2004). Bidirectional signaling mediated by ephrin-B2 and EphB2 controls urorectal development. Dev Biol *271*, 272-290.

Dufour, A., Egea, J., Kullander, K., Klein, R., and Vanderhaeghen, P. (2006). Genetic analysis of EphA-dependent signaling mechanisms controlling topographic mapping in vivo. Development *133*, 4415-4420.

Dufour, A., Seibt, J., Passante, L., Depaepe, V., Ciossek, T., Frisen, J., Kullander, K., Flanagan, J.G., Polleux, F., and Vanderhaeghen, P. (2003). Area specificity and topography of thalamocortical projections are controlled by ephrin/Eph genes. Neuron *39*, 453-465.

Eblen, S.T., Slack, J.K., Weber, M.J., and Catling, A.D. (2002). Rac-PAK signaling stimulates extracellular signal-regulated kinase (ERK) activation by regulating formation of MEK1-ERK complexes. Mol Cell Biol *22*, 6023-6033.

Edwards, D.C., Sanders, L.C., Bokoch, G.M., and Gill, G.N. (1999). Activation of LIM-kinase by Pak1 couples Rac/Cdc42 GTPase signalling to actin cytoskeletal dynamics. Nat Cell Biol *1*, 253-259.

Egea, J., and Klein, R. (2007). Bidirectional Eph-ephrin signaling during axon guidance. Trends Cell Biol *17*, 230-238.

Erskine, L., and Herrera, E. (2007). The retinal ganglion cell axon's journey: insights into molecular mechanisms of axon guidance. Dev Biol *308*, 1-14.

Erskine, L., Reijntjes, S., Pratt, T., Denti, L., Schwarz, Q., Vieira, J.M., Alakakone, B., Shewan, D., and Ruhrberg, C. (2011). VEGF signaling through neuropilin 1 guides commissural axon crossing at the optic chiasm. Neuron *70*, 951-965.

Erskine, L., Williams, S.E., Brose, K., Kidd, T., Rachel, R.A., Goodman, C.S., Tessier-Lavigne, M., and Mason, C.A. (2000). Retinal ganglion cell axon guidance in the mouse optic chiasm: expression and function of robos and slits. J Neurosci *20*, 4975-4982.

Falk, J., Bechara, A., Fiore, R., Nawabi, H., Zhou, H., Hoyo-Becerra, C., Bozon, M., Rougon, G., Grumet, M., Puschel, A.W.*, et al.* (2005). Dual functional activity of semaphorin 3B is required for positioning the anterior commissure. Neuron *48*, 63-75.

Fan, X., Labrador, J.P., Hing, H., and Bashaw, G.J. (2003). Slit stimulation recruits Dock and Pak to the roundabout receptor and increases Rac activity to regulate axon repulsion at the CNS midline. Neuron *40*, 113-127.

Fawcett, J.P., Georgiou, J., Ruston, J., Bladt, F., Sherman, A., Warner, N., Saab, B.J., Scott, R., Roder, J.C., and Pawson, T. (2007). Nck adaptor proteins control the organization of neuronal circuits important for walking. Proc Natl Acad Sci U S A *104*, 20973-20978.

Feldheim, D.A., Kim, Y.I., Bergemann, A.D., Frisen, J., Barbacid, M., and Flanagan, J.G. (2000). Genetic analysis of ephrin-A2 and ephrin-A5 shows their requirement in multiple aspects of retinocollicular mapping. Neuron *25*, 563-574.

Feldheim, D.A., Vanderhaeghen, P., Hansen, M.J., Frisen, J., Lu, Q., Barbacid, M., and Flanagan, J.G. (1998). Topographic guidance labels in a sensory projection to the forebrain. Neuron *21*, 1303-1313.

Fournier, A.E., Nakamura, F., Kawamoto, S., Goshima, Y., Kalb, R.G., and Strittmatter, S.M. (2000). Semaphorin3A enhances endocytosis at sites of receptor-F-actin colocalization during growth cone collapse. J Cell Biol *149*, 411-422.

Frisen, J., Yates, P.A., McLaughlin, T., Friedman, G.C., O'Leary, D.D., and Barbacid, M. (1998). Ephrin-A5 (AL-1/RAGS) is essential for proper retinal axon guidance and topographic mapping in the mammalian visual system. Neuron *20*, 235-243.

Fujikawa, K., Iwata, T., Inoue, K., Akahori, M., Kadotani, H., Fukaya, M., Watanabe, M., Chang, Q., Barnett, E.M., and Swat, W. (2010). VAV2 and VAV3 as candidate disease genes for spontaneous glaucoma in mice and humans. PLoS One *5*, e9050.

Fukuda, T., Kawano, H., Ohyama, K., Li, H.P., Takeda, Y., Oohira, A., and Kawamura, K. (1997). Immunohistochemical localization of neurocan and L1 in the formation of thalamocortical pathway of developing rats. J Comp Neurol *382*, 141-152.

Fukuda, Y., Sawai, H., Watanabe, M., Wakakuwa, K., and Morigiwa, K. (1989). Nasotemporal overlap of crossed and uncrossed retinal ganglion cell projections in the Japanese monkey (Macaca fuscata). J Neurosci *9*, 2353-2373.

Gale, N.W., Holland, S.J., Valenzuela, D.M., Flenniken, A., Pan, L., Ryan, T.E., Henkemeyer, M., Strebhardt, K., Hirai, H., Wilkinson, D.G.*, et al.* (1996). Eph receptors and ligands comprise two major specificity subclasses and are reciprocally compartmentalized during embryogenesis. Neuron *17*, 9-19.

Galisteo, M.L., Chernoff, J., Su, Y.C., Skolnik, E.Y., and Schlessinger, J. (1996). The adaptor protein Nck links receptor tyrosine kinases with the serine-threonine kinase Pak1. J Biol Chem *271*, 20997-21000.

Garcia-Frigola, C., Carreres, M.I., Vegar, C., Mason, C., and Herrera, E. (2008). Zic2 promotes axonal divergence at the optic chiasm midline by EphB1-dependent and -independent mechanisms. Development *135*, 1833-1841.

Garel, S., Yun, K., Grosschedl, R., and Rubenstein, J.L. (2002). The early topography of thalamocortical projections is shifted in Ebf1 and Dlx1/2 mutant mice. Development *129*, 5621-5634.

Garrity, P.A., Rao, Y., Salecker, I., McGlade, J., Pawson, T., and Zipursky, S.L. (1996). Drosophila photoreceptor axon guidance and targeting requires the dreadlocks SH2/SH3 adapter protein. Cell *85*, 639-650.

Gauthier, L.R., and Robbins, S.M. (2003). Ephrin signaling: One raft to rule them all? One raft to sort them? One raft to spread their call and in signaling bind them? Life Sci *74*, 207-216.

Gedeon, A.K., Nelson, J., Gecz, J., and Mulley, J.C. (2003). X-linked mild non-syndromic mental retardation with neuropsychiatric problems and the missense mutation A365E in PAK3. Am J Med Genet A *120A*, 509-517.

Genander, M., Halford, M.M., Xu, N.J., Eriksson, M., Yu, Z., Qiu, Z., Martling, A., Greicius, G., Thakar, S., Catchpole, T.*, et al.* (2009). Dissociation of EphB2 signaling pathways mediating progenitor cell proliferation and tumor suppression. Cell *139*, 679-692.

Georgakopoulos, A., Litterst, C., Ghersi, E., Baki, L., Xu, C., Serban, G., and Robakis, N.K. (2006). Metalloproteinase/Presenilin1 processing of ephrinB regulates EphB-induced Src phosphorylation and signaling. EMBO J *25*, 1242-1252.

Gerety, S.S., and Anderson, D.J. (2002). Cardiovascular ephrinB2 function is essential for embryonic angiogenesis. Development *129*, 1397-1410.

Giger, R.J., Cloutier, J.F., Sahay, A., Prinjha, R.K., Levengood, D.V., Moore, S.E., Pickering, S., Simmons, D., Rastan, S., Walsh, F.S.*, et al.* (2000). Neuropilin-2 is required in vivo for selective axon guidance responses to secreted semaphorins. Neuron *25*, 29-41.

Godement, P., Salaun, J., and Mason, C.A. (1990). Retinal axon pathfinding in the optic chiasm: divergence of crossed and uncrossed fibers. Neuron *5*, 173-186.

Godement, P., Salaun, J., and Metin, C. (1987). Fate of uncrossed retinal projections following early or late prenatal monocular enucleation in the mouse. J Comp Neurol *255*, 97-109.

Godement, P., Wang, L.C., and Mason, C.A. (1994). Retinal axon divergence in the optic chiasm: dynamics of growth cone behavior at the midline. J Neurosci *14*, 7024-7039.

Gray, J.A., Sheffler, D.J., Bhatnagar, A., Woods, J.A., Hufeisen, S.J., Benovic, J.L., and Roth, B.L. (2001). Cell-type specific effects of endocytosis inhibitors on 5-hydroxytryptamine(2A) receptor desensitization and resensitization reveal an arrestin-, GRK2-, and GRK5-independent mode of regulation in human embryonic kidney 293 cells. Mol Pharmacol *60*, 1020-1030.

Hale, C.F., Dietz, K.C., Varela, J.A., Wood, C.B., Zirlin, B.C., Leverich, L.S., Greene, R.W., and Cowan, C.W. (2011). Essential role for vav Guanine nucleotide exchange factors in brain-derived neurotrophic factor-induced dendritic spine growth and synapse plasticity. J Neurosci *31*, 12426-12436.

Hall, A. (1998). Rho GTPases and the actin cytoskeleton. Science *279*, 509-514.

Hall, A., and Lalli, G. (2010). Rho and Ras GTPases in axon growth, guidance, and branching. Cold Spring Harb Perspect Biol *2*, a001818.

Harada, T., Harada, C., and Parada, L.F. (2007). Molecular regulation of visual system development: more than meets the eye. Genes Dev *21*, 367-378.

Harbott, L.K., and Nobes, C.D. (2005). A key role for Abl family kinases in EphA receptor-mediated growth cone collapse. Mol Cell Neurosci *30*, 1-11.

Hattori, M., Osterfield, M., and Flanagan, J.G. (2000). Regulated cleavage of a contact-mediated axon repellent. Science *289*, 1360-1365.

Hayashi, K., Ohshima, T., Hashimoto, M., and Mikoshiba, K. (2007). Pak1 regulates dendritic branching and spine formation. Dev Neurobiol *67*, 655-669.

Hebert, J.M., and McConnell, S.K. (2000). Targeting of cre to the Foxg1 (BF-1) locus mediates loxP recombination in the telencephalon and other developing head structures. Dev Biol *222*, 296-306.

Henkemeyer, M., Itkis, O.S., Ngo, M., Hickmott, P.W., and Ethell, I.M. (2003). Multiple EphB receptor tyrosine kinases shape dendritic spines in the hippocampus. J Cell Biol *163*, 1313-1326.

Henkemeyer, M., Orioli, D., Henderson, J.T., Saxton, T.M., Roder, J., Pawson, T., and Klein, R. (1996). Nuk controls pathfinding of commissural axons in the mammalian central nervous system. Cell *86*, 35-46.

Herrera, E., Brown, L., Aruga, J., Rachel, R.A., Dolen, G., Mikoshiba, K., Brown, S., and Mason, C.A. (2003). Zic2 patterns binocular vision by specifying the uncrossed retinal projection. Cell *114*, 545-557.

Hertel, C., Coulter, S.J., and Perkins, J.P. (1985). A comparison of catecholamine-induced internalization of beta-adrenergic receptors and receptor-mediated endocytosis of epidermal growth factor in human astrocytoma cells. Inhibition by phenylarsine oxide. J Biol Chem *260*, 12547-12553.

Hevner, R.F., Miyashita-Lin, E., and Rubenstein, J.L. (2002). Cortical and thalamic axon pathfinding defects in Tbr1, Gbx2, and Pax6 mutant mice: evidence that cortical and thalamic axons interact and guide each other. J Comp Neurol *447*, 8-17.

Himanen, J.P., Chumley, M.J., Lackmann, M., Li, C., Barton, W.A., Jeffrey, P.D., Vearing, C., Geleick, D., Feldheim, D.A., Boyd, A.W.*, et al.* (2004). Repelling class discrimination: ephrin-A5 binds to and activates EphB2 receptor signaling. Nat Neurosci *7*, 501-509.

Himanen, J.P., and Nikolov, D.B. (2003). Eph signaling: a structural view. Trends Neurosci *26*, 46-51.

Himanen, J.P., Rajashankar, K.R., Lackmann, M., Cowan, C.A., Henkemeyer, M., and Nikolov, D.B. (2001). Crystal structure of an Eph receptor-ephrin complex. Nature *414*, 933-938.

Hindges, R., McLaughlin, T., Genoud, N., Henkemeyer, M., and O'Leary, D. (2002a). EphB forward signaling controls directional branch extension and arborization required for dorsal-ventral retinotopic mapping. Neuron *35*, 475-487.

Hindges, R., McLaughlin, T., Genoud, N., Henkemeyer, M., and O'Leary, D.D. (2002b). EphB forward signaling controls directional branch extension and arborization required for dorsal-ventral retinotopic mapping. Neuron *35*, 475-487.

Hing, H., Xiao, J., Harden, N., Lim, L., and Zipursky, S.L. (1999). Pak functions downstream of Dock to regulate photoreceptor axon guidance in Drosophila. Cell *97*, 853-863.

Hirai, H., Maru, Y., Hagiwara, K., Nishida, J., and Takaku, F. (1987). A novel putative tyrosine kinase receptor encoded by the eph gene. Science *238*, 1717-1720.

Ho, S.K., Kovacevic, N., Henkelman, R.M., Boyd, A., Pawson, T., and Henderson, J.T. (2009). EphB2 and EphA4 receptors regulate formation of the principal inter-hemispheric tracts of the mammalian forebrain. Neuroscience *160*, 784-795.

Holland, S.J., Gale, N.W., Gish, G.D., Roth, R.A., Songyang, Z., Cantley, L.C., Henkemeyer, M., Yancopoulos, G.D., and Pawson, T. (1997). Juxtamembrane tyrosine residues couple the Eph family receptor EphB2/Nuk to specific SH2 domain proteins in neuronal cells. EMBO J *16*, 3877-3888.

Holland, S.J., Gale, N.W., Mbamalu, G., Yancopoulos, G.D., Henkemeyer, M., and Pawson, T. (1996). Bidirectional signalling through the EPH-family receptor Nuk and its transmembrane ligands. Nature *383*, 722-725.

Hossain, M., Ahmed, G., Naser, I.B., Shinmyo, Y., Ito, A., Riyadh, M.A., Felemban, A., Song, X., Ohta, K., and Tanaka, H. (2013). The combinatorial guidance activities of draxin and Tsukushi are essential for forebrain commissure formation. Dev Biol *374*, 58-70.

Hu, T., Shi, G., Larose, L., Rivera, G.M., Mayer, B.J., and Zhou, R. (2009). Regulation of process retraction and cell migration by EphA3 is mediated by the adaptor protein Nck1. Biochemistry *48*, 6369-6378.

Hu, Z., Yue, X., Shi, G., Yue, Y., Crockett, D.P., Blair-Flynn, J., Reuhl, K., Tessarollo, L., and Zhou, R. (2003). Corpus callosum deficiency in transgenic mice expressing a truncated ephrin-A receptor. J Neurosci *23*, 10963-10970.

Huang, H., Feng, X., Zhuang, J., Frohlich, O., Klein, J.D., Cai, H., Sands, J.M., and Chen, G. (2010). Internalization of UT-A1 urea transporter is dynamin dependent and mediated by both caveolae- and clathrin-coated pit pathways. Am J Physiol Renal Physiol *299*, F1389-1395.

Innocenti, G.M., Aggoun-Zouaoui, D., and Lehmann, P. (1995). Cellular aspects of callosal connections and their development. Neuropsychologia *33*, 961-987.

Islam, S.M., Shinmyo, Y., Okafuji, T., Su, Y., Naser, I.B., Ahmed, G., Zhang, S., Chen, S., Ohta, K., Kiyonari, H.*, et al.* (2009). Draxin, a repulsive guidance protein for spinal cord and forebrain commissures. Science *323*, 388-393.

Ito, A., Shinmyo, Y., Abe, T., Oshima, N., Tanaka, H., and Ohta, K. (2010). Tsukushi is required for anterior commissure formation in mouse brain. Biochem Biophys Res Commun *402*, 813-818.

Iwasato, T., Katoh, H., Nishimaru, H., Ishikawa, Y., Inoue, H., Saito, Y.M., Ando, R., Iwama, M., Takahashi, R., Negishi, M.*, et al.* (2007). Rac-GAP alpha-chimerin regulates motor-circuit formation as a key mediator of EphrinB3/EphA4 forward signaling. Cell *130*, 742-753.

Jacobs, E.C., Campagnoni, C., Kampf, K., Reyes, S.D., Kalra, V., Handley, V., Xie, Y.Y., Hong-Hu, Y., Spreur, V., Fisher, R.S.*, et al.* (2007a). Visualization of corticofugal projections during early cortical development in a tau-GFP-transgenic mouse. Eur J Neurosci *25*, 17-30.

Jacobs, T., Causeret, F., Nishimura, Y.V., Terao, M., Norman, A., Hoshino, M., and Nikolic, M. (2007b). Localized activation of p21-activated kinase controls neuronal polarity and morphology. J Neurosci *27*, 8604-8615.

Jaffe, A.B., and Hall, A. (2005). Rho GTPases: biochemistry and biology. Annu Rev Cell Dev Biol *21*, 247-269.

Jouandet, M.L. (1982). Neocortical and basal telencephalic origins of the anterior commissure of the cat. Neuroscience *7*, 1731-1752.

Jouandet, M.L., and Gazzaniga, M.S. (1979). Cortical field of origin of the anterior commissure of the rhesus monkey. Exp Neurol *66*, 381-397.

Jouandet, M.L., and Hartenstein, V. (1983). Basal telencephalic origins of the anterior commissure of the rat. Exp Brain Res *50*, 183-192.

Jurney, W.M., Gallo, G., Letourneau, P.C., and McLoon, S.C. (2002). Rac1-mediated endocytosis during ephrin-A2- and semaphorin 3A-induced growth cone collapse. J Neurosci *22*, 6019-6028.

Just, M.A., Cherkassky, V.L., Keller, T.A., and Minshew, N.J. (2004). Cortical activation and synchronization during sentence comprehension in high-functioning autism: evidence of underconnectivity. Brain *127*, 1811-1821.

Kadison, S.R., Makinen, T., Klein, R., Henkemeyer, M., and Kaprielian, Z. (2006). EphB receptors and ephrin-B3 regulate axon guidance at the ventral midline of the embryonic mouse spinal cord. J Neurosci *26*, 8909-8914.

Kamiguchi, H., Hlavin, M.L., Yamasaki, M., and Lemmon, V. (1998). Adhesion molecules and inherited diseases of the human nervous system. Annu Rev Neurosci *21*, 97-125.

Katz, M.J., Lasek, R.J., and Silver, J. (1983). Ontophyletics of the nervous system: development of the corpus callosum and evolution of axon tracts. Proc Natl Acad Sci U S A *80*, 5936-5940.

Kawakatsu, T., Ogita, H., Fukuhara, T., Fukuyama, T., Minami, Y., Shimizu, K., and Takai, Y. (2005). Vav2 as a Rac-GDP/GTP exchange factor responsible for the nectin-induced, c-Src- and Cdc42-mediated activation of Rac. J Biol Chem *280*, 4940-4947.

Kayser, M.S., McClelland, A.C., Hughes, E.G., and Dalva, M.B. (2006). Intracellular and trans-synaptic regulation of glutamatergic synaptogenesis by EphB receptors. J Neurosci *26*, 12152-12164.

Kayser, M.S., Nolt, M.J., and Dalva, M.B. (2008). EphB receptors couple dendritic filopodia motility to synapse formation. Neuron *59*, 56-69.

Keeble, T.R., Halford, M.M., Seaman, C., Kee, N., Macheda, M., Anderson, R.B., Stacker, S.A., and Cooper, H.M. (2006). The Wnt receptor Ryk is required for Wnt5a-mediated axon guidance on the contralateral side of the corpus callosum. J Neurosci *26*, 5840-5848.

Keynes, R., and Lumsden, A. (1990). Segmentation and the origin of regional diversity in the vertebrate central nervous system. Neuron *4*, 1-9.

King, C.C., Gardiner, E.M., Zenke, F.T., Bohl, B.P., Newton, A.C., Hemmings, B.A., and Bokoch, G.M. (2000). p21-activated kinase (PAK1) is phosphorylated and activated by 3-phosphoinositide-dependent kinase-1 (PDK1). J Biol Chem *275*, 41201-41209.

Kullander, K., Croll, S.D., Zimmer, M., Pan, L., McClain, J., Hughes, V., Zabski, S., DeChiara, T.M., Klein, R., Yancopoulos, G.D.*, et al.* (2001a). Ephrin-B3 is the midline barrier that prevents corticospinal tract axons from recrossing, allowing for unilateral motor control. Genes Dev *15*, 877-888.

Kullander, K., and Klein, R. (2002). Mechanisms and functions of Eph and ephrin signalling. Nat Rev Mol Cell Biol *3*, 475-486.

Kullander, K., Mather, N.K., Diella, F., Dottori, M., Boyd, A.W., and Klein, R. (2001b). Kinase-dependent and kinase-independent functions of EphA4 receptors in major axon tract formation in vivo. Neuron *29*, 73-84.

Kuwajima, T., Yoshida, Y., Takegahara, N., Petros, T.J., Kumanogoh, A., Jessell, T.M., Sakurai, T., and Mason, C. (2012). Optic chiasm presentation of Semaphorin6D in the context of Plexin-A1 and Nr-CAM promotes retinal axon midline crossing. Neuron *74*, 676-690.

Kwan, K.Y., Lam, M.M., Krsnik, Z., Kawasawa, Y.I., Lefebvre, V., and Sestan, N. (2008). SOX5 postmitotically regulates migration, postmigratory differentiation, and projections of subplate and deep-layer neocortical neurons. Proc Natl Acad Sci U S A *105*, 16021-16026.

Kwan, K.Y., Sestan, N., and Anton, E.S. (2012). Transcriptional co-regulation of neuronal migration and laminar identity in the neocortex. Development *139*, 1535-1546.

Lakhina, V., Falnikar, A., Bhatnagar, L., and Tole, S. (2007). Early thalamocortical tract guidance and topographic sorting of thalamic projections requires LIM-homeodomain gene Lhx2. Dev Biol *306*, 703-713.

Lauderdale, J.D., Davis, N.M., and Kuwada, J.Y. (1997). Axon tracts correlate with netrin-1a expression in the zebrafish embryo. Mol Cell Neurosci *9*, 293-313.

Lee, R., Petros, T.J., and Mason, C.A. (2008). Zic2 regulates retinal ganglion cell axon avoidance of ephrinB2 through inducing expression of the guidance receptor EphB1. J Neurosci *28*, 5910-5919.

Leekam, S.R., Nieto, C., Libby, S.J., Wing, L., and Gould, J. (2007). Describing the sensory abnormalities of children and adults with autism. J Autism Dev Disord *37*, 894-910.

Lett, R.L., Wang, W., and O'Connor, T.P. (2009). Semaphorin 5B is a novel inhibitory cue for corticofugal axons. Cereb Cortex *19*, 1408-1421.

Li, L., Tasic, B., Micheva, K.D., Ivanov, V.M., Spletter, M.L., Smith, S.J., and Luo, L. (2010). Visualizing the distribution of synapses from individual neurons in the mouse brain. PLoS One *5*, e11503.

Li, W., Fan, J., and Woodley, D.T. (2001). Nck/Dock: an adapter between cell surface receptors and the actin cytoskeleton. Oncogene *20*, 6403-6417.

Lindwall, C., Fothergill, T., and Richards, L.J. (2007). Commissure formation in the mammalian forebrain. Curr Opin Neurobiol *17*, 3-14.

Little, G.E., Lopez-Bendito, G., Runker, A.E., Garcia, N., Pinon, M.C., Chedotal, A., Molnar, Z., and Mitchell, K.J. (2009). Specificity and plasticity of thalamocortical connections in Sema6A mutant mice. PLoS Biol *7*, e98.

Liu, B.P., and Burridge, K. (2000). Vav2 activates Rac1, Cdc42, and RhoA downstream from growth factor receptors but not beta1 integrins. Mol Cell Biol *20*, 7160-7169.

Lopez-Bendito, G., Cautinat, A., Sanchez, J.A., Bielle, F., Flames, N., Garratt, A.N., Talmage, D.A., Role, L.W., Charnay, P., Marin, O*., et al.* (2006). Tangential neuronal migration controls axon guidance: a role for neuregulin-1 in thalamocortical axon navigation. Cell *125*, 127-142.

Lopez-Bendito, G., Chan, C.H., Mallamaci, A., Parnavelas, J., and Molnar, Z. (2002). Role of Emx2 in the development of the reciprocal connectivity between cortex and thalamus. J Comp Neurol *451*, 153-169.

Lopez-Bendito, G., Flames, N., Ma, L., Fouquet, C., Di Meglio, T., Chedotal, A., Tessier-Lavigne, M., and Marin, O. (2007). Robo1 and Robo2 cooperate to control the guidance of major axonal tracts in the mammalian forebrain. J Neurosci *27*, 3395-3407.

Lopez-Bendito, G., and Molnar, Z. (2003). Thalamocortical development: how are we going to get there? Nat Rev Neurosci *4*, 276-289.

Lu, W., Katz, S., Gupta, R., and Mayer, B.J. (1997). Activation of Pak by membrane localization mediated by an SH3 domain from the adaptor protein Nck. Curr Biol *7*, 85-94.

Madisen, L., Zwingman, T.A., Sunkin, S.M., Oh, S.W., Zariwala, H.A., Gu, H., Ng, L.L., Palmiter, R.D., Hawrylycz, M.J., Jones, A.R.*, et al.* (2010). A robust and high-throughput Cre reporting and characterization system for the whole mouse brain. Nat Neurosci *13*, 133-140.

Malartre, M., Ayaz, D., Amador, F.F., and Martin-Bermudo, M.D. (2010). The guanine exchange factor vav controls axon growth and guidance during Drosophila development. J Neurosci *30*, 2257-2267.

Manser, E., Leung, T., Salihuddin, H., Zhao, Z.S., and Lim, L. (1994). A brain serine/threonine protein kinase activated by Cdc42 and Rac1. Nature *367*, 40-46.

Manser, E., Loo, T.H., Koh, C.G., Zhao, Z.S., Chen, X.Q., Tan, L., Tan, I., Leung, T., and Lim, L. (1998). PAK kinases are directly coupled to the PIX family of nucleotide exchange factors. Mol Cell *1*, 183-192.

Marston, D.J., Dickinson, S., and Nobes, C.D. (2003). Rac-dependent trans-endocytosis of ephrinBs regulates Eph-ephrin contact repulsion. Nat Cell Biol *5*, 879-888.

Mason, C.A., and Sretavan, D.W. (1997). Glia, neurons, and axon pathfinding during optic chiasm development. Curr Opin Neurobiol *7*, 647-653.

Mason, C.A., and Wang, L.C. (1997). Growth cone form is behavior-specific and, consequently, position-specific along the retinal axon pathway. J Neurosci *17*, 1086-1100.

McConnell, S.K. (1995). Constructing the cerebral cortex: neurogenesis and fate determination. Neuron *15*, 761-768.

McPhie, D.L., Coopersmith, R., Hines-Peralta, A., Chen, Y., Ivins, K.J., Manly, S.P., Kozlowski, M.R., Neve, K.A., and Neve, R.L. (2003). DNA synthesis and neuronal apoptosis caused by familial Alzheimer disease mutants of the amyloid precursor protein are mediated by the p21 activated kinase PAK3. J Neurosci *23*, 6914-6927.

Mendes, S.W., Henkemeyer, M., and Liebl, D.J. (2006). Multiple Eph receptors and B-class ephrins regulate midline crossing of corpus callosum fibers in the developing mouse forebrain. J Neurosci *26*, 882-892.

Metin, C., Deleglise, D., Serafini, T., Kennedy, T.E., and Tessier-Lavigne, M. (1997). A role for netrin-1 in the guidance of cortical efferents. Development *124*, 5063-5074.

Minshew, N.J., and Williams, D.L. (2007). The new neurobiology of autism: cortex, connectivity, and neuronal organization. Arch Neurol *64*, 945-950.

Mizuno, A., Villalobos, M.E., Davies, M.M., Dahl, B.C., and Muller, R.A. (2006). Partially enhanced thalamocortical functional connectivity in autism. Brain Res *1104*, 160-174.

Molnar, Z., Adams, R., and Blakemore, C. (1998a). Mechanisms underlying the early establishment of thalamocortical connections in the rat. J Neurosci *18*, 5723-5745.

Molnar, Z., Adams, R., Goffinet, A.M., and Blakemore, C. (1998b). The role of the first postmitotic cortical cells in the development of thalamocortical innervation in the reeler mouse. J Neurosci *18*, 5746-5765.

Molnar, Z., and Blakemore, C. (1991). Lack of regional specificity for connections formed between thalamus and cortex in coculture. Nature *351*, 475-477.

Molnar, Z., and Blakemore, C. (1995). How do thalamic axons find their way to the cortex? Trends Neurosci *18*, 389-397.

Molnar, Z., and Cordery, P. (1999). Connections between cells of the internal capsule, thalamus, and cerebral cortex in embryonic rat. J Comp Neurol *413*, 1-25.

Molnar, Z., Garel, S., Lopez-Bendito, G., Maness, P., and Price, D.J. (2012). Mechanisms controlling the guidance of thalamocortical axons through the embryonic forebrain. Eur J Neurosci *35*, 1573-1585.

Moon, M.S., and Gomez, T.M. (2010). Balanced Vav2 GEF activity regulates neurite outgrowth and branching in vitro and in vivo. Mol Cell Neurosci *44*, 118-128.

Movilla, N., and Bustelo, X.R. (1999). Biological and regulatory properties of Vav-3, a new member of the Vav family of oncoproteins. Mol Cell Biol *19*, 7870-7885.

Nakagawa, S., Brennan, C., Johnson, K.G., Shewan, D., Harris, W.A., and Holt, C.E. (2000). Ephrin-B regulates the Ipsilateral routing of retinal axons at the optic chiasm. Neuron *25*, 599-610.

Nguyen, T.V., Galvan, V., Huang, W., Banwait, S., Tang, H., Zhang, J., and Bredesen, D.E. (2008). Signal transduction in Alzheimer disease: p21-activated kinase signaling requires C-terminal cleavage of APP at Asp664. J Neurochem *104*, 1065-1080.

Nofer, J.R., Feuerborn, R., Levkau, B., Sokoll, A., Seedorf, U., and Assmann, G. (2003). Involvement of Cdc42 signaling in apoA-I-induced cholesterol efflux. J Biol Chem *278*, 53055-53062.

North, H.A., Zhao, X., Kolk, S.M., Clifford, M.A., Ziskind, D.M., and Donoghue, M.J. (2009). Promotion of proliferation in the developing cerebral cortex by EphA4 forward signaling. Development *136*, 2467-2476.

O'Leary, D.D., and Koester, S.E. (1993). Development of projection neuron types, axon pathways, and patterned connections of the mammalian cortex. Neuron *10*, 991-1006.

O'Leary, D.D., Schlaggar, B.L., and Tuttle, R. (1994). Specification of neocortical areas and thalamocortical connections. Annu Rev Neurosci *17*, 419-439.

O'Leary, D.M., Gerfen, C.R., and Cowan, W.M. (1983). The development and restriction of the ipsilateral retinofugal projection in the chick. Brain Res *312*, 93-109.

Orioli, D., Henkemeyer, M., Lemke, G., Klein, R., and Pawson, T. (1996). Sek4 and Nuk receptors cooperate in guidance of commissural axons and in palate formation. EMBO J *15*, 6035-6049.

Oster, S.F., Bodeker, M.O., He, F., and Sretavan, D.W. (2003). Invariant Sema5A inhibition serves an ensheathing function during optic nerve development. Development *130*, 775-784.

Ozaki, H.S., and Wahlsten, D. (1992). Prenatal formation of the normal mouse corpus callosum: a quantitative study with carbocyanine dyes. J Comp Neurol *323*, 81-90.

Pak, W., Hindges, R., Lim, Y.S., Pfaff, S.L., and O'Leary, D.D. (2004). Magnitude of binocular vision controlled by islet-2 repression of a genetic program that specifies laterality of retinal axon pathfinding. Cell *119*, 567-578.

Palmieri, S.J., Nebl, T., Pope, R.K., Seastone, D.J., Lee, E., Hinchcliffe, E.H., Sluder, G., Knecht, D., Cardelli, J., and Luna, E.J. (2000). Mutant Rac1B expression in Dictyostelium: effects on morphology, growth, endocytosis, development, and the actin cytoskeleton. Cell Motil Cytoskeleton *46*, 285-304.

Pascall, J.C., and Brown, K.D. (2004). Intramembrane cleavage of ephrinB3 by the human rhomboid family protease, RHBDL2. Biochem Biophys Res Commun *317*, 244-252.

Pasquale, E.B. (2005). Eph receptor signalling casts a wide net on cell behaviour. Nat Rev Mol Cell Biol *6*, 462-475.

Paxinos, G.H., G. Watson, C. Koutcherov, Y. Wang, H. (2007). Atlas of the Developing Mouse Brain at E17.5, P0, and P6, First edn (Elsevier).

Petros, T.J., Bryson, J.B., and Mason, C. (2010). Ephrin-B2 elicits differential growth cone collapse and axon retraction in retinal ganglion cells from distinct retinal regions. Dev Neurobiol *70*, 781-794.

Petros, T.J., Rebsam, A., and Mason, C.A. (2008). Retinal axon growth at the optic chiasm: to cross or not to cross. Annu Rev Neurosci *31*, 295-315.

Petros, T.J., Shrestha, B.R., and Mason, C. (2009). Specificity and sufficiency of EphB1 in driving the ipsilateral retinal projection. J Neurosci *29*, 3463-3474.

Pires-Neto, M.A., and Lent, R. (1993). The prenatal development of the anterior commissure in hamsters: pioneer fibers lead the way. Brain Res Dev Brain Res *72*, 59-66.

Plump, A.S., Erskine, L., Sabatier, C., Brose, K., Epstein, C.J., Goodman, C.S., Mason, C.A., and Tessier-Lavigne, M. (2002). Slit1 and Slit2 cooperate to prevent premature midline crossing of retinal axons in the mouse visual system. Neuron *33*, 219-232.

Polleux, F., Giger, R.J., Ginty, D.D., Kolodkin, A.L., and Ghosh, A. (1998). Patterning of cortical efferent projections by semaphorin-neuropilin interactions. Science *282*, 1904-1906.

Powell, A.W., Sassa, T., Wu, Y., Tessier-Lavigne, M., and Polleux, F. (2008). Topography of thalamic projections requires attractive and repulsive functions of Netrin-1 in the ventral telencephalon. PLoS Biol *6*, e116.

Price, D.J., Kennedy, H., Dehay, C., Zhou, L., Mercier, M., Jossin, Y., Goffinet, A.M., Tissir, F., Blakey, D., and Molnar, Z. (2006). The development of cortical connections. Eur J Neurosci *23*, 910-920.

Raper, J., and Mason, C. (2010). Cellular strategies of axonal pathfinding. Cold Spring Harb Perspect Biol *2*, a001933.

Rash, B.G., and Richards, L.J. (2001). A role for cingulate pioneering axons in the development of the corpus callosum. J Comp Neurol *434*, 147-157.

Raybaud, C., and Girard, N. (2005). Malformations of the telencephalic commissures. *Pediatric neuroradiology*, 41-69.

Rebsam, A., Petros, T.J., and Mason, C.A. (2009). Switching retinogeniculate axon laterality leads to normal targeting but abnormal eye-specific segregation that is activity dependent. J Neurosci *29*, 14855-14863.

Richards, L.J., Plachez, C., and Ren, T. (2004). Mechanisms regulating the development of the corpus callosum and its agenesis in mouse and human. Clin Genet *66*, 276-289.

Robichaux, M.A., Chenaux, G., Ho, H.Y., Soskis, M.J., Dravis, C., Kwan, K.Y., Sestan, N., Greenberg, M.E., Henkemeyer, M., and Cowan, C.W. (2013). Transient EphB Receptor Forward Signaling Coordinates Area-specific Cofasciculation of Reciprocal Thalamic and Cortical Axons during Brain Development.

Rouiller, E.M., and Welker, E. (2000). A comparative analysis of the morphology of corticothalamic projections in mammals. Brain Res Bull *53*, 727-741.

Sahay, A., Molliver, M.E., Ginty, D.D., and Kolodkin, A.L. (2003). Semaphorin 3F is critical for development of limbic system circuitry and is required in neurons for selective CNS axon guidance events. J Neurosci *23*, 6671-6680.

Sahin, M., Greer, P.L., Lin, M.Z., Poucher, H., Eberhart, J., Schmidt, S., Wright, T.M., Shamah, S.M., O'Connell, S., Cowan, C.W.*, et al.* (2005). Eph-dependent tyrosine phosphorylation of ephexin1 modulates growth cone collapse. Neuron *46*, 191-204.

Sakai, J.A., and Halloran, M.C. (2006). Semaphorin 3d guides laterality of retinal ganglion cell projections in zebrafish. Development *133*, 1035-1044.

Sanders, S.J., Murtha, M.T., Gupta, A.R., Murdoch, J.D., Raubeson, M.J., Willsey, A.J., Ercan-Sencicek, A.G., DiLullo, N.M., Parikshak, N.N., Stein, J.L.*, et al.* (2012). De novo mutations revealed by whole-exome sequencing are strongly associated with autism. Nature *485*, 237-241.

Schmandke, A., and Strittmatter, S.M. (2007). ROCK and Rho: biochemistry and neuronal functions of Rho-associated protein kinases. Neuroscientist *13*, 454-469.

Schmidt, A., and Hall, A. (2002). Guanine nucleotide exchange factors for Rho GTPases: turning on the switch. Genes Dev *16*, 1587-1609.

Schuebel, K.E., Movilla, N., Rosa, J.L., and Bustelo, X.R. (1998). Phosphorylation-dependent and constitutive activation of Rho proteins by wild-type and oncogenic Vav-2. EMBO J *17*, 6608-6621.

Seibt, J., Schuurmans, C., Gradwhol, G., Dehay, C., Vanderhaeghen, P., Guillemot, F., and Polleux, F. (2003). Neurogenin2 specifies the connectivity of thalamic neurons by controlling axon responsiveness to intermediate target cues. Neuron *39*, 439-452.

Sells, M.A., Knaus, U.G., Bagrodia, S., Ambrose, D.M., Bokoch, G.M., and Chernoff, J. (1997). Human p21-activated kinase (Pak1) regulates actin organization in mammalian cells. Curr Biol *7*, 202-210.

Sells, M.A., Pfaff, A., and Chernoff, J. (2000). Temporal and spatial distribution of activated Pak1 in fibroblasts. J Cell Biol *151*, 1449-1458.

Serafini, T., Colamarino, S.A., Leonardo, E.D., Wang, H., Beddington, R., Skarnes, W.C., and Tessier-Lavigne, M. (1996). Netrin-1 is required for commissural axon guidance in the developing vertebrate nervous system. Cell *87*, 1001-1014.

Shamah, S.M., Lin, M.Z., Goldberg, J.L., Estrach, S., Sahin, M., Hu, L., Bazalakova, M., Neve, R.L., Corfas, G., Debant, A.*, et al.* (2001). EphA receptors regulate growth cone dynamics through the novel guanine nucleotide exchange factor ephexin. Cell *105*, 233-244.

Shatz, C.J., and Sretavan, D.W. (1986). Interactions between retinal ganglion cells during the development of the mammalian visual system. Annu Rev Neurosci *9*, 171-207.

Shekarabi, M., and Kennedy, T.E. (2002). The netrin-1 receptor DCC promotes filopodia formation and cell spreading by activating Cdc42 and Rac1. Mol Cell Neurosci *19*, 1-17.

Shekarabi, M., Moore, S.W., Tritsch, N.X., Morris, S.J., Bouchard, J.F., and Kennedy, T.E. (2005). Deleted in colorectal cancer binding netrin-1 mediates cell substrate adhesion and

recruits Cdc42, Rac1, Pak1, and N-WASP into an intracellular signaling complex that promotes growth cone expansion. J Neurosci *25*, 3132-3141.

Shen, K., and Cowan, C.W. (2010). Guidance molecules in synapse formation and plasticity. Cold Spring Harb Perspect Biol *2*, a001842.

Shintani, T., Ihara, M., Sakuta, H., Takahashi, H., Watakabe, I., and Noda, M. (2006). Eph receptors are negatively controlled by protein tyrosine phosphatase receptor type O. Nat Neurosci *9*, 761-769.

Shu, T., Butz, K.G., Plachez, C., Gronostajski, R.M., and Richards, L.J. (2003a). Abnormal development of forebrain midline glia and commissural projections in Nfia knock-out mice. J Neurosci *23*, 203-212.

Shu, T., and Richards, L.J. (2001). Cortical axon guidance by the glial wedge during the development of the corpus callosum. J Neurosci *21*, 2749-2758.

Shu, T., Sundaresan, V., McCarthy, M.M., and Richards, L.J. (2003b). Slit2 guides both precrossing and postcrossing callosal axons at the midline in vivo. J Neurosci *23*, 8176-8184.

Shukla, D.K., Keehn, B., and Muller, R.A. (2011). Tract-specific analyses of diffusion tensor imaging show widespread white matter compromise in autism spectrum disorder. J Child Psychol Psychiatry *52*, 286-295.

Silver, J., Lorenz, S.E., Wahlsten, D., and Coughlin, J. (1982). Axonal guidance during development of the great cerebral commissures: descriptive and experimental studies, in vivo, on the role of preformed glial pathways. J Comp Neurol *210*, 10-29.

Silver, J., and Ogawa, M.Y. (1983). Postnatally induced formation of the corpus callosum in acallosal mice on glia-coated cellulose bridges. Science *220*, 1067-1069.

Slack-Davis, J.K., Eblen, S.T., Zecevic, M., Boerner, S.A., Tarcsafalvi, A., Diaz, H.B., Marshall, M.S., Weber, M.J., Parsons, J.T., and Catling, A.D. (2003). PAK1 phosphorylation of MEK1 regulates fibronectin-stimulated MAPK activation. J Cell Biol *162*, 281-291.

Songyang, Z., Shoelson, S.E., McGlade, J., Olivier, P., Pawson, T., Bustelo, X.R., Barbacid, M., Sabe, H., Hanafusa, H., Yi, T.*, et al.* (1994). Specific motifs recognized by the SH2 domains of Csk, 3BP2, fps/fes, GRB-2, HCP, SHC, Syk, and Vav. Mol Cell Biol *14*, 2777-2785.

Soskis, M.J., Ho, H.Y., Bloodgood, B.L., Robichaux, M.A., Malik, A.N., Ataman, B., Rubin, A.A., Zieg, J., Zhang, C., Shokat, K.M.*, et al.* (2012). A chemical genetic approach reveals distinct EphB signaling mechanisms during brain development. Nat Neurosci *15*, 1645-1654.

Sretavan, D.W. (1990). Specific routing of retinal ganglion cell axons at the mammalian optic chiasm during embryonic development. J Neurosci *10*, 1995-2007.

Srivastava, N., Robichaux, M.A., Chenaux, G., Henkemeyer, M., and Cowan, C.W. (2013). EphB2 receptor forward signaling controls cortical growth cone collapse via Nck and Pak. Mol Cell Neurosci *52*, 106-116.

Stein, E., Zou, Y., Poo, M., and Tessier-Lavigne, M. (2001). Binding of DCC by netrin-1 to mediate axon guidance independent of adenosine A2B receptor activation. Science *291*, 1976-1982.

Stepanek, L., Stoker, A.W., Stoeckli, E., and Bixby, J.L. (2005). Receptor tyrosine phosphatases guide vertebrate motor axons during development. J Neurosci *25*, 3813-3823.

Suto, F., Ito, K., Uemura, M., Shimizu, M., Shinkawa, Y., Sanbo, M., Shinoda, T., Tsuboi, M., Takashima, S., Yagi, T.*, et al.* (2005). Plexin-a4 mediates axon-repulsive activities of both secreted and transmembrane semaphorins and plays roles in nerve fiber guidance. J Neurosci *25*, 3628-3637.

Swiercz, J.M., Kuner, R., Behrens, J., and Offermanns, S. (2002). Plexin-B1 directly interacts with PDZ-RhoGEF/LARG to regulate RhoA and growth cone morphology. Neuron *35*, 51-63.

Temereanca, S., and Simons, D.J. (2004). Functional topography of corticothalamic feedback enhances thalamic spatial response tuning in the somatosensory whisker/barrel system. Neuron *41*, 639-651.

Thompson, H., Barker, D., Camand, O., and Erskine, L. (2006a). Slits contribute to the guidance of retinal ganglion cell axons in the mammalian optic tract. Dev Biol *296*, 476-484.

Thompson, H., Camand, O., Barker, D., and Erskine, L. (2006b). Slit proteins regulate distinct aspects of retinal ganglion cell axon guidance within dorsal and ventral retina. J Neurosci *26*, 8082-8091.

Tole, S., Gutin, G., Bhatnagar, L., Remedios, R., and Hebert, J.M. (2006). Development of midline cell types and commissural axon tracts requires Fgfr1 in the cerebrum. Dev Biol *289*, 141-151.

Tolias, K.F., Bikoff, J.B., Kane, C.G., Tolias, C.S., Hu, L., and Greenberg, M.E. (2007). The Rac1 guanine nucleotide exchange factor Tiam1 mediates EphB receptor-dependent dendritic spine development. Proc Natl Acad Sci U S A *104*, 7265-7270.

Torborg, C.L., and Feller, M.B. (2004). Unbiased analysis of bulk axonal segregation patterns. J Neurosci Methods *135*, 17-26.

Torii, M., and Levitt, P. (2005). Dissociation of corticothalamic and thalamocortical axon targeting by an EphA7-mediated mechanism. Neuron *48*, 563-575.

Turner, M., and Billadeau, D.D. (2002). VAV proteins as signal integrators for multi-subunit immune-recognition receptors. Nat Rev Immunol *2*, 476-486.

van der Bliek, A.M., Redelmeier, T.E., Damke, H., Tisdale, E.J., Meyerowitz, E.M., and Schmid, S.L. (1993). Mutations in human dynamin block an intermediate stage in coated vesicle formation. J Cell Biol *122*, 553-563.

Wahl, S., Barth, H., Ciossek, T., Aktories, K., and Mueller, B.K. (2000). Ephrin-A5 induces collapse of growth cones by activating Rho and Rho kinase. J Cell Biol *149*, 263-270.

Wiencken-Barger, A.E., Mavity-Hudson, J., Bartsch, U., Schachner, M., and Casagrande, V.A. (2004). The role of L1 in axon pathfinding and fasciculation. Cereb Cortex *14*, 121-131.

Williams, S.E., Grumet, M., Colman, D.R., Henkemeyer, M., Mason, C.A., and Sakurai, T. (2006). A role for Nr-CAM in the patterning of binocular visual pathways. Neuron *50*, 535-547.

Williams, S.E., Mann, F., Erskine, L., Sakurai, T., Wei, S., Rossi, D.J., Gale, N.W., Holt, C.E., Mason, C.A., and Henkemeyer, M. (2003). Ephrin-B2 and EphB1 mediate retinal axon divergence at the optic chiasm. Neuron *39*, 919-935.

Williams, S.E., Mason, C.A., and Herrera, E. (2004). The optic chiasm as a midline choice point. Curr Opin Neurobiol *14*, 51-60.

Wolff, J.J., Gu, H., Gerig, G., Elison, J.T., Styner, M., Gouttard, S., Botteron, K.N., Dager, S.R., Dawson, G., Estes, A.M*., et al.* (2012). Differences in white matter fiber tract development present from 6 to 24 months in infants with autism. Am J Psychiatry *169*, 589-600.

Wright, A.G., Demyanenko, G.P., Powell, A., Schachner, M., Enriquez-Barreto, L., Tran, T.S., Polleux, F., and Maness, P.F. (2007). Close homolog of L1 and neuropilin 1 mediate guidance of thalamocortical axons at the ventral telencephalon. J Neurosci *27*, 13667-13679.

Wybenga-Groot, L.E., Baskin, B., Ong, S.H., Tong, J., Pawson, T., and Sicheri, F. (2001). Structural basis for autoinhibition of the Ephb2 receptor tyrosine kinase by the unphosphorylated juxtamembrane region. Cell *106*, 745-757.

Xia, W., Wong, E.W., Mruk, D.D., and Cheng, C.Y. (2009). TGF-beta3 and TNFalpha perturb blood-testis barrier (BTB) dynamics by accelerating the clathrin-mediated endocytosis of integral membrane proteins: a new concept of BTB regulation during spermatogenesis. Dev Biol *327*, 48-61.

Xu, N.J., and Henkemeyer, M. (2009). Ephrin-B3 reverse signaling through Grb4 and cytoskeletal regulators mediates axon pruning. Nat Neurosci *12*, 268-276.

Yi, C., Wilker, E.W., Yaffe, M.B., Stemmer-Rachamimov, A., and Kissil, J.L. (2008). Validation of the p21-activated kinases as targets for inhibition in neurofibromatosis type 2. Cancer Res *68*, 7932-7937.

Yokoyama, N., Romero, M.I., Cowan, C.A., Galvan, P., Helmbacher, F., Charnay, P., Parada, L.F., and Henkemeyer, M. (2001). Forward signaling mediated by ephrin-B3 prevents contralateral corticospinal axons from recrossing the spinal cord midline. Neuron *29*, 85-97.

Zhang, D., Udagawa, N., Nakamura, I., Murakami, H., Saito, S., Yamasaki, K., Shibasaki, Y., Morii, N., Narumiya, S., Takahashi, N.*, et al.* (1995). The small GTP-binding protein, rho p21, is involved in bone resorption by regulating cytoskeletal organization in osteoclasts. J Cell Sci *108 (Pt 6)*, 2285-2292.

Zhao, L., Ma, Q.L., Calon, F., Harris-White, M.E., Yang, F., Lim, G.P., Morihara, T., Ubeda, O.J., Ambegaokar, S., Hansen, J.E.*, et al.* (2006). Role of p21-activated kinase pathway defects in the cognitive deficits of Alzheimer disease. Nat Neurosci *9*, 234-242.

Zhong, J.L., Banerjee, M.D., and Nikolic, M. (2003). Pak1 and its T212 phosphorylated form accumulate in neurones and epithelial cells of the developing rodent. Dev Dyn *228*, 121-127.

Zhou, C., Qiu, Y., Pereira, F.A., Crair, M.C., Tsai, S.Y., and Tsai, M.J. (1999). The nuclear orphan receptor COUP-TFI is required for differentiation of subplate neurons and guidance of thalamocortical axons. Neuron *24*, 847-859.

Zimmer, M., Palmer, A., Kohler, J., and Klein, R. (2003). EphB-ephrinB bi-directional endocytosis terminates adhesion allowing contact mediated repulsion. Nat Cell Biol *5*, 869-878.

Zisch, A.H., Kalo, M.S., Chong, L.D., and Pasquale, E.B. (1998). Complex formation between EphB2 and Src requires phosphorylation of tyrosine 611 in the EphB2 juxtamembrane region. Oncogene *16*, 2657-2670.